Charles University
Faculty of Science

Study programme: Anatomy and physiology of plants

Mgr. Zdeňka Kubátová

FUNCTIONAL ANALYSIS OF SELECTED EXO70 EXOCYST SUBUNITS IN PLANTS

FUNKČNÍ ANALÝZA VYBRANÝCH PODJEDNOTEK EXOCYSTU EXO70 U ROSTLIN

Doctoral thesis

Supervisor: Mgr. Ivan Kulich, Ph.D.
Consultant: prof. RNDr. Viktor Žárský, CSc.

Prague, 2020

Student's declaration

I hereby declare that I have written this thesis by myself, that I have listed all information sources and literature used and that this thesis was submitted only once and has not been used to apply for another academic title.

Prohlášení studenta

Prohlašuji, že jsem závěrečnou práci zpracovala samostatně a že jsem uvedla všechny použité informační zdroje a literaturu. Tato práce ani její podstatná část nebyla předložena k získání jiného nebo stejného akademického titulu.

In Prague/ V Praze: _____ _____

Mgr. Zdeňka Kubátová

Supervisor's declaration

I hereby confirm that contribution of Zdeňka Kubátová to the published work corresponds to what she declares here.

Prohlášení školitele

Prohlašuji, že podíl Zdeňky Kubátové na předložených publikacích odpovídá tomu, co v této disertační práci deklaruje.

In Prague/ V Praze: _____ _____

Mgr. Ivan Kulich, Ph.D.

Acknowledgements

Research presented in this thesis was conducted under the kind and thorough guidance of my supervisor Ivan Kulich to whom I would like to thank the most. For his scientific passion, which has been and always will be an amazing inspiration for me, and especially for his supportive leadership and amiable attitude that allowed me to improve day by day.

I would like to thank Viktor Žárský for the opportunity given to me in his laboratory, for a critical conceptual view of my work and experienced revisions of publications and texts, thanks to which I learned a lot.

I would also like to thank my colleagues in our laboratory for a positive and collaborative environment, for many constructive discussions and multiple encouraging words about thesis writing.

Further, I would like to thank our technician Marta Čadyová for her immense technical support of our laboratory, including my experiments.

Special thanks go to Antonín Vojtík Jr. for typesetting and graphical layout of this thesis, to Marek Romášek for language proofreading and to Peter Sabol for plentiful comments and corrections of the text.

And last I thank my family, especially my parents and my husband for their infinite support during my studies.

Research presented in this thesis was supported by these grants:

Grant Agency of Charles University
grant 387515

Grant Agency of Charles University
grant 658112

Czech Science Foundation
grant 14-27329P

Czech Science Foundation
grant 18-12579S

Czech Ministry of Education
grant NPUI LO1417

Abbreviations

Arabidopsis	*Arabidopsis thaliana*
CASP	CASPARIAN STRIP MEMBRANE DOMAIN PROTEIN
CesA	cellulose synthase
CSC	Cellulose synthase complex
DAB	3,3'-diaminobenzidine
GFP	green fluorescent protein
GSL	GLUCAN SYNTHASE-LIKE
GTPase	guanosine triphosphatase
Fig.	Figure
H_2O_2	hydrogen peroxide
MT	microtubule
NADPH	nicotinamide adenine dinucleotide phosphate
PA	phosphatidic acid
PIP_2	phosphatidylinositol 4,5-bisphosphate
ROP	Rho of plants
ROS	reactive oxygen species
SCW	secondary cell wall
UDP	uridine diphosphate
UV	ultraviolet

Abstract

Arabidopsis thaliana trichomes are large unicellular epidermal outgrowths with a specific development and intriguing shape, which makes them an excellent cell type for our research of cell polarization mechanisms. Cell polarity is essential for plant development and the exocyst complex is one of its key regulators. It is an octameric protein complex that mediates polarized exocytosis and growth by targeted tethering of secretory vesicles to the plasma membrane. Its EXO70 subunit functions as a landmark for exocytosis site and physically binds the target membrane through interaction with phospholipids. A remarkable multiplication of EXO70 subunit paralogs in land plant genomes is well documented, but the functional diversity of these paralogs remains to be described.

In trichomes we revealed the specific role of the EXO70H4 paralog in secondary cell wall deposition, especially in callose synthase delivery. We documented formation of a thick secondary cell wall during the maturation phase of wild type trichome development and a lack of it in the *exo70H4* mutant. Moreover, we showed evidence for silica deposition dependency on callose synthesis. Further, we unveiled the formation of apical and basal plasma membrane domains, which differ in their phospholipid composition and ability to bind different EXO70 paralogs. Our results have a potential of broader implications thanks to the putative role of EXO70H4 in the response to pathogens and thanks to its evolutionary conservation among other angiosperm species.

Abstrakt

Unikátnost trichomů *Arabidopsis thaliana* tkví ve spojení jejich jednobuněčnosti a specifického tvaru, a tak jsme trichomy využili jako skvělý modelový systém pro výzkum mechanismů buněčné polarizace. Vývoj rostlinného těla je silně určen mechanismy buněčné polarizace a proteinový komplex exocyst je jedním z jejich klíčových regulátorů. Exocyst je tvořen osmi různými podjednotkami a při polarizované exocytóze váže sekretorické váčky na cílové membráně. Podjednotka EXO70 pomocí interakce s fosfolipidy značí konkrétní místo exocytózy na cílové membráně. Pozoruhodné zmnožení genů podjednotky EXO70 v rostlinných genomech je již obstojně zdokumentováno, nicméně zmapování funkční rozrůzněnosti jednotlivých paralogů zatím schází.

Studiem trichomů jsme odhalili specifickou funkci paralogu EXO70H4 ve vývoji sekundární buněčné stěny trichomu a především sekreci kalózo-syntáz. V divokém trichomu jsme popsali utváření tlusté sekundární buněčné stěny během fáze dozrávání a její absenci u mutanta *exo70H4*. Dále jsme prokázali vztah mezi ukládáním křemíku a přítomností kalózy. Také jsme odhalili rozdělení plazmatické membrány trichomu na apikální a bazální doménu plazmatické membrány, které se liší složením fosfolipidů a schopností vázat různé paralogy EXO70. Naše výsledky mají potenciál širšího využití díky pravděpodobné funkci proteinu EXO70H4 v obraně před patogeny a díky jeho evoluční konzervovanosti napříč jinými druhy krytosemenných rostlin.

1 Introduction

This thesis summarizes the results obtained by research of *Arabidopsis thaliana* (Arabidopsis) trichomes during my Ph.D. studies and it is based on my previous findings from my Master's thesis. In trichomes we studied the mechanisms of secondary cell wall (SCW) thickening and a role of polar exocytosis in this process. Our results shed light on callose synthase secretion and its connection with silica deposition. Further, we bring new conclusions about the role of the EXO70 subunit of the exocyst complex, particularly the EXO70H4 paralog. We defined its function in polarized SCW formation and the organization of plasma membrane domains.

1.1 Arabidopsis trichomes

Arabidopsis trichomes are non-secreting cells of epidermal origin with many exclusive attributes which made them a fruitful model in several cell biology research areas. Their regular distribution on the leaf was suitable for genetic studies of epidermal cell patterning, cell fate determination and the coordination of cell division and differentiation (Hülskamp et al., 1994). They have been suggested to passively contribute to light reflection properties of the leaf (Suo et al., 2013), ultraviolet (UV) light protection (Yan et al., 2012), herbivore defense (Handley et al., 2005; Jakoby et al., 2008; Dai et al., 2010; Frerigmann et al., 2012) and mechanosensing (Zhou et al., 2017). Nevertheless, due to only a small amount of evidence, our understanding of their role and function is still very limited.

Despite being single-celled, they grow into precisely polarized structures with three branches. This outstanding process of trichome shaping was used as a potent model for the study of cell morphogenesis and polarized processes - growth, secretion, etc. (Szymanski et al., 2000). The bottom of the cell forms a bulging base, which is the only part of the trichome in contact with other epidermal and mesophyll cells, while the upper parts (stalk and three branches) outgrow above the epidermis. Trichome cell development can be divided into six stages (Hülskamp, 2004) with tightly regulated steps. Several rounds of endoreduplication during the first phase of trichome development result in a multiplication of nuclear genome, leading to a significantly enlarged cell size and content. During the growing and shaping phases the trichome reaches its typical shape, forming most frequently three long branches with sharp tips. The growth completion is followed by the last phase - the maturation of the cell wall. This phase of trichome development has been, for unknown reasons, largely omitted by researchers in the field and therefore unexploited.

Only a few mutants with a phenotypic deviation in cell wall differentiation have been identified so far. Several mutations affect surface papillae formation; such mutants are known as “glassy hair”, because the trichomes seem to be more transparent in comparison to wild type. The first glassy hair mutants identified are *chablis*, *chardonnay* and *retsina* (Hülskamp et al., 1994) and others are *trichome birefringence* (Hülskamp et al., 1994; Potikha and Delmer, 1995), *noeck* (Esch et al., 2003), *glabrous 3-shapeshifter* (Jakoby et al., 2008), *homeodomain glabrous 2* (Marks et al., 2009), *constitutive pathogen resistance 5* (Brininstool et al., 2008) and *glassy hair 1 and 3* (Suo et al., 2013). Then there are mutants with an impaired cell wall composition, like *murus 2* (Vanzin et al., 2002), *murus 3* (Madson et al., 2003) and those with altered autofluorescence like *fah 1* (Chapple et al., 1992) and *bright trichomes 1* (Ruegger and Chapple, 2001; Sinlapadech et al., 2007). Despite some new evidence that has emerged during the last years, no significant

progress in discovering detailed mechanisms of trichome cell wall maturation has been made. We tried to change this lack of knowledge by a detailed study of the wild type trichome and by its comparison with the *exo70H4* mutant, which exhibits defective cell wall maturation. Our research finally brought insight into processes occurring during this stage and it showed a deep potential of trichomes as a model for polar SCW biogenesis.

1.2 Secondary cell wall in plants

Each plant cell is encased by elastic but tough cellulosic cell wall, which is essential for cell development, growth regulation and its protection, while at the same time it enables communication and exchange of substances between cells (Somerville, 2004). The cell wall consists of structural proteins, enzymes and secondary compounds but predominantly of polysaccharides with different composition and structure - homopolysaccharides and heteropolysaccharides.

Heteropolysaccharides, principally pectins and hemicelluloses, are synthesized in the Golgi apparatus and secreted to the apoplast, where they are incorporated into a growing cell wall matrix and frequently modified (Mohnen, 2008; Scheller and Ulvskov, 2010). This is not the case for homopolysaccharides, cellulose and callose, whose synthesis is executed directly on the plasma membrane by synthase complexes. Cell wall composition varies a lot depending on the species, tissues, cell types and developmental stage; for instance, primary and secondary cell walls differ significantly by characteristic chemical composition. Ubiquitously present primary cell walls are thin but strong enough to resist turgor pressure, while facilitating morphogenetic processes thanks to their flexibility and expandability. On the contrary, SCWs are deposited after the completion of growth only in a small portion of specialized cells with a specific structure and function involving prominent cell wall thickenings. SCWs provide mechanical support to cells and thus to the whole plant body, because they are tough and rigid, although still plastic.

The plant cell wall fundamentally influences the cell shape by determining the direction and amount of cell growth. Morphological and developmental impacts of cell wall properties promote functional specialization of cells. Differentiated cell types are often characterized by an accumulation of SCW which tends to be profoundly adapted to its function.

1.2.1 Secondary cell wall composition and properties

Secondary cell walls are precisely arranged mixtures of several fibrous molecules and a cross-linked matrix. They differ from primary cell walls in their characteristic composition, as primary cell walls are predominantly made of cellulose and hemicelluloses (cross-linking glycans; cellulose-hemicellulose network) and a pectin matrix, whereas SCWs are made of cellulose, hemicelluloses (xylan, glucomannan), proteins and lignin (and other aromatics). Cellulose is the load-bearing unit composed of microfibrils, which act as a framework for interlinkage with hemicelluloses. Hemicelluloses are of great importance for the assembly of SCW and its mechanical strength. Lignin is a hydrophobic and inert compound which impregnates the cellulose-hemicellulose network and provides additional rigidity and hydrophobicity.

The particular ratio between the main components (and thus the structure) varies among plant species, tissues, cells and even cell regions and it is influenced by developmental and environmental aspects. This is enabled by a precise management of SCW production in time and space, via regulation of gene expression, component biosynthesis and modifications, targeted secretion, patterned deposition and assembly. Intricate coordination of these processes results in a tremendous structural and pattern variability and thereby the diversity of functions of SCWs. Several of them are of immense interest for humans, because of their impact on agriculture, industry and human well being.

The emergence of SCW was one of the crucial features in the plant transition to the land, and lignified SCWs are a great example of such evolutionary adaptations. Thickened SCWs are strong but still plastic, provide shape and support to the cells, giving thus strength to the aerial parts of the plant. Primary cell walls are deposited during the cell growth, are flexible and strong at the same time to promote morphogenesis and resist turgor. On the contrary, SCW deposition usually comes after growth completion and is very variable depending on cell type and function.

1.2.2 Secondary cell wall formation

The transition from primary to SCW production encompasses substantial changes in biosynthetic machinery, remodelling of transcriptomic cascades and redirection of the secretory pathway (Li et al., 2016). Different cellulose synthase complexes (CSCs) and matrix polysaccharides are produced and the cytoskeleton is rearranged during the process (Cosgrove and Jarvis, 2012). While the primary cell wall is synthesized and deposited evenly on the surface, the SCW synthesis is typically focused to specific domains and its maturation is typically completed by lignification and often followed by programmed cell death (Zhong and Ye, 2009).

Secondary cell wall formation is a complex process of coordinated biosynthesis and targeted secretion, allowing patterned deposition and assembly of SCW. SCWs are generally not deposited uniformly, creating intricate patterned thickenings. Mechanisms in charge of this precise targeting have been partially uncovered using convenient cell models with prominent SCW structures. For example, tracheary elements of vascular plants turned out to be a practical model for decoding the specific molecular machinery of SCW deposition, which comprises focused biosynthesis, polarized secretion and precise transcriptional regulation (Oda and Fukuda, 2012; Zhong and Ye, 2014).

During SCW biosynthesis, the usual cargo of polarized secretion are enzymes, SCW polysaccharides and CSCs and callose synthase complexes. For instance, the investigation of organized synthesis of cellulose microfibrils started to shed light upon this area. Compelling evidence in the literature shows that cortical microtubules (MTs) are of significant importance for both targeting of CSCs to the plasma membrane and for their subsequent movement along them. Cellulose microfibrils are produced in an oriented way by CSCs, which are guided by cortical MTs as shown for example by fluorescent fusion studies (Paradez et al., 2006) or experiments with anti-cytoskeletal drugs (Baskin, 2001; Gu et al., 2010). Several genes involved in organizing cellulose microfibrils have been identified already. Protein CELLULOSE SYNTHASE INTERACTING 1 was found to act as a scaffold protein guiding CSC alongside cortical MTs (Bringmann et al., 2012; Li et al., 2012). Discovery of this protein disproved the previous working model, where cortical MTs spatially restrict lateral diffusion of the CSCs. Also, other proteins associated with MT turnover also play a role in the cellulose fiber orientation. Such proteins include kinesin-like FRAGILE

FIBER 1 (Zhong et al., 2002) or katanin-like FRAGILE FIBER 2 (Burk and Ye, 2002). More genes identified in SCW patterning can be found in a recent review (Zhong and Ye, 2015).

Further, MTs are important for localized deposition of other SCW components, as it was demonstrated in tracheary elements, where MT bundles spatially localize underneath the plasma membrane domains of forming SCW thickenings (Oda et al., 2005) and at the same time they are absent from resting areas (microtubule-depleting plasma membrane domains), where secondary thickening does not occur (Oda and Fukuda, 2013). Moreover, cortical MT-positive plasma membrane domains are enriched not only in CSCs but also in laccases (oxidative enzymes catalyzing lignin polymerization), and they are distinctly separate from the adjacent primary wall domains, which have to maintain higher plasticity (Schuetz et al., 2014). Just as MTs shape SCW deposition, so do proteins which influence MTs. Arrangement of MTs is regulated by a range of proteins and factors including several MT-associated proteins (MAPs), Rho of plants (ROP) guanosine triphosphatases (GTPases; again well reviewed in Zhong and Ye, 2015). There is also an impact on the evolutionarily conserved network of transcriptional factors which spatially and temporally coordinate the transition to genes involved in SCW biosynthesis and deposition (Zhong et al., 2010). Until now, numerous transcriptional master switches of SCW genes transcription have been identified in the superfamily of No Apical Meristem (NAC) domain transcriptional regulators and the MYB family (also extensively reviewed in Zhong and Ye, 2015).

1.3 Callose in plant cell walls

Callose is a widespread polysaccharide of specialized plant cell walls with a linear structure of β-(1,3)-glucan with some (1,6)-branches. In certain aspects it is comparable to cellulose and it is also produced directly on the plasma membrane by membrane-associated enzymes. Nonetheless, unlike cellulose, which crystallizes exclusively into linear β-(1,4)-glucan microfibrils with high tensile strength, callose has an amorphous gel-like structure. Thus, cellulose provides general structural firmness to the cell and callose is purposed for local sealing of the spaces in the cell wall. Additionally, its nature is often rather ephemeral with only temporary existence regulated by multiple stress-related processes, while cellulose is the solid and lasting structural cell wall component.

1.3.1 Biological role of callose

The list of biological roles of callose within the plant body is impressively multifarious. It is substantial for cell plate formation during cytokinesis (Samuels, 1995; Verma, 2001) and for several cell differentiation and developmental processes, typically in cells with specialized cell walls like phloem (Evert and Derr, 1964; Sjolund, 1997; Xie et al., 2010b), in multiple stages of pollen development (McCormick, 1993), and for plasmodesmata permeability at the neck region (Iglesias and Meins, 2000; Bucher et al., 2001). Besides these roles, callose deposition is the typical plant response in stress-related processes triggered by mechanical injury or chemical damage from biotic infections and other environmental stresses (Stone and Clarke, 1992).Polymerization of uridine diphosphate (UDP) glucose into callose is catalyzed by callose synthase proteins directly on the plasma membrane. Genetic studies in Arabidopsis have identified 12 putative members of the callose synthase family whose expression and activity are presumably tissue- and cell-type specific and highly regulated by environmental or physiological and developmental signals (Verma and Hong, 2001; Dong et al., 2005; Dong et al., 2008).

1.3.2 Callose synthase proteins

Two distinct nomenclatures are in use for these genes, the first one being *GSL* for GLUCAN SYNTHASE-LIKE as reported by Richmond and Somerville (2001), and the second *CalS* for CALLOSE SYNTHASE according to Verma and Hong (2001). The *GSL* nomenclature system will be employed in this work. Members of this family mostly contain around 2000 amino acids, which makes them some of the largest proteins in plants. They have 14 -16 predicted transmembrane domains and a cytoplasmic region with a large central catalytic domain comprising a UDP-glucose catalytic site and a glycosyltransferase domain (Brownfield et al., 2009). Most *GSL* genes consist of 40 - 50 exons, with the exception of *GSL1* and *GSL5*, which have a strikingly low intron number (1 and 2, respectively).

Given the potential and the important function of GSL proteins, it may seem surprising that the elementary knowledge regarding their precise biological role, molecular mechanism and localization of many of them is only fragmentary and in several cases it has not been elucidated in any detail yet. To briefly summarize existing findings, until now, multiple GSL proteins have been found to act in pollen development and fertility: GSL1 (Enns et al., 2005), GSL2 (Dong et al., 2005; Xie et al., 2010a), GSL5 (Shi et al., 2015), GSL8 and GSL10 (Töller et al., 2008; Huang et al., 2009). Three have been reported to be involved in cell plate formation during cell division: GSL6 (Hong et al., 2001a), GSL8 (Chen et al., 2009; Thiele et al., 2009) and GSL10 (Töller et al., 2008). GSL5 has been extensively studied for its role in defensive papillae formation during pathogen infection (Jacobs et al., 2003; Nishimura et al., 2003). GSL7 was shown to maintain important functions during sieve plate pores formation in the phloem (Xie et al., 2010b; Barratt et al., 2011). Several GSLs operate in plasmodesmata regulation: GSL4 and GSL6 (Cui and Lee, 2016), GSL7 (Xie et al., 2010b) and GSL8 (Guseman et al., 2010), GSL12 (Vatén et al., 2011). Biological role of three out of the twelve GSLs in Arabidopsis, GSL3, GSL9 and GSL1, remains undiscovered so far.

1.3.3 GLUCAN-SYNTHASE LIKE 5

This thesis focuses on GSL5, also well known from the plant pathogen research field as POWDERY MILDEW RESISTANT 4. Multiple lines of evidence in the literature imply GSL5 as the main callose synthase involved in stress response (Vogel and Somerville, 2000; Nishimura et al., 2003), especially in pathogen-induced callose deposition (Jacobs et al., 2003; Nishimura et al., 2003). Its role in pathogen-induced stress response has been broadly studied over the last two decades with the focus on callose deposition during papillae formation. Papilla is a local reinforcement of the cell wall produced in order to restrict the invasion of germinating pathogen spores on the leaf surface, and callose has been considered as its main firming component (Ellinger and Voigt, 2014; Voigt, 2016).

Mutation in *GSL5* increases the level of resistance to powdery mildew fungi through the activation of SA signaling (Nishimura et al., 2003), although overexpression of *GSL5* leads to a complete resistance to powdery mildew penetration (Ellinger et al., 2013). GTPases were hypothesized as possible regulators of callose synthesis upon pathogen attack, which was recently supported experimentally by the identification of RabA4c GTPase as a direct interactor of GSL5 (Ellinger et al., 2014). RabA4c overexpression induced an increase in GSL5-dependent callose deposition leading to fungal penetration resistance, which implied GSL5 as the effector of this GTPase (Ellinger et al., 2014).

Involvement of GSL5 not only in callose production but also in signaling processes was recognized by the identification of its synergistic impact on pathogen response regulation together with a negative regulator of salicylic acid-dependent defense - ENHANCED DISEASE RESISTANCE 1. Mutation in this gene improves disease resistance linked with salicylic and jasmonic acid signaling pathway in response to powdery mildew (Wawrzynska et al., 2010). Simultaneous mutation of *edr1* and *gsl5* led to vast mesophyll cell death in response to pathogen attack as a consequence of the synergistic impact of these mutations on the signaling pathway of salicylic and jasmonic acid. So it seems that callose synthase or callose itself is involved in the suppression of salicylic and jasmonic acid-induced defense. Moreover, it implies that not the loss of callose but an excessively active salicylic acid signalling is the real and previously overlooked cause of the improved resistance in *gsl5* mutants.

Recently, two homologs of a conserved protein, UBIQUITIN-ASSOCIATED DOMAIN-CONTAINING PROTEIN 2, were identified to act in GSL5 accumulation. Mutation of this gene causes a reduction of GSL5, leading to an impaired pathogen-induced callose deposition, and conversely, constitutive overexpression of GSL5 restores pathogen-induced callose synthesis in this mutant (Wang et al., 2019).

1.3.4 Callose synthase trafficking and regulation

Despite the importance of callose deposition in plant development and defense, the exact details of GSL biosynthesis and subsequent processes (assembly, trafficking, regulation) are only fragmentary and no significant progress has been made in recent years in this field. Incomparably more evidence can be found regarding cellulose synthase proteins (CesAs), which have been in the centre of researchers' focus over the last few years. Very briefly, CesAs are synthesized in the endoplasmic reticulum and conceivably assembled in the endomembrane system to form a hexamer rosette CSCs containing 18-36 individual CesA proteins (Somerville, 2004; Crowell et al., 2009; Gutierrez et al., 2009; Newman et al., 2013). Multiple *CesA* genes are present in genomes of higher plants, ten in the case of Arabidopsis (*CesA1 - CesA10*) and distinct CesA proteins typically form a functional rosette complex (Taylor, 2000). Regarding CesA subcellular localization, many fluorescent protein fusion studies and immunological data demonstrate CesAs to be localized to subcellular compartments and to be transported to the plasma membrane via CesA-containing vesicles named Microtubule-Associated Cellulose Synthase Compartments (Crowell et al., 2009) or Small CesA-containing compartments (Gutierrez et al., 2009).

In the case of GSLs it remains unclear whether they act in complex like CesAs do, and if so, to what extent and whether these complexes are homo- or hetero-oligomeric. Verma and Hong (2001) proposed a model of a putative callose synthase complex, in which GSLs interact with UDP-glucose transferase, annexin, sucrose synthase and monomeric GTPase. And there are likely other accessory proteins interacting with the callose synthase complex, plausibly tissue-specific. This might be the case of the cell plate-associated protein phragmoplastin, which was indicated to be part of the callose synthase complex in cytokinesis (Hong et al., 2001b), or monomeric GTPase RabA4c during pathogen attack, where GSL5 acts as its effector protein (Ellinger et al., 2014). Small GTPases might play a significant role in plant callose synthase regulation similarly as they do in yeast, where the addition of guanosine triphosphate is necessary for yeast 1,3-β-glucan synthase activity. In yeast, Rho1p GTPase was demonstrated to be one of the components of the 1,3-β-glucan synthase complex (Qadota et al., 1996). Accordingly in plants, ROP1 functions as a molecular switch controlling GSL6 activity via interaction with UDP-glucose transferase 1 (UGT1). Small GTPases could act as translators of spatial and temporal signals from upstream pathways to the callose synthase complex.

Another well known direct regulators of callose deposition and biosynthesis are calcium ions. External Ca^{2+} is essential for callose synthesis in many plants and the presence of $CaCl_2$ was shown to increase callose synthase activity by 50 times (Kauss, 1985; Kauss et al., 1990; Nedukha, 2015). For instance, increased levels of intracellular calcium enhanced callose production in the subintinal layer in the microspores (Nedukha, 2015; Parra-Vega et al., 2015). On the contrary, inhibition of callose synthase in Arabidopsis increased sensitivity to low Ca conditions, which resulted in necrosis, leaf expansion failure and reduced ectopic callose (Shikanai et al., 2020). These symptoms were more severe in case of *gsl10* mutant suggesting that *GSL10* is important for the alleviation of defects caused by the calcium deficiency. Although a substantial amount of data about role of calcium in callose regulation has been acquired, we still know surprisingly little about the mechanistic details of direct activation of callose synthases by Ca^{2+} on the plasma membrane and other aspects of their relation.

Observations from tobacco pollen tubes indicate that the putative callose synthase complex is presumably assembled in the endoplasmic reticulum (Cai et al., 2011), but the subsequent trafficking to the plasma membrane and its specific regulation remain to be elucidated, although fragmentary and inconclusive evidence is slowly emerging. Trafficking of GSL through trans-Golgi network was observed in Arabidopsis (Cai et al., 2011; Drakakaki et al., 2012) and transport via multivesicular bodies was recorded in barley (Böhlenius et al., 2010), which was supported by brefeldin A experiments blocking callose deposition in Arabidopsis leaves upon fungal attack (Nielsen et al., 2012). Additionally, vesicle-like bodies were reported to translocate GSL5 from the plasma membrane to the pathogen attack penetration sites, where fluorescently tagged GSL5 was detected in bodies via confocal microscopy, suggesting exosome-based transport of the enzyme (Ellinger et al., 2013).

1.4 Silica in plant cell walls

Silicon is a ubiquitous soil element with well-known beneficial effects in agricultural applications (enhancing growth and yields, chiefly under stress) and with increasing evidence in the literature of its phytoprotective roles. The underlying mechanisms of silica influence on plant physiology and metabolism have been the subject of vast research and discussions till today, yet they still remain undefined and debated (Coskun et al., 2019; Exley and Guerriero, 2019). Silica has been suggested to improve mechanical strength of aerial parts of the plant body and to promote protection against various diseases and exogenous stresses, including plant pathogens (viruses, fungi, bacteria and herbivores), metal toxicities, drought and salinity stress, and temperature extremes (Epstein, 2001; Epstein, 2009; Luyckx et al., 2017). Weathering of siliceous minerals produces monosilicic acid ($Si(OH)_4$), which is the only form of silicon taken up from the soil by plants (Mitani et al., 2005). Monosilicic acid is transported upward in the water-conducting tissues to a final destination (sink), where high concentrations of polysilicic acid induce further polymerization process. This step is irreversible and produces non-crystalline and non-birefringent amorphous silica gel of polysilicic acid (Kaufman et al., 1981). In the extracellular matrix, silica forms complexes with several plant cell wall components and causes crosslinking of cell wall polymers, resulting in cell wall reinforcement similar to lignin in lignified walls (Currie and Perry, 2007).

1.4.1 Silica uptake and deposition

The mechanisms and capability of silica uptake and accumulation significantly differ between plant species and particular genotypes. Monocots are known silica hyperaccumulators, in some cases reaching up to 10 % of silica in dry weight, while the majority of dicots contain less than 0.1 % (Epstein, 1994). The greater part of silica content is located in the stem and only small amounts polymerize in the root tissues. Typical sites of silica accumulation are cell walls, cell lumens and intracellular spaces (Sangster et al., 2001).

Structural and chemical mechanisms of silica deposition at the single-cell level are still a topic of debates with two scenarios being repeated - passive and active. The passive deposition is described as a spontaneous process tightly linked to transpiration, which by dehydration causes the condensation and precipitation of silicic acid. The active way of silica deposition comprises biological factors which catalyze the process of silicification. Due to different and sometimes contradictory results coming from diverse species and cell types, there is no simple and universal mechanism for silica deposition. Initial knowledge of silica uptake mechanisms came out from the research of marine diatoms; nevertheless, silica absorption in higher plants differs significantly. The first evidence of silica active transport in plants came from rice, where a silica transporter from the aquaporin NIP (Nodulin-26 like Intrinsic Protein) subfamily was identified (Tamai and Ma, 2003; Ma et al., 2004) and until the present day, several members of NIP2 subgroup were proved to be active silica transporters in rice, named Low silicon rice - OsLsi (Ma and Yamaji, 2006; Ma et al., 2007; Yamaji et al., 2008). Other silica transporters have been identified in multiple species, for example in wheat (Grégoire et al., 2012; Montpetit et al., 2012; Deshmukh et al., 2013), horsetail (Grégoire et al., 2012), barley (Chiba et al., 2009; Yamaji et al., 2012), maize (Mitani et al., 2009), pumpkin (Mitani et al., 2011), soybean (Deshmukh et al., 2013) and cucumber (Wang et al., 2014). So far, no close functional homolog of the Low silicon rice genes has been found in the Arabidopsis genome, which is in accordance with its silica non-accumulating nature. However, Arabidopsis is still a convenient heterologous system or genetic model for studying silica transporters (Grégoire et al., 2012; Montpetit et al., 2012; Deshmukh et al., 2013).

1.4.2 Biosilica formation mechanisms

The process of $Si(OH)_4$ precipitation in organic environment is termed biosilicification and seems to be affected by a broad field of factors, including silica concentration, temperature, pH and presence of several biomolecules. As possible cell wall macromolecules with silicification-catalyzing abilities were identified, for example, polysaccharides, lignin, other phenylpropanoids, proteins, lipids and ions. Many different biomolecules, mostly cell wall components, have been shown as possible templating factors for silica polymerization in plants and an increasing number of *in vitro* and *in vivo* studies bring examples of specific cell wall components with an effect on biosilica formation. Silica was found to bind to hemicelluloses in rice suspension culture (He et al., 2013a) and it was also shown to associate with pectins (Gierlinger et al., 2008; Leroux et al., 2013), lignin and some polyphenolic compounds (Inanaga et al., 1995; Watteau and Villemin, 2001; Fang and Ma, 2006). In addition, it was speculated that mixed-linkage (1-3,1-4)-β-D-glucans might potentially be a functional environment for silica condensation in horsetail (Fry et al., 2008), which was later confirmed in rice (Kido et al., 2015).

1.4.3 Relationship between silica and callose

The first evidence of callose-driven biosilicification was experimentally established in a well-known silica hyperaccumulator, *Equisetum arvense*. Work of Law and Exley (2011) showed that foci of callose deposition copied/mimicked the sites of silicification; and their *in vitro* assay demonstrated the ability of callose to promote $Si(OH)_4$ precipitation from an undersaturated solution of silicic acid. This was later supported by analogical data in hydroponic studies of Arabidopsis (Brugiére and Exley, 2017), where the induction of callose synthesis by overexpression of GSL5 callose synthase generated more intense biosilica accumulation in the leaf tissue, while *gsl5* mutants practically lacked callose and accordingly deposited less silica. This data has been confirmed by pathogen assays and trichome cell wall stainings where callose deposition was also conditional for consequent silica deposition, demonstrating the link between callose synthesis and silica deposition.

1.5 Exocyst complex in plant polarity and cell wall biogenesis

The transition of plants to the land and their sessile life strategy provoked plenty of evolutionary novelties which modulated plants into the form we know nowadays. Precisely coordinated polarity at the level of organs, tissues, cells and organelles is one of the basic ingredients in the plants' success in the battle of life in a constantly changing environment full of mobile predators and continuously evolving pathogens. Specifically polarized secretion enables important functional and spatiotemporal regulation and plasticity within one cell, provided mainly by targeted transport of cargos to the selected destination in correct amount and timing. The final destination of the cargo is defined by many aspects of the secretory machinery and tethering protein complexes are one of them. They attach the vesicle membrane in close proximity to the target membrane and thus facilitate subsequent steps of fusion. Particular destinations are operated by different multisubunit tethering complexes (Koumandou et al., 2007; Klinger et al., 2013; Vukašinović and Žárský, 2016), namely Transport protein particle (TRAPP) I–III, Golgi-associated retrograde protein (GARP) and endosome-associated retrograde protein (EARP) complexes, conserved oligomeric Golgi (COG) complex, class C core vacuole/endosome tethering (CORVET), homotypic fusion and protein sorting (HOPS), depends on SLY1-20 (Dsl1) and the exocyst. Polar secretion of post-Golgi vesicles through the conventional secretory pathway to the plasma membrane is executed by the exocyst complex (He and Guo, 2009; Zhang et al., 2010). Evolutionarily conserved across eukaryotes, it was first described in yeast, where it was originally identified and broadly studied in budding processes (TerBush et al., 1996; Guo et al., 1999). It is a large complex with eight conserved subunits - Sec3, Sec5, Sec6, Sec8, Sec10, Sec15, Exo70, Exo84 (TerBush et al., 1996). In yeast and animals there is commonly but not always only one copy of each subunit in the genome (Martin-Urdiroz et al., 2016).

1.5.1 Multiplication of EXO70 subunit in land plant genomes

Land plants' genomes usually contain several paralogs of the exocyst subunits (Elias et al., 2003; Cvrčková et al., 2012). In the case of the core subunits (SEC6, SEC8, SEC10) plus SEC3 and SEC5, none or only a few duplications occurred (single or low copy subunits), whereas in the case of SEC15, EXO70

and EXO84 multiple duplications resulted in families with several, sometimes numerous isoforms (Cvrčková et al., 2012). This phenomenon is significant and seems to be evolutionarily connected with the transition of plants to the land.

The most prominent multimerization was detected in the case of the EXO70 subunit with several dozens of paralogs per genome, resulting in for example 23 isoforms in Arabidopsis (Synek et al., 2006). This considerable genomic EXO70 multiplicity was proposed as the possible basis for the establishment and organization of distinct recycling domains within one cell (Zárský et al., 2009; Zárský and Potocký, 2010). However, no evidence was given for a long time that the EXO70 proteins are functionally distinct or that they possess the capacity to decorate different membranes within a single cell.

Divergent membrane lipid-binding properties were suggested as a possible mechanism for EXO70 specificity to different membrane domains. Interactions of proteins and membrane phospholipids are of substantial importance for plant cell polarity establishment and membrane trafficking regulation (Sekereš et al., 2015) and it has been already shown in yeast and mammals that a specific interaction of the Exo70 C-terminus with phosphatidylinositol 4,5-bisphosphate is responsible for the targeting of the exocyst complex to the plasma membrane (He et al., 2007; Liu et al., 2007). The first evidence of EXO70 paralogs preference to different plasma membrane domains and phospholipids within one cell was demonstrated in *Nicotiana tabacum* pollen tube on NtEXO70A1 and NtEXO70B1 (Sekereš et al., 2017), but the particular phospholipids to which most of the plant EXO70 subunits bind remain unexplored.

Functional specialization of diverse EXO70 paralogs seems very probable and coevolution with pathogens was suggested as its substantial driving force (Žárský et al., 2019). Current state of knowledge about EXO70 subunits in plants, focusing on Arabidopsis, was summarized in a review included in this thesis - Article 4 (Žárský et al., 2019).

1.5.2 Exocyst complex and its role in secondary cell wall formation

The exocyst complex has been already implicated in SCW development and to briefly summarize its mode of action in SCW formation, data from CesA secretion, tracheary elements, seed coats and Casparian strip formation should be discussed. The exocyst was previously proposed to contribute to the secretion of CSCs to the plasma membrane (Bashline et al., 2014; Vukašinović et al., 2017). Indeed, this was later corroborated by reporting its role in *de novo* secretion of CesAs to discrete loci of the plasma membrane in cooperation with protein CELLULOSE SYNTHASE INTERACTING 1 and plant specific protein PATROL 1 (Zhu et al., 2018).

Various studies have disclosed the exocyst complex function in MT-dependent xylem formation (Li et al., 2013; Oda et al., 2015; Vukašinović et al., 2017). MT-dependent localization of the exocyst subunits was documented using Arabidopsis VASCULAR NAC DOMAIN 7 tracheary element inducible system (Vukašinović et al., 2017). The study showed exocyst-mediated trafficking in a developing tracheary element and the contribution of the EXO70A1 paralog to localized secretion of the SCW material. SCW deposition was impaired in tracheary elements of exocyst mutants probably due to mislocalization of cellulose synthase.

The exocyst's contribution to seed coat deposition was manifested by defects in pectin coat structure in *sec8* and *exo70A1* mutants, which had mis-localized deposition of pectinous mucilage in seed coat volcano cells (Kulich et al., 2010). It is not exactly like the SCW deposition, as seed pectinous mucilage is delivered into the apoplastic space between primary and secondary cell walls, but it is still a good example of the exocyst role in polarized and highly specialized cell wall morphogenesis.

The ring-like Casparian strip in root epidermis is a great illustration of a polarized SCW structure and its precise localization is known to be defined by CASPARIAN STRIP MEMBRANE DOMAIN PROTEINS (CASPs). Recently, EXO70A1 was identified as the crucial component for proper Casparian strip formation, because depletion of *exo70A1* leads to disruption of CASPs localization into random microdomains but does not affect CASPs secretion (Kalmbach et al., 2017). Thus, the EXO70A1 was deduced to sustain spatially coordinated CASP protein localization, which is later translated into precise deposition and modification of the Casparian strip.

1.5.3 Involvement of exocyst complex in establishment of polar membrane domains

Information about the underlying mechanisms of the maintenance of asymmetric protein allocation at distinct membrane domains is increasing and it seems clear that several cellular processes might be involved. A combination of reduced lateral diffusion of the proteins within the membrane and a spatially defined polar exocytosis and selective endocytosis were proposed formerly (Kleine-Vehn et al., 2011; Martiniere et al., 2012). Typical domain polarities in plant cells are apical-basal and inner-outer lateral polarity and thus at least four domains with a specific composition and function likely coexist within one cell (Zárský et al., 2009; Alassimone et al., 2010; Roppolo et al., 2011).

A well-established model for membrane polarization are the PIN-FORMED (PIN) auxin efflux carriers in the root. Their characteristic polar localization is crucial for spatial regulation of auxin transport (Kleine-Vehn et al., 2011; Łangowski et al., 2016). In root epidermis, which represents the interface between the root and the soil, distinct intracellular distribution of proteins is also critical for dealing with entirely different functions of inner and outer region of the cell (Langowski et al., 2010). Root epidermis is also a great model cell type with localized plasma membrane microdomains, where precise localization of CASP proteins into a ring-like microdomain enables polarized deposition of SCW to form diffusion barrier called the Casparian strip (Alassimone et al., 2010; Roppolo et al., 2011). Distinct membrane domains have also been identified in pollen tubes. There, the plasma membrane domains of active endocytosis and exocytosis are well separated (Derksen et al., 1995; Moscatelli et al., 2007; Bove et al., 2008). A similar situation was described in another cell type with tip growth - root hairs, where the apical zone, sub-apical zone, and shank are distinguished (Cole and Fowler, 2006). Further examples can be found in structures polarly formed in response to pathogens (Dörmann et al., 2014).

Diversification of EXO70 subunit genes and a demand for operating different cortical domains together indicate a possible role for different EXO70 paralogs in the coordination of polar secretion into distinct docking platforms in a single cell. A variety of other players from the secretory machinery might be involved in orchestrating these processes, like Rab GTPases, SNARE protein isoforms and several types of recycling endosomes along with a dynamic crosstalk between proteins and membrane lipids (Zárský et al., 2009; Sekereš et al., 2015).

In support of this hypothesis, first evidence of such specific domain localization of EXO70s now starts to appear. EXO70B1 was shown to localize to internal compartments instead of the plasma membrane and to colocalize with the autophagosomal marker within the vacuole upon treatment with concanamycin A (Kulich et al., 2013). EXO70A1 accumulates transiently in the central endodermal plasma membrane, where it determines the position of the Casparian strip (Kalmbach et al., 2017). In *Medicago truncatula* EXO70I was shown to operate in arbuscular mycorrhizal symbiosis, where it is necessary for the creation of a subdomain of the periarbuscular membrane (Zhang et al., 2015).

At this moment, however, simultaneous visualization of multiple EXO70 paralogs within a single cell is necessary. First such evidence comes from tobacco growing pollen tube, exhibiting distinct localization of NtEXO70A1 and NtEXO70B1 into mutually exclusive domains of the plasma membrane (Sekereš et al., 2017). This study also revealed unequal colocalization of NtEXO70A1 and NtEXO70B1 with markers of plasma membrane phospholipids (phosphatidic acid and phosphatidylinositol 4,5-bisphosphate). Our work brings additional confirmation of such membrane domain differentiation and of distinct preferences of EXO70 paralogs for these membrane domains.

2 Aims of the thesis

The research communicated in this thesis is based on previous results of our laboratory and follows my investigations presented in my Master's thesis. There I already worked on the EXO70H4 subunit of the exocyst complex and described the lack of SCW formation in trichomes of the *exo70H4* mutant. The formation of the SCW in general is an unexploited topic and thus we decided to use the comparison of Arabidopsis wild type trichomes with *exo70H4* mutant trichomes as a suitable model for unraveling its mechanisms. Our hypotheses were formulated and gradually updated based on the successive findings. We have aimed to address the following fundamental biological questions.

2.1 Biological question 1

As EXO70H4 is one of the most upregulated transcripts in the Arabidopsis trichome (Jakoby et al., 2008), is it indispensable for the trichome development?

Subqueries

Does mutation of *EXO70H4* affect the development of trichome shape? To which part of trichome development does EXO70H4 contribute the most? Is the UV upregulation known from the literature biologically relevant (Oravecz et al., 2006)?

2.2 Biological question 2

How does EXO70H4 contribute to polarized delivery of SCW components in trichome?

Subqueries

What cell wall components are deposited in an EXO70H4-dependent manner? Is EXO70H4 necessary for callose synthase delivery in the trichome?

2.3 Biological question 3

Is the function of EXO70H4 unique and different from other EXO70 paralogs?

Subqueries

Are different EXO70 paralogs functionally redundant or do they cover different functions? Do EXO70 paralogs function differently in specialized cell types by recruiting the exocyst subunits into specific endomembrane recycling domains? Do other EXO70 paralogs localize the same as EXO70H4 or differently in the trichome?

2.4 Biological question 4

Is there a distinct distribution of plasma membrane lipids and EXO70s in the trichome cell?

Subqueries

What is the phospholipid composition of the plasma membrane in the trichome? Are there any specific phospholipid domains formed? Which phospholipids interact with EXO70H4? Do EXO70 paralogs differ in phospholipid binding preferences? What is the relationship between EXO70H4 localization and the formation of plasma membrane lipid domains?

3 Article summary

The first and the second article was published under my maiden name - Vojtíková, the third and the fourth publication was published under my married name - Kubátová.

3.1 Article 1: Cell Wall Maturation of Arabidopsis Trichomes Is Dependent on Exocyst Subunit EXO70H4 and Involves Callose Deposition

Ivan Kulich*, **Zdeňka Vojtíková***, Matouš Glanc, Jitka Ortmannová, Sergio Rasmann, Viktor Žárský
Published in May 2015. DOI: https://doi.org/10.1104/pp.15.00112

My contribution: participation in construct preparation and transformation; aniline blue staining, measurements and quantification; cell wall thickness microscopy; yeast two hybrid experiments; ectopic cell division study;

In wild type trichome we described SCW deposition and maturation process specific for apical trichome domain. Besides, our study resulted in the characterization of cell wall structural component named the Ortmannian ring, which is formed on the bottom edge of the apical domain and seems to act as the border-defining element. Both EXO70H4-dependent processes of SCW thickening and the Ortmannian ring biogenesis are strongly stimulated by UV-B irradiation. Additionally, we detected that apical SCW of mature trichome contains autofluorescent (probably phenolic) compounds and a considerable amount of callose microdomain accumulations. Callose is secreted there in a strikingly patterned manner and it is definitely not a wounding callose, but rather an example of a previously neglected developmental callose deposition event. All these wild type trichome characteristics are impaired in the *exo70H4* mutant. Trichomes of *exo70H4* mutants lack the SCW apical domain, because its secretion is EXO70H4-dependent and so cell wall autofluorescence is significantly decreased in the mutant and callose is not deposited at all or in a very random pattern.

---

* These authors contributed equally to the article.

3.2 Article 2: Exocyst Subunit EXO70H4 Has a Specific Role in Callose Synthase Secretion and Silica Accumulation

Ivan Kulich*, **Zdeňka Vojtíková***, Peter Sabol, Jitka Ortmannová, Vilém Neděla, Eva Tihlaříková, Viktor Žárský
Published in March 2018. DOI: https://doi.org/10.1104/pp.17.01693

My contribution: construct preparation and transgenic line preparation; measurement quantification; data validation; cross-complementation study (cloning, transformation, selection, microscopy, figure preparation); overview of EXO70 paralogs localization in the trichome; aniline blue stainings; help with manuscript preparation and editing;

Confocal microscopy of fluorescently tagged EXO70H4 constructs revealed localization strikingly resembling the callose pattern. EXO70H4 also localized into microdomains in the apical domain of the plasma membrane, cell wall ingrowths and the Ortmannian ring. And since other selected exocyst subunits localized in a similar way and colocalized with EXO70H4 signal, we concluded that the EXO70H4 paralog indeed acts as part of the exocyst complex in trichome SCW polarized secretion. To address the functional specificity of the EXO70H4 paralog, we performed a cross-complementation experiment of the *exo70H4* mutant phenotype with 18 selected Arabidopsis EXO70 paralogs under the EXO70H4 promoter. Unexpectedly, only EXO70H4 itself was able to complement the *exo70H4* mutation phenotype, while no other EXO70 paralog complemented the phenotype even partially. Thus, the function of EXO70H4 seems to be substantially unique, being a reliable evidence for EXO70 paralog functional diversification.

Since EXO70H4 localization resembled to a great extent the callose deposition pattern, we started to unveil feasible connection between the callose synthase secretion and the exocyst complex. Indeed, we discovered colocalization of fluorescently tagged EXO70H4 with GSL5 and GSL10 constructs in microdomains in the apical part of the trichome. Also, we showed impaired GSL5 secretion into the plasma membrane in *exo70H4* background and thus our results establish the exocyst as an important player in oriented callose synthase delivery to the plasma membrane. The exocyst had already been speculated to operate in the delivery of CSCs to the plasma membrane (Bashline et al., 2014), and recently it was indeed reported in control of *de novo* secretion of CSCs to the plasma membrane (Vukašinović et al., 2017; Zhu et al., 2018). Our work resulted in the discovery of such a relation between the exocyst and the delivery of callose synthase to the plasma membrane in Arabidopsis.

Using energy-dispersive X-ray microanalysis we reported a high content of silica in the wild type trichome, while no silica was detected in *exo70H4* nor the *gsl5* mutant trichome. Because the *exo70H4* mutant is deficient in callose secretion but not in its biosynthesis, while the *gsl5* mutant has impaired callose biosynthesis but not delivery, it implicates that both delivery and biosynthesis are essential for the silicification of the cell wall.

---

* These authors contributed equally to the article.

3.3 Article 3: *Arabidopsis* Trichome Contains Two Plasma Membrane Domains with Different Lipid Compositions Which Attract Distinct EXO70 Subunits

Zdeňka Kubátová, Přemysl Pejchar, Martin Potocký, Juraj Sekereš, Viktor Žárský and Ivan Kulich
Published in August 2019. DOI: https://doi.org/10.3390/ijms20153803

My contribution: construct preparation and transformation; majority of the experiments; validation of the data from confocal microscopy; trichome ontogenesis observations; over-expression study (cloning, transformation, selection, microscopy, figure preparation); interpretation of the data; original draft preparation; manuscript editing and final compilation; preparation of figures for the manuscript;

We revealed the formation of two distinct plasma membrane domains with dissimilar lipid composition. Briefly, the apical domain accumulates phosphatidic acid and phosphatidylserine, while the basal domain is enriched in phosphatidylinositol 4,5-bisphosphate. A clear border between these two plasma membrane domains is depicted by the Ortmannian ring, which is also rich in phosphatidic acid and phosphatidylserine but depleted of phosphatidylinositol 4,5-bisphosphate. Such a sharp borderline is missing in the *exo70H4* mutant, where apical-basal polarity of the plasma membrane domains is preserved only partially and the basal domain seems to spread upwards into the apical domain.

By transmission electron microscopy we examined the identity of microdomains observed in the apical SCW of wild type trichome. These microdomains or ingrowths were nicely visible in aniline blue callose staining and with fluorescently tagged plasma membrane proteins, which seemed to be entrapped in them. Transmission electron microscopy images indeed revealed membranous structures captured inside the cell wall. These pockets apparently were of cytoplasmic origin but often fully detached from the cytoplasm.

Biological function, relevance and potential impact of these findings on prospective research will be discussed below.

3.4 Article 4: Three subfamilies of exocyst EXO70 family subunits in land plants: early divergence and ongoing functional specialization

Viktor Žárský, Juraj Sekereš, **Zdeňka Kubátová**, Tamara Pečenková, Fatima Cvrčková
Published in October 2019. DOI: https://doi.org/10.1093/jxb/erz423

My contribution: participation in the writing and editing of the manuscript (mainly EXO70H4 paragraph and EXO70H chapter); Table 1. assembly; final compilation and formatting;

The first comprehensive review about EXO70 paralogs in plants. It focuses on phylogenetics, evolutionary aspect of the topic and summarizes so far revealed biological functions of different EXO70 paralogs.

— The aforementioned publications are listed at the end of the thesis (Published articles).

4 Unpublished data

4.1 Hydrogen peroxide is almost absent from the cell walls of *exo70H4* trichomes

Arabidopsis trichomes were tested for the presence of hydrogen peroxide (H_2O_2), one of reactive oxygen species. Rosette leaves were subjected to the *in situ* detection of H_2O_2 by staining with 3,3'-diaminobenzidine (DAB) according to the protocol of Daudi and O'Brien (2012). H_2O_2 oxidizes the DAB and generates dark brown precipitates by which the presence and distribution of H_2O_2 can be detected in plant cells. This method is suitable also for cell walls of Arabidopsis trichomes and it displayed H_2O_2 accumulation in the apical cell wall of mature trichomes.

The brown precipitate was mainly formed in the shape of a wide band at the bottom of the apical domain, just above the Ortmannian ring (Fig. 1 a); sometimes it blurredly diffused upwards through the stalk (Fig. 1 b) and sometimes both patterns combined (Fig. 1 c). Interestingly, unlike in the case of callose, deposition in the form of rings or dots was not observed, only the pattern of bands was formed. Brown precipitate staining was not present in all wild type trichomes and the percentage of positive trichomes varied during several repetitions. No decisive factor responsible for that has been identified yet. The highest number of stained trichomes was found at the distal part of the leave, where the trichomes are older on average.

Nothing like the bands seen in wild type trichomes was detected in *exo70H4* trichomes and most of the trichomes totally lacked DAB precipitates in their cell walls (Fig. 1 d). Sporadically, DAB precipitates were formed at the branch tips of trichomes in certain areas of the leaf (Fig. 1 e, f). These results suggest that EXO70H4 may be directly or indirectly involved in the production of H_2O_2 in trichomes.

Figure 1

Hydrogen peroxide accumulation in wild type and *exo70H4* trichomes

Staining with 3,3'-diaminobenzidine displayed brown precipitates declaring presence of hydrogen peroxide in the apical domain of the wild type trichomes above the Ortmannian ring (a, b, c) and its absence in *exo70H4* mutant (d) or occasional staining of *exo70H4* branch tips (e, f). Scale bars are 20 µm long.

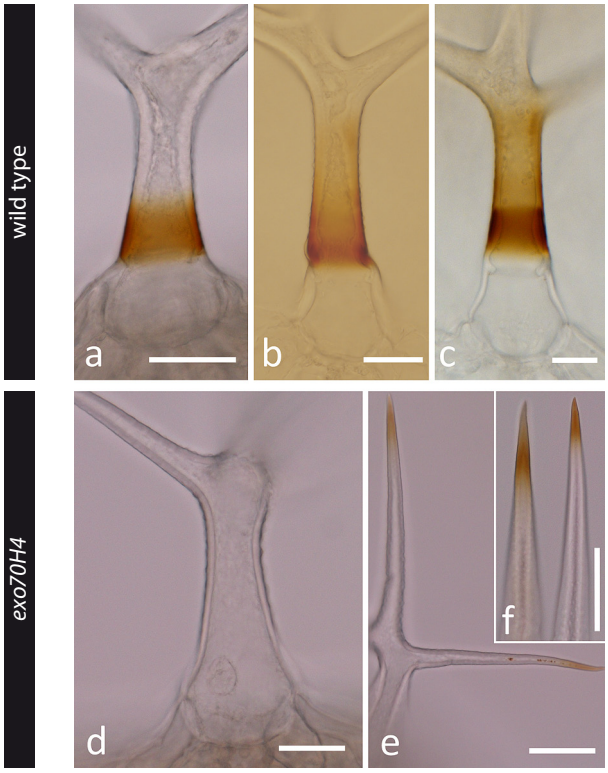

4.2 Cadmium and zinc accumulation in wild type and *exo70H4* trichomes

Wild type and *exo70H4* mutant plants were watered with 1 mM $ZnCl_2$ or 1 mM $CdCl_2$. Control sets of plants were irrigated with water or a 1 mM solution of KCl. Rosette leaves of 3-week-old plants were stained for the presence of metals by diphenylthiocarbazone (dithizone) (Seregin and Ivanov, 1997). This compound is highly sensitive to several metal ions like cadmium, lead, zinc, copper, nickel and others; and it forms colored complexes with them (Sandell, 1945). The color of the precipitate depends on the particular metal.

In the wild type trichomes, strong zinc and cadmium deposition was detected in the apical cell wall of trichomes in plants irrigated with metal-containing respective metal solutions. Plants watered with 1 mM $ZnCl_2$ exhibited intense pink precipitates of dithizone complexes with zinc. Correspondingly, plants watered with 1 mM $CdCl_2$ displayed orange precipitates of cadmium-dithizonate complex but to our surprise also pink precipitates of zinc-dithizonate complex, however much weaker than in $ZnCl_2$ experiment. Control sets of plants also contained this weak pink signal for the presence of zinc, but did not display the orange signal for cadmium. We explained that by common zinc contamination from the soil or tap water. Control plants, watered with the solution of 1 mM KCl, did not display any significant differences in overall growth or in trichomes in comparison to the water control and the metal-treated plants, ruling out a possible general effect of ionic stress.

Typically, rings and bands were stained at the bottom of the apical domain of the wild type trichome cell wall (Fig. 2 a, b) and sometimes a diffused coloration of the stalk or of the whole apical part was visible. In the *exo70H4* mutant, no staining was observed in trichomes (Fig. 2 c, d), suggesting that mutant trichomes fail to function as a sink for metal deposition or that EXO70H4 has a putative role in the delivery of metals to the cell wall, which is disturbed in the mutant.

Figure 2

Zinc and cadmium accumulation in wild type and *exo70H4* trichomes

Plants watered with 1 mM $ZnCl_2$ (left column) or 1 mM $CdCl_2$ (right column) were stained with diphenylthiocarbazone for presence of zinc (pink) and cadmium (orange). Deposits of metals were detected in the apical domain of the wild type trichome cell wall above the Ortmannian ring - zinc (a), cadmium (b). Such deposits were absent in *exo70H4* trichomes (c, d). Scale bar is 20 µm long.

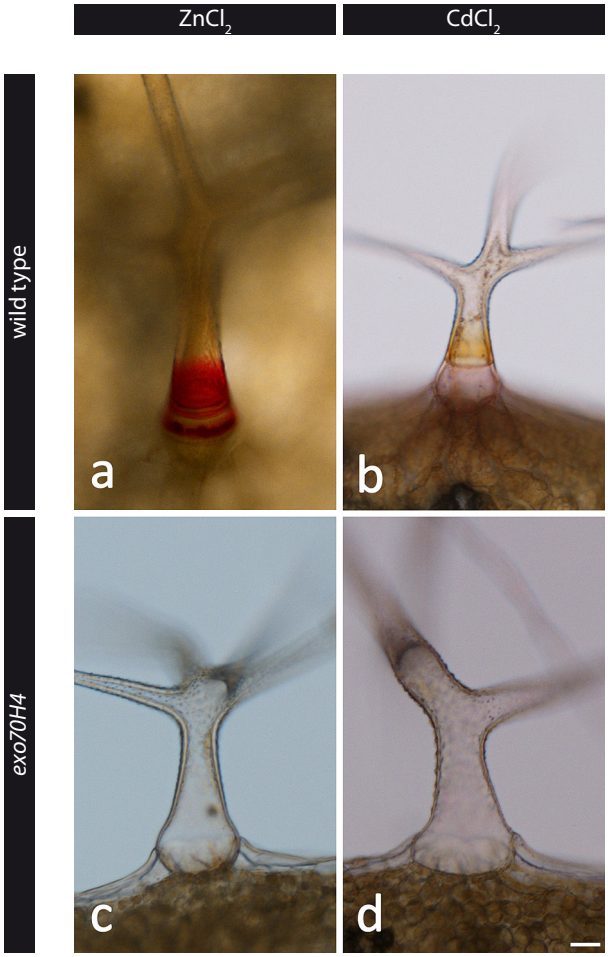

5 Discussion

Over the years our attention focused on the EXO70H4 paralog, the 11th most up-regulated gene in the mature trichome (Jakoby et al., 2008). Our work on trichomes led to description of two different domains within one cell and of a substantially delineated border in between them - the Ortmannian ring. While a basic characterisation of these structures has been done, we are just starting to unravel the molecular mechanisms of their establishment and the biological function of this impressive cellular polarization.

5.1 Causalities between the Ortmannian ring development and trichome membrane domain formation

The establishment of the Ortmannian ring represents a significant and easily quantifiable aspect of trichome cell wall maturation. Our understanding of its proper function and causality of its origin is still poor, despite the obtained data. We cannot clearly decide whether the formation of the Ortmannian ring is the cause of the domain separation or rather its consequence. One possible explanation is that it defines the borderline between the domains prior to their arrangement. Alternatively, it simply contributes to the preservation of already organized domains or perhaps it is only a side product of some process involved in domain organization or of some process going on in the apical domain and as such it would not be essential for domain separation. All these possibilities should still come into consideration. Very plausibly it is a result of two concurrently running developmental programmes of the reinforcement of the upper and lower cell wall domains in the trichome.

Studying domain establishment in the context of trichome ontogenesis could bring the desired explanation. Neither plasma membrane domains (as defined by lipid composition and EXO70 binding - Kubátová et al., 2019), SCW domains nor the Ortmannian ring are yet formed at stage 4 (elongation), when branches have already been founded, extensively elongating until the trichome reaches its final shape at stage 5 (extension). However, it is clear from the ontogenetic stages of trichome initiation and development that the basal (immersed in the epidermis) and apical (protruding from the epidermis) domains of the trichome are initiated and start to develop between stage 1 (endoreduplication and radial cell expansion) and stage 2 (emergence of the trichome from the plane of the leaf (Hülskamp, 2004). Hence the plasma membrane domains related to the SCW biogenesis form at some point between the fifth and sixth stage from the pre-existing basal and apical domains and a more exact resolution is necessary to distinguish what comes first - either the boundary or the domain gradient. To conclude, only very limited information is available regarding the exact biological function of the Ortmannian ring. Apparently, it could be a physical barrier initiated and accumulated at the junction between apical and basal domains at the stage of SCW deposition. If so, it needs to be tested whether it fully separates the apical and basal cell wall and whether it also restricts lateral mobility of the plasma membrane proteins.

5.2 Significance of plasma membrane lipid composition for binding of different EXO70 paralogs

A specific lipid composition and the role of particular phospholipids in distinct microdomains is quite a fresh topic in plant cell biology and our understanding of how such membrane polarity is established, regulated and maintained remains poor. Phosphatidylinositol phosphates represent less than one percent of membrane lipids; nevertheless, they are highly important for signalling, regulation of all membrane trafficking events and protein recruitment and activation. Recognition of their complex subcellular localization is thus of utmost importance.

5.2.1 Polarized distribution of phosphatidylinositol phosphates

Our study of phospholipid markers in the mature trichome discovered a strong polarization of some plasma membrane phospholipids. Phosphatidic acid (PA) marker was strongly accumulated in the apical domain while phosphatidylinositol 4,5-bisphosphate (PIP_2) marker was found exclusively at the basal domain.

An additional example of PIP_2 and PA separation was formerly described in growing tobacco pollen tubes (Potocký et al., 2014). That study showed PA marker to localize into a belt-like pattern in the subapical region of the plasma membrane, right behind the tip of the growing pollen tube. Conversely, PIP_2 maximum was established at the tip of the growing pollen tube and markers of PIP_2 and PA overlapped partially at the border of apical and subapical zone and this overlap defines possibly yet another functional domain. The functional relevance of these three domains in the pollen tube is not clear, but several lines of evidence point to the role of PA/PIP_2 and PA-rich domains in clathrin-mediated endocytosis and that of the PIP_2 domain in exocytosis. Interactions of PIP_2 (Martin, 2015) and PA (Liu et al., 2013) with several components of both exocytotic and endocytotic pathways were identified previously in Opisthokont models. In the growing pollen tube, plenty of membrane material is secreted during the build-up of a new cell wall and excess membrane is recycled by accurate regulation of endocytosis, including clathrin-mediated endocytosis which takes place behind the apex (Bove et al., 2008). The zone of clathrin-mediated endocytosis overlaps with PA/PIP_2 and PA-rich regions and thus PA was speculated to function as a putative regulator of clathrin-mediated endocytosis machinery in growing pollen tubes (Potocký et al., 2014). Interestingly, it was also previously implicated in clathrin-mediated endocytosis regulation in mammals (Antonescu et al., 2010). Mechanically, PA with its small polar head group spontaneously induces the negative membrane curvature (Kooijman et al., 2005), enabling the formation of vesicles or protrusions.

Based on this data it is feasible that a similar regulation of the plasma membrane area might take place during the thickening of the trichome apical SCW, where large amounts of cell wall material has to be deposited, much like in the pollen tube. Thereby, strong PA marker accumulation at this region indirectly points to clathrin-mediated endocytosis as another important process in trichome SCW deposition, which has not been studied yet. Moreover, an absence of PIP_2 from the apical trichome domain implies its dispensability for EXO70H4-dependent cell wall thickening in the trichome maturation.

Polarized distribution of plasma membrane phospholipids depends on phosphoinositol-converting enzyme localization and activity (Heilmann and Heilmann, 2015). These have not been studied in the trichome yet, deserving more attention in the near future.

5.2.2 Distinct preference of EXO70 paralogs for binding to phosphatidylinositol phosphates

In addition to phospholipid polarization, we found a remarkable polarization of distinct EXO70 paralogs in the trichome. In our ectopic expression study we took representative EXO70 paralogs from different families and expressed them under the EXO70H4 promoter in the trichome. The majority of them remained cytoplasmic, but some of them localized to the plasma membrane or one of its domains. Particularly EXO70H8 hyper-accumulated in the apical PA-rich domain, similar to EXO70H4, while EXO70A1 (weakly also EXO70A2) labeled mainly the basal PIP_2-rich domain. From yeast and mammals it is known that the EXO70 subunit directly binds PIP_2 (He et al., 2007; Liu et al., 2007). PIP_2 microdomains were thus proposed to be involved in exocyst regulation. A conserved PIP_2 binding site was indeed identified in the Arabidopsis EXO70A1 paralog (Zárský et al., 2009) and our data from its localization studies are in accordance with that. On the other hand, we brought evidence of different binding properties of other EXO70 paralogs, particularly EXO70H4 and EXO70H8, which bound to the PA-rich domain and not to the PIP_2-rich domain. This difference in lipid binding properties between EXO70H4 and EXO70A1 was confirmed by a lipid binding assay, where EXO70H4 indeed did not bind to PIP_2 but it did bind to phosphatidylserine and PA.

The only analogous result of distinct localization and phospholipid preference of distinct EXO70 paralogs was described in a study of natively expressed tobacco EXO70 paralogs in tobacco growing pollen tubes (Sekereš et al., 2017). There, NtEXO70B1 localized to the outer subapical region, while NtEXO70A1 localized to the near subapical region and these two domains were mutually exclusive. Interestingly, NtEXO70B1 colocalized with the marker of PA and also with a marker of clathrin-mediated endocytosis, suggesting the role of NtEXO70B1 in endocytosis rather than in exocytosis or in another process specific to this region. NtEXO70A1 localized to the overlapping region of PA and PIP_2 markers and not to the very apex, where only PIP_2 is present and so possibly localization of EXO70A1 demands the presence of both of them (Sekereš et al., 2017). This is in consistent with our results from mature trichome, where EXO70A1 accumulated mainly at the basal PIP_2 rich domain, which also labeled weakly with the PA marker. The fact that NtEXO70B1 was largely excluded from the pollen tube apical PIP_2-rich region coincides with EXO70H4 exclusion from the basal PIP_2-rich region in mature trichome. Interestingly, the GFP-EXO70B1 protein was cytoplasmic in the trichome, while being plasma membrane-bound in the adjacent epidermal cells. PA is abundant in both trichome and epidermal cells and therefore, other unknown factors (phosphorylation, interacting partners, etc.) contribute to the EXO70 localization. For instance, RPM1 INTERACTING PROTEIN4 (RIN4) has been recently shown to recruit EXO70B1 to the plasma membrane (Sabol et al., 2017) and it is downregulated in the trichome. Another factor in this mosaic could be the conditional binding of peripheral membrane proteins, because many proteins recognize several lipids instead of being specific to only one species and they also bind at the same time to activated small GTPases and other membrane proteins (Moravcevic et al., 2012; Pleskot et al., 2015). In any case, our data clearly show the influence of local distribution of specific phospholipids on the recruitment of EXO70 paralogs.

5.3 Role of callose in trichome development and implications for other epidermal cells

Callose deposition is a very prominent aspect of trichome maturation, yet, its biological relevance is not clear. As we have shown, callose is not required for secondary metabolite accumulation. It was, however, essential for cell wall silicification, which may be an indispensable cell wall maturation process for trichomes in other species as well, for instance in *Urtica dioica* with highly silicified trichomes. Indeed, trichomes of *Urtica dioica* also display large callose deposits.

5.3.1 Patterns of callose deposition in the apical domain of trichome secondary cell wall

Callose is deposited in intriguing patterns which might help us to discover its structural relevance. Despite overall high variability in callose patterns, three basic motifs appear and diversely combine - the Ortmannian ring, a wide callosic band and a pattern of speckles. The Ortmannian ring labels the lowest margin of the apical SCW domain, occasionally it is formed repeatedly one above another in one trichome cell and sporadically it is not present at all. The callosic band is usually formed in the zone above the Ortmannian ring in the middle of the stalk of the apical domain. As in the case of the Ortmannian ring, it is not always visible. The stippled callosic cell wall ingrowths spread downwards from the tips of the branches to the stalk up to the band or ring area, if the band is not present. Although trichomes with all three patterns formed are considered to be the most common, any combination of these patterns is possible. Sometimes only a single motif is formed or any combination of two of them. It varies even within trichomes on a single leaf. Underlying mechanisms and the reason for this patterning are unknown. The observations of the callose pattern variability may simply imply that the callose patterns develop in time. As callose is actively deposited by callose synthases and removed from the cell wall by β-1,3-glucanases (Levy et al., 2007), its localization may be different during different stages of development. Alternatively, callose patterns themselves may be a form of Turing patterns changing dramatically with a slight change of the external conditions.

5.3.2 Polymer network of callose and cellulose

In respect to callose synthase delivery and callose apposition to the cell wall, interesting findings have been published during the last years. The classical model of callose deposition in between the existing cellulose layer and the plasma membrane was recently shown not to be the only option. In Arabidopsis leaves attacked by powdery mildew, direct interaction of callose and cellulose at the sites of attempted fungal penetration was documented by super resolution fluorescence imaging methods (Eggert et al., 2014). Cellulose and callose form a polymer network there, and callose is deposited into the space between pre-existing cellulose fibrils through intramural nanopores in a gel-like form. Intriguingly, experiments with GSL5 overexpression led to an expansion of this cellulose-callose network and formation of a callose layer even beyond the cellulose layer (Eggert et al., 2014; Voigt, 2014). This indicates that callose deposition and organisation within the apical domain of a trichome can be even more complicated than it seems.

A recent study has demonstrated that the addition of callose increases cellulose resilience in high strain conditions by raising its plasticity or toughness and thus the ability of the cell wall to gradually deform rather than tear apart under such conditions (Abou-Saleh et al., 2018). These observations shed new light on the textbook definition of callose as an element of cell wall stiffness. Moreover, such an effect on the apical domain of the trichome could be important for the mechanosensing properties of the trichome discussed above.

5.3.3 Comparison of the trichome and defence papilla cell wall biogenesis

In our work, we have mostly focused on the role of EXO70H4 in the trichome cell wall biogenesis. However, we have accumulated some unpublished evidence that *exo70H4-1* mutants also differ in the fungal pathogen defence. Under control conditions, EXO70H4 is expressed exclusively in trichomes; nonetheless, according to our results the EXO70H4 promoter itself has the capacity to drive EXO70H4 expression also in other epidermal cell types and it can be activated upon pathogen attack. The epidermal activity of the promoter was shown by a green fluorescent protein (GFP) reporter assay, where EXO70H4p::GFP:GFP reporter construct displayed activity throughout the plant. A supporting line of evidence came from the expression of different GFP-EXO70 paralogs under the EXO70H4 promoter, which also resulted in a strong GFP signal in all epidermal cells. GFP-EXO70H4 localization under its native promoter is restricted to the trichome and can only be induced in other cell types 4 - 6 hours after treatment with flagellin peptide 22 (Kulich et al., 2018). Expression triggered by pathogen attack stimuli is not homogeneous across the epidermis, but rather mosaic within single cells with domains of strong signal. These domains develop cell wall autofluorescence similar to that of the apical cell wall of trichomes. On top of that, the composition of the pathogen-induced defensive papilla is very similar to trichome apical SCW. These defensive cell wall appositions are rich in callose, silica and autofluorescent phenolic compounds in the same way as the trichome apical SCW and so the possible role of EXO70H4 in defence against pathogens starts to be apparent. Such pathogen-driven EXO70H4 expression might be a part of the defensive cell wall biogenesis module. A similar module may be constitutively active in the trichome, rapidly forming the cell wall rich in phenolic compounds and callose. Callose deposition in defensive papillae would possibly act as a scaffold for silica accumulation, which thereafter enhances cell wall defence properties against fungal pathogen attack (Ghanmi et al., 2004; Fauteux et al., 2006; Vivancos et al., 2015).

Another indication of EXO70H4 contribution to defence against pathogens came from stomata, where thermal screening of Arabidopsis mutants identified EXO70H4 role in bacterial-specific stomatal response, possibly through regulation of callose deposition (Rodrigues Oblessuc et al., 2019). In this work *exo70H4-3* mutants suffered from an increased susceptibility to stomatal reopening by *Salmonella enterica* but not by *Pseudomonas syringae*. In their follow-up work these authors extended their study with *Escherichia coli* and showed that *exo70H4-3* has defective stomatal closure also after inoculation by these human enterobacteria (Oblessuc et al., 2020). In addition, they demonstrated that the role of EXO70H4 in the apoplast differs from that in stomata, because in mesophyll cells EXO70H4 contributes to the defence against *Salmonella enterica* and *Pseudomonas syringae*, but not *Escherichia coli* (Oblessuc et al., 2020). And lastly, since the inoculation of *exo70H4-3* mutant by any of the three bacteria tested resulted in a lower number of callose deposits in comparison to wild type, they suggested a contribution of EXO70H4 to the bacteria-induced callose deposition in Arabidopsis leaves (Oblessuc et al., 2020). Thus, it is not possible to simply restrict the biological role of EXO70H4 solely to the trichome.

5.4 Environmental reasons for the trichome cell wall heterogeneity

The existence of two or more plasma membrane or cell wall domains within one cell is one of plant cell polarization strategies and different EXO70s were previously proposed to operate in distinct domains within one cell (Zárský et al., 2009; Zárský and Potocký, 2010). The biological relevance of two distinct domains in the trichome needs to be explained. It probably enables the trichome cell to fulfill simultaneously two distinct but interdependent functions. The aerial part (apical) interacts with the environment and protects the plant both against physical and biotic adversities, while the basal part communicates with the plant and it is responsible for the supplementation of nutrients, material exchange and signal transduction. The apical part undergoes a substantial SCW thickening accompanied by deposition of callose and silica. The definition of exact biological functions of each domain is still at the beginning and we can only speculate based on the accessible data.

5.4.1 Cell wall phenolic compounds and UV protection

The functions of Arabidopsis trichomes have been enigmatic so far. There are, nevertheless, hints indicating their contribution to UV and herbivore protection (Yan et al., 2012). In accordance, transcription of EXO70H4 was indeed reported to be induced by UV-B light in a CONSTITUTIVE PHOTOMORPHOGENIC 1-dependent way (Oravecz et al., 2006) and down-regulated by methyl jasmonate (Hruz et al., 2008), a volatile plant defense hormone of the response to herbivores and wounding. The UV-B-induced EXO70H4 expression and apical domain SCW thickening (Kulich et al., 2015) indicate a possible role of the apical trichome domain in UV protection. Our speculation is that UV-protective properties of trichomes might be crucial for shoot apical meristem conservation. At the beginning of rosette development, young emerging leaves, already full of mature trichomes, form a hairy barrier around and above the shoot apical meristem. Thanks to this protective shelter from trichomes, the shoot apical meristem is strongly shielded from UV irradiance, which can be very harmful. Silica deposition was also indicated in UV tolerance in leaf epidermis (Goto et al., 2003) and in membrane damage protection (Shen et al., 2010), thus it could contribute to the UV-protective role of the trichome as well.

5.4.2 Trichome as mechanosensor

The Arabidopsis trichome was also indicated as a force-focusing mechanoreceptor that deforms at its base region in response to mechanical force (Liu et al., 2016; Zhou et al., 2017). This well corresponds with our observations of the thin cell wall at the base of the trichome and a stiff apical cell wall, so when mechanical force is applied along the reinforced apical zone, the trichome bends below the Ortmannian ring at the basal zone with the thin cell wall. Biological explanation of this mechanosensing was postulated later when it was shown that small mechanical disturbances caused by herbivores can induce signal transduction through cytosolic Ca^{2+} and apoplastic pH shifts and hence activate the physiological response (Zhou et al., 2017). Another work from this field proposed trichomes to have vibrational modes with the same frequency as the sounds of feeding caterpillars, and suggested that trichomes act as mechanical antennae (Liu et al., 2017).

5.4.3 Functional implications of trichome silicification

Callose has been known for a long time for its relationship with silica accumulation, but the underlying mechanisms are largely unknown. Our work demonstrates that for silicification of the apical trichome cell wall both callose synthase delivery and callose biosynthesis are important. Although the functional significance of the Arabidopsis trichome silicification is unclear, multiple lines of evidence appear. For example, by some means it might act in defence against herbivores as it was several times suggested previously (James, 2003; Connick, 2011; Reynolds et al., 2016). Numerous examples of the alleviative effect of silica in heavy metal stress and detoxification, salt stress, priming and more were exhaustively reviewed in (Guerriero et al., 2016).

In respect to our field of study it is noteworthy to mention the alleviating effect of silica under NaCl stress (Yeo et al., 1999; Shi et al., 2013; Zhu and Gong, 2014). Because together with publicly accessible microarray data showing that EXO70H4 is upregulated by salt stress, it opens a new potential direction of investigation. Moreover, in rice suspension culture the association of silica with hemicelluloses was documented as important factor for cadmium detoxification (Ma et al., 2015). Also silica and cadmium co-precipitation was found in rice cell wall (He et al., 2013b) and gelatinous metasilicic acid (H_2SiO_3) was shown to retain heavy metals in rice (Gu et al., 2011). Thus, the role of silica in heavy metal protection is very likely possible in trichomes.

The alleviative effect of silica was manifested also in pumpkin leaves (*Cucurbita moschata*) upon treatment with manganese (Mn) or both Mn and silica together. Moreover, an electron probe X-ray microanalysis of pumpkin leaves detected high concentrations of Mn at the base of the leaf trichomes of both plants treated with Mn or Mn and silica, but around necrotic lesions only after treatment with Mn without silica supply (Iwasaki and Matsumura, 1999). Higher concentrations of Mn and more focused region of its deposition were detected at the trichome base in case of silica supply. These data implicate a role of silica in alleviation from Mn toxicity by Mn localized accumulation at the base of the trichome.

These observations from pumpkin leaves indicate the importance of trichome base for sequestration of toxic elements and indicate role of Si in it. In accordance with this, increased content of Si was detected in the trichome base of *Arabidopsis halleri* and *Arabidopsis lyrata* (Sarret et al., 2009). In this study, elemental profile of the trichome clearly demonstrated remarkable increase of Si deposition exactly at the zone of the high zinc deposition at the base of the trichome. We found analogous Si enrichment at the zone of the Ortmannian ring and above it in Arabidopsis wild type trichomes, which was also the place of zinc accumulation (Kulich et al., 2018). Large amount of Si was detected also in the trichome tips of Arabidopsis, together with cadmium and mangan (Isaure et al., 2006), thus this region might be also important for sequestration of toxic compounds.

Taken together, these observations from Arabidopsis and other species indicate that silicification of the trichome cell wall might have alleviative role in trichome cell wall, where several toxic compounds accumulate.

5.4.4 Trichomes as sink for toxic compounds

Compartmentation of toxic compounds is one of tolerance strategies in plants. Typical sink for harmful compound sequestration are trichomes, because they represent a tissue external to the leaf and toxic substances can be effectively isolated there from the plant tissues (Choi et al., 2001; Domínguez-Solís et al., 2004). Indeed, heavy metals have been detected in trichome cell walls in *Brassicaceae*, including *Arabidopsis thaliana* (Gutierrez-Alcala et al., 2000; Ager et al., 2002; Ager, 2003; Dar et al., 2015). For instance, *Brassica juncea* (indian mustard) accumulated cadmium mainly in the leaf trichomes, apparently at the beginning of their stalk (Salt et al., 1995). Another *Brassicaceae* species is a well known model of metal tolerance and hyperaccumulation in plants - *Arabidopsis halleri* (Roosens et al., 2008). Its leaves have been analyzed by several X-ray based methods and its trichomes, especially their lower parts, have been identified as hot spots of accumulation of zinc, cadmium and other transition metals - Mn, Fe, Cr, Cu, Ni (Küpper et al., 2000; Zhao et al., 2000; Sarret et al., 2002; Hokura et al., 2006; Fukuda et al., 2008; Sarret et al., 2009; Isaure et al., 2015). These elements were distributed adjacent to the cell surface, often recognizably in the form of a ring. Similarly, enrichment of heavy metals was identified in upper part of the trichomes of non-hyperaccumulating species, *Arabidopsis lyrata* (Sarret et al., 2009; Isaure et al., 2015) and *Arabidopsis thaliana* (Ager et al., 2002; Isaure et al., 2006). Actually, in Arabidopsis, Isaure et al. (2006) reported cadmium and mangan accumulation in a strip in the middle of the trichome stalk and moreover, in the tip of the branches.

Our work previously demonstrated copper deposition (Kulich et al., 2015), zinc and cadmium deposition (chapter 4 of this thesis) in Arabidopsis trichomes at the zone of the Ortmannian ring and above it. On the contrary, no deposition of heavy metals was detected in *exo70H4* trichome cell wall, indicating a role of exocytosis in heavy metal sequestration. And involvement of the exocyst in metal tolerance was indeed formerly identified in Arabidopsis and barley (Hirschi et al., 2000). Further, a transcriptomic analysis identified regulation of OsExo70s by heavy metal stress in rice and strong induction of NbExo70D1 by copper treatment in tobacco (Lin et al., 2013). Taken together, the cell wall of Brassicaceae trichomes serves as a sequestering sink for heavy metals and the participation of the exocyst on heavy metal delivery to the cell wall becomes more and more apparent.

According to Isaure et al. (2006), trichomes were the main site of cadmium compartmentation in the Arabidopsis leaf, whereas only traces of cadmium accumulated in the epidermis and the mesophyll. Similar sequestration of cadmium from leaves to the trichomes was found in *Arabidopsis lyrata*, where trichomes contained 40 % of cadmium in the leaf (Huguet et al., 2006). Different situation seems to be in *Arabidopsis halleri*, the metal hyperaccumulating species, where trichomes were only minor sink in comparison to other leave tissues, despite the apparent enrichment of metals in the base of the trichomes (Küpper et al., 2000; Sarret et al., 2002). Thus, it is tempting to speculate about relevance of trichomes as metal sequestration sink and presumably they seem to be more important for the non-tolerant plants than for the hyperaccumulators.

In addition to trichome function in metal sequestration from metabolically active cells of the leaf, it is noteworthy to mention also their active physiological role in the metal detoxification. For instance, the expression of two distinct isoforms of metallothionein (Cys-rich proteins implicated in the detoxification of heavy metals) increased in Arabidopsis trichomes in experiments with copper treatment (García-Hernández et al., 1998). Metallothionein function in metal tolerance and homeostasis in plants has been observed in several Arabidopsis ecotypes (Murphy and Taiz, 1995). Role in metal detoxification

is known also for glutathione and indeed its elevated biosynthesis in Arabidopsis trichomes has been reported (Gutierrez-Alcala et al., 2000). The total content of glutathione in Arabidopsis trichomes was more than 300-fold higher in comparison to other epidermal cells. These results suggest considerable capacity of the trichome vacuole to sequestrate xenobiotics and heavy metals via glutathione conjugation.

5.4.5 Reactive oxygen species in the apical trichome cell wall domain

Reactive oxygen species (ROS) are free radicals derived from molecular oxygen, which are commonly produced by plant cell metabolism. Sensitive and fragile balance between their production and breakdown decides their role within the cell. At low concentrations they perform as important second messengers (signaling components) but at high concentrations they induce progressive oxidative damage. Orchestrating the delicate equilibrium of their concentrations requires responsive and complicated network of plenty of mechanisms that together maintain the oxygen homeostasis in the cell (Mittler et al., 2011; Sharma et al., 2012; Mhamdi and Van Breusegem, 2018; Noctor et al., 2018).

The production of ROS in plants is a very complex network of reactions involving a plenty of enzymes and interlinked pathways of responses to diverse stimuli. One of the most abundant ROS is hydrogen peroxide, H_2O_2, a non-radical and relatively stable ROS (Das and Roychoudhury, 2014). Enzymes involved in H_2O_2 metabolism in Arabidopsis are known to reside mainly in mitochondria, chloroplasts, peroxisomes and apoplast (Černý et al., 2018). Given our results showing accumulation of H_2O_2 in the apoplast of trichome stalk, this discussion will focus on H_2O_2 present in the apoplast. Redox reactions producing H_2O_2 in the apoplast are of great importance and intensively studied due to their role in maintaining cell wall integrity via promoting cell wall stiffening, loosening, lignin formation and suberization (Wrzaczek et al., 2013; Jovanović et al., 2018).

Peroxidases are typical enzymes responsible for the majority of these processes (Jovanović et al., 2018). In addition to the apoplastic H_2O_2 generated by cell-wall-associated peroxidases (Gross, 1977; Martinez et al., 1998; Kim et al., 2010), involvement of plasma membrane NADPH oxidases is also significant. They catalyse the extracellular production of superoxide from molecular oxygen (Sagi and Fluhr, 2001). This extracellular superoxide promptly changes into other ROS, typically into H_2O_2. Dismutation of superoxide into H_2O_2 is spontaneous or catalysed via cell wall superoxide dismutases (Bannister and Hill, 1980).

Our unpublished data displayed the production of H_2O_2 in wild type trichome apoplast and its disruption in *exo70H4* mutant trichomes. Based on the little information we have so far, it is difficult to guess the origin and role of H_2O_2 in the trichome. Such accumulation of H_2O_2 (visualized by DAB) was already spotted in trichomes of mulberry plants under copper(Cu)-deficient conditions (Tewari et al., 2006). Authors explained that as a result of oxidative stress in the Cu-deficient plants and as a consequence of impaired H_2O_2 scavenging machinery in plants under Cu-deficiency stress. Another example of H_2O_2 accumulation (visualized by DAB) was reported in Arabidopsis wild type trichomes in context of environmental stresses, particularly UV-B irradiation (Bouché et al., 2003). However our investigation conducted on unstressed plants suggests that H_2O_2 production in the Arabidopsis trichome apoplast is more likely a developmental event. Possibly it acts in some cell wall modifications, as H_2O_2 is known for instance to operate in peroxidative-cross-linking of cell wall polysaccharides and phenolics (Kjellbom et al., 1997; Kerr and Fry, 2004) and to accelerate strengthening of cell walls (Zarra et al., 1999). Though, H_2O_2 in the apoplast of the apical domain of trichome could play role as substrate for the processes of cell wall

peroxidases, such as modification of cell wall rigidity through polysaccharide cross-linking, suberization and lignification (Wrzaczek et al., 2013; Jovanović et al., 2018). Further but still indirect evidence for H_2O_2 role in cell wall modifications comes from our data showing that the main region of H_2O_2 accumulation in the trichome is the zone of stalk above the Ortmannian ring. Precisely this part becomes rigid during the maturation and thus plenty of cell wall modifications take place in this region, while the basal part of the trichome remains flexible and is prone to bending (Liu et al., 2016); (Zhou et al., 2017).

Interestingly, the H_2O_2 accumulation was frequently found in a pattern of band with sharp edges. This phenomenon points at very precise targeting of some H_2O_2-involving process within the cell wall and such polarization and sharp limits of the pattern even imply some relation with plasma membrane organization. Perchance, some plasma membrane-resident protein, like NADPH oxidase, produces H_2O_2 into the apoplast in such organized way because the protein itself is highly polarized at the plasma membrane. Equivalent ROS-dependent regulation of plant cell wall through polarization of NADPH oxidases was already described in Casparian strip formation in the root epidermis (Fujita et al., 2020). The Casparian strip is a precisely polarized band of lignified cell wall around every cell of the root endodermis and it can be considered as considerably analogous structure to the Orthmannian ring. Though analogous mechanisms can be speculated to act in their polarization. In the Casparian strip formation, it was shown, that the polar localization of a signaling kinase is crucial for local production of extracellular ROS, which is then necessary for precisely localized lignification of the Casparian strip (Fujita et al., 2020). Particularly, the asymmetrically localized kinase SCHENGEN1 directly phosphorylates NADPH oxidases at specific plasma membrane domain and though locally induces spatially restricted production of extracellular ROS (Fujita et al., 2020). Such ROS are used as a critical co-substrate for lignin production by apoplastic cell wall peroxidases and though SCHENGEN1 polarized localization defines the Casparian strip zone via local activation of NADPH-dependent ROS production (Fujita et al., 2020).

The regulation of ROS production and transmission is slowly being described. For example aquaporins (Henzler and Steudle, 2000) or vesicle trafficking complexes, including exocyst were already implicated in these processes (Sanderfoot et al., 2000; Leshem et al., 2006; Trinh et al., 2014). Increasing evidence suggests functional connection between EXO70s and ROS. NbExo70D1 was found to operate in ROS production under heavy metal (Trinh et al., 2014) and salt (Lin et al., 2013) stresses. These studies particularly indicated that NbExo70D1 acts in NADPH oxidase-mediated ROS production and chromium-induced ROS production. Taken together, these indications and our data from *exo70H4* mutant, link between NADPH oxidase-mediated ROS production and exocyst seems to be plausible future outcome, which has to be verified.

5.5 Evolutionarily conserved role of EXO70H4 paralog

Good evidence for evolutionarily conserved function of EXO70H4 came out from transcriptome profiling of *Cucumis sativus*, where EXO70H4 was identified as a highly upregulated gene in fruit trichomes (Chen et al., 2014). This transcriptomic analysis revealed a 406-fold increase of *CsEXO70H4* in wild type cucumber in comparison to a mutant without the trichomes. Very interestingly, in glandular trichomes of female cannabis flowers, a putative EXO70H4 paralog was also found to be upregulated, together with the rest of the exocyst subunits (Livingston et al., 2019).

Trichomes of a thousand shapes and structures, multicellular and unicellular, non-secretory and glandular exist on plant surfaces; their structural diversity is enormous (Werker, 2000) and so is their phylogenetic diversity (Tissier, 2012). Nevertheless, our results as well as previously published data point to a possibility that the function of EXO70H4 in trichomes is evolutionarily conserved among various land plant lineages, giving the findings in Arabidopsis a broader application.

6 Conclusions

The main topic of the Ph.D. thesis and experiments presented was the exocyst complex with the focus on the EXO70H4 subunit. We have accumulated experimental evidence for the functional diversification of EXO70 paralogs and a specific function of EXO70H4. We described the basic characteristics of the SCW deposited in wild type Arabidopsis trichome during the maturation phase. This final stage of trichome development had always been overlooked and we were the first to report callose deposition in Arabidopsis trichomes, which extends the typical text book list of callose developmental distribution. On top of that, we discovered an intriguing anatomical cell wall structure, which we named the Ortmannian ring and which in mature trichomes visibly separates apical and basal trichome domains. The Arabidopsis trichome is a highly polarized cell with a huge potential as a model not only in the research of mechanisms of cellular polarization, but especially also for the mechanistic analysis of the SCW formation.

From the phenotypic defects of *EXO70H4* depletion during the trichome cell wall maturation, which include mis-localization or a total lack of callose deposition, lowered cell wall autofluorescence and a total loss of apical SCW, we unraveled the importance of EXO70H4 for trichome SCW formation. Colocalization studies of EXO70H4 and GSL5 and GSL10 in the trichome, together with GSL5 delocalization in the *exo70H4* background manifested the central role of the exocyst complex in polarized secretion of callose synthase to the apical plasma membrane. We thus documented one of the first mechanistic details of callose synthase secretion and their regulation. More attention should be paid to this topic due to the important role of callose in plant defence against pathogens and due to its importance for agriculture. Based on our preliminary results of EXO70H4 function in pathogen defence and thanks to the resemblance of trichome SCW to the defensive papilla buildup during pathogen interactions, our results might have implications for the phytopathological field in the future. We have shown that heavy metal deposition in trichomes is dependent on EXO70H4. Similarly, our discovery of silica deposition in wild type trichome and a clear demonstration of the relationship between callose and silica deposition have broader implications. Trichome SCW might serve as a favorable environment for detailed studies of silica, an enigmatic cell wall component.

Finally, our studies of plasma membrane phospholipid composition in the trichome brought the last evidence of striking polarization of the trichome cell. Two distinct plasma membrane domains are visible at the end of the trichome cell development and EXO70H4 is necessary for their final definition. The accurate polarization of cellular domains and accessibility of trichomes makes them a very prominent cell type for investigation of detailed mechanisms not only of cell polarization and biological relevance of two domains within one cell, but also for mechanistic analyses of SCW biogenesis. Moreover, our cross-complementation experiment showed dissimilar preference of EXO70 paralogs to the two lipid plasma membrane domains in trichome, which was another strong piece of evidence for EXO70 paralog differentiation

and ability to recruit the exocyst complex to specific endomembrane recyclation domains within one cell. Our pioneer work explored uncharted territories of trichome development, bringing along new insight into its several aspects.

7 Závěr

Disertační práce byla zaměřena na komplex exocyst a to hlavně jeho podjednotku EXO70, konkrétně paralog EXO70H4. Naše práce přinesla významné výsledky potvrzující funkční rozrůzněnost paralogů EXO70 a jedinečnost funkce paralogu EXO70H4. Charakterizovali jsme vlastnosti sekundární buněčné stěny divokého trichomu Arabidopsis, která se ukládá během maturace. Tato závěrečná fáze vývoje trichomu byla výzkumníky notoricky přehlížena a tak jsme k našemu překvapení jako první popsali ukládání kalózy v trichomu Arabidopsis, čímž jsme rozšířili klasický učebnicový seznam výskytu kalózy v ontogenezi rostlin. Navíc jsme objevili fascinující anatomickou strukturu buněčné stěny, kterou jsme pojmenovali Ortmannové kroužek. Jedná se o vysoce polarizovanou kalózovou strukturu s obrovským potenciálem pro výzkum mechanismů buněčné polarizace, obdobně jako Caspariho proužek v endodermis kořene.

Studiem fenotypických odchylek buněčné stěny mutanta *exo70H4* jsme stanovili význam proteinu EXO70H4 pro budování sekundární buněčné stěny apikální domény trichomu. Odhalili jsme, že se tento protein lokalizuje na plazmatické membráně v zóně Ortmannové kroužku a v tečkovitém vzoru po celé apikální doméně. Výsledky kolokalizační studie proteinů EXO70H4 s GSL5 a s GSL10 spolu s delokalizací GSL5 proteinu v *exo70H4* pozadí jasně potvrdily význam komplexu exocyst pro polarizovanou sekreci kalózo-syntáz na plazmatickou membránu. Přinesli jsme tak první detailní vhled do mechanismů sekrece kalózo-syntáz, které však z větší části stále zůstávají nepopsány. Tomuto tématu by v budoucnosti mělo být věnováno více pozornosti vzhledem k významu kalózy v obraně rostlin proti patogenům a tudíž její důležitosti pro zemědělství. Trichomy by mohly sloužit jako užitečný výzkumný model s možným přesahem a aplikací výsledků do oboru fytopatologie. Podobně náš objev křemíku v buněčné stěně divokého trichomu Arabidopsis a jasná demonstrace vztahu mezi kalózou a ukládáním křemíku může mít širší implikace do dalších oborů. Sekundární buněčná stěna trichomu může sloužit jako vhodné výzkumné prostředí pro detailní studium křemíku, jehož dosavadní výzkum skýtá mnoho neobjeveného a záhadného.

Nakonec naše studium složení fosfolipidů plazmatické membrány trichomu přineslo další důkaz enormní úrovně polarizace trichomové buňky. Tyto dvě různé domény plazmatické membrány se formují na konci vývoje trichomu a protein EXO70H4 je potřebný pro jejich precizní formování. V rostlinách není mnoho buněčných typů s obdobnou úrovní polarizace domén, což z trichomů dělá velmi mocný nástroj studia detailů buněčné polarizace a biologického významu existence dvou domén v rámci jedné buňky. Navíc naše experimenty s dalšími paralogy EXO70 prokázaly rozdílné preference jednotlivých paralogů k těmto doménám a tím přinesly další silný důkaz diferenciace paralogů EXO70 a jejich schopnosti navádět komplex exocyst do specifických recyklačních endomembránových domén v jedné buňce. Naše práce se věnovala neprozkoumané oblasti buněčného vývoje trichomu a byla tak průkopnická v mnoha ohledech. Doufáme, že na budoucí výzkumníky, kteří navážou na námi postavené základy, čekají ještě zajímavější zjištění.

8 Published articles

8.1 Article 1

12 pages (43—54)

Cell Wall Maturation of Arabidopsis Trichomes Is Dependent on Exocyst Subunit EXO70H4 and Involves Callose Deposition[1][OPEN]

Ivan Kulich[2]*, Zdenka Vojtíková[2], Matouš Glanc, Jitka Ortmannová, Sergio Rasmann[3], and Viktor Zárský

Department of Experimental Plant Biology, Faculty of Sciences, Charles University, 12844 Prague, Czech Republic (I.K., Z.V., M.G., J.O., V.Z.); Institute of Experimental Botany, Academy of Sciences of the Czech Republic, 16502 Prague, Czech Republic (J.O., V.Z.); and Department of Ecology and Evolution, University of Lausanne, CH–1015 Lausanne, Switzerland (S.R.)

Arabidopsis (*Arabidopsis thaliana*) leaf trichomes are single-cell structures with a well-studied development, but little is understood about their function. Developmental studies focused mainly on the early shaping stages, and little attention has been paid to the maturation stage. We focused on the EXO70H4 exocyst subunit, one of the most up-regulated genes in the mature trichome. We uncovered EXO70H4-dependent development of the secondary cell wall layer, highly autofluorescent and callose rich, deposited only in the upper part of the trichome. The boundary is formed between the apical and the basal parts of mature trichome by a callose ring that is also deposited in an EXO70H4-dependent manner. We call this structure the Ortmannian ring (OR). Both the secondary cell wall layer and the OR are absent in the *exo70H4* mutants. Ecophysiological aspects of the trichome cell wall thickening include interference with antiherbivore defense and heavy metal accumulation. Ultraviolet B light induces EXO70H4 transcription in a CONSTITUTIVE PHOTOMORPHOGENIC1-dependent way, resulting in stimulation of trichome cell wall thickening and the OR biogenesis. EXO70H4-dependent trichome cell wall hardening is a unique phenomenon, which may be conserved among a variety of the land plants. Our analyses support a concept that Arabidopsis trichome is an excellent model to study molecular mechanisms of secondary cell wall deposition.

Driven by selection pressure on reproductive success, the surface layers of land plants continually evolve to endure biotic and abiotic stresses. This has resulted in the dynamic evolution of different epidermis and derived structures, such as trichomes, across species and genotypes. Trichomes particularly can be of different forms, even within one individual plant. Because they are unessential for plant survival in laboratory conditions, trichomes became popular targets of genetic developmental analyses in the model plant Arabidopsis (*Arabidopsis thaliana*); until now, the focus was mostly on trichomes patterning/initiation and early morphogenetic processes. Nevertheless, trichome development has been shown to be modulated by abiotic stresses in Arabidopsis and other systems. Yamasaki et al. (2007), for instance, showed that UV-B irradiation was responsible for increasing the number of cells and the amount of polyphenolic compounds in trichomes. Roles in the drought and heat stresses (Ehleringer, 1982; Grammatikopoulos and Manetas, 1994; Espigares and Peco, 1995; Pérez-Estrada et al., 2000) and heavy metal detoxification and deposition (Salt et al., 1995; Pérez-Estrada et al., 2000; Servin et al., 2012; Jr and Kupper, 2014) also have been described. Additionally, different forms of trichomes have been linked to increased plant resistance against herbivores across different species of plants (for review, see Riddick and Simmons, 2014).

Arabidopsis trichomes are nonglandular hairs with epidermal origin. Unlike most plants with multicellular trichomes, Arabidopsis trichomes are unicellular (but undergo four endoreduplication cycles; Hülskamp et al., 1994). Despite unicellularity, Arabidopsis trichomes reach an extremely polarized shape, with bulged stalk and three to four branches. Development has been well characterized genetically (Hülskamp et al., 1994; Folkers et al., 1997; for review, see Marks et al., 1991), and it has been divided into six stages: initiation, polar expansion, branching, branch growth, diffuse growth, and maturation of cell wall (Szymanski et al., 1998, 2000). Nevertheless, interest has remained firmly focused on the first five stages, when trichome growth and formation occur, with rather less attention paid to the stage of trichome maturation. Only a few mutants with defective trichome maturation have been identified to date. For instance, the

[1] This work was supported by the Grant Agency of Czech Republic (grant no. 14–27329P), the Grant Agency of Charles University (grant no. 658112), the Czech Ministry of Education (grant no. NPUI LO1417), and the City of Prague (grant no. OPPK CZ.2. 16/3.1.00/24014 for the transmission electron microscope used in this study).

[2] These authors contributed equally to the article.

[3] Present address: Institute of Biology, University of Neuchâtel, CH–2000 Neuchâtel, Switzerland.

* Address correspondence to kulich@natur.cuni.cz.

The author responsible for distribution of materials integral to the findings presented in this article in accordance with the policy described in the Instructions for Authors (www.plantphysiol.org) is: Ivan Kulich (kulich@natur.cuni.cz).

[OPEN] Articles can be viewed without a subscription.

www.plantphysiol.org/cgi/doi/10.1104/pp.15.00112

group of glassy mutants lacks surface papillae, rendering them a lustrous and transparent appearance. These include *chablis*, *chardonnay*, *retsina* (Hülskamp et al., 1994), *glassy hair1* (*GLH1*), *GLH2*, *GLH3*, *GLH4*, and *GLH6* (Suo et al., 2013). Unfortunately, only phenotype description and chromosomal position mapping of glassy genes have been published. A similar situation prevails with mutant *underdeveloped trichome* (Haughn and Somerville, 1988) and *constitutive expression of PR genes5* (Brininstool et al., 2008). Mapped mutations affecting the trichome cell wall include several transcription factors and cell wall enzymes. *murus2* mutation is in the fucosyltransferase1, resulting in underdeveloped trichome papillae (Vanzin et al., 2002), similar to *murus3* mutation in the xyloglucan galactosyltransferase (Madson et al., 2003). Mutants named *trichome birefringence* lack the birefringence of the trichomes, which is primarily caused by paracrystalline cellulose. The precise role of these proteins is, however, still unclear (Potikha and Delmer, 1995; Bischoff et al., 2010). Transcription factors involved in the trichome cell wall development include HOMEODOMAIN GLABROUS2 (Marks et al., 2009) and MYB DOMAIN PROTEIN106 (NOECK; Jakoby et al., 2008). Both of these mutants also have underdeveloped trichome papillae.

Only recently has the potential of Arabidopsis trichomes as a model for cell wall biogenesis been recognized (Suo et al., 2013). In fact, most of the published work on cell walls formation was done on stem/xylem or whole-plant analysis and is related to cell wall component biosynthesis (Liepman et al., 2010), with recent emphasis on transcriptional networks reconstructed from transcriptional analyses (Wang et al., 2012).

Exocytosis is a constituent process in cell wall formation, and we are interested in how delivery/targeting and tethering of secretory vesicles to the plasma membrane are involved in Arabidopsis trichome cell wall maturation. Exocyst is an evolutionarily conserved protein complex in all eukaryotes and plays an important role in polarized exocytosis (Elias et al., 2003; Munson and Novick, 2006; Cvrcková et al., 2012). The exocyst complex consists of eight subunits (SEC3, SEC5, SEC6, SEC8, SEC10, SEC15, EXO70, and EXO84). Although it has been initially described in yeast (*Saccharomyces cerevisiae*; TerBush et al., 1996), homologs of all of the subunits have been described in plants (Elias et al., 2003), where they also form a complex (Hála et al., 2008). The role of the exocyst complex is tethering and docking of the post-Golgi vesicles to plasma membrane. SEC3 and EXO70 proteins are believed to be spatial landmarks on the plasma membrane, marking the place of the vesicle fusion (Finger et al., 1998; He et al., 2007). This can be shown by artificial targeting of the SEC3 to the mitochondrial outer membrane, which is followed by relocalization of the remaining exocyst subunits and secretion into the mitochondrion (Luo et al., 2014). The vesicle is attached by the exocyst near to the acceptor target membrane, whereas SNARE proteins mediate the rest of the fusion process. Polarized exocytosis mediated by exocyst enables effective control of growth and final shape of plant cells and tissues. The role of polarized exocytosis in cell wall formation is crucial and makes possible the creation of extremely polarized cells, such as root hairs, or pollen tubes (Cole et al., 2005; Cole and Fowler, 2006; Synek et al., 2006; Zárský et al., 2009).

Interestingly, some of exocyst subunits are found in multiple copies in terrestrial plant genomes (Elias et al., 2003; Hála et al., 2008; Cvrcková et al., 2012). The most protruding is multiplication of subunit EXO70. For example, the genome of *Physcomitrella patens* encodes 13 paralogs of the EXO70 subunit, *Vitis vinifera* encodes 15 paralogs, and *Oryza sativa* encodes 47 paralogs (Cvrcková et al., 2012). The Arabidopsis genome encodes 1 copy of exocyst subunits SEC6 and SEC8, 2 copies of SEC3, SEC5, SEC10, and SEC15, 3 copies of EXO84, and strikingly, 23 copies of EXO70 (Elias et al., 2003; Hála et al., 2008; Cvrcková et al., 2012). It still remains unclear whether the functions of EXO70 paralogs are redundant or specialized, but new findings suggest that at least some EXO70 paralogs have entirely different functions than the most studied and most conserved EXO70A1. Early data show that the transcription of some EXO70 paralogs is up-regulated in specific tissues or under specific conditions. For example, EXO70B2 and EXO70H1 are strongly up-regulated by pathogen elicitors (Pecenkova et al., 2011). Other recent works report the first evidence, to our knowledge, of functional diversification of some EXO70 paralogs, with possible roles in autophagy (Kulich et al., 2013). Formation of other double-membrane bodies has been reported for the EXO70E2 subunit (Wang et al., 2010). Overexpression of EXO70E2 also induces double-membrane structures in animal cells (Ding et al., 2014). This may reflect an exocyst-independent effect of EXO70 on the membrane curvature, which was reported in animal cells (Zhao et al., 2013).

Here, we focus on the EXO70H4 paralog, which is the 11th most up-regulated gene in the mature trichome (Jakoby et al., 2008). Arabidopsis trichomes functions are mostly associated with herbivore defense and UV protection (Yan et al., 2012). Corresponding with this, it was indicated that EXO70H4 is up-regulated by UV-B irradiation in a CONSTITUTIVE PHOTOMORPHOGENIC1 (COP1)-dependent manner (Oravecz et al., 2006) and that it is down-regulated by methyl jasmonate (MeJA; Hruz et al., 2008). MeJA is a volatile plant defense hormone, which is important, especially in response to herbivores and wounding. A recent transcriptome profiling study has identified the cucumber (*Cucumis sativus*) EXO70H4 paralog as also being highly up-regulated during the cucumber fruit trichome development, suggesting that similar mechanisms are present among various land plants (Chen et al., 2014).

In this report, we studied and compared Arabidopsis trichomes maturation between the wild type and *EXO70H4* subunit mutants. Our work has resulted in the description of a component and structure in Arabidopsis trichomes, which we named Ortmannian ring (OR). Additionally, our data highlight that EXO70H4 plays a role in Arabidopsis trichome cell wall maturation

as well as plant response to UV-B irradiation and herbivore attack.

RESULTS

Two Arabidopsis SALK insertional mutants in the *EXO70H4* single-exon gene were used for this study: *exo70H4-1* and *exo70H4-3* (SALK_023593 and SALK_003200, respectively). Annotated position of the insertions was verified by sequencing of the flanking regions. Both lines have transfer DNA insertion in the single exon of the *EXO70H4* gene, and recessive homozygotes exhibit identical phenotypic deviations. *exo70H4-1* has a tandem insertion, disrupting the coding sequence (CDS) 47 bp from the start codon, and *exo70H4-3* has a single insertion, disrupting CDS 580 bp from the start codon (Fig. 1A). According to reverse transcription (RT)-PCR, both mutations prevent synthesis of the full-length RNA, with partial transcripts present (Fig. 1B). Because the phenotypes were identical, most of the following work has been done on the *exo70H4-1* allele. Transformation of the *exo70H4-1* mutant with the genomic fragment, including the promoter (895 bp) and the C-terminal fluorescent marker tagRFP (*Entacmaea quadricolor* red fluorescent protein), has restored the wild-type phenotype of the trichomes (Supplemental Fig. S1).

To test whether EXO70H4 is an exocyst subunit, we performed yeast two-hybrid analysis, which has resulted in interactions with SEC5a, SEC6, and the C terminus of EXO84b and also, a weak interaction with SEC15a (Supplemental Fig. S2).

Overall plant size, structure, and trichome morphogenesis of mutant plants are not affected. However, mutant plants have leaf trichomes that lack rigidity and are more flexible and bendable compared with the wild type. For example, in a blinded study, we were able to precisely distinguish 100% of the mutants from the wild types by touching the leaves (n = 40). This difference is because of the apparently thinner cell walls of mutant trichomes compared with the wild type (Fig. 1C). These observations imply that deposition of cell wall components is defective in *exo70H4* mutants during the trichome maturation phase. At this phase, wild-type trichome cell wall undergoes massive secondary thickening, which progressively fills up trichome inner space. This thickening is mostly pronounced in the branch tips (Fig. 1C) and can be easily measured (Fig. 1D). This extensive deposition results in cytoplasm reduction and recession toward the stalk.

OR, Cell Wall Structure of the Mature Arabidopsis Trichome

During our observation of the trichome cell wall thickening, we noticed a distinct circular thickening of cell wall at the basal region of the stalk (Fig. 1C). This ring, present above the surrounding epidermal cells, appears to divide the trichome into two different domains. Staining with decolorized aniline blue has revealed that the ring is a callose-rich structure (Fig. 2A).

To show that such circular formation is a normal part of Arabidopsis trichome maturation, we captured photographs of whole 24-d-old rosettes stained by aniline blue (Fig. 2B) by automated stitching of individual microscopic frames in three focal depths. With this resolution, we could detect the presence of the callose ring in all leaf trichomes. First, callose rings appear in the oldest trichomes and grow on the apex. Second, a wave of maturation continues, and rings also appear in the leaf base. Because this ring was not studied before, we propose naming it OR after author J.O., who first spotted it.

The OR acts as a boundary and apparently divides the trichome cell wall into two clearly distinct domains—apical (branches and stalk) and basal (bulge). The cell wall in the apical domain shows strong autofluorescence upon UV-B excitation (Fig. 3), it has surface papillae, and it undergoes massive secondary

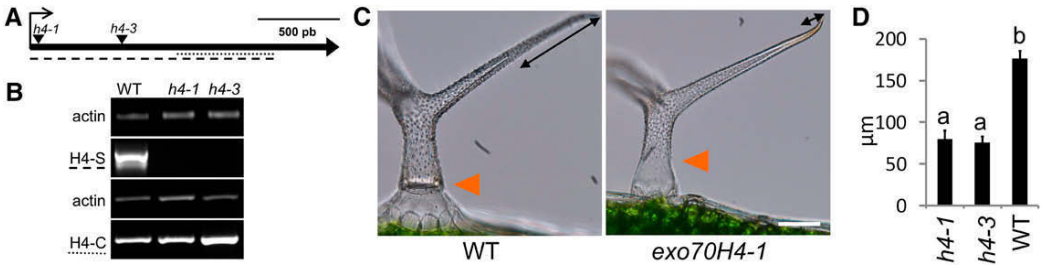

Figure 1. *exo70H4* mutants show trichome cell wall thickening defects. A, Insertions in *exo70H4-1* and *exo70H4-3* mutants disrupt the single exon of *EXO70H4*. B, H4-S and H4-C fragments (shown in A as dashed and dotted lines, respectively) amplified by RT-PCR. C, Phenotypes of the wild type (WT) versus *exo70H4-1* mutant in the trichome tip cell wall (double arrow line) and basal (orange triangle) parts. Bar = 20 μm. D, Quantification of the apical thickening on *exo70H4-1* and *exo70H4-3* mutants. Letters above bars mean significant differences (honestly significant difference [HSD] Tukey post hoc test, $P < 0.01$). Error bars represent SE. Similar results were obtained in three biological replicas.

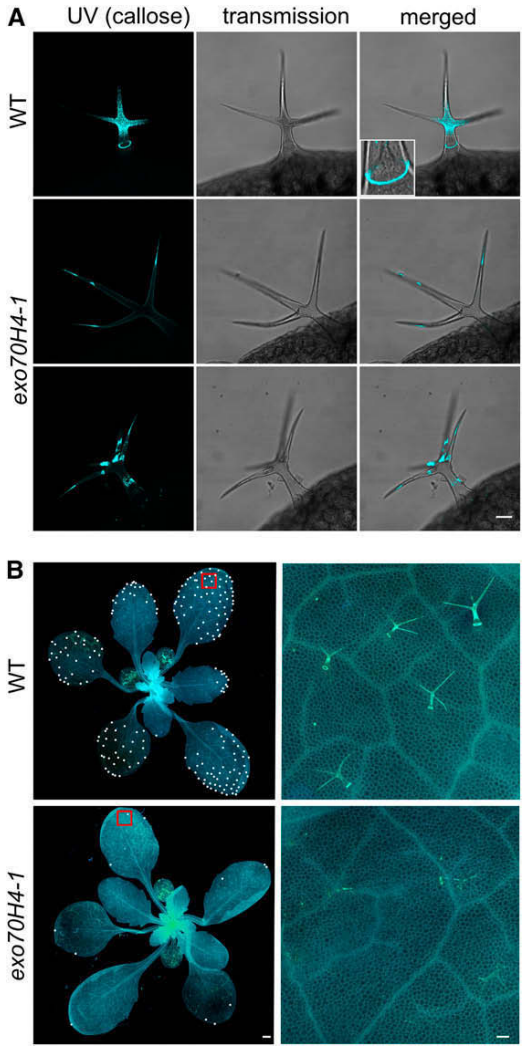

Figure 2. Visualization of the OR. A, Aniline blue staining of the wild type (WT) and *exo70H4-1* mutant. The distinct callose ring is what we termed OR. Bar = 20 μm. B, Whole-rosette aniline blue staining of the 23-d-old wild-type and *exo70H4-1* mutant plants. White dots, Trichomes with the OR already visible; red rectangles, the positions of the zoomed areas. Bars = 1 mm (left); 50 μm (right).

thickening during the maturation phase. In contrast, the basal domain lacks autofluorescence (Fig. 3A) and papillae (Fig. 1C), and its cell wall remains thin. The *exo70H4-1* mutant lacks the OR and most of the callose in the vast majority of the trichomes (more than 95%). *exo70H4-1* trichomes either lack the callose entirely or it can be detected within the cytoplasm in the form of ectopic fibrous bodies (Fig. 2A). No major differences in callose deposition were spotted elsewhere (plasmodesmatal plugs after wounding and vasculature; data not shown). Papillae do develop in the *exo70H4* mutant; however, their distribution is not limited by any clear border area (Fig. 1C).

exo70H4 Mutants Lack a Highly Autofluorescent Internal Cell Wall Layer That Is Bordered by the OR in the Wild Type

In the trichomes of the wild type, the internal cell wall layer can be easily recognized. This layer shows strong autofluorescence, especially upon excitation with 405 nm and emission maxima at 485 nm (Fig. 3B). Interestingly, this high autofluorescence is found only in the upper part of the trichome above the OR (Fig. 3A).

Autofluorescence of the inner cell wall layer is rapidly increased by trichome breakage or damage (Fig. 3, C and D). Because the damaged trichomes were killed by their breakage, gain of autofluorescence was likely caused by oxidation of the inner cell wall layer. This statement is supported by treatment with reducing agents (40 mM mercaptoethanol), which suppressed the autofluorescence buildup after breakage (Fig. 3E). With or without physical damage, *exo70H4* mutants show dramatically decreased autofluorescence compared with the wild type because of the absence of the whole inner cell wall layer. The remaining autofluorescence was more equally distributed within the mutant cell wall (Fig. 3A). The absence of the inner trichome cell wall layer also explains differential calcofluor white (CW) staining of isolated *exo70H4-1* trichome versus the wild type. Whereas in wild-type trichome, only the trichome base was stained, in the mutant, the apical domain was also stained (Supplemental Fig. S3). Hence, the callose-rich inner trichome cell wall layer likely insulates the apical trichome domain and prevents cellulose from staining.

To further characterize EXO70H4-dependent cell wall thickening, we have observed transmission electron microscopy (TEM) sections in isolated trichomes. Our sectioning confirmed that the wild-type trichome contains two clearly distinct cell wall layers—an electron-dense external layer and an internal layer. The internal layer is limited to the apical part of the trichome above the OR, where it forms a bulge of thick cell wall. This second internal cell wall layer is completely absent from *exo70H4* mutant trichomes (Fig. 4, A–D). Immunogold labeling of the callose has revealed that OR is usually U-shaped on cross section bordering the secondary cell wall (Fig. 4, E and F). Results of the immunogold labeling were consistent with aniline blue staining, with callose detected primarily in the OR and less frequently in the secondary cell wall above it. Because the staining was rather weak and specific, we have detected no immunogold particles in the other parts of the section.

By extensive observation of trichomes in different stages of their maturation, we were able to summarize the thickening progress. The secondary cell wall thickening is accompanied by growth of the OR, which is U-shaped on the cross section and widens in the latest stages of the trichome maturation (Fig. 5).

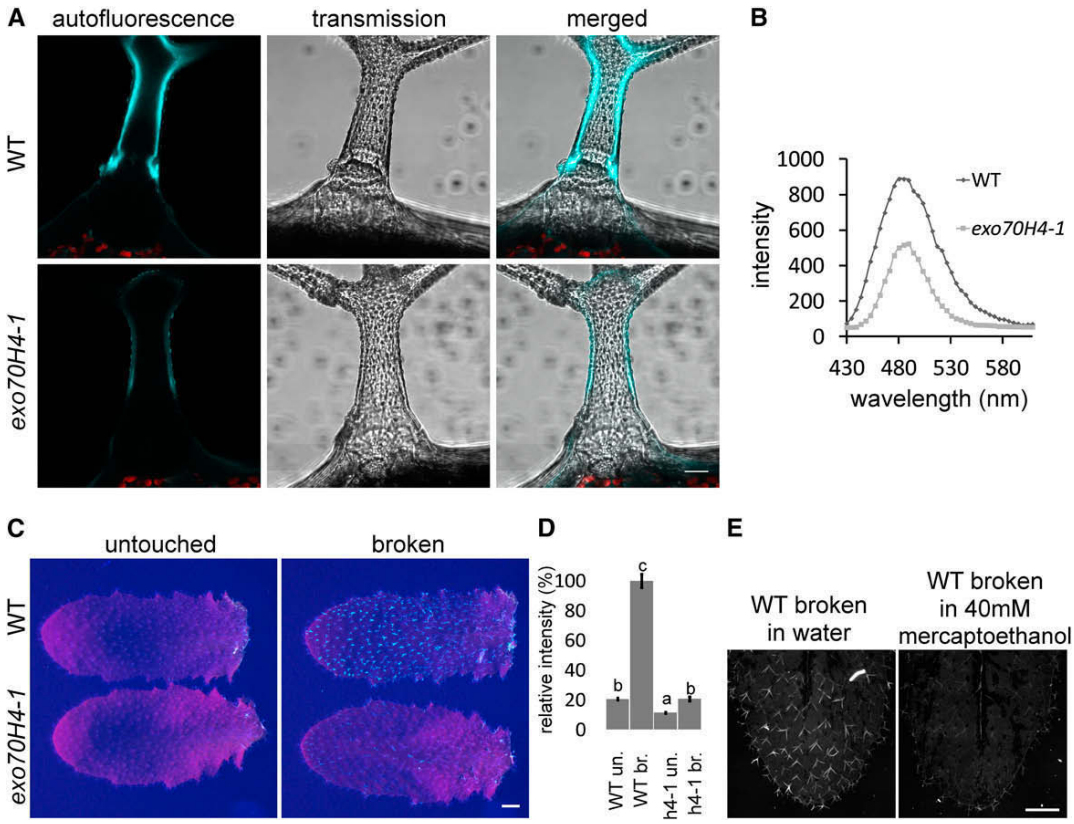

Figure 3. Autofluorescence of the *exo70H4-1* and wild-type (WT) trichomes. A, Autofluorescence of the mature trichome cell wall of wild-type and *exo70H4-1* trichomes. Bar = 20 μm. B, λ-Scan of the trichome autofluorescence reveals a single peak at 485 nm. C, Visualization of the autofluorescence gain after physical damage of trichomes. Bar = 1 mm. D, Quantification of the autofluorescence of the untouched (un.) and broken (br.) trichomes from C. Error bars represent SE. Different letters above bars mean significant differences (HSD Tukey post hoc test, $P < 0.05$). Eighty trichomes per sample were measured. Similar results were obtained from more than three biological replicas. E, Reduction of autofluorescence gain in reducing environment. Bar = 1 mm.

UV-B-Induced EXO70H4 Expression Promotes Cell Wall Thickening and OR Biogenesis

According to several published microarray experiments (Hruz et al., 2008), *EXO70H4* transcription is induced by UV-B irradiation. This induction is, moreover, COP1 dependent, linking expression of EXO70H4 with an already known UV response pathway (Oravecz et al., 2006). However, MeJA (a major regulator of necrotrophic pathogen and herbivore response; Jander and Howe, 2008) inhibits *EXO70H4* transcription (Hruz et al., 2008). Therefore, we have designed experiments to test whether these environmental factors do affect trichome maturation in an EXO70H4-dependent manner.

We have isolated trichomes from fifth and sixth leaves of 24-d-old plants that were treated by UV-B irradiation and/or MeJA for 5 d. Isolated trichomes were then stained with decolorized aniline blue to visualize the OR. As can be seen in Figure 6A, UV irradiation clearly stimulates the callose ring formation, whereas MeJA suppresses it. If both treatments were applied simultaneously, their effects subtracted, resulting in OR abundance similar to in wild-type plants.

We have also examined the effect of UV-B on cell wall thickening in the trichome stalk above the OR. Despite the large defects of cell wall thickening in the trichome apices (Fig. 1C), the differences were rather small but highly significant; UV-B treatment stimulated wild-type thickening by about 10% in contrast to no stimulation in the *exo70H4* mutant. Combined UV and MeJA treatment caused the 10% thickening in both the wild type and *exo70H4*, indicating that this particular mutant phenotype is complemented by an unknown MeJA-dependent mechanism under these combined treatment conditions (Fig. 6B).

Ecophysiological Aspects of Trichome Cell Wall Thickening

Because trichomes have been previously reported to also play a role in anti-herbivore protection, we next asked whether thick secondary walls of wild-type trichomes facilitate plant resistance against insect pests. For this, we performed a weight gain experiment using

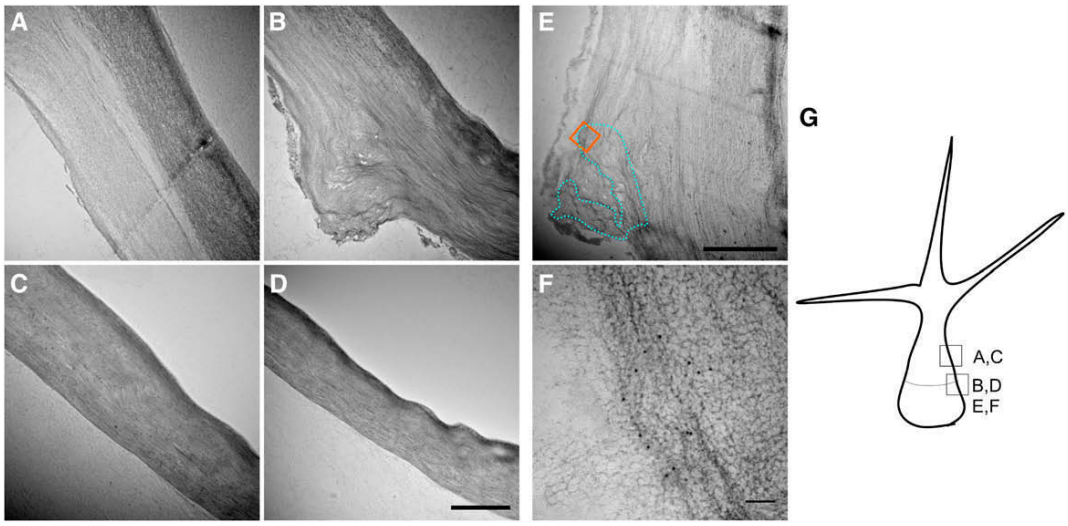

Figure 4. TEM micrographs of wild-type and *exo70H4-1* trichomes. A, Wild-type cell wall above the OR has two distinct layers. B, Wild-type cell wall at the OR. Above the OR, two layers can be recognized, but only one layer is visible beneath the OR. C, *exo70H4-1* cell wall at the place corresponding to A. Only one cell wall layer is visible. D, *exo70H4-1* cell wall at the place corresponding to B. No OR is visible. E, The blue dotted line highlights the region that forms the OR according to the immunogold labeling. The orange square represents the approximate position of F. F, Detail on the immunogold labeling by the anticallose antibody. The position of F is highlighted by the orange square in E. G, Position and orientation of micrographs depicted for better orientation. Bars = 2 μm (A–E) and 100 nm (F).

a specialist herbivore (cabbage butterfly [*Pieris brassicae*]) and a generalist herbivore (Egyptian cotton leafworm [*Spodoptera littoralis*]). First instar caterpillars were placed on both wild-type and *exo70H4* plants for 7 d, after which dry weight gain was measured. For both herbivore species, caterpillars grew less on the *exo70H4* mutants compared with on wild-type plants (Supplemental Fig. S4A). In accordance, we also observed that endogenous MeJA content in *exo70H4* mutants was generally higher than in wild-type plants (Supplemental Fig. S4B). Because jasmonic acid (JA) induction has been linked to increased herbivore resistance in Arabidopsis, we suggest that the influence of trichome stiffness is hazed by other effects, likely MeJA-induced glucosinolate synthesis and overall resistance.

Copper Is Accumulated in the Cell Wall of the OR and above It

Trichomes of other species are well known to accumulate heavy metals, so we were interested if they could be detected in the secondary cell wall and the OR. We have observed second and third true leaves of 24-d-old plants watered by 2 mM $CuSO_4$ and water. Then, copper was stained using dithiooxamide. The copper mainly accumulated in the OR and the cell wall band right above it, whereas it was not detected in the samples watered by regular water. Also, copper was not detected in the *exo70H4-1* mutant, where the whole secondary cell wall is absent (Supplemental Fig. S5).

OR Is Not Likely a Rudiment of Cytokinesis

Arabidopsis trichomes are of unicellular origin; however, DNA endoreduplication suggests their multicellular origin (Hülskamp et al., 1994). In the multicellular trichomes of cucumber, EXO70H4 paralogs are also highly up-regulated (Chen et al., 2014). In these trichomes, the two apical cells also accumulate big amounts of callose, and callose rings are common at the cell divisions (Supplemental Fig. S6).

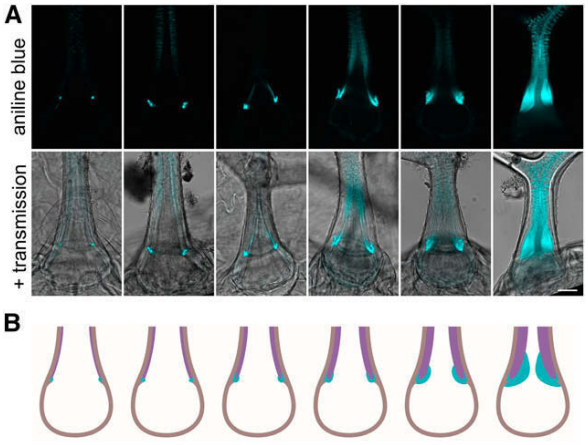

Figure 5. Development of the OR. A, Stages of the trichome maturation accompanied by the secondary cell wall thickening and OR growth. Bar = 20 μm. B, Graphical portrayal of A. Cyan, The OR; purple, the secondary cell wall above the OR; brown, the primary cell wall (respective cellulose-rich cell wall).

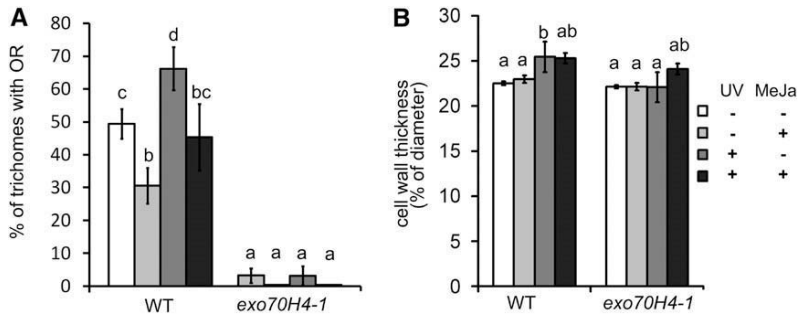

Figure 6. Stimulation of secondary cell wall deposition by UV-B. A, Percentage of trichomes with the OR is increased by the UV and decreased by the MeJA treatment in wild-type (WT) trichomes. B, Relative cell wall thickness of the cell wall in the trichome stalk above the OR. Different letters above bars mean significant differences using the χ^2 test in A ($P < 0.01$) and ANOVA with the HSD Tukey post hoc test ($P < 0.05$) in B. Error bars represent SE. The measurements were made in three biological replicas on more than 20 plants and more than 100 trichomes per treatment and genotype.

Hence, we asked whether Arabidopsis OR is a rudiment of cell plate formation. To address this question, we used the microtubules reporter MICROTUBULE ASSOCIATED PROTEIN4-GFP (MAP4-GFP)-expressing Arabidopsis plant. A band of microtubules distantly resembling a preprophasic band was observed in many trichomes during our observations, and we spotted a correlation between the nucleus position and OR biogenesis (Fig. 7, A–D). Previous studies concluded the final position of the nucleus at the point of the third branching (Hülskamp et al., 1994). We carefully monitored position dynamics of the nucleus in maturing trichomes and realized that, in finally matured/thickened wild-type trichomes, the nucleus, in fact, moved back to basal position. In wild-type trichomes without OR, the nucleus was mostly spotted at the branching point. However, the position of the nucleus was much more basal in the trichomes with OR (Fig. 7, A–C). To test the possibility that OR is a rudiment of cytokinesis, we observed OR in the *Siamese* (*sim*) mutant (GABI_170C01). *SIM* encodes an Interactors of Cdc2 kinase/Kip-related protein cell cycle inhibitor, and mutation in this gene results in ectopic trichome cell divisions (Walker et al., 2000). Surprisingly, these trichomes did not divide in the OR domain (Fig. 7E). Moreover, additional ORs were present in newly divided branches. Hence, this observation did not support the hypothesis that the OR would be a simple rudiment of preprophase or cytokinesis.

DISCUSSION

Here, we show that the final stages of trichome development (i.e. trichome maturation) are characterized by the deposition of an additional layer of the cell wall. Because it is clearly distinguishable and deposited in the last stage of trichome development, we refer to this layer as the secondary cell wall, although biochemical analysis suggested that it has primary wall-like composition (Marks et al., 2008). Strong argument for this cell wall being secondary is the fact that this layer is only formed in the apical part of the trichome and not in the base. The secondary cell wall layer is bordered by a previously undescribed structure, which we propose to name the OR. OR not only borders the secondary cell wall but also, limits the surface papillae distribution, which is much more delimited in the *exo70H4* mutant.

The scenario of OR being a phylogenetic relic of preprophase is unlikely, although our observations do not rule out any other link to the cell cycle. Other phenomena observed can also be explained by different mechanisms. It was shown previously in multiple cases that the nucleus moves toward places with massive secretion (for example, during plant-microbe interactions; Griffis et al., 2014). Also, microtubular structures are often present in active secretory plasma membrane domains, such as the mucilage secretion domain of the outer layer of Arabidopsis seed coat (McFarlane et al., 2008).

OR has been anecdotally spotted before, however, without any additional attention. In figure 1m in Potikha and Delmer (1995), a callose ring was noticed in the trichome, but it was interpreted as a circular wound response. Here, we show that the OR constantly appears with trichome maturation, resulting in nearly 100% of the mature trichomes having the OR. In sum, we propose that, as the trichome maturates, most of its volume is filled up by the callose-rich cell wall, and this thickening is accompanied by the growth of the OR. It should be also noted that callose patterns in the secondary cell wall may vary and are not always as we described here as general pattern. The most common patterns above the OR are small speckles spreading down from the branch tips. Other than the OR, a wide callose band repeatedly appears on the stalk. Interestingly, sometimes not only one OR but two or more are formed. Controlling mechanisms and conditions of these patterns remain unclear and have yet to be studied.

Role of the OR and the Autofluorescent Secondary Cell Wall Layer

The precise role of OR is yet unknown; however, because it borders the autofluorescent and callose-rich inner layer of the cell wall, it likely has a structural

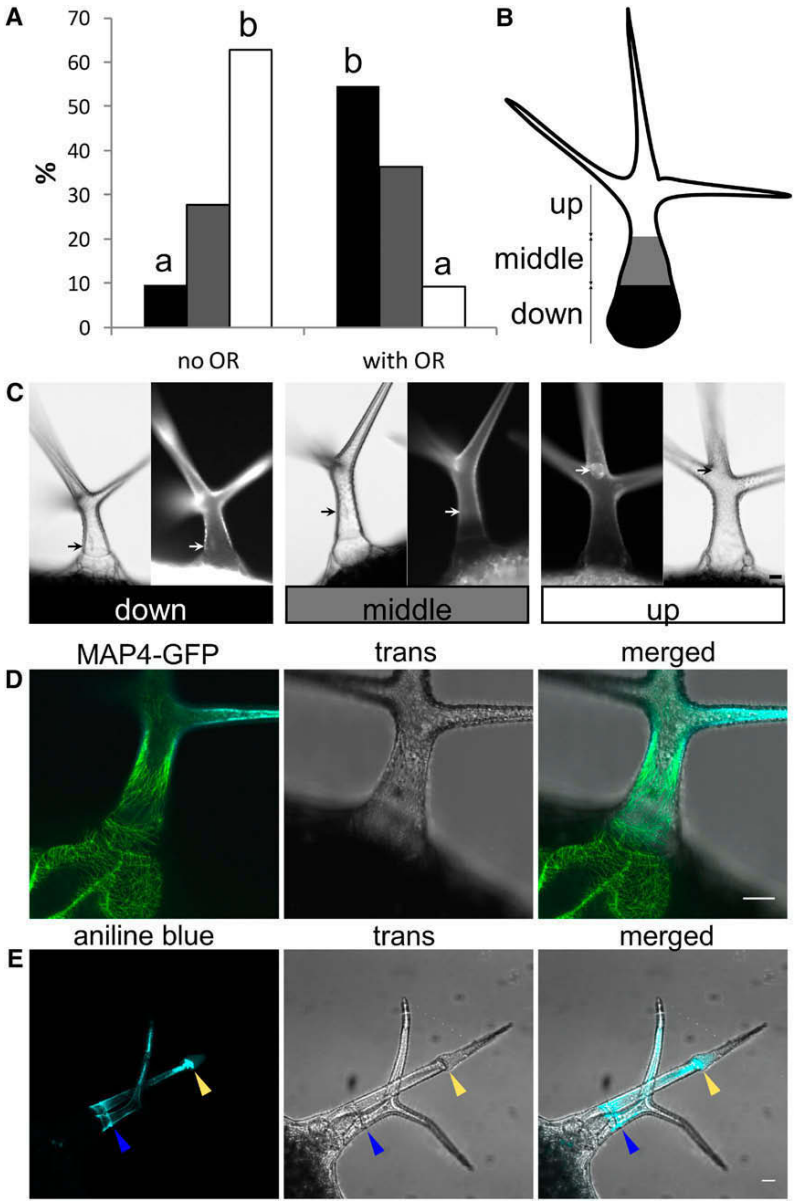

Figure 7. OR biogenesis: link to the nucleus movements and the cell cycle. A, Position of the nuclei in the trichomes before and after the OR formation. Percentage of nuclei located in the lower part of the stalk (black), the middle of the stalk (gray), and the upper part of the stalk (white). Different letters above bars mean significant differences (χ^2 test; $P < 0.0005$); more than 100 trichomes per sample from more than 10 plants were used. Similar results were obtained from three biological replicas. B, Scheme displaying how nucleus position was categorized into three groups. C, Examples of the nucleus (stained by 4′,6-diamino-phenylindole) positions evaluated in A. D, Band of microtubules at the base, which can be spotted before OR biogenesis. E, *sim* mutant ectopic cell divisions (yellow arrow) do not take place at the OR (blue arrow). Bars = 20 μm.

role. The role of the inner layer may be more general and important for many ecophysiological aspects, including UV protection and heavy metal detoxification. Because many toxic compounds, including secondary metabolites, are expected to be deposited in the trichome cell wall, the OR may limit their localization from spreading into other tissues. For example, sequestration of heavy metals in trichomes has been described in both hyperaccumulating and nonaccumulating plant species (Martell, 1974; Salt et al., 1995; Krämer et al., 1997; MacFarlane and Burchett, 1999; Servin et al., 2012; Jr and Kupper, 2014). *Arabidopsis halleri* is a well-known heavy metal hyperaccumulator, with strong evidence for accumulation of zinc, cadmium, and other heavy metals in trichomes. Subcellular localization is in accordance with our results with striking cellular distribution in a narrow ring or thick band at the trichome base (Küpper et al., 2000; Zhao et al., 2000; Sarret et al., 2002; Fukuda et al., 2008), corresponding to the secondary cell wall above the OR. There is also evidence of cadmium hyperaccumulation in trichomes of Arabidopsis (Ager et al., 2002). Jakoby et al. (2008) have shown that zinc transporters and copper chaperones are on the list of the 5% most up-regulated genes in the mature trichome. Hence, the Arabidopsis trichome secondary cell wall may be a permanent storage for toxic heavy metals, which we show here with copper. In this regard, Arabidopsis simple trichomes are analogous to the

glandular trichomes of other species, which also usually have cell wall domains specialized for phytochemical deposition (Turner and Croteau, 2004; Ramirez et al., 2012). Heavy-metal stress has been shown previously to up-regulate the secretory pathway genes in *O. sativa*, including EXO70FX14 and EXO70FX15, which were induced by the copper stress. Similarly, *Nicotiana benthamiana EXO70* is up-regulated by the copper stress and required for the heavy metal-induced reactive oxygen species production (Lin et al., 2013).

We do not yet know the nature of the autofluorescent compounds stored in the trichome secondary cell wall. We have tried multiple lignin stainings, which all gave us negative results, with both healthy and broken trichomes (data not shown).

Interestingly, the whole process of callose accumulation, cell wall thickening, and OR development is enhanced by UV-B irradiation. Trichomes, indeed, play a role in the UV stress response, and their density is increased in plants exposed to UV-B (Yan et al., 2012). UV-B-induced trichome cell wall thickening is in accordance with these results. Induction of EXO70H4 by UV light, resulting in trichome cell wall thickening, indicates a possible function in apical meristem protection against damaging ROS production, although we have not yet performed experiments to confirm this.

The inner trichome cell wall layer also contains a lot of callose, and its absence in *exo70H4* mutants does not cause a change in the trichome birefringence (data not shown). Therefore, the birefringent cell wall layer is likely the outer one, which is also more electron dense on the TEM and contains dense cellulose fibers. This observation is also supported by our CW staining, in which the inner cell wall layer was not stained by the CW in contrast to the *exo70H4* mutant. The presence of ectopic fibrous callose patches in *exo70H4* mutants suggests that callose rather than callose synthase is one of EXO70H4-dependent cargoes. Because the whole internal cell wall layer is callose rich, its development may be callose dependent. Occasional presence of the OR in the *exo70H4* mutant is likely caused by existence of a very close paralog *EXO70H3*, which is a twin gene next to *EXO70H4*, similar to *SEC10a* and *SEC10b* (Vukašinovic et al., 2014). *EXO70H3* shows a pollen-specific expression; however, like many other genes, there may be some ectopic expression in the sporophyte. In Arabidopsis pollen, more EXO70 subunits of the H group are expressed, which is probably why *exo70H3* has viable and functional pollen with normal size of the callose plugs (data not shown).

To our surprise, simultaneous application of both UV-B and MeJA induced cell wall thickening in both the *exo70H4* mutant and the wild type without the induction of the OR biogenesis. This may be caused by up-regulation of another EXO70 paralog (for example, EXO70H7, which is stimulated by MeJA on the transcriptional level; Hruz et al., 2008) or another exocyst-independent mechanism.

Because our larval weight experiment did not reveal any importance of *exo70H4*-mediated cell wall thickening for herbivore resistance, we speculate that EXO70H4 is essential for default UV-B-induced thickening, which may be modulated upon herbivore attack. Trichome stiffness itself, however, may still be important to protect against another herbivore species (for example, slugs), and it may be a more general way to improve plant fitness.

Exocyst and Trichome: Questions of the Future Cell Wall Biogenesis Investigation

According to the transcriptomic data (Oravecz et al., 2006; Jakoby et al., 2008), *EXO70H4* is one of the most up-regulated genes in the mature trichome. Surprisingly, this high expression was not noticed in GUS reporter promoter activity assays (Li et al., 2010). This may be because of early observations of too young trichomes combined with very low permeability of old ones.

The EXO70H4 paralog up-regulation in cucumber trichomes (Chen et al., 2014) is a clue that mechanisms of the cell wall thickening in Arabidopsis described here may be a more general phenomenon for land plants that also include multicellular trichome types.

Other (core) exocyst subunits are not dramatically up-regulated in the trichome. Hence, there is a question of the stoichiometry of the complex. Recently, mammalian EXO70 was shown to also function independently from the rest of the exocyst complex in a way analogous to Bin–Amphiphysin–Rvs domain proteins functioning in a membrane deformation (Zhao et al., 2013). We cannot yet exclude the possibility of exocyst-independent function; however, it is worth noting that EXO70H4 interacts with other exocyst subunits in the yeast two-hybrid assays (Supplemental Fig. S2). The stoichiometry question could be explained by post-transcriptional regulation of the EXO70H4 level, which is the case in many other Arabidopsis EXO70s (Stegmann et al., 2012), or possibly, high doses of this subunit are important to compete with the other EXO70s for the rest of the complex, thus modulating its function as proposed in Zárský et al., 2013. Our work aims to answer some of these questions and includes more general analysis of exocyst-dependent callose deposition processes in defense responses.

MATERIALS AND METHODS

Plant Growth and Conditions

T-DNA insertion lines of Arabidopsis (*Arabidopsis thaliana*) were obtained from the Nottingham Arabidopsis Stock Centre (Scholl et al., 2000). These lines were crossed with MAP4-GFP lines (Marc et al., 1998). Plants were grown in Jiffy soil pellets under long-day conditions with illumination of 100 μm m^{-2} s^{-1} photosynthetically active radiation (OSRAM L 58W/930). Plants were planted, placed into paper boxes, and sealed from above by filter foils. Rosco 226 (UV filter) and Rosco 130 (control filter) were used.

Subsequently, plants were exposed to UV-B radiation for 5 d under LT 36W/958 T8 BIOVITAL NARVA fluorescent tubes (which contain UV-B emission peaks) and/or treated with MeJA by installation of slices of filter

papers soaked in the MeJA amount corresponding to a concentration of 0.8 μL L^{-1} box volume (also for 5 d).

In high-light conditions, plants were grown under 700 μm m^{-2} s^{-1} photosynthetically active radiation with Philips HPI-T Plus 400W/645 E40 light bulbs (also with UV-B peak).

Genotype Analysis

The following primers were used for genotyping: *exo70H4-1*, left primer (LP), TGGGATTTCGTTTCACAGTTC and right primer (RP), AATCCGTCATGACGTTGGTAG; exo70H4-3, LP, AACAAACCTGAAGCCATGATG and RP, GTTGCTGTAGTCAGCGAGGAG; Salk LBb 1.3, ATTTTGCCGATTTCGGAAC; GABI_170C01, LP, ATGGATTAACTTGGCATGTGG and RP, TGAAAATGTACTTTTTGGCCAC; and Gabi LB 08409, ATATTGACCATCATACTCATTGC.

The following primers were used for cloning fragments for genomic complementation: EXO70H4 Pst1_for, AAGCTGCAGGCTACAGGAGGCTGGATCATC; and EXO70H4 Kpn1_rev, TCAGGTACCGACATGGATTGCCTTGACCG.

The following primers were used for testing its presence: H4seq3 for, CCGGAGATCATTAATACTAAAA; and TagRFPrev, ATCAACTCTTCACCTTTACTCACCAT.

This fragment has been subcloned into the TagRFP AS-N vector (Evrogen), transferred to the binary vector pBGW (Karimi et al., 2002) by the Clontech LR clonase recombination, and sequenced.

Transcript Detection and Semiquantitative RT-PCR

For detection of transcript in *exo70H4-1* and *exo70H4-3* mutants, RNA was isolated from 100 mg of 7-d-old seedlings grown on Murashige and Skoog plates. RT-PCR was done with the Fermentas First-Strand cDNA Synthesis Kit with 1 μg of total RNA, which was double DNAsed. The following primer pairs were used for transcript detection: GTTTTCCGGCTGCTTGACAT with TATAGCTGCCGGCGAATTGT for the 3′-terminal region and TTTCCATGGTGACGAGAAAAGCAATGAT (forward primer for cloning *EXO70H4* cds) with TATAGCTGCCGGCGAATTGT for the insertion spanning RT-PCR.

Trichome Isolation and Staining

Fifth and sixth leaves were selected from plants (24 d after germination) grown in various conditions (see "Plant Growth and Conditions"). Trichomes were then isolated using a method described in Marks et al. (2008) with minor modifications (phosphate-buffered saline buffer and 100 mM EGTA incubated for 1 h at 50°C).

To stain for the callose, isolated trichomes or whole rosettes were washed for 3 h in acetic acid:ethanol (1:3), washed three times in deionized water, and incubated overnight in aniline blue solution (150 mM KH_2PO_4 and 0.01% [w/v] aniline blue, pH 9.5). This solution without aniline blue was used as a control to check autofluorescence background. For copper staining, after acetic acid-ethanol fixation, samples were washed in 70% (v/v) ethanol and then incubated overnight in a 0.1% (w/v) solution of dithiooxamide in 70% (v/v) ethanol.

Microscopy

Images were acquired with a Leica LCS 510 Confocal Microscope with ×63/1.2 and ×20/0.8 water immersion objectives. A 405-nm laser with an emission window of 470 to 490 nm was used for autofluorescence observation, and a 405-nm laser with an emission window of 490 to 510 nm was used for aniline blue. A 488-nm laser with an emission window of 510 to 530 nm was used for GFP observations. For whole-rosette pictures, a Nikon Eclipse 90i with a ×4 objective was used. Each rosette picture consists of numerous frames that were fused automatically by NIS Elements AR software. Each frame is a maximal projection of three frames with 50 μm of *Z* distance.

TEM and Immunogold Labeling

For TEM, isolated trichomes were fixed for 24 h in 2.5% (v/v) glutaraldehyde in 0.1 M cacodylate buffer (pH 7.2) at 4°C and postfixed in 2% (w/v) OsO_4 in the same buffer. Fixed samples were dehydrated through an ascending ethanol and acetone series and embedded in Epon-Araldite.

On-section immunogold labeling was done using mouse anticallose primary antibody and goat anti-mouse 10-nm golden particles (25128; Aurion) with a standard procedure recommended by the supplier with these conditions: 5% (w/v) bovine serum albumin in phosphate-buffered saline buffer was used as a blocking reagent, and goat monoclonal anti-β-1-3 Glucan from Biosupplies Australia Pty. Ltd. in a concentration 10 μg mL^{-1} was applied for 1 h.

Herbivore Weight Gain Experiments

To measure the specificity of resistance in the Arabidopsis wild type and *exo70H4* mutants, including *exo70H4-1* and *exo70H4-3*, we performed an experiment with two different herbivores: the highly generalist herbivore Egyptian cotton leafworm (*Spodoptera littoralis*; Lepidoptera, Noctuidae) and the cabbage family specialist herbivore cabbage butterfly (*Pieris brassicae*; Lepidoptera, Pieridae). Eggs of Egyptian cotton leafworms were provided by Syngenta, and first instar larvae were obtained by placing eggs at 30°C for 3 d. First instar larvae of cabbage butterflies were provided by Philippe Reymond (University of Lausanne) and obtained from rearing insects on cabbage (*Brassica oleracea*) in controlled greenhouse conditions. All plants were grown in a growth chamber (short days, 20°C, and 55% relative humidity) with a 3:1 mix of commercial potting soil (Orbo-2; Schweizer AG):perlite, and they were 6 weeks old at the time of the experiment. After initial growth, plants were individually surrounded with 330-mL-volume deli plastic cups with the bottoms cut off, and one Egyptian cotton leafworm or one cabbage butterfly larvae (n = 11–13 larvae per herbivore treatment) was added to each plant. Cups were then covered with fine-meshed nylon nets to prevent larvae from escaping, and larvae were allowed to feed for 7 d, after which all surviving larvae were flash frozen in liquid nitrogen, oven dried for 4 d at 50°C, and weighed. An additional four to six plants were set aside, and they were treated in the same way but left herbivore free for measuring constitutive jasmonate production (see below). The main effects of the three different genotypes (the wild type, *exo70H4-1*, and *exo70H4-3*), the two herbivore species (Egyptian cotton leafworm and cabbage butterfly), and their interaction were analyzed with two-way ANOVA.

JA content in leaves was analyzed by collecting one leaf per plant. The extraction was performed by grinding 200 mg of fresh leaves to a powder and mixing with 990 μL of extraction solvent (ethylacetate:formic acid at 99.5:0.5) and 10 μL of internal standards (containing isotopically labeled d5-JA at a concentration of 100 ng mL^{-1}) in a mixer mill at 30 Hz. After centrifugation and evaporation of the supernatant, the residue was resuspended in 100 μL of 70% (v/v) MeOH. Five microliters of solution was injected for ultra-high-performance liquid chromatography-mass spectrometry/mass spectrometry analysis following the same conditions as in Glauser et al. (2014). The final concentration of JA is expressed in nanograms per gram times fresh weight. The main effects of the three different genotypes (the wild type, *exo70H4-1*, and *exo70H4-3*), the herbivore treatment (Egyptian cotton leafworm, cabbage butterfly, and control), and their interaction on JA concentrations were analyzed with two-way permutation ANOVA using the lmPerm package in R (Wheeler, 2010).

Yeast Two-Hybrid Assays

The yeast (*Saccharomyces cerevisiae*) two hybrid was performed as described previously (Hála et al., 2008). We used the Matchmaker GAL4 Two-Hybrid System 3 (Clontech) following the manufacturer's instructions. We used constructs prepared by Hála et al. (2008), Fendrych et al. (2010), and Pecenková et al. (2011), and *EXO70H4* cds was amplified from genomic DNA and subcloned into the pGBKT7 vector between *Nco*I and *Sal*I using these primers: For_EXO70H4_*Nco*I, TTTCCATGGTGACGAGAAAAGCAATGAT; and Rev_EXO70H4_*Sal*I, TTTGTCGACTTAGGACATGGATTGCCTTGAC. From this vector, EXO70H4 cds was recloned into pGADT7 using *Nde*I and *Xho*I restriction sites.

Supplemental Data

The following supplemental materials are available.

Supplemental Figure S1. Genetic complementation of the *exo70H4-1* mutant.

Supplemental Figure S2. Yeast two-hybrid interactions of EXO70H4 and other exocyst subunits.

Supplemental Figure S3. Calcofluor white staining of the wild-type and *exo70H4-1* mutant trichomes.

Supplemental Figure S4. Herbivore studies on *exo70H4* mutants.

Supplemental Figure S5. Copper accumulation in wild-type and *exo70H4-1* trichomes.

Supplemental Figure S6. Callose in the cucumber trichome.

ACKNOWLEDGMENTS

We thank Dr. Miroslav Hyliš for extensive help with the TEM microscopy, Juraj Sekereš for data mining from transcriptomic databases, and Marta Čadyová for technical support.

Received January 24, 2015; accepted March 10, 2015; published March 12, 2015.

LITERATURE CITED

Ager FJ, Ynsa MD, Domínguez-Solís JR, Gotor C, Respaldiza MA, Romero LC (2002) Cadmium localization and quantification in the plant Arabidopsis thaliana using micro-PIXE. Nucl Instrum Methods Phys Res B **189:** 494–498

Bischoff V, Nita S, Neumetzler L, Schindelasch D, Urbain A, Eshed R, Persson S, Delmer D, Scheible WR (2010) *TRICHOME BIREFRINGENCE* and its homolog *AT5G01360* encode plant-specific DUF231 proteins required for cellulose biosynthesis in Arabidopsis. Plant Physiol **153:** 590–602

Brininstool G, Kasili R, Simmons LA, Kirik V, Hülskamp M, Larkin JC (2008) Constitutive Expressor of Pathogenesis-related Genes5 affects cell wall biogenesis and trichome development. BMC Plant Biol **8:** 58

Chen C, Liu M, Jiang L, Liu X, Zhao J, Yan S, Yang S, Ren H, Liu R, Zhang X (2014) Transcriptome profiling reveals roles of meristem regulators and polarity genes during fruit trichome development in cucumber (Cucumis sativus L.). J Exp Bot **65:** 4943–4958

Cole RA, Fowler JE (2006) Polarized growth: maintaining focus on the tip. Curr Opin Plant Biol **9:** 579–588

Cole RA, Synek L, Zarsky V, Fowler JE (2005) SEC8, a subunit of the putative Arabidopsis exocyst complex, facilitates pollen germination and competitive pollen tube growth. Plant Physiol **138:** 2005–2018

Cvrcková F, Grunt M, Bezvoda R, Hála M, Kulich I, Rawat A, Zárský V (2012) Evolution of the land plant exocyst complexes. Front Plant Sci **3:** 159

Ding Y, Wang J, Chun Lai JH, Ling Chan VH, Wang X, Cai Y, Tan X, Bao Y, Xia J, Robinson DG, et al (2014) Exo70E2 is essential for exocyst subunit recruitment and EXPO formation in both plants and animals. Mol Biol Cell **25:** 412–426

Ehleringer J (1982) The influence of water stress and temperature on leaf pubescence development in encelia farinosa. Am J Bot **69:** 670–675

Elias M, Drdova E, Ziak D, Bavlnka B, Hala M, Cvrckova F, Soukupova H, Zarsky V (2003) The exocyst complex in plants. Cell Biol Int **27:** 199–201

Espigares T, Peco B (1995) Mediterranean annual pasture dynamics: impact of autumn drought. J Ecol **83:** 135–142

Fendrych M, Synek L, Pecenková T, Toupalová H, Cole R, Drdová E, Nebesárová J, Sedinová M, Hála M, Fowler JE, et al (2010) The *Arabidopsis* exocyst complex is involved in cytokinesis and cell plate maturation. Plant Cell **22:** 3053–3065

Finger FP, Hughes TE, Novick P (1998) Sec3p is a spatial landmark for polarized secretion in budding yeast. Cell **92:** 559–571

Folkers U, Berger J, Hülskamp M (1997) Cell morphogenesis of trichomes in Arabidopsis: differential control of primary and secondary branching by branch initiation regulators and cell growth. Development **124:** 3779–3786

Fukuda N, Hokura A, Kitajima N, Terada Y, Saito H, Abe T, Nakai I (2008) Micro X-ray fluorescence imaging and micro X-ray absorption spectroscopy of cadmium hyper-accumulating plant, Arabidopsis halleri ssp. gemmifera, using high-energy synchrotron radiation. J Anal At Spectrom **23:** 1068–1075

Glauser G, Vallat A, Balmer D (2014) Hormone profiling. Methods Mol Biol **1062:** 597–608

Grammatikopoulos G, Manetas Y (1994) Direct absorption of water by hairy leaves of Phlomis fruticosa and its contribution to drought avoidance. Can J Bot **72:** 1805–1811

Griffis AHN, Groves NR, Zhou X, Meier I (2014) Nuclei in motion: movement and positioning of plant nuclei in development, signaling, symbiosis, and disease. Front Plant Sci **5:** 129

Hála M, Cole R, Synek L, Drdová E, Pecenková T, Nordheim A, Lamkemeyer T, Madlung J, Hochholdinger F, Fowler JE, et al (2008) An exocyst complex functions in plant cell growth in *Arabidopsis* and tobacco. Plant Cell **20:** 1330–1345

Haughn GW, Somerville CR (1988) Genetic control of morphogenesis in Arabidopsis. Dev Genet **9:** 73–89

He B, Xi F, Zhang X, Zhang J, Guo W (2007) Exo70 interacts with phospholipids and mediates the targeting of the exocyst to the plasma membrane. EMBO J **26:** 4053–4065

Hruz T, Laule O, Szabo G, Wessendorp F, Bleuler S, Oertle L, Widmayer P, Gruissem W, Zimmermann P (2008) Genevestigator v3: a reference expression database for the meta-analysis of transcriptomes. Adv Bioinforma **2008:** 420747

Hülskamp M, Misŕa S, Jürgens G (1994) Genetic dissection of trichome cell development in Arabidopsis. Cell **76:** 555–566

Jakoby MJ, Falkenhan D, Mader MT, Brininstool G, Wischnitzki E, Platz N, Hudson A, Hülskamp M, Larkin J, Schnittger A (2008) Transcriptional profiling of mature Arabidopsis trichomes reveals that *NOECK* encodes the MIXTA-like transcriptional regulator MYB106. Plant Physiol **148:** 1583–1602

Jander G, Howe G (2008) Plant interactions with arthropod herbivores: state of the field. Plant Physiol **146:** 801–803

Karimi M, Inzé D, Depicker A (2002) GATEWAY vectors for Agrobacterium-mediated plant transformation. Trends Plant Sci **7:** 193–195

Krämer U, Grime GW, Smith JAC, Hawes CR, Baker AJM (1997) Micro-PIXE as a technique for studying nickel localization in leaves of the hyperaccumulator plant Alyssum lesbiacum. Nucl Instrum Methods Phys Res B **130:** 346–350

Kulich I, Pecenková T, Sekereš J, Smetana O, Fendrych M, Foissner I, Höftberger M, Zárský V (2013) Arabidopsis exocyst subcomplex containing subunit EXO70B1 is involved in autophagy-related transport to the vacuole. Traffic **14:** 1155–1165

Küpper H, Lombi E, Zhao FJ, McGrath SP (2000) Cellular compartmentation of cadmium and zinc in relation to other elements in the hyperaccumulator Arabidopsis halleri. Planta **212:** 75–84

Li S, van Os GMA, Ren S, Yu D, Ketelaar T, Emons AMC, Liu CM (2010) Expression and functional analyses of *EXO70* genes in Arabidopsis implicate their roles in regulating cell type-specific exocytosis. Plant Physiol **154:** 1819–1830

Liepman AH, Wightman R, Geshi N, Turner SR, Scheller HV (2010) Arabidopsis - a powerful model system for plant cell wall research. Plant J **61:** 1107–1121

Lin CY, Trinh NN, Fu SF, Hsiung YC, Chia LC, Lin CW, Huang HJ (2013) Comparison of early transcriptome responses to copper and cadmium in rice roots. Plant Mol Biol **81:** 507–522

Luo G, Zhang J, Guo W (2014). The role of Sec3p in secretory vesicle targeting and exocyst complex assembly. Mol Biol Cell **25:** 3813–3822

MacFarlane GR, Burchett MD (1999) Zinc distribution and excretion in the leaves of the grey mangrove, Avicennia marina (Forsk.). Vierh Environ Exp Bot **41:** 167–175

Madson M, Dunand C, Li X, Verma R, Vanzin GF, Caplan J, Shoue DA, Carpita NC, Reiter WD (2003) The *MUR3* gene of *Arabidopsis* encodes a xyloglucan galactosyltransferase that is evolutionarily related to animal exostosins. Plant Cell **15:** 1662–1670

Marc J, Granger CL, Brincat J, Fisher DD, Kao Th, McCubbin AG, Cyr RJ (1998) A GFP-MAP4 reporter gene for visualizing cortical microtubule rearrangements in living epidermal cells. Plant Cell **10:** 1927–1940

Marks MD, Betancur L, Gilding E, Chen F, Bauer S, Wenger JP, Dixon RA, Haigler CH (2008) A new method for isolating large quantities of *Arabidopsis* trichomes for transcriptome, cell wall and other types of analyses. Plant J **56:** 483–492

Marks MD, Esch J, Herman P, Sivakumaran S, Oppenheimer D (1991) A model for cell-type determination and differentiation in plants. Symp Soc Exp Biol **45:** 77–87

Marks MD, Wenger JP, Gilding E, Jilk R, Dixon RA (2009) Transcriptome analysis of Arabidopsis wild-type and gl3-sst sim trichomes identifies four additional genes required for trichome development. Mol Plant **2:** 803–822

Martell EA (1974) Radioactivity of tobacco trichomes and insoluble cigarette smoke particles. Nature **249:** 215–217

McFarlane HE, Young RE, Wasteneys GO, Samuels AL (2008) Cortical microtubules mark the mucilage secretion domain of the plasma membrane in Arabidopsis seed coat cells. Planta **227:** 1363–1375

McNear DH Jr, Kupper JV (2014) Mechanisms of trichome-specific Mn accumulation and toxicity in the Ni hyperaccumulator Alyssum murale. Plant Soil **377:** 407–422

Munson M, Novick P (2006) The exocyst defrocked, a framework of rods revealed. Nat Struct Mol Biol **13:** 577–581

Oravecz A, Baumann A, Máté Z, Brzezinska A, Molinier J, Oakeley EJ, Adám E, Schäfer E, Nagy F, Ulm R (2006) CONSTITUTIVELY PHOTOMORPHOGENIC1 is required for the UV-B response in *Arabidopsis*. Plant Cell **18:** 1975–1990

Pecenková T, Hála M, Kulich I, Kocourková D, Drdová E, Fendrych M, Toupalová H, Zársky V (2011) The role for the exocyst complex subunits Exo70B2 and Exo70H1 in the plant-pathogen interaction. J Exp Bot **62:** 2107–2116

Pérez-Estrada LB, Cano-Santana Z, Oyama K (2000) Variation in leaf trichomes of Wigandia urens: environmental factors and physiological consequences. Tree Physiol **20:** 629–632

Potikha T, Delmer DP (1995) A mutant of Arabidopsis thaliana displaying altered patterns of cellulose deposition. Plant J **7:** 453–460

Ramirez AM, Stoopen G, Menzel TR, Gols R, Bouwmeester HJ, Dicke M, Jongsma MA (2012) Bidirectional secretions from glandular trichomes of pyrethrum enable immunization of seedlings. Plant Cell **24:** 4252–4265

Riddick EW, Simmons AM (2014) Do plant trichomes cause more harm than good to predatory insects? Pest Manag Sci **70:** 1655–1665

Salt DE, Prince RC, Pickering IJ, Raskin I (1995) Mechanisms of cadmium mobility and accumulation in Indian mustard. Plant Physiol **109:** 1427–1433

Sarret G, Saumitou-Laprade P, Bert V, Proux O, Hazemann JL, Traverse A, Marcus MA, Manceau A (2002) Forms of zinc accumulated in the hyperaccumulator *Arabidopsis halleri*. Plant Physiol **130:** 1815–1826

Scholl RL, May ST, Ware DH (2000) Seed and molecular resources for Arabidopsis. Plant Physiol **124:** 1477–1480

Servin AD, Castillo-Michel H, Hernandez-Viezcas JA, Diaz BC, Peralta-Videa JR, Gardea-Torresdey JL (2012) Synchrotron micro-XRF and micro-XANES confirmation of the uptake and translocation of TiO_2 nanoparticles in cucumber (Cucumis sativus) plants. Environ Sci Technol **46:** 7637–7643

Stegmann M, Anderson RG, Ichimura K, Pecenkova T, Reuter P, Zársky V, McDowell JM, Shirasu K, Trujillo M (2012) The ubiquitin ligase PUB22 targets a subunit of the exocyst complex required for PAMP-triggered responses in *Arabidopsis*. Plant Cell **24:** 4703–4716

Suo B, Seifert S, Kirik V (2013) Arabidopsis GLASSY HAIR genes promote trichome papillae development. J Exp Bot **64:** 4981–4991

Synek L, Schlager N, Eliás M, Quentin M, Hauser MT, Zársky V (2006) AtEXO70A1, a member of a family of putative exocyst subunits specifically expanded in land plants, is important for polar growth and plant development. Plant J **48:** 54–72

Szymanski DB, Jilk RA, Pollock SM, Marks MD (1998) Control of GL2 expression in Arabidopsis leaves and trichomes. Development **125:** 1161–1171

Szymanski DB, Lloyd AM, Marks MD (2000) Progress in the molecular genetic analysis of trichome initiation and morphogenesis in Arabidopsis. Trends Plant Sci **5:** 214–219

TerBush DR, Maurice T, Roth D, Novick P (1996) The Exocyst is a multiprotein complex required for exocytosis in Saccharomyces cerevisiae. EMBO J **15:** 6483–6494

Turner GW, Croteau R (2004) Organization of monoterpene biosynthesis in Mentha: immunocytochemical localizations of geranyl diphosphate synthase, limonene-6-hydroxylase, isopiperitenol dehydrogenase, and pulegone reductase. Plant Physiol **136:** 4215–4227

Vanzin GF, Madson M, Carpita NC, Raikhel NV, Keegstra K, Reiter WD (2002) The mur2 mutant of Arabidopsis thaliana lacks fucosylated xyloglucan because of a lesion in fucosyltransferase AtFUT1. Proc Natl Acad Sci USA **99:** 3340–3345

Vukašinovic N, Cvrcková F, Eliáš M, Cole R, Fowler JE, Zársky V, Synek L (2014) Dissecting a hidden gene duplication: the Arabidopsis thaliana SEC10 locus. PLoS ONE **9:** e94077

Walker JD, Oppenheimer DG, Concienne J, Larkin JC (2000) SIAMESE, a gene controlling the endoreduplication cell cycle in Arabidopsis thaliana trichomes. Development **127:** 3931–3940

Wang J, Ding Y, Wang J, Hillmer S, Miao Y, Lo SW, Wang X, Robinson DG, Jiang L (2010) EXPO, an exocyst-positive organelle distinct from multivesicular endosomes and autophagosomes, mediates cytosol to cell wall exocytosis in *Arabidopsis* and tobacco cells. Plant Cell **22:** 4009–4030

Wang S, Yin Y, Ma Q, Tang X, Hao D, Xu Y (2012) Genome-scale identification of cell-wall related genes in Arabidopsis based on co-expression network analysis. BMC Plant Biol **12:** 138

Wheeler RE (2010) multResp(lmPerm). The R Project for Statistical Computing. http://www.r-project.org/ (January 14, 2015)

Yamasaki S, Noguchi N, Mimaki K (2007) Continuous UV-B irradiation induces morphological changes and the accumulation of polyphenolic compounds on the surface of cucumber cotyledons. J Radiat Res (Tokyo) **48:** 443–454

Yan A, Pan J, An L, Gan Y, Feng H (2012) The responses of trichome mutants to enhanced ultraviolet-B radiation in Arabidopsis thaliana. J Photochem Photobiol B **113:** 29–35

Zársky V, Cvrcková F, Potocký M, Hála M (2009) Exocytosis and cell polarity in plants - exocyst and recycling domains. New Phytol **183:** 255–272

Zársky V, Kulich I, Fendrych M, Pecenková T (2013) Exocyst complexes multiple functions in plant cells secretory pathways. Curr Opin Plant Biol **16:** 726–733

Zhao FJ, Lombi E, Breedon T, McGrath SP (2000) Zinc hyperaccumulation and cellular distribution in *Arabidopsis halleri*. Plant Cell Environ **23:** 507–514

Zhao Y, Liu J, Yang C, Capraro BR, Baumgart T, Bradley RP, Ramakrishnan N, Xu X, Radhakrishnan R, Svitkina T, et al (2013) Exo70 generates membrane curvature for morphogenesis and cell migration. Dev Cell **26:** 266–278

8.2 Article 2

12 pages (57—68)

Exocyst Subunit EXO70H4 Has a Specific Role in Callose Synthase Secretion and Silica Accumulation[1][OPEN]

Ivan Kulich,[a,2,3] Zdeňka Vojtíková,[a,2] Peter Sabol,[a] Jitka Ortmannová,[a,b] Vilém Nedela,[c] Eva Tihlaříková,[c] and Viktor Zárský[a,b]

[a]Department of Experimental Plant Biology, Faculty of Sciences, Charles University, Prague, Czech Republic
[b]Institute of Experimental Botany, Academy of Sciences of the Czech Republic, Prague, Czech Republic
[c]Institute of Scientific Instruments of the Academy of Sciences of the Czech Republic, Brno, Czech Republic

ORCID IDs: 0000-0002-0458-6470 (I.K.); 0000-0001-9507-5600 (P.S.); 0000-0001-7626-1520 (J.O.); 0000-0001-6029-5435 (V.N.); 0000-0002-7983-2971 (E.T.); 0000-0002-5301-0339 (V.Z.).

Biogenesis of the plant secondary cell wall involves many important aspects, such as phenolic compound deposition and often silica encrustation. Previously, we demonstrated the importance of the exocyst subunit EXO70H4 for biogenesis of the trichome secondary cell wall, namely for deposition of the autofluorescent and callose-rich cell wall layer. Here, we reveal that EXO70H4-driven cell wall biogenesis is constitutively active in the mature trichome, but also can be activated elsewhere upon pathogen attack, giving this study a broader significance with an overlap into phytopathology. To address the specificity of EXO70H4 among the EXO70 family, we complemented the *exo70H4-1* mutant by 18 different Arabidopsis (*Arabidopsis thaliana*) EXO70 paralogs subcloned under the EXO70H4 promoter. Only EXO70H4 had the capacity to rescue the *exo70H4-1* trichome phenotype. Callose deposition phenotype of *exo70H4-1* mutant is caused by impaired secretion of PMR4, a callose synthase responsible for the synthesis of callose in the trichome. PMR4 colocalizes with EXO70H4 on plasma membrane microdomains that do not develop in the *exo70H4-1* mutant. Using energy-dispersive x-ray microanalysis, we show that both EXO70H4- and PMR4-dependent callose deposition in the trichome are essential for cell wall silicification.

The exocyst is a protein complex conserved across all eukaryotes, composed of eight subunits with a rod-like shape. Its main function described in yeast is tethering secretory vesicles to the plasma membrane (PM; Munson and Novick, 2006). Two exocyst subunits, SEC3 and EXO70, were described as spatial landmarks for polarized secretion in yeast. It was clearly shown that SEC3 is capable of working as a landmark by itself, whereas EXO70 likely requires additional signaling factors to work (Luo et al., 2014), such as small GTPases (Wu et al., 2010). The rest of the complex, also referred to as the exocyst core, is associated with secretory vesicles and is regulated via RAB GTPase interactions (Robinson et al., 1999). Most of the time, all exocyst subunits form a relatively stable holocomplex in yeast (Heider et al., 2016; Picco et al., 2017). The interaction of the exocyst core with SEC3 and EXO70 subunits at the PM mediates the tethering of the vesicle to the membrane, followed by the SNARE protein-mediated fusion of the vesicle with the membrane (Heider and Munson, 2012; Yue et al., 2017). Besides conventional roles, the animal EXO70 protein was shown to induce membrane curvature (Zhao et al., 2013).

In comparison with yeast and mammalian genomes, which encode only one or two EXO70s, land plant genomes encode a high number of EXO70 paralogs, which likely emerged during land colonization. The Arabidopsis (*Arabidopsis thaliana*) genome encodes 23 EXO70 paralogs (Elias et al., 2003; Cvrcková et al., 2012). EXO70A1, the most basal EXO70, has been shown to be involved in the secretion of membrane proteins such as PIN1 or BRI1 (Drdová et al., 2013). It

[1] This work was supported by the Grant Agency of Czech Republic (grant nos. 14-27329P and GF16-34887L), the Czech Ministry of Education (grant no. NPUI LO1417), and the Grant Agency of Charles University [grant no. GA UK(CZ) 387515]. Microscopy was performed in the Laboratory of Confocal and Fluorescence Microscopy cofinanced by the European Regional Development Fund and the state budget of the Czech Republic (project nos. CZ.1.05/4.1.00/16.0347 and CZ.2.16/3.1.00/21515).

[2] These authors contributed equally to the article.

[3] Address correspondence to kulich@natur.cuni.cz.

Author contributions are as follows: I.K., construct preparation and transformation, callose synthase observations, colocalization and the cross-complementation studies (callose stainings and microscopy), callose synthase localization in the *exo70H4-1* mutant background, manuscript preparation; Z.V., construct and transgenic line preparation, cross-complementation study, microscopy of all 18 cross-complementations, aniline blue stainings, manuscript preparation; P.S., flg22- and chitin-induced EXO70H4 up-regulation, western blots, cloning of PMR4, manuscript editing; J.O., flg22-induced EXO70H4 up-regulation; V.N., ESEM studies, silica quantification, consultations on ESEM and EDS, figure preparation; E.T., ESEM studies, operating the ESEM microscope, acquiring images; V.Z., group leader work (consultations, manuscript editing).

The author responsible for distribution of materials integral to the findings presented in this article in accordance with the policy described in the Instructions for Authors (www.plantphysiol.org) is: Ivan Kulich (kulich@natur.cuni.cz).

[OPEN] Articles can be viewed without a subscription.
www.plantphysiol.org/cgi/doi/10.1104/pp.17.01693

also is crucial for the proper development of the Casparian strip (Kalmbach et al., 2017). EXO70A1 also is recruited to the microtubules decorating xylem secondary cell wall thickenings in a COG/VETH-dependent manner, where EXO70A1 recruits the exocyst complex and is responsible for the development of the cell wall thickenings (Oda et al., 2015; Vukašinovic et al., 2017). Another example of the exocyst recruitment was shown on EXO70B1, which is recruited to the PM by RIN4 (Sabol et al., 2017). Thus, besides direct lipid interaction, plant EXO70s also seem to be recruited by other proteins. Besides secretion, the EXO70B1 subunit functions in autophagy (Kulich et al., 2013), immune responses (Stegmann et al., 2013; Zhao et al., 2015), and stomatal opening (Hong et al., 2016; Seo et al., 2016). EXO70H1 and EXO70B2 were shown to facilitate the defense papilla buildup (Pecenková et al., 2011). Recently, we showed a role of the EXO70H4 paralog in Arabidopsis trichome cell wall maturation (Kulich et al., 2015).

Arabidopsis leaf trichomes are unicellular outgrowths with very specific polarized shape and two to four (but most frequently three) sharp branches. Their shape is easily and visibly distorted by numerous mutations, which, together with their large size and good accessibility, led to their popularity as a model for studies of plant cell morphogenesis (Hülskamp et al., 1994). They have been especially vital for studies of microtubule- and actin-dependent morphogenetic events (Saedler et al., 2004; Tian et al., 2015), but also serve as a model for deposition of cell wall components (Sinlapadech et al., 2007; Bischoff et al., 2010).

We previously demonstrated that the Arabidopsis trichome cell wall consists of two distinct domains, the basal thin cell wall of the bulb and apical thick cell wall. These domains are separated by a callose-rich structure named the Ortmannian ring (OR). Only the apical cell wall domain consists of an outer and inner layer. We showed that the development of the inner cell wall layer depends on the exocyst subunit EXO70H4 (Kulich et al., 2015). However, we did not provide a detailed description, subcellular localization, and the functional context of EXO70H4. Here, we focused on the EXO70H4-dependent callose deposition, as the lack of callose is one of the most prominent defects of the *exo70H4-1* mutant and because callose deposition is of great interest due to its involvement in plant immunity.

Callose is a cell wall polymer, β-1-3-glucan that is involved in many plant developmental processes, such as cell plate formation (Hong et al., 2001), the development of phloem (Bonke et al., 2003), stomata (Guseman et al., 2010), pollen, and pollen tube, as well as regulations of plasmodesmatal permeability (Iglesias and Meins, 2000). It also is deposited in response to abiotic and biotic stress stimuli like wounding, pathogen invasion, or heavy metals exposure (Frye and Innes, 1998; Blümke et al., 2013; Ellinger et al., 2013, 2014).

In contrast to cellulose, a β-1-4-glucan that is crystallized into permanent microfibrils, callose is deposited as an amorphous plug, and often only transiently, because it is specifically and rapidly degraded by the hydrolytic enzymes β-1-3-glucanases (Levy et al., 2007). Callose is synthesized at the PM by large glucan synthase complexes called callose synthases (CalS) or glucan synthase-like (GSL). The Arabidopsis genome contains 12 CalS genes, which fall into two groups (Verma and Hong, 2001). *CalS* from the first group contain up to 50 exons and are some of the longest genes found in the Arabidopsis genome. The second group consists of *CalS11* (*GSL1*) and *CalS12* (*GSL5*), containing two and three exons, respectively (Hong et al., 2001). Different CalS are expressed in a tissue-specific way in response to diverse physiological conditions (Dong et al., 2008).

It is supposed that callose synthases are transported to the sites of callose synthesis by vesicle trafficking and that the cytoskeleton and endomembrane system are necessary for callose synthase distribution, transport, and positioning (Cai et al., 2011; Drakakaki et al., 2012). Despite pilot observations of callose synthase transport by vesicle-like bodies (Cai et al., 2011; Drakakaki et al., 2012; Nielsen et al., 2012), strong evidence is missing.

In this study, we worked with two callose synthase proteins: CalS9 (GSL10) and CalS12. CalS9 is known to act in male gametophyte development with mutants defective in pollen mitotic division (Töller et al., 2008; Huang et al., 2009), and it is one of the most transcribed callose synthases in the trichome (Jakoby et al., 2008). CalS12, also known as powdery mildew resistant 4 (PMR4), is a stress-induced callose synthase (Vogel and Somerville, 2000). Knockout mutants lack pathogen-induced callose deposits (Jacobs et al., 2003; Ellinger et al., 2013). One of the possible roles for the callose deposits may be inducing mechanical stiffness in the cell wall by supporting its silicification.

Silica is a nonessential micronutrient absorbed by plants in the form of silicic acid, $Si(OH)_4$, and deposited in different amounts into cell walls of various tissues and structures. Typically, trichome cell walls of many plants are encrusted with silica. Some observations suggest that silica deposition may be related to callose synthesis. The co-occurrence of callose and silica deposition was previously shown in several plant species, including silica hyperaccumulators, for example, in the common horsetail (*Equisetum arvense*; Law and Exley, 2011), in epidermal trichomes of numerous species (Waterkeyn and Dupont, 1982), *Selaginella* (Webster, 1992), and Arabidopsis (Brugiére and Exley, 2017). Callose was suggested as an inducing rather than catalyzing element of silicification, operating as a supportive matrix for the specific condensation of silicic acid into silica nanoparticles (Brugiére and Exley, 2017). There also is evidence that carbohydrates other than callose can act as organic matrices for silicification (Perry et al., 1987; Leroux et al., 2013; Guerriero et al., 2016), but also that in some cases no carbohydrates are needed (Hodson, 2016).

Despite this considerable evidence for the dependency of silica deposition on callose synthesis, a comprehensive analysis was still missing. In this report, we

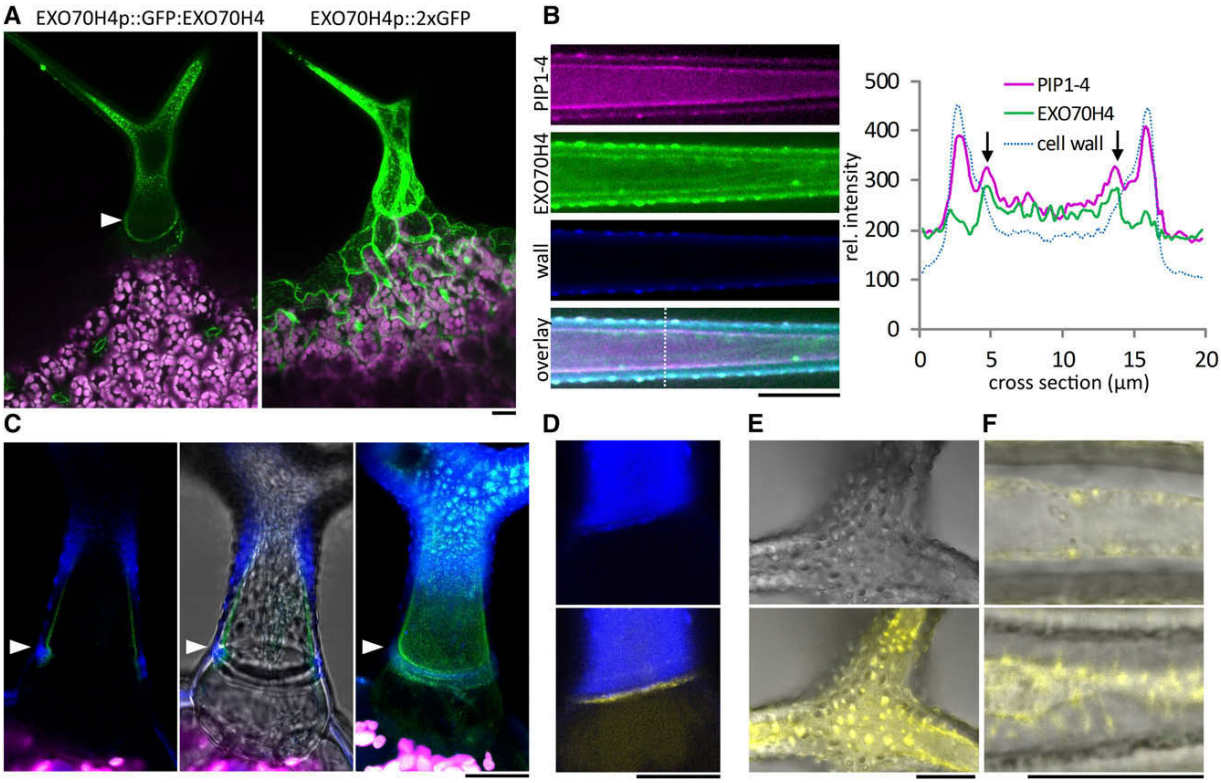

Figure 1. EXO70H4 localization in the trichome. A, EXO70H4 (green) under its native promoter is only visible in the trichome (left), but the EXO70H4 promoter is active also in other epidermal cells (right). Magenta represents chlorophyll; arrowhead points at the OR. B, EXO70H4 colocalizes with PM marker PIP1-4. Graph on the right represents plot of the profile depicted as white dotted line on the left. C, EXO70H4p::mGFP:EXO70H4 (green) localizes to the OR (white arrowheads) and the apical domain above the OR, which produces a highly autofluorescent cell wall (blue). Chlorophyll is in magenta. Left, Single section; middle, single section with transmission; right, z projection. D, A detail of the OR labeled by mCH-EXO70H4 (yellow) and the border of the apical autofluorescent cell wall domain (blue) and the basal domain. Top, Autofluorescence; bottom, autofluorescence and mCH-EXO70H4. E, Detailed view of the mCH-EXO70H4-positive cell wall ingrowths. Top, Transmission; bottom, transmission and mCH-EXO70H4. F, Plasmolysis of a trichome with labeled mCH-EXO70H4, without (top) and with (bottom) developed cell wall ingrowths. The differential attachment of the PM to the cell wall is visible. Bars = 20 μm.

demonstrate that callose is indispensable for silica deposition in Arabidopsis trichomes.

RESULTS

EXO70H4 Is Localized to the OR and a PM Domain above It

To observe the localization of the EXO70H4 protein, we generated native promoter-driven constructs with an N-terminal GFP and with mCHERRY (GFP-EXO70H4, mCH-EXO70H4). These constructs were proven to be functional, as they fully complemented the *exo70H4-1* mutation described previously (Kulich et al., 2015). In the absence of stress, EXO70H4 constructs were exclusively expressed in the trichome; however, the EXO70H4 promoter also was active in other epidermal cells, showing the capacity of EXO70H4 to be activated elsewhere (Fig. 1A). This also was true for other EXO70 paralogs expressed under the EXO70H4 promoter (see further), suggesting posttranscriptional regulation of EXO70H4. To show whether GFP-EXO70H4 localizes to specific PM domains, we looked for colocalization with the well-established PM marker mCHERRY-PIP1-4 (Geldner et al., 2009; Fig. 1B). Unfortunately, PIP1-4 is almost completely degraded in the mature trichome.

The localization of EXO70H4 very well matches the callose-rich and autofluorescent cell wall shown in Kulich et al. (2015). The XFP-EXO70H4 signal is always present at the OR and above it (apical domain) throughout trichome cell wall development (Fig. 1, A, C, and D). The presence of the EXO70H4 signal was always accompanied by cell wall autofluorescence. The basal PM domain beneath the OR is devoid of GFP-EXO70H4 (Fig. 1, A and D). Identical results were obtained using the mCHERRY construct mCH-EXO70H4 (Fig. 1, D–F). In young trichomes, the

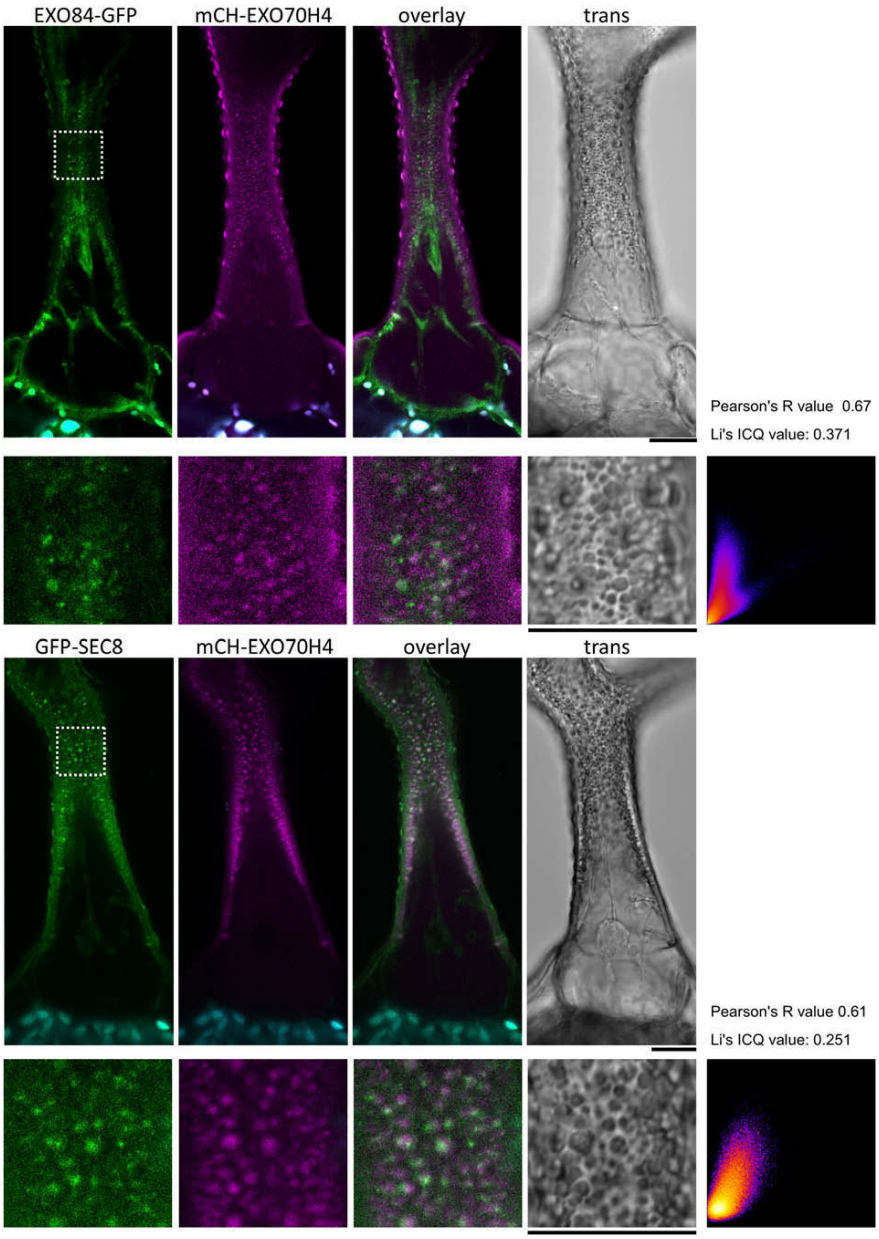

Figure 2. Colocalization of the core exocyst subunits with EXO70H4. SEC8 and EXO84 under their own natural promoters largely localize to the cytoplasm and partially localize to the EXO70H4-positive compartments. The ratio of both signals changes over time. Bars = 20 μm.

signal above the OR is homogeneous. In older trichomes, the signal becomes more speckled and accumulates at the differential interference contrast-visible cell wall ingrowths, which are a common feature of older trichomes (Fig. 1E). Upon plasmolysis, the mCH-EXO70H4 signal is easily separated from the cell wall of the young trichomes but is attached to the cell wall that has developed ingrowths along cytoplasmic strands (Fig. 1F). To confirm that these are actual cell wall ingrowths, we investigated the trichome cell wall from the inside using environmental scanning electron microscopy (ESEM; Supplemental Fig. S1).

On these ingrowths, mCH-EXO70H4 transiently colocalizes with the core exocyst subunits GFP-SEC8 and EXO84-GFP expressed under their respective natural promoters (Fig. 2). The core exocyst subunit signal is, however, visible also in the cytoplasm and in other membrane domains, suggesting their general function in secretion. These data fit with our previous yeast two-hybrid study, where EXO70H4 also physically

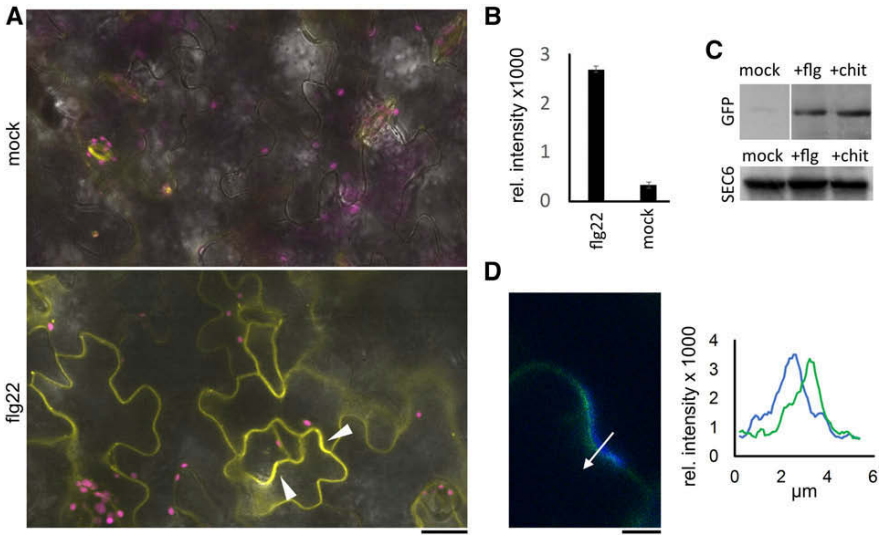

Figure 3. EXO70H4 up-regulation by flg22 in the leaf pavement cells. A, Representative images of leaves 5 h after flg22 treatment (spraying by 1 μM flg22 in 0.05% Silwet and 0.05% Silwet as control). Yellow, mCH-EXO70H4; magenta, chlorophyll; grays, transmission. Arrowheads depict domains with enchiched EXO70H4 signal. Scale bar = 20 μm. B, Quantification of the EXO70H4 signal intensity out of 10 plants and 100 cells. Similar results were obtained in three independent replicates, with both GFP- and mCHERRY-labeled constructs. C, Up-regulation of EXO70H4 in total cell extract from whole rosettes of GFP-EXO70H4 plants, 5 h after flg22 and chitin treatment. The white line is where one empty lane was left on the gel due to overflow. SEC6 was used as a loading control. D, GFP-EXO70H4 (green) forms a microdomain with enriched signal. This is accompanied by development of cell wall autofluorescence (blue). The arrow shows the position of the plot profile in D. Scale bar = 5 μm. Right, Plot profile demonstrating spatial separation of EXO70H4 and cell wall autofluorescence.

interacted with the Arabidopsis exocyst subunits SEC5A, SEC6, and EXO84b (Kulich et al., 2015).

Flg22 Induces EXO70H4 Expression in Epidermal Pavement Cells

Because the composition of the trichome inner cell wall layer highly resembles the pathogen-induced cell wall appositions, we investigated whether there is a possible function of EXO70H4 beyond the trichome. As shown in Figure 1A, the EXO70H4 promoter has a capacity to drive EXO70H4 expression in other epidermal cells, but the EXO70H4 protein is absent. Public microarray data suggest an elevation of the *EXO70H4* mRNA signal upon flg22 treatment. Therefore, we applied 1 μM flg22 by spraying on the mature Arabidopsis rosettes (24 d old). Four hours after the treatment, the first visible signal appeared in the epidermal pavement cells and peaked approximately 5 h after induction (Fig. 3A). The signal disappeared again 12 h after induction. We got similar results with both GFP and mCHERRY lines and quantified the fluorescence intensity (Fig. 3B). These results are supported by the western blot analysis of the total cell extract using an anti-GFP antibody and document similar up-regulation using chitin as elicitor (Fig. 3C). In many cells, the EXO70H4 signal was not evenly distributed across the cell surface and formed small domains of higher signal intensity. These domains developed cell wall autofluorescence similar to the autofluorescence of the trichome apical cell wall (Fig. 3D).

EXO70H4 Differs from Other Arabidopsis EXO70 Paralogs in Its Function and Subcellular Localization

To learn more about the specificity of EXO70H4 function, we performed a cross-complementation analysis, in which we subcloned multiple EXO70 paralogs under the EXO70H4 promoter. We subcloned 18 different EXO70 paralogs in the same fashion under EXO70H4 promoter (EXO70H4p::GFP:EXO70XY). We selected at least one gene from each subfamily (A–G) and all members of the subfamily H. Then, we transformed these constructs into the *exo70H4-1* mutant background and observed the development of trichome autofluorescence (Fig. 4, A and B) and trichome callose deposition (Supplemental Fig. S2). Both of these parameters provided us with identical results. Apart from EXO70H4, no other paralog could restore either the callose or autofluorescence, suggesting that the function of EXO70H4 is highly specific.

Most EXO70 paralogs showed no PM localization in the trichome (Supplemental Fig. S3). While EXO70A1 was uniformly distributed over the whole PM of the trichome (even beneath the OR; Fig. 4C), EXO70B1 and most of the other EXO70 paralogs showed cytoplasmic and nuclear localization.

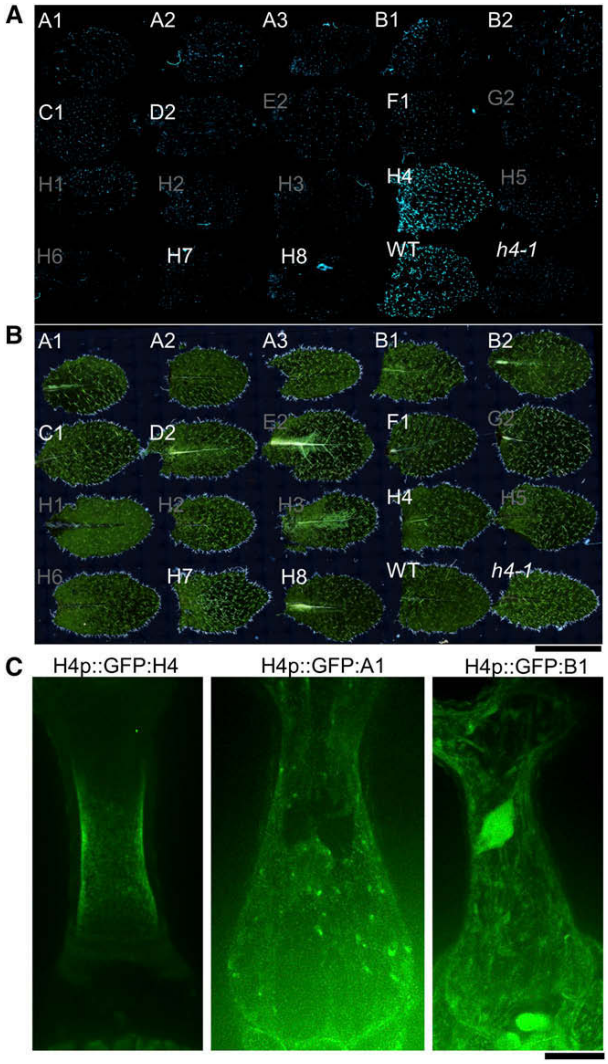

Figure 4. Complementation of the *exo70H4-1* mutant by multiple EXO70 paralogs. A, Autofluorescence of trichomes on leaves of individual transgenic lines (A1 stands for *exo70H4-1* complemented by EXO70H4p::GFP:EXO70A1, etc.), plus wild-type control (WT) and *exo70H4-1* mutant (*h4-1*). Gray letters label lines where no GFP signal was observed in the trichome. B, Dark-field view of A. Large images (A and B) consist of 475 tiles. Scale bar = 500 μm. C, Localization of selected EXO70 paralogs under the EXO70H4 promoter in *exo70H4-1* background (H4p::GFP:H4 stands for EXO70H4p::GFP:EXO70H4, etc.). Localizations of all 18 tested EXO70 paralogs are shown in Supplemental Figure S3.

Despite using an identical experimental setup, some of the EXO70 proteins (H1, E2, G2, H2, H3, H5, and H6) were not detected in the trichome, and therefore, we cannot exclude that some of these have the capacity to complement EXO70H4 on the protein level (Supplemental Fig. S3). This may be due to microRNA (miRNA) regulation of the EXO70 mRNA. We identified several miRNAs that may interfere with EXO70. The number of predicted interfering RNAs (based on Yi et al. [2015] database) is enhanced in the EXO70H subfamily (Supplemental Table S1).

EXO70H4 Is Essential for PM Localization of Callose Synthases in the Trichome

Since we showed that callose is absent from the *exo70H4-1* mutant trichomes (Kulich et al., 2015), we further investigated the callose synthase delivery to the PM. We worked with two callose synthases and generated ubiquitin promoter-driven callose synthase constructs UBQ::GFP:PMR4 (GFP-PMR4) and UBQ::GFP:CALS9 (GFP-CALS9). Here, we focus on PMR4, which is essential for the callose production in the trichome. We obtained similar results using CALS9. These can be found in the supplements (Supplemental Fig. S4).

As reported previously, *pmr4* mutants lack pathogen-induced callose deposits (Jacobs et al., 2003; Ellinger et al., 2013). In our hands, *pmr4* trichomes also lacked the visible callose, stained with aniline blue (Fig. 5A). This phenotype was complemented by transforming the *pmr4* mutant plants with GFP-PMR4 (Fig. 5B), demonstrating the functionality of this construct. In contrast to *exo70H4-1*, *pmr4* trichomes are mechanically stiff and show wild type-like autofluorescence (Fig. 5C).

Next, we introduced UBQ::GFP:PMR4 into the wild type and the *exo70H4-1* mutant line. In the wild-type trichome, the signal of both callose synthases was visible in immobile membrane speckles at the PM and also on mobile membrane bodies, possibly representing multiple steps of the secretory pathway (Fig. 6A). To separate mobile PMR4 fraction from the immobile PM dots, we performed time-series imaging and minimal-intensity projections (Fig. 6B). In the *exo70H4-1* mutant plants, the signal from the PM speckles was lost, suggesting a secretory defect of both of these callose synthases (Fig. 6, B–D).

By colocalization of EXO70H4p::mCHERRY:EXO70H4 with UBQ::GFP:PMR4, we show that the callose synthase speckles also are EXO70H4 positive (Fig. 6A). As described above, the signal of callose synthases was first visible in smaller transient speckles on the PM of young trichomes and developed later into large speckles. Taken together, our data show the dependency of callose synthase secretion on the EXO70H4 protein.

Silica Accumulation Is Dependent on Callose Deposition and Thus on the EXO70H4-Dependent PMR4 Secretion

While doing our ESEM studies of untreated biological samples (Tihlaríková et al., 2013; Nedela et al., 2015), we applied energy-dispersive x-ray spectroscopy for a semiquantitative analysis of elements in the trichome. Surprisingly, apart from heavy metals, we noticed a significant amount of silica in the domain above the OR.

This silica encrustation was absent in *exo70H4-1* mutant trichomes. To determine whether this was a direct effect of the *exo70H4-1* mutation, we next included a *pmr4* mutant (which lacks callose in the trichome), and we increased the amount of silica in the soil by watering with sodium silicate solution (final concentration 2 mM). As shown in Figure 7, both the *pmr4* and the *exo70H4-1* mutants had dramatically reduced silica levels in the trichomes. Therefore, we conclude that callose deposition is essential for cell wall silicification and that the *exo70H4-1* silica phenotype is a secondary phenotype, contingent on the impaired callose synthase delivery and the subsequent absence of callose synthesis.

DISCUSSION

In our previous study, we demonstrated the EXO70H4-dependent development of the callose-rich cell wall in the Arabidopsis trichome. Here, we show that EXO70H4 acts by promoting the secretion of callose synthase. Surprisingly, no other EXO70 subcloned under the EXO70H4 promoter was able to complement the *exo70H4-1* phenotype, despite high sequence similarity of some paralogs (Cvrcková et al., 2012). Since EXO70 proteins in general act as spatial landmarks for secretion, it is likely that the specificity of EXO70 paralogs reflects their differential target binding capacities. EXO70H4 decorates a specific PM subdomain in the trichome, while the most ancestral EXO70A1 localizes all over the trichome PM. This is consistent with the previous model of multiple recycling domains within one cell (Zárský et al., 2009). We also observed that some of the EXO70 paralogs with cytoplasmic localization in the trichome localize to the PM in the pavement cells (e.g. EXO70B1), suggesting differential regulatory mechanisms.

The cross-complementation analysis suggests that the EXO70H4-positive trichome PM domains have a highly distinctive character and cannot be recognized by other EXO70 paralogs. Previously, it was proposed that the EXO70 paralogs differ just in their expression pattern (Li et al., 2010). In this study, we demonstrate that there is functional divergence between the paralogs. This also is supported by other studies showing specific EXO70 roles (Kulich et al., 2013; Zhao et al., 2015) and recently by the specific PM domain localizations of NtEXO70A1 and NtEXO70B1 in tobacco (*Nicotiana tabacum*) pollen tubes (Sekereš et al., 2017).

Since EXO70 proteins are putative landmarks for secretion, the specificity of EXO70 paralogs could mainly be determined by different localization signals. For example, during xylogenesis, EXO70A1 localization to cortical microtubules is maintained by COG-VETH proteins (Oda et al., 2015; Vukašinovic et al., 2017). Also, as we showed recently, EXO70B1 PM localization can be achieved by protein-protein interaction with NOI family proteins (Sabol et al., 2017). We speculate that a similar mechanism, but with different proteins, may be responsible for the specific localization of many EXO70 paralogs, causing their functional diversity. Whether the process of EXO70H4 localization is mediated by specific lipid-binding properties or by interacting proteins is the subject of our follow-up study.

The initially homogenous PM signal of GFP-EXO70H4 develops later into stable speckles, which then form ingrowths of the cell wall. Similar behavior of the exocyst subunits was observed during xylogenesis, where EXO70A1-tagRFP first localized dispersedly to the PM and later on gradually organized into a bundled pattern (Vukašinovic et al., 2017). Such stabilization of the polarity was observed previously in budding yeast (*Saccharomyces cerevisiae*; Brennwald and Rossi, 2007). The mechanism of this stabilization in plants is not yet known, but in our opinion it may be achieved by a positive feedback loop, whereby the original EXO70 attracts vesicles with more exocyst subunits.

Unfortunately, not all the EXO70 constructs in our cross-complementation study were expressed in the trichome. We explain this by a predicted RNA interference regulation, which is common among stress-induced transcripts (Sunkar and Zhu, 2004), or by ubiquitination, which was previously manifested as a possible step in EXO70 protein regulation (Samuel et al., 2009; Stegmann et al., 2012; Seo et al., 2016). Very likely, EXO70s are subjected to a high degree of regulation at multiple levels.

Here, we show a secretory defect of the *exo70H4-1* mutation on one type of cargo: two callose synthases, which both localized and behaved similarly despite their functional classification. Of these, only CALS12 was biologically relevant for callose synthesis in the trichome. More cargo affected by the *exo70H4-1* mutation must exist, since the trichomes lacking only callose and silica in the case of the *pmr4* mutation are still mechanically relatively stiff and accumulate autofluorescent compounds and metals, unlike *exo70H4-1* mutants.

The inner cell wall of the trichome shares many similarities with the pathogen-induced cell wall (being rich in callose, silica, and phenolic compounds; Russo and Bushnell, 1989; Ghanmi et al., 2004), and as we show here, EXO70H4 has the capacity to contribute to such a cell wall biogenesis, since the EXO70H4 protein appears in nontrichome cells upon bacterial elicitor treatment, allowing PMR4 and other cargo secretion and callose synthesis. Deposited callose thereafter acts as a matrix for silica accumulation, which is known to modulate physical properties of the cell wall and acts as an important line of defense against fungal pathogens (Ghanmi et al., 2004; Fauteux et al., 2006; Vivancos et al., 2015). The exact relationship between callose and the silica accumulation was enigmatic for a long time, although it was clear that these processes are related (Law and Exley, 2011; Exley, 2015). First evidence that callose may be essential for silica deposition was provided recently (Brugiére and Exley, 2017), using chemical staining of silica. In our study, we extend these

observations with quantitative and statistically processed data. We also show that callose is not essential for the accumulation of phenolic compounds in the cell wall in contrast to some observations that lignification precedes silicification (Zhang et al., 2013).

While Arabidopsis trichomes contain relatively little silica, trichomes of species such as nettle (*Urtica dioica*) are well known for their silicified cell wall (Sangster and Hodson, 2007). Cucumber (*Cucumis sativus*) trichomes also contain silica, and supplementing plants with silica leads to physically stiffer trichomes (Samuels, 1993). In cucumber, basal cells of the trichomes (sometimes referred to as cells surrounding the trichome or the trichome spine) were the site of maximal silica deposition (Samuels et al., 1991a, 1991b; Chérif et al., 1992). Transcriptomic analyses have revealed that wild-type cucumber contains 406-fold more *CsEXO70H4* transcript than the trichome-less *tbh* mutant (Chen et al., 2014). This suggests that the mechanisms we describe in the Arabidopsis trichome may have more general implications for eurosids.

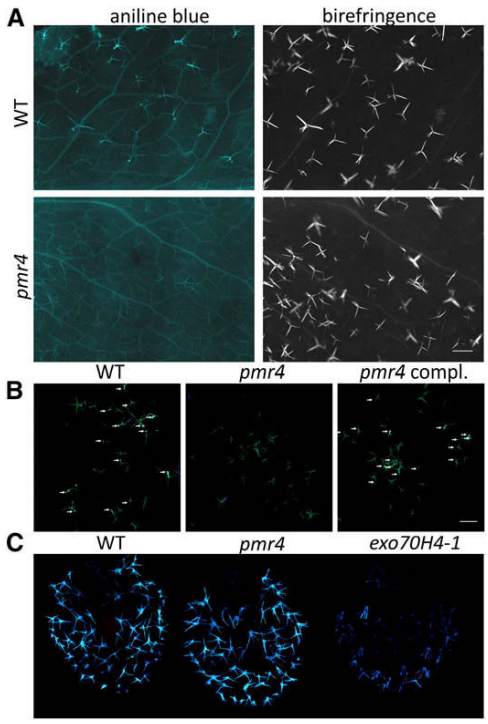

Figure 5. Trichome phenotype of *pmr4* mutant. A, Aniline blue staining of callose (left) and cellulose birefringence in polarized light (right) for *pmr4* (top) and wild type (WT; bottom) leaves. B, Aniline blue staining of callose on isolated trichomes of wild type, *pmr4*, and *pmr4* mutant complemented with UBQ::GFP:PMR4 construct (*pmr4* compl.); arrows point to trichomes with developed callose structures. Scale bar = 500 μm. C, Autofluorescence of phenolic compounds in broken (dead) trichomes of wild type, *pmr4*, and *exo70H4-1*, respectively.

MATERIALS AND METHODS

Plant Material and Growth

If not indicated otherwise, plants were grown in standard growth chamber conditions (long day 16 h:8 h, 100 μM photosynthetically active radiation m^{-2} s^{-1}). LT 36W/958 T8 BIOVITAL NARVA fluorescent tubes were used. These contain a UV-B peak. All plants were grown in Jiffy soil pellets. The *exo70H4-1* mutant was described previously (Kulich et al., 2015), as well as the *pmr4-1* mutant (Vogel and Somerville, 2000). As a control, a wild-type sibling of the *exo70H4-1* mutant was used. As a control for the *exo70H4-1* × *rdr6-12* double mutant, *rdr6-12* (Peragine et al., 2004) was used.

Callose Staining and Autofluorescence Visualization

To stain for callose, whole leaves were washed for 3 h in acetic acid:ethanol (1:3) solution, washed three times in deionized water, and incubated overnight in aniline blue solution (150 mM KH_2PO_4 and 0.01% [w/v] aniline blue, pH 9.5). Trichomes were then imaged on leaves or brushed off and imaged.

For autofluorescence development, leaves were placed in between two microscopy slides and dried up overnight. Fifth and sixth leaves of the 24- to 28-d-old rosettes were used for the aniline blue staining and the third youngest visible leaf for autofluorescence observations.

PAMP Treatments

Flg22 (1 μM) or chitosan solution (150 mg/L) with 0.05% Silwet Star wetting agent was sprayed onto the 24-d-old Arabidopsis (*Arabidopsis thaliana*) rosettes stably transformed with XFP-EXO70H4. Silwet Star (0.05%) was used as a control. Signal was observed 4 to 5 h after the treatment. This experiment was done in triplicate. Spraying was critical factor for the EXO70H4 up-regulation. Protein extract from whole rosettes was used for the western blot analysis, using primary anti-GFP and anti-SEC6 antibodies (Agrisera; AS15 2987 and AS13 2686, respectively).

Construct and Transgenic Line Preparation

For the cloning of all EXO70 paralogs, a multisite gateway approach was used. The EXO70H4 promoter (1 kb upstream) was subcloned into pDONORP4-P1r. GFP in pEN-L1-F-L2 (GFP) was obtained from Karimi et al. (2007). pEN-L1-mCherry-L2 was obtained from Mylle et al. (2013); however, since this construct had a stop codon, we used it as a template to generate a new pDONOR 221-mCherry construct. EXO70 coding sequences were amplified in one or two steps (with att extension primers) and subcloned into the pDONOR P2R-P3 using Gateway BP clonase (Invitrogen). Then, multisite reactions were performed using the EXO70H4 promoter, GFP, EXO70 coding sequence, and destination vector pB7m34GW (BASTA plant selection; Karimi et al., 2007). pDONOR vectors were sequenced using M13 primers. The destination binary constructs were sequenced using M13 primers and two GFP primers (see primer list in Supplemental Table S2). To clone callose synthase PMR4, the genomic fragment was subcloned into pDONOR 221 using Gateway BP clonase and then transferred into the pUBN-GFP vector (Grefen et al., 2010) using Gateway LR clonase. Since the CalS9 genomic fragment is too long to amplify, we isolated the cDNA. This was stitched together from two parts, as none of transcripts had all 42 introns properly spliced. GFP-SEC8 and EXO84b-GFP lines were described previously (Fendrych et al., 2013). All primers in this study are listed in Supplemental Table S2.

All prepared constructs were electroporated into *Agrobacterium tumefaciens* GV3101 competent cells. The floral dip method (Clough and Bent, 1998) of plant transformation was used, and the transformants were selected on soil by spraying with BASTA (150 mg/L of glufosinate-NH_4). At least five individual transformants were observed in each experiment, and at least two biological replicates were made.

Light Microscopy

Zeiss LSM880 with C-Apochromat 40×/1.2 W Korr FCS M27 objective was used for Figures 1, 4, and 5 [GFP (488): 508–540 nm, chlorophyll (488) 650–721 nm, cell wall autofluorescence (405) 426–502, mCHERRY (561) 597–641]. For Figure 4C and Supplemental Figures S3 and S4, we used

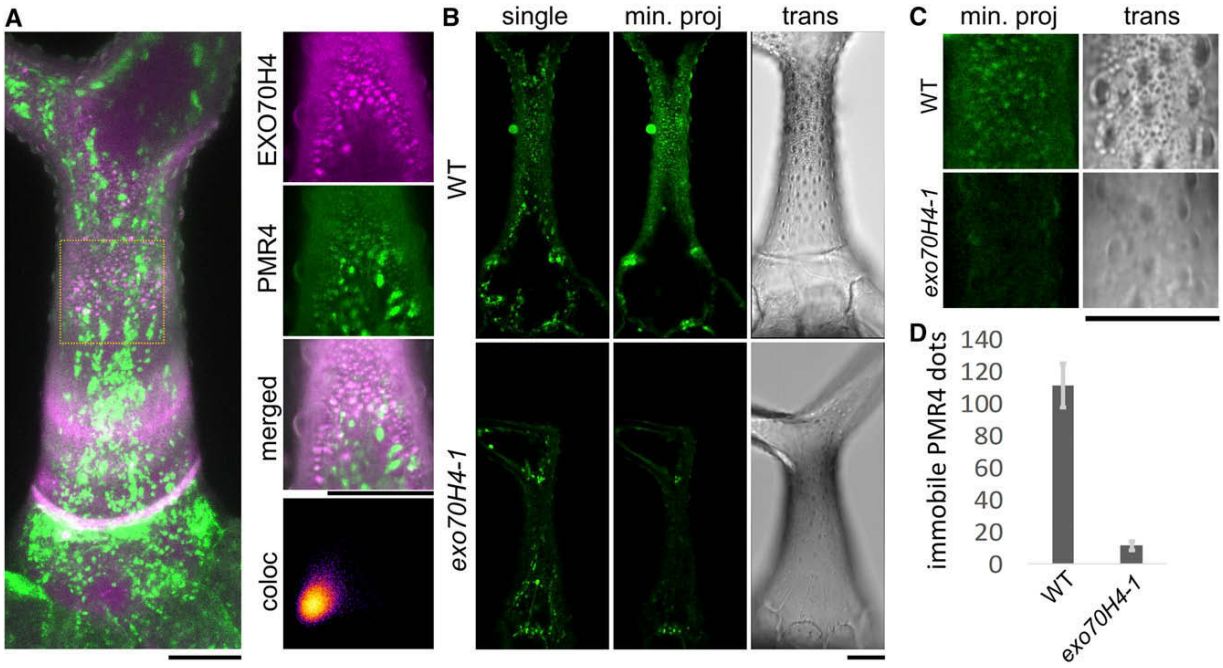

Figure 6. EXO70H4 recruits PMR4 to the ingrowths of the trichome cell wall. A, Left, Overall view of the trichome expressing mCH-EXO70H4 (magenta) and GFP-PMR4 (green). Projection of 14 sections. Yellow dotted square depicts detailed view on the right. Right, Detailed view of a single section with cell wall ingrowths decorated by EXO70H4 and PMR4 with a 2D histogram for the colocalization (Pearson's R value, 0.35; Li's ICQ value, 0,127). B, PMR4-positive cell wall ingrowths are absent in the *exo70H4-1* mutant. In the single frame, both the mobile endomembrane fraction and the immobile ingrowths are visible. The mobile fraction is reduced by minimal intensity projection (min. proj.). C, A detail of the ingrowths from B. D, Quantification of the immobile dots in a blind study using the minimal intensity projections. WT, Wild type; bars = 20 μm.

Yokogawa CSU-X1 on Nikon Ti-698 E platform, Agilent MLC400 laser box, and iXON camera (Andor) using filter stringent cubes for GFP and RFP. For Figure 4, A and B, and Supplemental Figure S2, Nikon Eclipse 90i with PlanApo 4×/0.2 objective and Nikon DsFi 2 camera were used. Images were processed using the Fiji platform (Schindelin et al., 2012).

ESEM and Energy-Dispersive X-Ray Microanalysis

For a semiquantitative energy-dispersive x-ray microanalysis (EDS), four trichomes from eight leaves were selected for each of the three samples (wild type, *pmr4*, and *exo70H4-1*), air dried, and placed on a carbon pad. To maximize

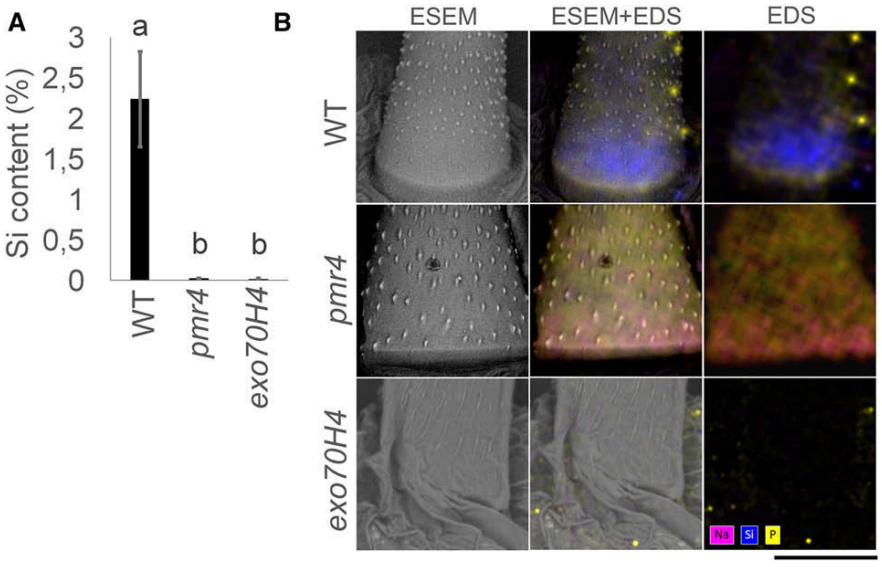

Figure 7. The presence of silica in Arabidopsis trichomes is dependent on callose. A, Quantification of the silica content in multiple genotypes grown on a soil containing 2 mM sodium silicate. Error bars represent SES. Letters above the bars: mean significant differences (HSD Tukey post hoc test, $P < 0.01$). B, Examples of trichomes accumulating silicon (blue signal). The accumulation is prominent in the apical domain above the OR. Note that the *exo70H4-1* cell wall collapsed due to its mechanical properties. Elements such as sodium (magenta) and phosphate (yellow) also are indicated. Scale bar = 30 μm. WT, Wild type.

detection efficiency and accuracy of the analysis, trichomes were selected according to their shape and shadowing in x-ray maps using a solid-state detector of backscattered electrons and fast EDS mapping. Dried, chemical treatment-free, and conductive coating-free samples were imaged and analyzed using ESEM Quanta 650 FEG equipped with EDS silicon drift detector Bruker Quantax 400 XFlash 6/60 under beam energy 10 keV, beam current 100 pA, working distance 10 mm, and water vapor pressure 100 Pa. The ratio of silicon in the sample was calculated as the median values obtained from all trichomes for each sample.

The cell wall of the mature Arabidopsis trichome was in situ opened using two Kleindiek micromanipulators MM3A-EM, thus without any manipulation, cutting, or contamination outside the specimen chamber of ESEM. The inner surface of the trichome (Supplemental Fig. S1) was imaged using gaseous secondary electron detector under beam energy 10 keV, beam current 50 pA, working distance 11.5 mm, and water vapor pressure 170 Pa.

Supplemental Data

The following supplemental materials are available.

Supplemental Figure S1. ESEM view of the inner structure of the fresh mature Arabidopsis trichome cell wall.

Supplemental Figure S2. Complementation of the *exo70H4-1* mutant by multiple EXO70 paralogs.

Supplemental Figure S3. Overview of EXO70 paralog localization in the trichome.

Supplemental Figure S4. EXO70H4-dependent Cals9 delivery.

Supplemental Table S1. RNA interference of EXO70 paralogs.

Supplemental Table S2. List of primers used in this study.

ACKNOWLEDGMENTS

We thank Lukáš Fischer for the motivation to look for the putative EXO70s regulating miRNAs and our technician Marta Čadyová, Patrick Moxon, and Matouš Glanc for a significant improvement of the cloning methods and for constructs provided.

Received November 27, 2017; accepted January 2, 2018; published January 4, 2018.

LITERATURE CITED

Bischoff V, Nita S, Neumetzler L, Schindelasch D, Urbain A, Eshed R, Persson S, Delmer D, Scheible W-R (2010) TRICHOME BIREFRINGENCE and its homolog AT5G01360 encode plant-specific DUF231 proteins required for cellulose biosynthesis in Arabidopsis. Plant Physiol **153:** 590–602

Blümke A, Somerville SC, Voigt CA (2013) Transient expression of the *Arabidopsis thaliana* callose synthase PMR4 increases penetration resistance to powdery mildew in barley. Adv Biosci Biotechnol **04:** 810–813

Bonke M, Thitamadee S, Mähönen AP, Hauser M-T, Helariutta Y (2003) APL regulates vascular tissue identity in Arabidopsis. Nature **426:** 181–186

Brennwald P, Rossi G (2007) Spatial regulation of exocytosis and cell polarity: yeast as a model for animal cells. FEBS Lett **581:** 2119–2124

Brugiére T, Exley C (2017) Callose-associated silica deposition in Arabidopsis. J Trace Elem Med Biol **39:** 86–90

Cai G, Faleri C, Del Casino C, Emons AMC, Cresti M (2011) Distribution of callose synthase, cellulose synthase, and sucrose synthase in tobacco pollen tube is controlled in dissimilar ways by actin filaments and microtubules. Plant Physiol **155:** 1169–1190

Chen C, Liu M, Jiang L, Liu X, Zhao J, Yan S, Yang S, Ren H, Liu R, Zhang X (2014) Transcriptome profiling reveals roles of meristem regulators and polarity genes during fruit trichome development in cucumber (Cucumis sativus L.). J Exp Bot **65:** 4943–4958

Chérif M, Menzies JG, Benhamou N, Bélanger RR (1992) Studies of silicon distribution in wounded and Pythium ultimum infected cucumber plants. Physiol Mol Plant Pathol **41:** 371–385

Clough SJ, Bent AF (1998) Floral dip: a simplified method for Agrobacterium-mediated transformation of Arabidopsis thaliana. Plant J **16:** 735–743

Cvrcková F, Grunt M, Bezvoda R, Hála M, Kulich I, Rawat A, Zárský V (2012) Evolution of the land plant exocyst complexes. Front Plant Sci **3:** 159

Dong X, Hong Z, Chatterjee J, Kim S, Verma DPS (2008) Expression of callose synthase genes and its connection with Npr1 signaling pathway during pathogen infection. Planta **229:** 87–98

Drakakaki G, van de Ven W, Pan S, Miao Y, Wang J, Keinath NF, Weatherly B, Jiang L, Schumacher K, Hicks G, et al (2012) Isolation and proteomic analysis of the SYP61 compartment reveal its role in exocytic trafficking in Arabidopsis. Cell Res **22:** 413–424

Drdová EJ, Synek L, Pecenková T, Hála M, Kulich I, Fowler JE, Murphy AS, Zárský V (2013) The exocyst complex contributes to PIN auxin efflux carrier recycling and polar auxin transport in Arabidopsis. Plant J **73:** 709–719

Elias M, Drdova E, Ziak D, Bavlnka B, Hala M, Cvrckova F, Soukupova H, Zarsky V (2003) The exocyst complex in plants. Cell Biol Int **27:** 199–201

Ellinger D, Glöckner A, Koch J, Naumann M, Stürtz V, Schütt K, Manisseri C, Somerville SC, Voigt CA (2014) Interaction of the Arabidopsis GTPase RabA4c with its effector PMR4 results in complete penetration resistance to powdery mildew. Plant Cell **26:** 3185–3200

Ellinger D, Naumann M, Falter C, Zwikowics C, Jamrow T, Manisseri C, Somerville SC, Voigt CA (2013) Elevated early callose deposition results in complete penetration resistance to powdery mildew in Arabidopsis. Plant Physiol **161:** 1433–1444

Exley C (2015) A possible mechanism of biological silicification in plants. Front Plant Sci **6:** 853

Fauteux F, Chain F, Belzile F, Menzies JG, Bélanger RR (2006) The protective role of silicon in the Arabidopsis-powdery mildew pathosystem. Proc Natl Acad Sci USA **103:** 17554–17559

Fendrych M, Synek L, Pecenková T, Drdová EJ, Sekeres J, de Rycke R, Nowack MK, Zársky V (2013) Visualization of the exocyst complex dynamics at the plasma membrane of Arabidopsis thaliana. Mol Biol Cell **24:** 510–520

Frye CA, Innes RW (1998) An Arabidopsis mutant with enhanced resistance to powdery mildew. Plant Cell **10:** 947–956

Geldner N, Dénervaud-Tendon V, Hyman DL, Mayer U, Stierhof Y-D, Chory J (2009) Rapid, combinatorial analysis of membrane compartments in intact plants with a multicolor marker set. Plant J **59:** 169–178

Ghanmi D, McNally DJ, Benhamou N, Menzies JG, Bélanger RR (2004) Powdery mildew of Arabidopsis thaliana: a pathosystem for exploring the role of silicon in plant–microbe interactions. Physiol Mol Plant Pathol **64:** 189–199

Grefen C, Donald N, Hashimoto K, Kudla J, Schumacher K, Blatt MR (2010) A ubiquitin-10 promoter-based vector set for fluorescent protein tagging facilitates temporal stability and native protein distribution in transient and stable expression studies. Plant J **64:** 355–365

Guerriero G, Hausman J-F, Legay S (2016) Silicon and the plant extracellular matrix. Front Plant Sci **7:** 463

Guseman JM, Lee JS, Bogenschutz NL, Peterson KM, Virata RE, Xie B, Kanaoka MM, Hong Z, Torii KU (2010) Dysregulation of cell-to-cell connectivity and stomatal patterning by loss-of-function mutation in Arabidopsis chorus (glucan synthase-like 8). Development **137:** 1731–1741

Heider MR, Gu M, Duffy CM, Mirza AM, Marcotte LL, Walls AC, Farrall N, Hakhverdyan Z, Field MC, Rout MP, et al (2016) Subunit connectivity, assembly determinants and architecture of the yeast exocyst complex. Nat Struct Mol Biol **23:** 59–66

Heider MR, Munson M (2012) Exorcising the exocyst complex. Traffic **13:** 898–907

Hodson MJ (2016) The development of phytoliths in plants and its influence on their chemistry and isotopic composition. Implications for palaeoecology and archaeology. J Archaeol Sci **68:** 62–69

Hong D, Jeon BW, Kim SY, Hwang J-U, Lee Y (2016) The ROP2-RIC7 pathway negatively regulates light-induced stomatal opening by inhibiting exocyst subunit Exo70B1 in Arabidopsis. New Phytol **209:** 624–635

Hong Z, Delauney AJ, Verma DP (2001) A cell plate-specific callose synthase and its interaction with phragmoplastin. Plant Cell **13:** 755–768

Huang L, Chen X-Y, Rim Y, Han X, Cho WK, Kim S-W, Kim J-Y (2009) Arabidopsis glucan synthase-like 10 functions in male gametogenesis. J Plant Physiol **166:** 344–352

Hülskamp M, Misŕa S, Jürgens G (1994) Genetic dissection of trichome cell development in Arabidopsis. Cell **76:** 555–566

Iglesias VA, Meins F Jr (2000) Movement of plant viruses is delayed in a beta-1,3-glucanase-deficient mutant showing a reduced plasmodesmatal size exclusion limit and enhanced callose deposition. Plant J **21:** 157–166

Jacobs AK, Lipka V, Burton RA, Panstruga R, Strizhov N, Schulze-Lefert P, Fincher GB (2003) An Arabidopsis callose synthase, GSL5, is required for wound and papillary callose formation. Plant Cell **15:** 2503–2513

Jakoby MJ, Falkenhan D, Mader MT, Brininstool G, Wischnitzki E, Platz N, Hudson A, Hülskamp M, Larkin J, Schnittger A (2008) Transcriptional profiling of mature Arabidopsis trichomes reveals that NOECK encodes the MIXTA-like transcriptional regulator MYB106. Plant Physiol **148:** 1583–1602

Kalmbach L, Hématy K, De Bellis D, Barberon M, Fujita S, Ursache R, Daraspe J, Geldner N (2017) Transient cell-specific EXO70A1 activity in the CASP domain and Casparian strip localization. Nat Plants **3:** 17058

Karimi M, Bleys A, Vanderhaeghen R, Hilson P (2007) Building blocks for plant gene assembly. Plant Physiol **145:** 1183–1191

Kulich I, Pecenková T, Sekereš J, Smetana O, Fendrych M, Foissner I, Höftberger M, Zárský V (2013) Arabidopsis exocyst subcomplex containing subunit EXO70B1 is involved in autophagy-related transport to the vacuole. Traffic **14:** 1155–1165

Kulich I, Vojtíková Z, Glanc M, Ortmannová J, Rasmann S, Zárský V (2015) Cell wall maturation of Arabidopsis trichomes is dependent on exocyst subunit EXO70H4 and involves callose deposition. Plant Physiol **168:** 120–131

Law C, Exley C (2011) New insight into silica deposition in horsetail (Equisetum arvense). BMC Plant Biol **11:** 112

Leroux O, Leroux F, Mastroberti AA, Santos-Silva F, Van Loo D, Bagniewska-Zadworna A, Van Hoorebeke L, Bals S, Popper ZA, de Araujo Mariath JE (2013) Heterogeneity of silica and glycan-epitope distribution in epidermal idioblast cell walls in Adiantum raddianum laminae. Planta **237:** 1453–1464

Levy A, Erlanger M, Rosenthal M, Epel BL (2007) A plasmodesmata-associated β-1,3-glucanase in Arabidopsis. Plant J **49:** 669–682

Li S, van Os GMA, Ren S, Yu D, Ketelaar T, Emons AMC, Liu C-M (2010) Expression and functional analyses of EXO70 genes in Arabidopsis implicate their roles in regulating cell type-specific exocytosis. Plant Physiol **154:** 1819–1830

Luo G, Zhang J, Guo W (2014) The role of Sec3p in secretory vesicle targeting and exocyst complex assembly. Mol Biol Cell **25:** 3813–3822

Munson M, Novick P (2006) The exocyst defrocked, a framework of rods revealed. Nat Struct Mol Biol **13:** 577–581

Mylle E, Codreanu M-C, Boruc J, Russinova E (2013) Emission spectra profiling of fluorescent proteins in living plant cells. Plant Methods **9:** 10

Nedela V, Tihlaríková E, Hrib J (2015) The low-temperature method for study of coniferous tissues in the environmental scanning electron microscope. Microsc Res Tech **78:** 13–21

Nielsen ME, Feechan A, Böhlenius H, Ueda T, Thordal-Christensen H (2012) Arabidopsis ARF-GTP exchange factor, GNOM, mediates transport required for innate immunity and focal accumulation of syntaxin PEN1. Proc Natl Acad Sci USA **109:** 11443–11448

Oda Y, Iida Y, Nagashima Y, Sugiyama Y, Fukuda H (2015) Novel coiled-coil proteins regulate exocyst association with cortical microtubules in xylem cells via the conserved oligomeric golgi-complex 2 protein. Plant Cell Physiol **56:** 277–286

Pecenková T, Hála M, Kulich I, Kocourková D, Drdová E, Fendrych M, Toupalová H, Zársky V (2011) The role for the exocyst complex subunits Exo70B2 and Exo70H1 in the plant-pathogen interaction. J Exp Bot **62:** 2107–2116

Peragine A, Yoshikawa M, Wu G, Albrecht HL, Poethig RS (2004) SGS3 and SGS2/SDE1/RDR6 are required for juvenile development and the production of trans-acting siRNAs in Arabidopsis. Genes Dev **18:** 2368–2379

Perry CC, Williams RJP, Fry SC (1987) Cell wall biosynthesis during silicification of grass hairs. J Plant Physiol **126:** 437–448

Picco A, Irastorza-Azcarate I, Specht T, Böke D, Pazos I, Rivier-Cordey A-S, Devos DP, Kaksonen M, Gallego O (2017) The in vivo architecture of the exocyst provides structural basis for exocytosis. Cell **168:** 400–412.e18

Robinson NGG, Guo L, Imai J, Toh-E A, Matsui Y, Tamanoi F (1999) Rho3 of Saccharomyces cerevisiae, which regulates the actin cytoskeleton and exocytosis, is a GTPase which interacts with Myo2 and Exo70. Mol Cell Biol **19:** 3580–3587

Russo VM, Bushnell WR (1989) Responses of barley cells to puncture by microneedles and to attempted penetration by Erysiphe graminis f.sp. hordei. Can J Bot **67:** 2912–2921

Sabol P, Kulich I, Zárský V (2017) RIN4 recruits the exocyst subunit EXO70B1 to the plasma membrane. J Exp Bot **68:** 3253–3265

Saedler R, Mathur N, Srinivas BP, Kernebeck B, Hülskamp M, Mathur J (2004) Actin control over microtubules suggested by DISTORTED2 encoding the Arabidopsis ARPC2 subunit homolog. Plant Cell Physiol **45:** 813–822

Samuel MA, Chong YT, Haasen KE, Aldea-Brydges MG, Stone SL, Goring DR (2009) Cellular pathways regulating responses to compatible and self-incompatible pollen in Brassica and Arabidopsis stigmas intersect at Exo70A1, a putative component of the exocyst complex. Plant Cell **21:** 2655–2671

Samuels A (1993) The effects of silicon supplementation on cucumber fruit: changes in surface characteristics. Ann Bot **72:** 433–440

Samuels AL, Glass ADM, Ehret DL, Menzies JG (1991a) Mobility and deposition of silicon in cucumber plants. Plant Cell Environ **14:** 485–492

Samuels AL, Glass ADM, Ehret DL, Menzies JG (1991b) Distribution of silicon in cucumber leaves during infection by powdery mildew fungus (*Sphaerotheca fuliginea*). Can J Bot **69:** 140–146

Sangster AG, Hodson MJ (2007) Silica in higher plants. *In* D Evered, M O'Connor, eds, Novartis Foundation Symposia: Silicon Biochemistry. John Wiley & Sons, Chichester, UK, pp 90–111

Schindelin J, Arganda-Carreras I, Frise E, Kaynig V, Longair M, Pietzsch T, Preibisch S, Rueden C, Saalfeld S, Schmid B, et al (2012) Fiji: an open-source platform for biological-image analysis. Nat Methods **9:** 676–682

Sekereš J, Pejchar P, Šantrucek J, Vukašinovic N, Zárský V, Potocký M (2017) Analysis of exocyst subunit EXO70 family reveals distinct membrane polar domains in tobacco pollen tubes. Plant Physiol **173:** 1659–1675

Seo DH, Ahn MY, Park KY, Kim EY, Kim WT (2016) The N-terminal UND motif of the Arabidopsis U-box E3 ligase PUB18 is critical for the negative regulation of ABA-mediated stomatal movement and determines its ubiquitination specificity for exocyst subunit Exo70B1. Plant Cell **28:** 2952–2973

Sinlapadech T, Stout J, Ruegger MO, Deak M, Chapple C (2007) The hyper-fluorescent trichome phenotype of the brt1 mutant of Arabidopsis is the result of a defect in a sinapic acid: UDPG glucosyltransferase. Plant J **49:** 655–668

Stegmann M, Anderson RG, Ichimura K, Pecenkova T, Reuter P, Zársky V, McDowell JM, Shirasu K, Trujillo M (2012) The ubiquitin ligase PUB22 targets a subunit of the exocyst complex required for PAMP-triggered responses in Arabidopsis. Plant Cell **24:** 4703–4716

Stegmann M, Anderson RG, Westphal L, Rosahl S, McDowell JM, Trujillo M (2013) The exocyst subunit Exo70B1 is involved in the immune response of Arabidopsis thaliana to different pathogens and cell death. Plant Signal Behav **8:** e27421

Sunkar R, Zhu J-K (2004) Novel and stress-regulated microRNAs and other small RNAs from Arabidopsis. Plant Cell **16:** 2001–2019

Tian J, Han L, Feng Z, Wang G, Liu W, Ma Y, Yu Y, Kong Z (2015) Orchestration of microtubules and the actin cytoskeleton in trichome cell shape determination by a plant-unique kinesin. eLife **4:** e09351

Tihlaríková E, Nedela V, Shiojiri M (2013) In situ study of live specimens in an environmental scanning electron microscope. Microsc Microanal **19:** 914–918

Töller A, Brownfield L, Neu C, Twell D, Schulze-Lefert P (2008) Dual function of Arabidopsis glucan synthase-like genes GSL8 and GSL10 in male gametophyte development and plant growth. Plant J **54:** 911–923

Verma DP, Hong Z (2001) Plant callose synthase complexes. Plant Mol Biol **47:** 693–701

Vivancos J, Labbé C, Menzies JG, Bélanger RR (2015) Silicon-mediated resistance of Arabidopsis against powdery mildew involves mechanisms other than the salicylic acid (SA)-dependent defence pathway. Mol Plant Pathol **16:** 572–582

Vogel J, Somerville S (2000) Isolation and characterization of powdery mildew-resistant Arabidopsis mutants. Proc Natl Acad Sci USA **97:** 1897–1902

Vukašinovic N, Oda Y, Pejchar P, Synek L, Pecenková T, Rawat A, Sekereš J, Potocký M, Zárský V (2017) Microtubule-dependent targeting of the exocyst complex is necessary for xylem development in Arabidopsis. New Phytol **213:** 1052–1067

Waterkeyn L, Dupont C (1982) L'observation des dépôts pariétaux de silice au microscope électronique à balayage. Bulletin Societe Royale de Botanique de Belgique **115:** 156–160

Webster TR (1992) Developmental problems in Selaginella (Selaginellaceae) in an evolutionary context. Ann Mo Bot Gard **79:** 632–647

Wu H, Turner C, Gardner J, Temple B, Brennwald P (2010) The Exo70 subunit of the exocyst is an effector for both Cdc42 and Rho3 function in polarized exocytosis. Mol Biol Cell **21:** 430–442

Yi X, Zhang Z, Ling Y, Xu W, Su Z (2015) PNRD: a plant non-coding RNA database. Nucleic Acids Res **43:** D982–D989

Yue P, Zhang Y, Mei K, Wang S, Lesigang J, Zhu Y, Dong G, Guo W (2017) Sec3 promotes the initial binary t-SNARE complex assembly and membrane fusion. Nat Commun **8:** 14236

Zárský V, Cvrcková F, Potocký M, Hála M (2009) Exocytosis and cell polarity in plants - exocyst and recycling domains. New Phytol **183:** 255–272

Zhang C, Wang L, Zhang W, Zhang F (2013) Do lignification and silicification of the cell wall precede silicon deposition in the silica cell of the rice (Oryza sativa L.) leaf epidermis? Plant Soil **372:** 137–149

Zhao T, Rui L, Li J, Nishimura MT, Vogel JP, Liu N, Liu S, Zhao Y, Dangl JL, Tang D (2015) A truncated NLR protein, TIR-NBS2, is required for activated defense responses in the exo70B1 mutant. PLoS Genet **11:** e1004945

Zhao Y, Liu J, Yang C, Capraro BR, Baumgart T, Bradley RP, Ramakrishnan N, Xu X, Radhakrishnan R, Svitkina T, Guo W (2013) Exo70 generates membrane curvature for morphogenesis and cell migration. Dev Cell **26:** 266–278

8.3 Article 3

13 pages (71—83)

Arabidopsis Trichome Contains Two Plasma Membrane Domains with Different Lipid Compositions Which Attract Distinct EXO70 Subunits

Zdeňka Kubátová [1], Přemysl Pejchar [1,2], Martin Potocký [1,2], Juraj Sekereš [2], Viktor Žárský [1,2] and Ivan Kulich [1,*]

[1] Department of Experimental Plant Biology, Faculty of Science, Charles University, 12800 Prague, Czech Republic
[2] Institute of Experimental Botany, Czech Academy of Sciences, 165 02 Prague, Czech Republic
* Correspondence: kulich@natur.cuni.cz

Received: 21 June 2019; Accepted: 1 August 2019; Published: 3 August 2019

Abstract: Plasma membrane (PM) lipid composition and domain organization are modulated by polarized exocytosis. Conversely, targeting of secretory vesicles at specific domains in the PM is carried out by exocyst complexes, which contain EXO70 subunits that play a significant role in the final recognition of the target membrane. As we have shown previously, a mature *Arabidopsis* trichome contains a basal domain with a thin cell wall and an apical domain with a thick secondary cell wall, which is developed in an EXO70H4-dependent manner. These domains are separated by a cell wall structure named the Ortmannian ring. Using phospholipid markers, we demonstrate that there are two distinct PM domains corresponding to these cell wall domains. The apical domain is enriched in phosphatidic acid (PA) and phosphatidylserine, with an undetectable amount of phosphatidylinositol 4,5-bisphosphate (PIP_2), whereas the basal domain is PIP_2-rich. While the apical domain recruits EXO70H4, the basal domain recruits EXO70A1, which corresponds to the lipid-binding capacities of these two paralogs. Loss of EXO70H4 results in a loss of the Ortmannian ring border and decreased apical PA accumulation, which causes the PA and PIP_2 domains to merge together. Using transmission electron microscopy, we describe these accumulations as a unique anatomical feature of the apical cell wall—radially distributed rod-shaped membranous pockets, where both EXO70H4 and lipid markers are immobilized.

Keywords: cell wall; EXO70; exocyst complex; phosphatidic acid; phosphatidylinositol 4,5-bisphosphate; phospholipids; plasma membrane domains; polar exocytosis; trichome

1. Introduction

Despite their unicellularity, *Arabidopsis* trichomes grow into extraordinarily shaped and precisely polarized structures, which makes them a potent model of cell polarization and morphogenesis [1]. According to [2], trichome development can be divided into six stages. During the first stage, several rounds of endoreduplication lead to an increased DNA content and, later, to a remarkably large trichome cell. The second and third stages are crucial for trichome shaping because they involve oriented growth above the surface and two or three branching events. During the fourth and fifth stages, the branches elongate significantly and the trichome reaches its final size and shape. When the growth is complete, the trichome enters the last stage of its development, which is maturation of the cell wall. In this stage, the trichome is divided into two markedly different domains—the basal domain, with a thin cell wall, and the apical domain, with an extremely thick cell wall. This latter secondary cell wall (SCW) consists of at least two distinct layers—the outer, cellulose-rich layer and the inner,

callose-rich layer [3]. The inner layer is autofluorescent and silicified in a callose-dependent manner [4]. The apical cell wall domain also contains surface papillae, which accumulate cuticular waxes that may be different from those in other epidermal cells [5]. Basal and apical trichome domains are separated by a ring-shaped, callose-rich structure named the Ortmannian ring [3].

The development of this cell wall is dependent on the EXO70H4 exocyst subunit, which is necessary for callose synthase delivery to the plasma membrane (PM) [4]. EXO70H4 is a subunit of the exocyst complex, which is a eukaryotic protein complex involved in the tethering of post-Golgi secretory vesicles, which carry membrane and cell wall components to the PM [6]. The exocyst is composed of eight different subunits forming a functional complex, including Sec3, Sec5, Sec6, Sec8, Sec10, Sec15, Exo70, and Exo84 (for review, see [7,8]). Exo70 and Sec3 have a special position in the complex, as both of these subunits are able to directly bind to the target membrane lipids [9–11], thus regulating where the secretion will occur [12]. In yeast and mammals, the Exo70 subunit recruits the rest of the exocyst complex to the PM via a specific interaction of the EXO70 C-terminus with phosphatidylinositol 4,5-bisphosphate (PIP_2) [9,13]. Sec3 is then responsible for initiating the binary SNARE (Soluble NSF Attachment Protein Receptor) complex [14]. The crosstalk of phospholipids with their protein partners and its importance in plant cell polarity determination and membrane traffic regulation was summarized in [15].

The *Arabidopsis* genome contains 23 EXO70 paralogs [16–18]. This multiplicity of EXO70 subunits in plants led to the hypothesis that EXO70s may have divergent lipid-binding properties and thus regulate exocytosis in distinct PM domains within a single cell [19]. So far, there is one documented example of such domain separation observed for NtEXO70A1 and NtEXO70B1 paralogs in *Nicotiana tabacum* pollen tubes, where EXO70A1 was more apically localized than EXO70B1 [20]. There is also apparent functional specialization among the EXO70 paralogs, as neither EXO70A1, B1, nor any other of 18 tested paralogs can complement the *exo70H4-1* loss-of-function mutant phenotype [4]. In this study, we document the differential localization of EXO70H4 and EXO70A1 in the mature trichome and show that EXO70H4 is required for the development and separation of two PM domains with different compositions of signaling phospholipids and distinct abilities to attract other EXO70 members.

2. Results

2.1. Mature Arabidopsis Trichomes Contain Two Distinct Lipid Domains and EXO70H4 is Involved in Their Formation

To investigate the distribution of the PM lipids in the *Arabidopsis* trichome, we observed localization of several fluorescent phospholipid markers. We focused on phosphatidylinositol-4-phosphate (PI4P) [21], phosphatidylinositol 4,5-bisphosphate (PIP_2) [21], phosphatidic acid (PA) [22,23], and phosphatidylserine (PS) membrane lipid markers [23]. While the PIP_2 marker was localized almost exclusively to the trichome base beneath the Ortmannian ring (Figure 1), the PI4P and PA markers were distributed evenly around the whole PM, with their signals enhanced at the Ortmannian ring and in intramural pockets throughout the apical domain (Figure 1). However, the PI4P marker signal inside these intramural pockets was weaker than the PA marker signal, which is highly accumulated there (Figure 1). The identities of these pockets will be described in more detail in Section 2.3. The PS marker was mostly visible at the apical membrane domain (Figure 1 and Supplemental Video S1). No signal was observed at the base, but a weak signal may have remained undetected due to a strong cytoplasmic background of this marker line. Thus, we concluded that a mature *Arabidopsis* trichome contains two distinct membrane domains with different lipid compositions.

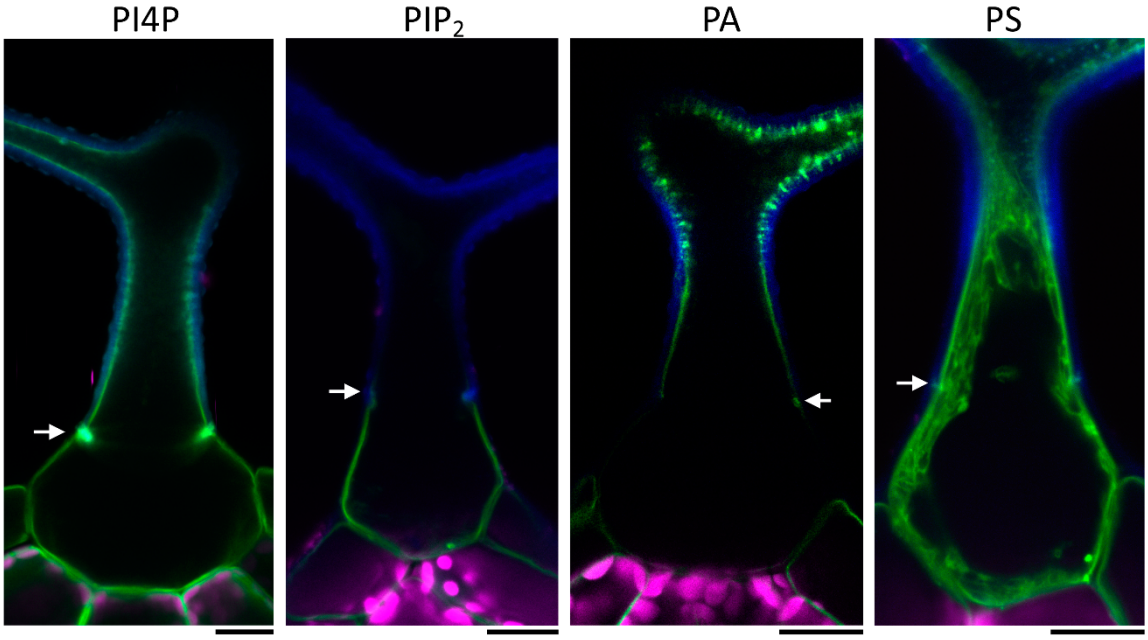

Figure 1. Representative images of different phospholipid markers in wild type mature trichome. PI4P—phosphatidylinositol-4-phosphate; PIP_2—phosphatidylinositol 4,5-bisphosphate; PA—phosphatidic acid; PS—phosphatidylserine. Blue—cell wall autofluorescence; magenta—chlorophyll autofluorescence; green—mCitrine or YFP (yellow fluorescent protein). White arrows point at the Ortmannian ring. Scale bars = 20 μm.

Next, we wanted to investigate when these two domains differentiated during trichome development. For this, we used a double marker line expressing a PA marker tagged with mCitrine and a PIP_2 marker tagged with mCherry (mCH), provided by the authors of [23]. In the wild type (WT) background, the distribution of the lipid markers was consistent with previous observations (Figure 2a). Distinct domains only appeared at stage 6 of trichome development, along with the establishment of the Ortmannian ring. In the WT trichomes of stage 4 (elongation), where the Ortmannian ring was not formed yet, PM domains were not visible (Figure 2b). The PIP_2 marker was evenly distributed all around the PM and the PA marker was not bound to the membrane at all (Figure 2b), suggesting that PA is not present in young trichome PM. Later, we introduced both lipid markers into the *exo70H4-1* mutant background, which was unable to finish the cell wall maturation [3]. Here, the membrane domains lacked a sharp border and were poorly visible (Figure 2c). We concluded that the establishment of the apical and basal membrane domains occurred while the EXO70H4-dependent SCW layer in the apical domain was formed, which depended on the SCW formation.

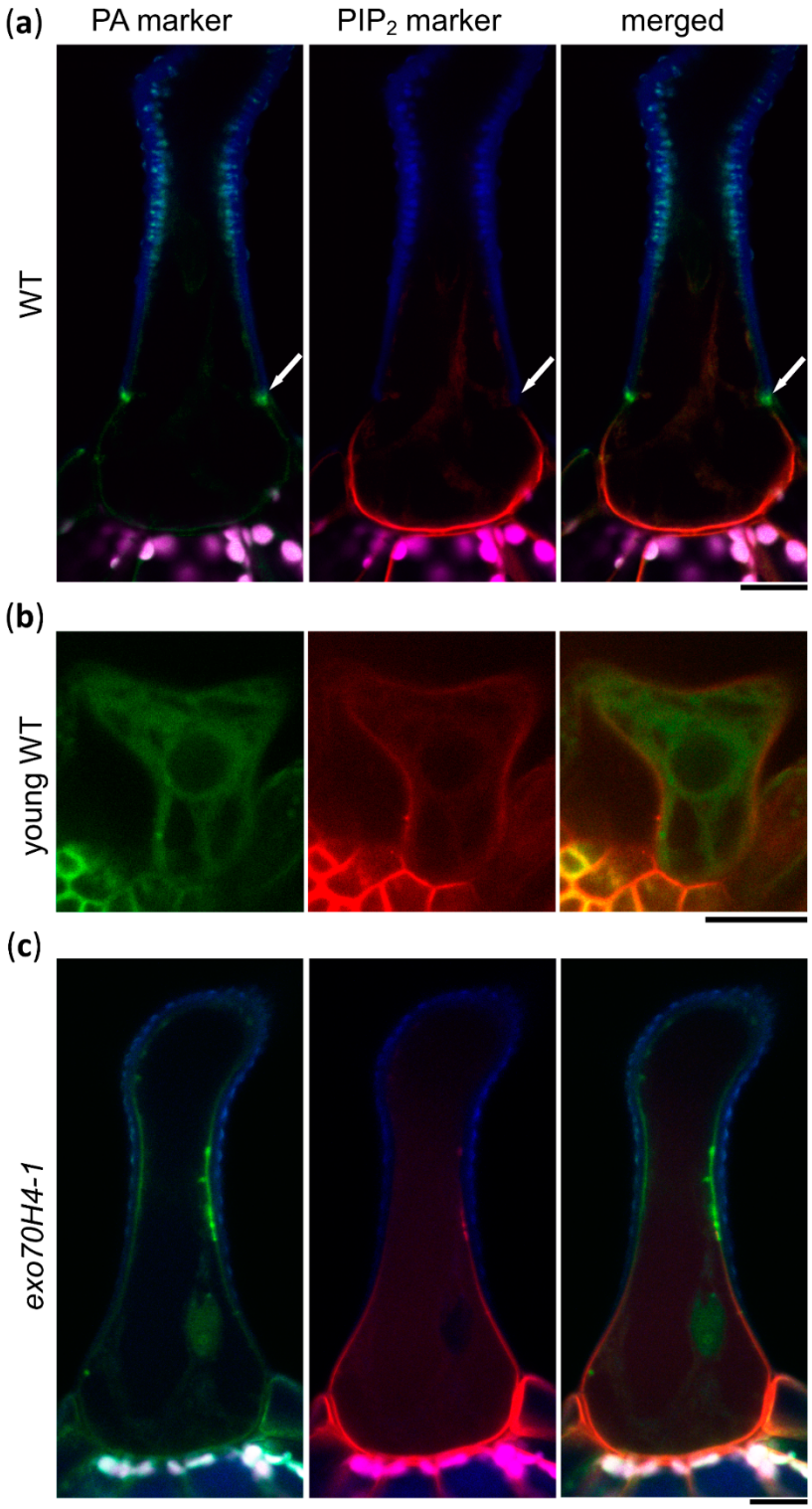

Figure 2. Lipid markers in WT and *exo70H4-1* trichomes. (**a**) Colocalization of PA and PIP_2 markers in WT trichome; (**b**) colocalization of PA and PIP_2 markers in WT trichome in the elongation stage; (**c**) colocalization of PA and PIP_2 markers in an *exo70H4-1* mutant background. Blue—cell wall autofluorescence; magenta—chlorophyll autofluorescence; green—YFP; red—mCherry. White arrows point at the Ortmannian ring. Scale bars = 20 μm.

2.2. Trichome Apical and Basal Plasma Membrane Domains Recruit Different EXO70 Proteins

To address the biological relevance of the trichome lipid domain distribution, we observed multiple EXO70 proteins under the control of the EXO70H4 promoter. EXO70A1 was previously found to bind to PIP_2 [24] and to localize to the PIP_2-rich region of the pollen tube [20]. Corresponding with its lipid affinity, EXO70A1 localized preferentially to the basal trichome domain and, in many cases, the apical trichome domain was completely devoid of EXO70A1, although there was a certain degree of variability and it was often seen also within the Ortmannian ring area (Figure 3a, Supplemental Figure S1). As reported previously [4], a lack of EXO70H4 resulted in EXO70A1 localizing all around the trichome PM (Figure 3a). To verify that EXO70A1 is natively present in *Arabidopsis* trichomes, we also generated a reporter construct of the EXO70A1 promoter fused to 2xGFP (green fluorescent protein). This revealed that EXO70A1 was indeed expressed in the mature trichome (Figure 3b).

EXO70H4 is known to localize to the apical trichome domain and to the Ortmannian ring [4]. To correlate its localization together with EXO70A1, we co-transformed EXO70H4p::mCHERRY-EXO70H4 (mCH-EXO70H4) with EXO70H4p::GFP-EXO70A1 (GFP-EXO70A1) In this case, the EXO70 isoforms localized to distinct and mostly non-overlapping PM domains that corresponded to the apical and basal trichome domains (Figure 3c).

We also investigated the localization of the remaining EXO70s, which we observed previously in the *exo70H4-1* mutant background [4]. This time, we expressed the constructs in a WT background to see their localization when it was unaffected by the *exo70H4-1* mutation. Eight paralogs were tested—EXO70A1, A2, B1, C1, D2, F1, H7, and H8. The only paralogs found to localize to the PM in the WT background in addition to EXO70A1 were EXO70A2 (localized similarly to EXO70A1) and EXO70H8. EXO70H8 strongly accumulated at the PA-rich domain in the apical part of the trichome, including Ortmannian ring and cell wall ingrowths. Although EXO70H8 mimicked EXO70H4 localization in the WT trichome, it was not capable of functionally complementing the *exo70H4-1* mutant phenotype in our previous cross-complementation study [4]. The other EXO70 paralogs that were tested remained in the cytoplasm or nucleus, as in the previous experiments in the *exo70H4-1* background.

Since the lipid-binding capacities of EXO70H4 have not yet been described, we performed a protein–lipid overlay assay with in vitro translated HA-tagged EXO70H4. This revealed a clear affinity to PS and conceivably PA, but no apparent binding to PIP_2 (Figure 3d). This corresponded well with the colocalization of EXO70H4 with PA and PS markers in the apical domain of the mature trichome. Based on these and previously published data, we concluded that different EXO70 proteins exhibit a specific capacity to bind membrane lipids and thus are recruited to distinct PM domains, contributing to the biogenesis of different cell wall domains within a single plant cell.

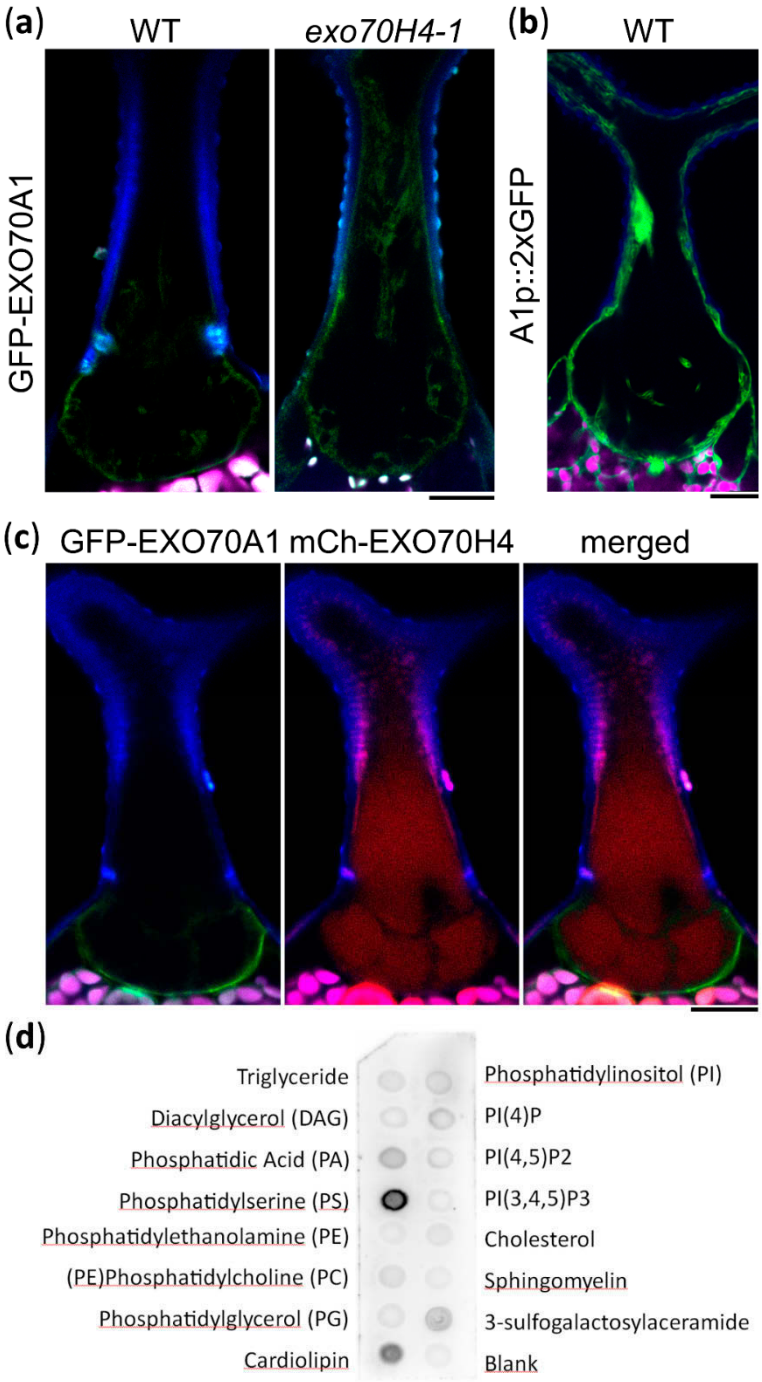

Figure 3. Trichome plasma membrane domains recruit different EXO70 proteins. (**a**) EXO70H4p::GFP-EXO70A1 (GFP-EXO70A1) preferentially localizes to the basal trichome domain in WT. This preference is lost in the *exo70H4-1* mutant. (**b**) EXO70A1p::GFP:GFP (A1p::2xGFP) expression marker in a WT trichome. (**c**) Colocalization of GFP-EXO70A1 with EXO70H4p::mCherry-EXO70H4 (mCh-EXO70H4). (**d**) Protein–lipid overlay assay of EXO70H4. Blue—cell wall autofluorescence; magenta—chlorophyll autofluorescence; green—GFP; red—mCherry. Scale bars = 20 μm.

2.3. The Apical Cell Wall Contains Entrapped Membranous Pockets

While observing the apical trichome domain, we noticed that a large portion of the signal came from within the cell wall. This was true for all of the constructs which localized to the apical membrane domain, including markers of PA, PS, PI4P, mCh-EXO70H4, GFP-EXO70H8, and occasionally also EXO70A1 and EXO70A2 with a weak signal. This strange intramural localization directed our further investigation. The signal within the SCW was distributed in a pattern remarkably similar to the callose deposits shown before [3,4]. The radially distributed rays of signal were visibly embedded within the cell wall and were well-apparent on fluorescence microscopy optical cuts of matured branches together with a wrinkled PM–SCW interface (Figure 4a,b). To be sure that this was indeed the fluorophore signal and not cell wall autofluorescence, we performed lambda scans in plants expressing GFP-EXO70H4, mCh-EXO70H4, YFP-PA marker, and untransformed control. In all of these cases, the expected emission peak was observed (Supplemental Figure S2), with no such peaks in the negative control. To check if these intramural signals were still connected to the rest of the cytoplasm, we performed a fluorescence recovery after photobleaching (FRAP) experiment on the PI4P marker, which revealed that there was no detectable recovery of the signal, unlike in the case of the signal bleached within the apparent continuum of the PM (Supplemental Figure S3). We therefore hypothesized that the intramural signal may come from the PM and cell interior, being physically entrapped within the cell wall pockets.

To investigate the SCW structure in more detail, we used transmission electron microscopy (TEM). This revealed internal cell wall structures, supporting our observations of oblong traversing pockets with light microscopy. TEM cross-sections of mature WT trichome branches displayed SCW-transpassing structures, probably aggregates of entrapped secretory lipid membranes, proteins, and the cell interior, often arranged in a radial pattern of concentric transpassing channels (Figure 4c, left). These intramural pockets were obviously separated from the continuum of cytoplasm (Figure 4c, middle), but their PM origin was apparent from images where pieces of electron-dense, non-cell wall materials were embedded into the cell wall (Figure 4c, right).

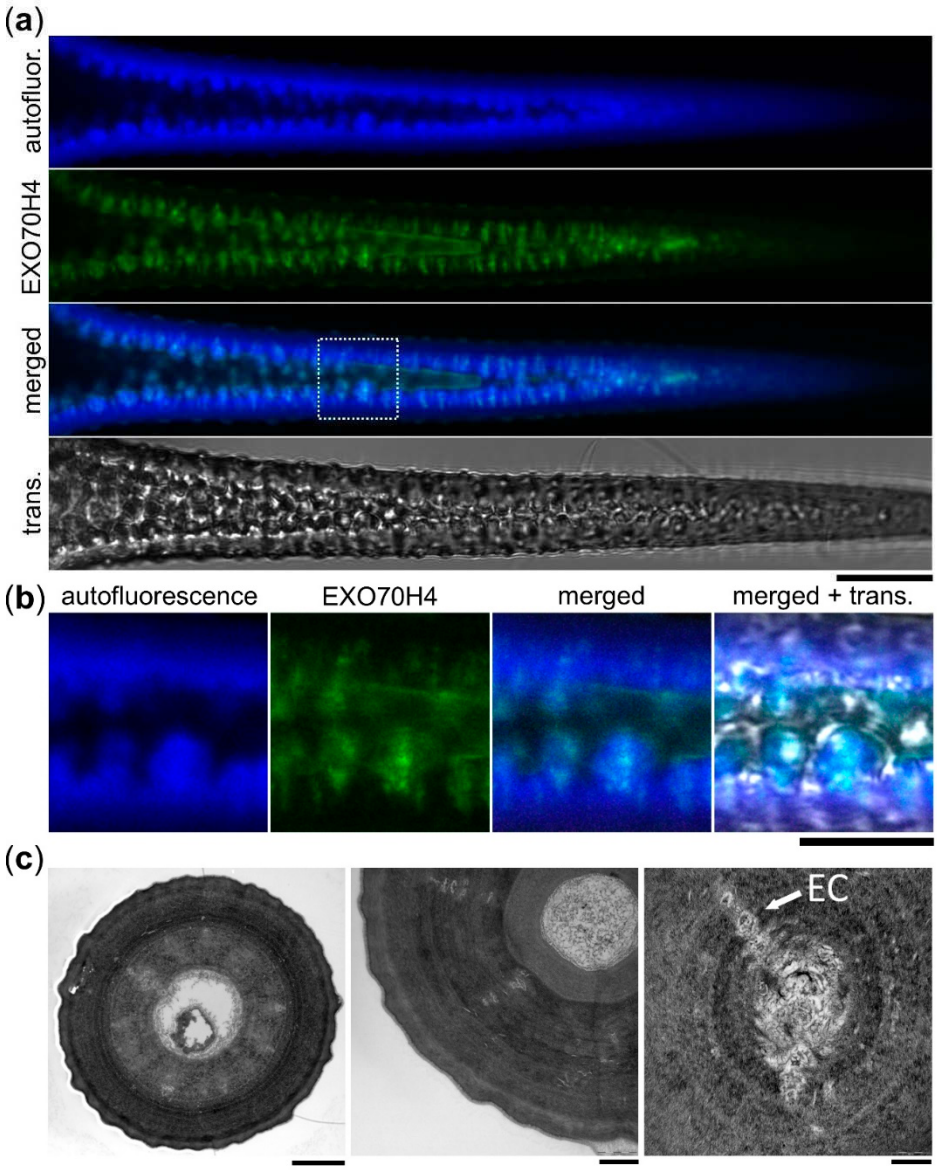

Figure 4. Plasma membrane proteins reside within the trichome apical cell wall. (**a**) GFP-EXO70H4 (EXO70H4) signal, cell wall autofluorescence (autofluor.), and transmission channel (trans.) at the branch of a mature WT trichome. The dotted square represents area enlarged in (**b**). Scale bar = 20 μm. (**b**) Detail of (**a**). Scale bar = 10 μm. (**c**) Left—TEM image of a cross-section of a trichome branch. Entrapped cell interior (EC) is visible as concentric rays. Scale bar = 3 μm. Middle—detail of entrapped cell interior obviously separated from the cytoplasm. Scale bar = 1 μm. Right—a detail of one concentric ray. Scale bar = 200 nm.

3. Discussion

We showed that the mature *Arabidopsis* trichome contains, along with two cell wall domains, two distinct PM domains that differ in their phospholipid composition and also in their ability to recruit different EXO70 proteins. EXO70A1 is recruited to the basal trichome domain, which is PIP_2-rich and contains a thin, pectin-rich cell wall [25]. EXO70H4 is recruited to the apical domain, which is PS- and PA-rich and has a thick, autofluorescent cell wall [3].

There are a number of different examples of cell types having different phospholipid domains and many of them can be linked with differential cell wall deposition. Pollen grains also accumulate PIP_2 at the site of the future aperture, which is an area marked with a thin cell wall [26]. Similarly, the pollen tube accumulates PIP_2 at its tip, while PS and PA are in the shank [22,23]. This corresponds

with the apical cell wall of the pollen tube being almost solely made of secreted pectins, while callose and cellulose are deposited in the shank [27]. This domain separation in the pollen tube is further marked by differential membrane localization of EXO70A1 and EXO70B1 in tobacco [20]. In contrast to the pollen tube, trichomes are extremely large and static structures. The border of the two membrane domains appears to be very sharp and defined by the Ortmannian ring. A lack of a sharp border between these two domains and a partial loss of polarity in the *exo70H4-1* mutant suggests that there is a positive feedback loop and that EXO70s have a role in domain development.

The observed lack of PIP_2 and abundance of PA in the apical domain could also imply that, in the apical domain, PIP_2 is metabolized to PA. In general, PA is formed through two pathways: First, by the direct hydrolysis of structural phospholipids by phospholipase D and second, through the consecutive actions of phospholipase C and diacylglycerol kinase, where the hydrolysis of PIP_2 produces inositol-1,4,5-trisphosphate (released into the cytosol) and diacylglycerol within the PM, which is quickly phosphorylated at the membrane into PA by diacylglycerol kinase. PA produced by phospholipase Dα1 is a crucial signaling lipid, mediating the abscisic acid response in guard cells, where its role in NADPH oxidase-mediated reactive oxygen species (ROS) production was clearly demonstrated [28]. Both PA and phospholipase Dα1 have previously been linked with ROS production [29]. NADPH oxidase-mediated ROS production acts in the plant defense response [30,31]. In plants, PA is also produced in response to several stress factors, including pathogen attack [32]. EXO70H4 is also induced by *flagellin 22* in epidermal pavement cells [4]. The apical cell wall domain of the trichome is also remarkably similar to the defense papillae, as they both accumulate callose deposits, phenolic compounds [33], and an extracellular signal of membrane proteins (such as SYP121—SYNTAXIN OF PLANTS 121 [34]). We therefore suggest that the mechanism and domain organization in the trichome may be a manifestation of a general response to pathogen attack, which runs constitutively in the trichome.

It was shown that binding of PA to its protein interactors is enhanced by a negative curvature stress and that a complex membrane lipid composition strongly influences lipid–protein interactions [35]. Surprisingly, EXO70 by itself is able to induce negative membrane curvature, specifically through the homodimerization mechanism, as was demonstrated in mammals [36]. Together, these biophysical properties could induce PM deformation sufficient to form extreme membrane curvatures, leading to the formation of membranous pockets within the SCW. Another factor contributing to the pocket formation may be the cuticular wax migration across the cell wall. The apical trichome domain displays several unique features, including surface papillae formation. Papillae start to form at stage 5 of trichome development (expansion) and continue developing during stage 6 (maturation). At these stages, the apical cell wall is already quite thick (>2 μm) [37]. Papillae are little bumps filled with lipophilic cuticular substances. These waxes differ from those of other epidermal cells by a high content of C35+ alkanes [5]. How these compounds get through the thick cell wall to the surface is not understood. Membranous pockets may drift along the migration routes of the cuticular waxes through the inner layer of the SCW. This feature may be very useful for the study of cuticular wax migration across the cell wall. Another intriguing possibility is that formation of these membranous pockets within the SCW is directly linked to the mechanism of callose deposition during SCW biogenesis—a possibility we aim to study.

4. Materials and Methods

4.1. Plant Material

Plants were grown in Jiffy soil pellets in standard growth chamber conditions (long day 16 h:8 h, 100–120 μM photosynthetically active radiation m^{-2} s^{-1}). The *exo70H4-1* mutant line was described previously [3]. As WT control, outcrossed WT plants were used. Seeds of PI4P and PIP_2 markers were obtained from Yvon Jaillais and are described in detail in [21]. From this set, we used line P21Y (mCitrine-2xPH FAPP PI4P binding domain), line P24Y (mCitrine-2xPH^{PLC} PIP_2 binding domain),

and line P24R (mCherry-2xPH^{PLC} PIP_2 binding domain). Two different PA markers were used in this study. In Figure 1, it was YFP:NES-2xSpo20p (cloning described below) and in Figure 2 and Supplemental Figure S2, it was a double marker line expressing a PA marker tagged with mCitrine (PAY) and a PIP_2 marker tagged with mCherry (P24R, mentioned above), provided by [23]. PS marker cloning is described below.

4.2. Confocal Microscopy

Confocal microscopy images were taken on Zeiss LSM880 with C-Apochromat 403/1.2 W Korr FCS M27 objective [GFP (488): 508–540 nm, chlorophyll (488) 650–721 nm, cell wall autofluorescence (405) 426–502, mCherry (561) 597–641]. Images were processed using the Fiji platform [38].

4.3. Trichome Isolation and TEM

Leaves of 4-week-old plants were collected and incubated for 3 h in falcon tubes in a solution of acetic acid:ethanol (1:3) and then washed three times with deionized water. Washed leaves were transferred to a solution of 150 mM KH_2PO_4 pH 9.5 and incubated overnight with shaking at 150–180 rpm. Released trichomes were collected by centrifugation (1 min, 1000 G, no break). For TEM, isolated trichomes were fixed for 24 h in 2.5% (*v*/*v*) glutaraldehyde in 0.1 M cacodylate buffer (pH 7.2) at 4 °C and postfixed in 2% (*w*/*v*) OsO4 in the same buffer. Fixed samples were dehydrated through an ascending ethanol and acetone series and embedded in Epon–Araldite.

4.4. Cloning and Stable Transgenic Line Preparation

For cloning of the expression reporter construct EXO70A1p::GFP:GFP, the multisite gateway approach was used. The EXO70A1 promoter (1 kb upstream, EXO70A1 prom for and EXO70A1 prom rev listed in Supplemental Table S1 were used) was subcloned into pDONORP4-P1r and sequenced using M13 primers. GFP constructs—pEN-L1-F-L2 and pEN-R2-GFP-L3,0—and destination vector pB7m34GW were obtained from [39]. An expression clone was assembled from these by a multisite reaction using Gateway LR clonase (Thermo Fischer, Waltham, MA, USA). All EXO70H4p::GFP-EXO70XY constructs used in this study were previously described in [4].

To prepare the construct for the PA marker (pUBQ::YFP:NES-2xSpo20p PABD), first NES-2xSpo20p was amplified from YFP:Spo20p-PABD [22] and cloned together with the ubiquitin (UBQ) promoter and YFP into the binary vector pHD71 (kindly provided by Dr. Benedikt Kost).

To prepare the construct for the PS marker (pUBQ::YFP:C2^{LACT}), YFP-C2^{LACT} from Lat52:YFP-C2^{LACT} [22] was cloned together with the UBQ promoter into the binary vector pHD71; the primers used are listed in Supplemental Table S1.

Final constructs were electroporated into competent cells of *Agrobacterium tumefaciens*, strain GV3101. Col-0 wild type plants were transformed by the floral dip method [40] and transformants were selected on kanamycin plates or soil by BASTA spraying (150 mg/L of glufosinate-ammonium). No fewer than five individual transformants were observed in each experiment and at least two biological replicates were made.

4.5. Protein–Lipid Overlay Assay

The protein–lipid overlay assay was performed using N-terminally HA-tagged EXO70H4 and echelon lipid strips. First, the EXO70H4 coding sequence was cloned into a pTNT vector (Promega, Fitchburg, WI, USA), optimized for in vitro coupled transcription and translation, using primers listed in Supplemental Table S1. The cloning was performed in two steps. First, the EXO70H4 coding sequence was amplified with the use of the primers EXO70H4-forward and EXO70H4-reverse. Subsequently, a megaprimer containing the HA-tag sequence and Kozak consensus sequence facilitating efficient translation initiation was used together with EXO70H4-reverse primer. The product was cloned into the pTNT vector via SalI and NotI restriction sites.

The construct was used as a template for in vitro coupled transcription and translation reactions using TNT® SP6 High-Yield Wheat Germ Protein Expression System (Promega), according to the manufacturer's instructions, in a total volume of 50 μL. To verify protein expression and stability, 10 μL of the yield was used in Western blotting. Since the protein was tagged on the N-terminus, Western blot analysis would have detected products of prematurely terminated translation, but none were observed (see Supplemental Figure S4).

The remaining 40 μL of the reaction product was used for the protein–lipid overlay assay. The echelon lipid strip (Elcheon Biosciences, Salt Lake City, UT, USA) was blocked for one hour in blocking solution (50 mM Tris, 150 mM NaCl, 0.05% Tween 20, pH 7.6 + 3% bovine serum albumine). After three washes in wash solution (50 mM Tris, 150 mM NaCl, 0.05% Tween 20, pH 7.6), the strip was incubated for two hours with primary mouse anti-HA antibody (Sigma-Aldrich, St. Louis, MO, USA) diluted 1:1000 in blocking solution. After three washes with wash solution, the strip was subsequently incubated with secondary anti-mouse antibody conjugated to horseradish peroxidase (Promega), diluted 1:20,000 in blocking solution. Finally, the strip was washed three times with wash solution and incubated for three minutes with Amersham ECL Prime Western Blotting Detection Reagent (GE Healthcare, Chicago, IL, USA) and imaged with Bio-Rad Laboratories (Hercules, CA, USA) Chemidoc gel imaging system. The experiment was repeated twice with consistent results.

Supplementary Materials: Supplementary Materials can be found at http://www.mdpi.com/1422-0067/20/15/3803/s1.

Author Contributions: Conceptualization, I.K. and V.Z.; validation, Z.K. and I.K.; investigation, Z.K., J.S. and I.K.; resources, P.P. and M.P.; writing—original draft preparation, Z.K. and I.K.; writing—review and editing, P.P., M.P., J.S. and V.Ž.; visualization, Z.K. and I.K.; supervision, I.K. and V.Z; funding acquisition, I.K.

Funding: This project was financed by Czech Science Foundation grant 18-12579S. Microscopy was performed in the Laboratory of Confocal and Fluorescence Microscopy co-financed by the European Regional Development Fund and the state budget of the Czech Republic (project no. CZ.1.05/4.1.00/16.0347). Part of income of V.Ž. is supported by the Ministry of Education, Youth and Sports of CR from European Regional Development Fund-Project "Centre for Experimental Plant Biology": No. CZ.02.1.01/0.0/0.0/16_019/0000738.

Acknowledgments: We would like to thank Yvon Jaillais for providing us with the lipid markers, Patrick Moxon for cloning EXO70A1 promoter, Jachym Metlicka for help with image preparation, and our technician, Marta Cadyova, for running the laboratory.

Conflicts of Interest: The authors declare no conflict of interest.

Abbreviations

FRAP	fluorescence recovery after photobleaching
mCh	mCherry
PA	phosphatidic acid
PI4P	phosphatidylinositol-4-phosphate
PIP_2	phosphatidylinositol 4,5-bisphosphate
PM	plasma membrane
PS	phosphatidylserine
SCW	secondary cell wall
TEM	transmission electron microscopy
WT	wild type

References

1. Szymanski, D.B.; Lloyd, A.M.; Marks, M.D. Progress in the molecular genetic analysis of trichome initiation and morphogenesis in Arabidopsis. *Trends Plant Sci.* **2000**, *5*, 214–219. [CrossRef]
2. Hülskamp, M. Plant trichomes: A model for cell differentiation. *Nat. Rev. Mol. Cell Biol.* **2004**, *5*, 471–480. [CrossRef] [PubMed]

3. Kulich, I.; Vojtíková, Z.; Glanc, M.; Ortmannová, J.; Rasmann, S.; Žárský, V. Cell wall maturation of Arabidopsis trichomes is dependent on exocyst subunit EXO70H4 and involves callose deposition. *Plant Physiol.* **2015**, *168*, 120–131. [CrossRef] [PubMed]
4. Kulich, I.; Vojtíková, Z.; Sabol, P.; Ortmannová, J.; Neděla, V.; Tihlaříková, E.; Žárský, V. Exocyst Subunit EXO70H4 Has a Specific Role in Callose Synthase Secretion and Silica Accumulation. *Plant Physiol.* **2018**, *176*, 2040–2051. [CrossRef] [PubMed]
5. Hegebarth, D.; Buschhaus, C.; Joubès, J.; Thoraval, D.; Bird, D.; Jetter, R. Arabidopsis ketoacyl-CoA synthase 16 (KCS16) forms C/C acyl precursors for leaf trichome and pavement surface wax. *Plant Cell Environ.* **2017**, *40*, 1761–1776. [CrossRef] [PubMed]
6. TerBush, D.R.; Maurice, T.; Roth, D.; Novick, P. The Exocyst is a multiprotein complex required for exocytosis in Saccharomyces cerevisiae. *EMBO J.* **1996**, *15*, 6483–6494. [CrossRef]
7. Hsu, S.-C.; TerBush, D.; Abraham, M.; Guo, W. The exocyst complex in polarized exocytosis. *Int. Rev. Cytol.* **2004**, *233*, 243–265.
8. Lepore, D.M.; Martínez-Núñez, L.; Munson, M. Exposing the Elusive Exocyst Structure. *Trends Biochem. Sci.* **2018**, *43*, 714–725. [CrossRef]
9. Liu, J.; Zuo, X.; Yue, P.; Guo, W. Phosphatidylinositol 4,5-Bisphosphate Mediates the Targeting of the Exocyst to the Plasma Membrane for Exocytosis in Mammalian Cells. *Mol. Biol. Cell* **2007**, *18*, 4483–4492. [CrossRef]
10. Zhang, X.; Orlando, K.; He, B.; Xi, F.; Zhang, J.; Zajac, A.; Guo, W. Membrane association and functional regulation of Sec3 by phospholipids and Cdc42. *J. Cell Biol.* **2008**, *180*, 145–158. [CrossRef]
11. Bendezú, F.O.; Vincenzetti, V.; Martin, S.G. Fission yeast Sec3 and Exo70 are transported on actin cables and localize the exocyst complex to cell poles. *PLoS ONE* **2012**, *7*, e40248. [CrossRef]
12. Luo, G.; Zhang, J.; Guo, W. The role of Sec3p in secretory vesicle targeting and exocyst complex assembly. *Mol. Biol. Cell* **2014**, *25*, 3813–3822. [CrossRef]
13. He, B.; Xi, F.; Zhang, X.; Zhang, J.; Guo, W. Exo70 interacts with phospholipids and mediates the targeting of the exocyst to the plasma membrane. *EMBO J.* **2007**, *26*, 4053–4065. [CrossRef]
14. Yue, P.; Zhang, Y.; Mei, K.; Wang, S.; Lesigang, J.; Zhu, Y.; Dong, G.; Guo, W. Sec3 promotes the initial binary t-SNARE complex assembly and membrane fusion. *Nat. Commun.* **2017**, *8*, 14236. [CrossRef]
15. Sekereš, J.; Pleskot, R.; Pejchar, P.; Žárský, V.; Potocký, M. The song of lipids and proteins: Dynamic lipid-protein interfaces in the regulation of plant cell polarity at different scales. *J. Exp. Bot.* **2015**, *66*, 1587–1598. [CrossRef]
16. Elias, M.; Drdova, E.; Ziak, D.; Bavlnka, B.; Hala, M.; Cvrckova, F.; Soukupova, H.; Zarsky, V. The exocyst complex in plants. *Cell Biol. Int.* **2003**, *27*, 199–201. [CrossRef]
17. Synek, L.; Schlager, N.; Eliás, M.; Quentin, M.; Hauser, M.-T.; Zárský, V. AtEXO70A1, a member of a family of putative exocyst subunits specifically expanded in land plants, is important for polar growth and plant development. *Plant J.* **2006**, *48*, 54–72. [CrossRef]
18. Cvrčková, F.; Grunt, M.; Bezvoda, R.; Hála, M.; Kulich, I.; Rawat, A.; Zárský, V. Evolution of the land plant exocyst complexes. *Front. Plant Sci.* **2012**, *3*, 159. [CrossRef]
19. Zárský, V.; Cvrcková, F.; Potocký, M.; Hála, M. Exocytosis and cell polarity in plants–exocyst and recycling domains. *New Phytol.* **2009**, *183*, 255–272. [CrossRef]
20. Sekereš, J.; Pejchar, P.; Šantrůček, J.; Vukašinović, N.; Žárský, V.; Potocký, M. Analysis of Exocyst Subunit EXO70 Family Reveals Distinct Membrane Polar Domains in Tobacco Pollen Tubes. *Plant Physiol.* **2017**, *173*, 1659–1675. [CrossRef]
21. Simon, M.L.A.; Platre, M.P.; Assil, S.; van Wijk, R.; Chen, W.Y.; Chory, J.; Dreux, M.; Munnik, T.; Jaillais, Y. A multi-colour/multi-affinity marker set to visualize phosphoinositide dynamics in Arabidopsis. *Plant J.* **2014**, *77*, 322–337. [CrossRef]
22. Potocký, M.; Pleskot, R.; Pejchar, P.; Vitale, N.; Kost, B.; Zárský, V. Live-cell imaging of phosphatidic acid dynamics in pollen tubes visualized by Spo20p-derived biosensor. *New Phytol.* **2014**, *203*, 483–494. [CrossRef]
23. Platre, M.P.; Noack, L.C.; Doumane, M.; Bayle, V.; Simon, M.L.A.; Maneta-Peyret, L.; Fouillen, L.; Stanislas, T.; Armengot, L.; Pejchar, P.; et al. A Combinatorial Lipid Code Shapes the Electrostatic Landscape of Plant Endomembranes. *Dev. Cell* **2018**, *45*, 465–480. [CrossRef]
24. Wu, C.; Tan, L.; van Hooren, M.; Tan, X.; Liu, F.; Li, Y.; Zhao, Y.; Li, B.; Rui, Q.; Munnik, T.; et al. Arabidopsis EXO70A1 recruits Patellin3 to the cell membrane independent of its role as an exocyst subunit. *J. Integr. Plant Biol.* **2017**, *59*, 851–865. [CrossRef]

25. Zhang, X.; Oppenheimer, D.G. A simple and efficient method for isolating trichomes for downstream analyses. *Plant Cell Physiol.* **2004**, *45*, 221–224. [CrossRef]
26. Lee, B.H.; Weber, Z.T.; Zourelidou, M.; Hofmeister, B.T.; Schmitz, R.J.; Schwechheimer, C.; Dobritsa, A.A. Arabidopsis Protein Kinase D6PKL3 Is Involved in the Formation of Distinct Plasma Membrane Aperture Domains on the Pollen Surface. *Plant Cell* **2018**, *30*, 2038–2056. [CrossRef]
27. Ferguson, C.; Teeri, T.T.; Siika-aho, M.; Read, S.M.; Bacic, A. Location of cellulose and callose in pollen tubes and grains of Nicotiana tabacum. *Planta* **1998**, *206*, 452–460. [CrossRef]
28. Zhang, Y.; Zhu, H.; Zhang, Q.; Li, M.; Yan, M.; Wang, R.; Wang, L.; Welti, R.; Zhang, W.; Wang, X. Phospholipase dalpha1 and phosphatidic acid regulate NADPH oxidase activity and production of reactive oxygen species in ABA-mediated stomatal closure in Arabidopsis. *Plant Cell* **2009**, *21*, 2357–2377. [CrossRef]
29. Sang, Y.; Cui, D.; Wang, X. Phospholipase D and phosphatidic acid-mediated generation of superoxide in Arabidopsis. *Plant Physiol.* **2001**, *126*, 1449–1458. [CrossRef]
30. Torres, M.A.; Dangl, J.L. Functions of the respiratory burst oxidase in biotic interactions, abiotic stress and development. *Curr. Opin. Plant Biol.* **2005**, *8*, 397–403. [CrossRef]
31. Torres, M.A.; Dangl, J.L.; Jones, J.D.G. Arabidopsis gp91phox homologues AtrbohD and AtrbohF are required for accumulation of reactive oxygen intermediates in the plant defense response. *Proc. Natl. Acad. Sci. USA* **2002**, *99*, 517–522. [CrossRef]
32. Testerink, C.; Munnik, T. Phosphatidic acid: A multifunctional stress signaling lipid in plants. *Trends Plant Sci.* **2005**, *10*, 368–375. [CrossRef]
33. Bélanger, R.R. *The Powdery Mildews: A Comprehensive Treatise*; Amer Phytopathological Society: Amer, India, 2002.
34. Assaad, F.F.; Qiu, J.-L.; Youngs, H.; Ehrhardt, D.; Zimmerli, L.; Kalde, M.; Wanner, G.; Peck, S.C.; Edwards, H.; Ramonell, K.; et al. The PEN1 syntaxin defines a novel cellular compartment upon fungal attack and is required for the timely assembly of papillae. *Mol. Biol. Cell* **2004**, *15*, 5118–5129. [CrossRef]
35. Putta, P.; Rankenberg, J.; Korver, R.A.; van Wijk, R.; Munnik, T.; Testerink, C.; Kooijman, E.E. Phosphatidic acid binding proteins display differential binding as a function of membrane curvature stress and chemical properties. *Biochim. Biophys. Acta* **2016**, *1858*, 2709–2716. [CrossRef]
36. Zhao, Y.; Liu, J.; Yang, C.; Capraro, B.R.; Baumgart, T.; Bradley, R.P.; Ramakrishnan, N.; Xu, X.; Radhakrishnan, R.; Svitkina, T.; et al. Exo70 generates membrane curvature for morphogenesis and cell migration. *Dev. Cell* **2013**, *26*, 266–278. [CrossRef]
37. Marks, M.D.; Gilding, E.; Wenger, J.P. Genetic interaction between glabra3-shapeshifter and siamese in Arabidopsis thaliana converts trichome precursors into cells with meristematic activity. *Plant J.* **2007**, *52*, 352–361. [CrossRef]
38. Schindelin, J.; Arganda-Carreras, I.; Frise, E.; Kaynig, V.; Longair, M.; Pietzsch, T.; Preibisch, S.; Rueden, C.; Saalfeld, S.; Schmid, B.; et al. Fiji: An open-source platform for biological-image analysis. *Nat. Methods* **2012**, *9*, 676–682. [CrossRef]
39. Karimi, M.; Bleys, A.; Vanderhaeghen, R.; Hilson, P. Building blocks for plant gene assembly. *Plant Physiol.* **2007**, *145*, 1183–1191. [CrossRef]
40. Clough, S.J.; Bent, A.F. Floral dip: A simplified method for Agrobacterium-mediated transformation of Arabidopsis thaliana. *Plant J.* **1998**, *16*, 735–743. [CrossRef]

8.4 Article 4

13 pages (85—98)

Three subfamilies of exocyst EXO70 family subunits in land plants: early divergence and ongoing functional specialization

Viktor Žárský[1,2,*], Juraj Sekereš[2], Zdeňka Kubátová[1], Tamara Pečenková[1,2] and Fatima Cvrčková[1]

[1] Department of Experimental Plant Biology, Faculty of Science, Charles University, Viničná 5, 128 44 Prague, Czech Republic
[2] Institute of Experimental Botany, v.v.i., Czech Academy of Sciences, Rozvojová 263, 165 02 Prague, Czech Republic

* Correspondence: viktor.zarsky@natur.cuni.cz

Received 18 April 2019; Editorial decision 6 September 2019; Accepted 10 October 2019

Editor: Howard Griffiths, University of Cambridge, UK

Abstract

Localized delivery of plasma membrane and cell wall components is an essential process in all plant cells. The vesicle-tethering complex, the exocyst, an ancient eukaryotic hetero-octameric protein cellular module, assists in targeted delivery of exocytosis vesicles to specific plasma membrane domains. Analyses of Arabidopsis and later other land plant genomes led to the surprising prediction of multiple putative EXO70 exocyst subunit paralogues. All land plant EXO70 exocyst subunits (including those of Bryophytes) form three distinct subfamilies—EXO70.1, EXO70.2, and EXO70.3. Interestingly, while the basal well-conserved EXO70.1 subfamily consists of multiexon genes, the remaining two subfamilies contain mostly single exon genes. Published analyses as well as public transcriptomic and proteomic data clearly indicate that most cell types in plants express and also use several different EXO70 isoforms. Here we sum up recent advances in the characterization of the members of the family of plant EXO70 exocyst subunits and present evidence that members of the EXO70.2 subfamily are often recruited to non-canonical functions in plant membrane trafficking pathways. Engagement of the most evolutionarily dynamic EXO70.2 subfamily of EXO70s in biotic interactions and defence correlates well with massive proliferation and conservation of new protein variants in this subfamily.

Keywords: Autophagy, defence, evolution, EXO70, exocyst, exocytosis, land plants, unconventional secretion.

Introduction

The exocyst complex and diversity of its EXO70 subunits in plants

Specific tethering protein complexes assist in vectorial delivery of trafficking cargos to distinct stations within the eukaryotic endomembrane system, acting mostly as effectors and regulators of small RAB and RHO GTPases (Koumandou *et al.*, 2007; Vukašinović and Žárský, 2016). One of them is the exocyst, an ancient eukaryotic hetero-octameric protein complex originally discovered in the context of polarized secretory vesicles tetheried at the plasma membrane (PM) in budding yeast (TerBush *et al.*, 1996; Munson and Novick, 2006; Novick, 2014). Driven by knowledge of the yeast exocyst, this complex was found also in animals and plants, and proven to be an ancestral cellular regulator traceable back

Abbreviations: ABA, abscisic acid; AIM, Atg8-interacting motif; CesA, cellulose synthase; flg22, flagellin; GFP, green fluorescent protein; HR, hypersensitive response; LOF, loss of function; MT, microtubule; MVB, multivesicular body; PA, phosphatidic acid; PIP_2, phosphatidylinositol bisphosphate; PM, plasma membrane; SA, salicylic acid; SCW, secondary cell wall; YFP, yellow fluorescent protein; WT, wild type.

to the last eukaryotic common ancestor (Koumandou *et al.*, 2007; Heider and Munson, 2012; Vaškovičová *et al.*, 2013; Wu and Guo, 2015). The exocyst consists of eight subunits (SEC3, SEC5, SEC6, SEC8, SEC10, SEC15, EXO84, and EXO70). By interacting with activated GTP-bound RHO GTPases, it localizes exocytotic membrane containers to specific PM cortical domains (Robinson *et al.*, 1999; Pommereit and Wouters, 2007). The SEC3 and EXO70 subunits target the complex by direct binding to phosphatidylinositol bisphosphate (PIP_2) (He *et al.*, 2007; Liu *et al.*, 2007). The exocyst also catalyses SNARE complex-mediated membrane fusion. This process is mechanistically best understood in the budding yeast, where the t-SNAREs Sso2p and Sec9p directly interact with Sec3p (Yue *et al.*, 2017) and Sec6p (Sivaram *et al.*, 2005), respectively. The *cis*-SNARE complex formation is further boosted by the direct interaction of Sec6p with the regulatory Sec1 protein (Morgera *et al.*, 2012).

Metazoan EXO70 functions within the exocyst complex in processes such as insulin secretion, neurite growth, cell migration, as well as midbody scission (Martin-Urdiroz *et al.*, 2016) and phagosome maturation (Rauch *et al.*, 2014). EXO70 is also involved in the autophagy as a part of an exocyst subcomplex (Bodemann *et al.*, 2011) and has several exocyst-independent roles, including membrane deformation resulting in the formation of actin-free cell protrusions by EXO70 oligomerization-induced negative membrane curvature (Zhao *et al.*, 2013). Independently from the rest of the exocyst, EXO70 stimulates Arp2/3-induced actin polymerization and branching (Liu *et al.*, 2012). Two different isoforms, E-EXO70 and M-EXO70, result from mammalian EXO70 alternative splicing, with only the M-EXO70 splice variant being able to activate the Arp2/3 complex. During the epithelial–mesenchymal transition, cells switch expression from E-EXO70 to M-EXO70, facilitating invadopodia formation and cell migration (Lu *et al.*, 2013). Several additional mammalian EXO70 splice variants with differential tissue expression were documented, but the functional significance of these variants is unclear. Surprisingly, EXO70 even seems to regulate pre-mRNA splicing (Dellago *et al.*, 2011).

Bioinformatic analyses predicted surprisingly many paralogues of the EXO70 exocyst subunit encoded by land plant genomes (Eliáš *et al.*, 2003; Synek *et al.*, 2006). The extraordinary evolutionary dynamics of plant EXO70 paralogues is begging for a functional explanation. In the Arabidopsis genome 23 and in rice 47 EXO70-encoding genes were identified (Cvrčková *et al.*, 2012). Land plant EXO70 paralogues can be divided into three well-defined monophyletic subfamilies—EXO70.1, EXO70.2, and EXO70.3. The EXO70.1 subfamily is the least evolutionarily dynamic, with its members closely related to single type EXO70A subunits encoded in Chlorophyta, fungal, and animal genomes (Fig. 1). Interestingly, while the EXO70.1 subfamily consists of multiexon genes, the remaining two subfamilies contain mostly single-exon (or, occasionally, single-intron) genes in Arabidopsis (Synek *et al.*, 2006), suggesting a possible derived character of EXO70.2 and EXO70.3 subfamilies, whose evolutionary history probably involved reverse transcription at some point. The same pattern of intron distribution was also confirmed in a recent study in wheat (Zhao *et al.*, 2018), although the phylogeny presented there, generated by a method known to be prone to produce artefacts for divergent sequences, would require a critical re-assessment.

Published analyses as well as public transcriptomic and proteomic data clearly indicate that most cell types in plants express and also use several different EXO70 isoforms (Žárský *et al.*, 2009, 2013; Pečenková *et al.*, 2011; Sekereš *et al.*, 2017; Kulich *et al.*, 2018). Ten years ago we proposed a hypothesis on the biological role of EXO70 multiplicity, assuming an exclusively exocytotic function of the exocyst and suggesting, in addition to tissue-specific roles, a function of particular EXO70s in distinct cortical secretory domains of individual plant cells (Žárský *et al.*, 2009).

The landscape of exocyst research both in plants and in animals was, however, transformed substantially by independent discoveries that versions of the exocyst complex are involved in the autophagy process and lysosome/vacuolar delivery pathway in mammals and plants (Bodemann *et al.*, 2011; Kulich *et al.*, 2013). Based on these discoveries and the follow-up studies of plant EXO70.2 subfamily exocyst paralogues summarized below, we formulate a new hypothesis implicating the EXO70.2 subfamily in often non-canonical secretory processes derived from, or related to, autophagy. The autophagy-related pathways include processes contributing to secondary cell wall (SCW) biogenesis, biotic interactions, and defence. Engagement of the most evolutionarily dynamic EXO70.2 subfamily of EXO70s in biotic interactions and defence correlates well with massive proliferation and conservation of new protein variants, resulting in six well-defined clades (B, C, D, E, F, and H) within this subfamily in angiosperms, with different clades undergoing massive amplification in monocots (F) and dicots (H). Also in conifers, mosses, and lycophytes, the most identified EXO70 paralogues belong to the EXO70.2 clade (Rawat *et al.*, 2017). The basal and least divergent EXO70.1 subfamily, comprising only one clade—the EXO70A isoforms—is clearly linked to the housekeeping exocytotic function of the exocyst, functionally related especially to cell growth and primary and secondary cell wall biogenesis. The third subfamily, EXO70.3, comprising EXO70G paralogues and in most plant families also the EXO70I clade (lost in Brassicaceae/Arabidopsis) remains currently almost fully uncharacterized.

In this review we sum up recent advances in the characterization of the numerous members of the family of plant EXO70 exocyst subunits, with focus on *Arabidopsis thaliana* (Table 1), and present evidence that members of the EXO70.2 subfamily are often recruited to non-canonical functions in plant secretory pathways.

The basal EXO70.1 subfamily comprising exclusively EXO70A isoforms

Arabidopsis EXO70A1 is the first described and so far best characterized land plant EXO70 isoform, closely related to opisthokont EXO70s (Synek *et al.*, 2006). Published data clearly indicate that the exocyst complex containing EXO70A regulates housekeeping exocytotic functions; this correlates well with rather stable and strong expression across

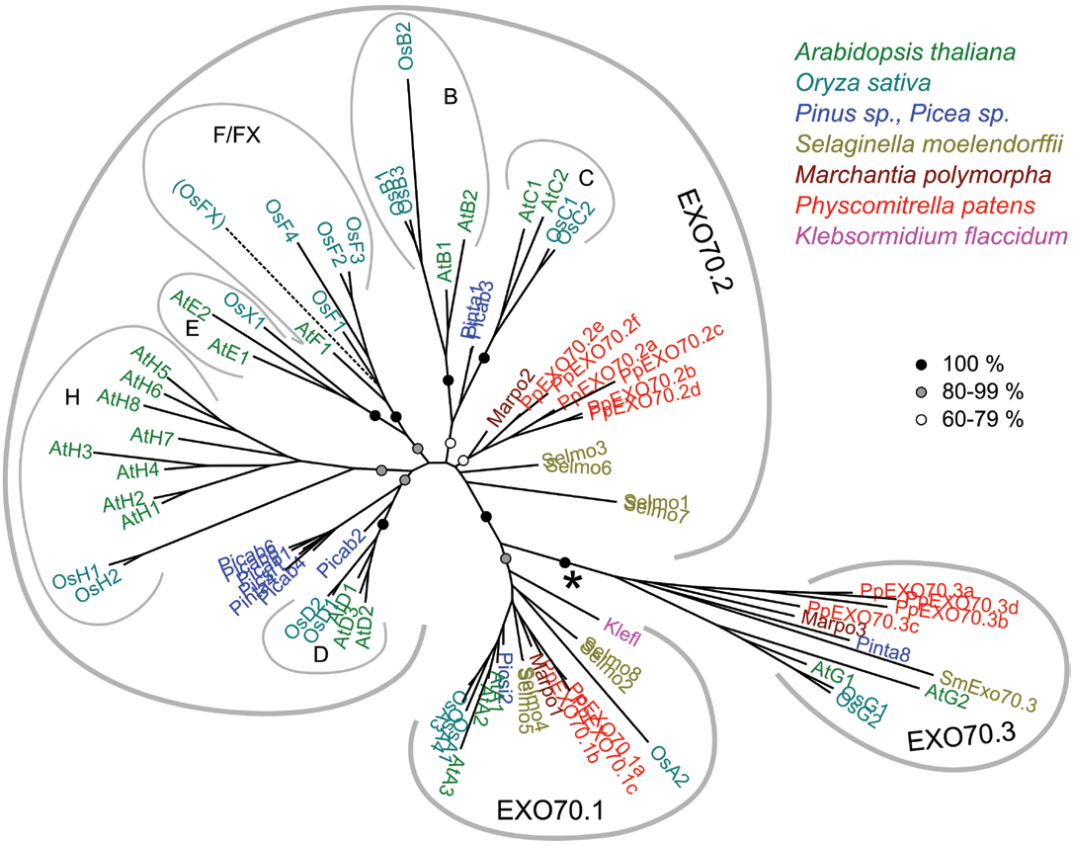

Fig. 1. Relationships between EXO70 subfamilies and lower order clades. The maximum likelihood phylogenetic tree was constructed using the method and a subset of data from our previous reports (Cvrčková *et al.*, 2012; Rawat *et al.*, 2017), with inclusion of the SmEXO70.3 sequence (Synek *et al.*, 2006). The FX clade was not included in the present analysis because of loss of resolution affecting mainly the non-angiosperm sequences; its position, based on a previous study (Cvrčková *et al.*, 2012), is indicated by a dashed line. The asterisk denotes the presumed position of the root, as inferred previously (Rawat *et al.*, 2017). For legibility, names of Arabidopsis and rice sequences are abbreviated: *A. thaliana* EXO70A1 as AtA1, rice EXO70B1 as OsB1, etc. For the remaining sequences, terminology follows our previous reports (Cvrčková *et al.*, 2012, Rawat *et al.*, 2017). Bootstrap support for deep (A to H clade level and below) branches is indicated by symbols (absence of a symbol means support <60%).

Arabidopsis sporophytic tissues (Synek *et al.*, 2006; Hála *et al.*, 2008; Fendrych *et al.*, 2010). A knockout mutant *exo70A1* also phenocopies defects of many core exocyst subunit mutants (Synek *et al.*, 2006; Hála *et al.*, 2008; Fendrych *et al.*, 2010). In the sporophyte, these shared defects include: slower hypocotyl elongation (Hála *et al.*, 2008), thinner and collapsed xylem SCW (Li *et al.*, 2013;Vukašinović *et al.*, 2017), impaired seed coat deposition mainly manifested as pectin deficiency (Kulich *et al.*, 2010), smaller and non-receptive stigmatic papillae (Synek *et al.*, 2006; Safavian *et al.*, 2015), reduced size of the root apical meristem and slower root cell elongation (Cole *et al.*, 2014), defective root hair growth (Wen *et al.*, 2005; Synek *et al.*, 2006), as well as impaired auxin transport due to slower PIN transporter recycling (Drdová *et al.*, 2013; Tan *et al.*, 2016) contributing to aberrant hypocotyl development in the dark (Drdová *et al.*, 2019). The elongation of *exo70A1* mutant root hairs is less stimulated in response to *Pseudomonas syringae*, and the mutant seedling roots are more susceptible to colonization by the bacteria than wild-type (WT) plants (Pečenková *et al.*, 2017). EXO70A1 shares subcellular localization with core exocyst subunits in many tissues, including root epidermis with polarization towards the outer lateral membrane domain (Fendrych *et al.*, 2013).

Exocyst function is essential for plant cytokinesis (Fendrych *et al.*, 2010; Rybak *et al.*, 2014). Loss-of-function (LOF) mutants *exo84b* (Fendrych *et al.*, 2010) and *sec6* (complemented in pollen by a lat52:SEC6 construct; Wu *et al.*, 2013) exhibit deformed seedlings and cell wall stubs resulting from defective cytokinesis. Although EXO70A1 co-localizes with the core exocyst subunits during both early cytokinesis and cell plate maturation, only the first phase of initial vesicle fusion is delayed in *exo70A1* mutants, but the defect is fully compensated during the cell plate progression. Thus, while loss of core exocyst subunits has dramatic consequences, only a transient defect in cell plate initiation was observed in Arabidopsis *exo70A1* LOF mutants, possibly due to functional redundancy with other EXO70 isoforms (Fendrych *et al.*, 2010).

Arabidopsis EXO70A2, the sister isoform of EXO70A1, is highly expressed in pollen (Loraine *et al.*, 2013; Synek *et al.*, 2017). It thus probably plays an analogous role in recruiting the exocyst to the area of active secretion around the pollen tube tip. In tobacco, NtEXO70A1a, and to some extent also

Table 1. *Summary of known functions and mutant phenotypes of* Arabidopsis thaliana *EXO70 paralogues*

Gene	AGI locus	Function or phenotype	References
EXO70.1 subfamily			
EXO70A1	At5g03540	Cytokinesis (cell plate initiation)	Fendrych *et al.* (2010); Rybak *et al.* (2014)
		Hypocotyl elongation	Hála *et al.* (2008)
		Root cell growth	Cole *et al.* (2014)
		Root hair growth	Synek *et al.* (2006); Wu *et al.* (2013)
		Smaller and non-receptive stigmatic papillae in mutants	Synek *et al.* (2006); Safavian *et al.* (2015)
		Seed coat deposition	Kulich *et al.* (2010)
		Aberrant hypocotyl development in dark-grown mutants	Drdová *et al.* (2019)
		Secondary cell wall biogenesis in endodermal Casparian bands	Kalmbach *et al.* (2017)
		Secondary cell wall deposition in developing xylem	Li *et al.* (2013); Oda *et al.* (2015); Vukašinović *et al.* (2017)
		PIN transporter recycling	Drdová *et al*. (2013); Tan *et al.* (2016)
		Binding to phosphatidylinositol 4,5-bisphosphate-rich PM domain in trichomes	Kubátová *et al.* (2019)
EXO70A2	At5g52340	High expression in pollen, role unknown	Loraine *et al.* (2013); Synek *et al.* (2017)
EXO70A3	At5g52350	Modulation of auxin-controlled root architecture development	Ogura *et al.* (2019)
EXO70.2 subfamily			
EXO70B1	At5g58430	Autophagy triggered by starvation and autophagy-related anthocyanin trafficking	Kulich *et al.* (2013)
		Immune response to pathogens, cell death	Stegmann *et al.* (2013; Zhao *et al.* (2015); Sabol *et al.* (2017)
		Light-induced stomatal opening	Hong *et al.* (2016); Seo *et al.* (2016)
EXO70B2	At1g07000	Formation of cell wall appositions in plant defence	Pečenková *et al*. (2011)
		Regulation of PAMP-induced signalling	Stegmann *et al.* (2012)
		Mannitol-induced stomatal closure	Seo *et al.* (2016)
EXO70C1	At5g13150	High expresion in root trichoblasts and pollen, role unknown	Grobei *et al.* (2009; Li *et al.* (2010); Synek *et al.* (2017)
EXO70C2	At5g13990	Negative regulation of tip growth	Synek *et al.* (2017)
EXO70D1	At1g72470	Unknown	
EXO70D2	At1g54090	Unknown	
EXO70D3	At3g14090	Unknown	
EXO70E1	At3g29400	Unknown	
EXO70E2	At5g61010	Unconventional secretory pathway or autophagy	Wang *et al.* (2010); Ding *et al.* (2014); Lin *et al.* (2015); P. Sabol *et al.* (unpublished results)
EXO70F1	At5g50380	Unknown	
EXO70H1	At3g55150	Defence against pathogens, mechanism unknown, nuclear localization	Pečenková *et al*. (2011)
EXO70H2	At2g39380	Iron transport and homeostasis, mechanism unknown	Xing *et al.* (2015)
EXO70H3	At3g09530	High expression in pollen, role unknown	Synek *et al.* (2017)
EXO70H4	At3g09520	Delivery of callose synthases to plasma membrane	Kulich *et al.* (2018)
		Secondary cell wall callose and silica deposition in trichomes	Kulich *et al.* (2015)
		Callose deposition during reaction to pathogen attack in epidermis	Kulich *et al.* (2018)
		Binding to phosphatidic acid and phosphatidylserine-rich PM domain in trichomes	Kubátová *et al.* (2019)
EXO70H5	At2g28640	High expression in pollen, role unknown	Synek *et al.* (2017)
EXO70H6	At1g07725	High expression in pollen, role unknown	Synek *et al.* (2017)
EXO70H7	At5g59730	Unknown	
EXO70H8	At2g28650	Unknown	
EXO70.3 subfamily			
EXO70G1	At4g31540	Unknown	
EXO70G2	At1g51640	Unknown	

Some of the genes with no experimental data available are not discussed in the text.

NtEXO70A2, are both expressed in pollen and localize to the same small exocytotically active subapical region of the pollen tube; however, tobacco NtEXO70A1b, which is not expressed in the male gametophyte, does not bind pollen tube PM (Sekereš *et al.*, 2017). EXO70A isoforms are thus involved in exocytosis in both sporophytes and gametophytes,

with pollen-specific isoforms possibly adapted to the extraordinary demand for vesicle fusion during rapid tip growth of pollen tubes.

Recently, a GWAS (genome-wide association study) identified Arabidopsis EXO70A3 as a modulator of auxin contribution to overall root architecture development, showing, for the first time, that this EXO70A paralogue is an important factor of natural genetic variability in deep- versus shallow-rooting Arabidopsis accessions (Ogura *et al.*, 2019).

A new pharmacological experimental intervention tool into the EXO70 function, endosidin2 (ES2), was described recently (Zhang *et al.*, 2016). This substance, discovered as an inhibitor of Arabidopsis exocytosis, was shown to specifically inhibit EXO70 homologues of eukaryotes, providing a new valuable possibility to address exocyst function in different cell types.

Since the EXO70.1 (EXO70A) isoforms are closest to opisthokont EXO70s and target exocysts to the PM in various tissues (Fendrych *et al.*, 2013; Kalmbach *et al.*, 2017), interaction with PM phospholipids can be expected to contribute to EXO70A PM targeting. Indeed, tobacco NtEXO70A1a localizes to a polar secretory domain where PIP_2 and phosphatidic acid (PA) overlap in the growing pollen tube (Sekereš *et al.*, 2017). EXO70A1 also co-localizes with PIP_2 in a prospective Casparian strip deposition site in differentiating endodermis (Kalmbach *et al.*, 2017). Importantly, besides Arabidopsis, a mutant in the EXO70A1 gene was also characterized in rice (Tu *et al.*, 2015). The mutant plants are dwarfed, with impaired cell elongation and differentiation (and also collapsed vascular xylem cell walls), and show a partial loss of apical dominance, clearly indicating conserved EXO70A function in all basal exocytotic processes across angiosperms.

Cellular context-dependent specific functions of Arabidopsis EXO70A1 in endodermis and xylem development

Possibly in every plant cell type there are several expressed EXO70 paralogues, resulting in the presence of several specific exocyst complexes. We proposed that this might support formation of distinct cortical exocytotic PM and cell wall domains (Žárský *et al.*, 2009, 2013). Surprisingly, recent studies indicate that even the same EXO70 paralogue, namely Arabidopsis EXO70A1, might function in several specific modes depending on the cellular context. An allele of EXO70A1 with a point mutation altering a putative C-terminal phospholipid-binding domain of the protein was found in a forward screen for genes engaged in Arabidopsis endodermis differentiation. Unlike the *exo70A1* LOF mutant, these point mutant plants do not exhibit gross developmental defects but show disturbed local SCW biogenesis in Casparian bands (Kalmbach *et al.*, 2017).

Defective xylem development was observed in the Arabidopsis *exo70A1* mutant, and was mistakenly interpreted as the sole primary cause of the whole-mutant developmental deviation syndrome (Li *et al.*, 2013). Using an inducible xylogenesis model system in Arabidopsis, Oda *et al.* (2015) surprisingly found that EXO70A1 protein localization in developing xylem depends on the microtubular (MT) cytoskeleton. This finding contrasts with our previous observations from root epidermal cells, where exocyst dynamics are largely independent of both actin and MT cytoskeletons and not affected even after a chronic pharmacological disturbance of the MTs (Fendrych *et al.*, 2013). In developing xylem, MT-dependent EXO70A1 localization is due to an indirect interaction between EXO70A1 and MTs mediated by xylem precursor cell-specific VESICLE TETHERING 1 and 2 (VETH1/2) proteins and the CONSERVED OLIGOMERIC GOLGI (COG) tethering complex subunit COG2 (Oda *et al.*, 2015). Our subsequent experiments revealed that several core exocyst subunits interact indirectly with the xylem-specific VETH1/2 adaptors via COG2 binding and that MT relocalization to the domains of future SCW deposition precedes exocyst localization to the same domain (Vukašinović *et al.*, 2017). Here we also observed for the first time that the delivery of cellulose synthase (CesA) complexes depends on the exocyst function (Vukašinović *et al.*, 2017). These observations are an important reminder that specific cellular contexts substantially affect protein function—in this case the same EXO70A1 paralogue functions in the biogenesis of different and cell type-specific cell wall domains.

EXO70.2 subfamily: a champion in evolutionary multiplication comprising six clades often involved in defence and non-canonical exocyst functions

Already the first systematic phylogenetic analysis of the immense land plant EXO70 diversity led us to propose that evolution of this gene family may be driven by competition with parasites, and that some EXO70s may participate in defence (Hála *et al.*, 2008). Indeed, pathogen/elicitor-induced EXO70B2 and EXO70H1 subunits are involved in the resistance against *P. syringae* and *Blumeria graminis* infections (Pečenková *et al.*, 2011). Phylogenetic analyses further confirm that the EXO70.2 subfamily, which comprises six well-defined clades, namely EXO70B, EXO70C, EXO70D, EXO70E, EXO70F, and EXO70H, is responsible for most of EXO70 diversification in land plants (see Fig. 1), often linked to defence. Evidence for a tendency of these EXO70s to form homo- or heterodimers slowly accumulates, while paralogues from other subfamilies seem incapable in this respect (Pečenková *et al.*, 2011; Fujisaki *et al.*, 2015; Z. Kubátová, unpublished data). Grasses have a specific, extraordinarily rapidly evolving subgroup FX within the EXO70F clade (Synek *et al.*, 2006; Cvrčková *et al.*, 2012).

EXO70B

The best characterized members of the EXO70.2 subfamily are both members of the Arabidopsis EXO70B clade, EXO70B1 and EXO70B2. Other angiosperm genomes often encode either only one EXO70B paralogue or paralogues that arose by independent duplications, not related to the evolution of Arabidopsis EXO70B1 and EXO70B2 (Cvrčková *et al.*, 2012). Therefore, some of the functional properties of EXO70B proteins discussed here are probably relevant mostly

for Brassicaceae; it is also possible that the EXO70B duplication in Brassicaceae led to separation of functions present in the unique EXO70B paralogue of other plant families.

Arabidopsis EXOB1: role in autophagy, stomatal regulation, and defence

EXO70B1 is highly expressed across many sporophytic and gametophytic tissues and, surprisingly, has a role in autophagy triggered by starvation (for either photosynthetic/sugar or nitrogen) and in autophagy-related direct import of anthocyanins to the vacuole, bypassing the Golgi apparatus (Kulich *et al.*, 2013). Vesicular autophagy-related anthocyanin trafficking involves EXO70B1 co-localization with the anthocyanin-containing compartments possibly initiated at the endoplasmic reticulum and also with the autophagy marker AUTOPHAGY-RELATED (ATG) protein ATG8f internalized into the vacuole (Kulich *et al.*, 2013). Mutants lacking EXO70B1 are nitrogen starvation sensitive, accumulate fewer autophagic bodies in the vacuole, and generate paramural bodies in the apoplast, possibly due to defective transport of autophagosomes or multivesicular bodies (MVBs) to the vacuole. Importantly, the *exo70A1exo70B1* double mutant displays phenotypic deviations of both single mutants, indicating no functional overlap between EXO70A1 and EXO70B1. *exo70B1* mutant plants also develop spontaneous leaf hypersensitive response (HR)-like lesions, with cells undergoing programmed cell death linked to salicylic acid (SA) hyperaccumulation (Kulich *et al.*, 2013), and have a reduced threshold for programmed cell death initiation after pathogen infection (Stegmann *et al.*, 2013; Zhao *et al.*, 2015). The onset of the HR-like phenotype varies depending on the cultivation conditions and appears with high incidence in plants older than 6 weeks (Kulich *et al.*, 2013). As a consequence of SA hyperaccumulation, the mutant is more resistant towards strictly biotrophic pathogens but displays reduced overall fitness (Stegmann *et al.*, 2013; Zhao *et al.*, 2015). Since SA hyperaccumulation is a common feature of autophagy mutants, and the SA analogue BTH [benzo (1,2,3) thiadiazole-7-carbothioic acid *S*-methyl ester] activates autophagy, the hypersensitive phenotype of *exo70B1* might be caused by impaired SA clearance due to its defective autophagy-related transport to the vacuole (Yoshimoto *et al.*, 2009; Kulich *et al.*, 2013; Kulich and Žárský, 2014).

A direct EXO70B1 interactor, TN2 (a TIR-NBS truncated NLR disease resistance protein), is required for SA and H_2O_2 accumulation, as well as for a spontaneous HR in *exo70B1* mutants (Zhao *et al.*, 2015). The TN2-driven HR involves direct phosphorylation of EXO70B1 by the TN2-interacting calcium-dependent protein kinase 5 (CDPK5), probably with an inhibitory effect (Liu *et al.*, 2017). It was hypothesized that EXO70B1 is targeted by an as yet unknown pathogen effector and that TN2 monitors EXO70B1 integrity, triggering a HR if EXO70B1 becomes compromised (Zhao *et al.*, 2015). Alternatively, TN2 could be normally degraded by an EXO70B1-dependent autophagy pathway to prevent excessive TN2-induced SA accumulation, which would occur in the absence of EXO70B1, since autophagy has been proposed as a possible mechanism for negative regulation of R proteins (Pečenková *et al.*, 2016). These mechanisms postulating either a direct or an indirect role for EXO70B1 in SA level control are not mutually exclusive. EXO70B1 could monitor TN2 activity under standard conditions, as well as facilitate degradation of excessive SA. An autophagy-related pathway involving EXO70B1 has been proposed as a general trafficking route of various secondary metabolites to the vacuole (Kulich and Žárský, 2014).

The role of EXO70B1 in plant immunity is not limited to SA-mediated indirect effects. Recently, we have shown (Sabol *et al.*, 2017) that EXO70B1 is translocated to the PM by RIN4 (RPM1 INTERACTING PROTEIN 4), a regulator of plant defence interacting with many plant R proteins. EXO70B1, unlike several other EXO70 isoforms tested, directly binds RIN4. Molecular details of EXO70B1 recruitment to the PM by RIN4 were investigated in a heterologous *Nicotiana benthamiana* system, showing that full-length RIN4 is required for this process and that upon RIN4 cleavage by the *P. syringae* effector protease, AvrRpt2, both RIN4 and EXO70B1 are released from the PM (Sabol *et al.*, 2017).

Furthermore, EXO70B1 also regulates stomatal opening and closure (Hong *et al.*, 2016). The *exo70B1* mutants exhibit slower light-induced stomatal opening than WT plants. EXO70B1 directly interacts with the Rho of plants (ROP) regulator RIC7 (ROP-interactive Cdc42- and Rac-interactive binding motif-containing protein 7). Both proteins are translocated to the PM by active ROP2 and are held inside the cytoplasm by dominant-negative ROP2 in biolistically transformed stomata of *Vicia faba* (Hong *et al.*, 2016). Since Arabidopsis *ric7* mutants display faster light-induced stomatal opening than WT plants, RIC7 probably also acts as a negative regulator of EXO70B1 activity during stomatal opening (Hong *et al.*, 2016). While mutation in the EXO70B1 gene has no effect on abscisic acid (ABA)-induced stomatal closure, upon treatment with 1 μM ABA (Hong *et al.*, 2016) the stomata of *exo70B1* close more slowly than those of WT plants upon the application of 10 μM ABA or mannitol; on the other hand, plants overexpressing EXO70B1 close their stomata faster under these conditions (Seo *et al.*, 2016).

The tobacco homologue NtEXO70B1 is distinctly expressed in pollen (Conze *et al.*, 2017; Sekereš *et al.*, 2017), and localizes to a specific subapical membrane domain in growing tobacco pollen tube, overlapping with the zone of active endocytosis marked by localization of the endocytic machinery; thus, the protein could play a direct or indirect role in the endocytosis. Alternatively, it could regulate an unknown minor secretory pathway in tobacco pollen, distinct from the bulk secretion regulated by EXO70A clade members (Sekereš *et al.*, 2017). Very low expression of B-clade EXO70 was reported in Arabidopsis pollen (summarized in Synek *et al.*, 2017). It is thus possible that the pollen function of EXO70B1 detected in Solanaceae might not be a general feature of pollen tubes in all Angiosperms. Tobacco NtEXO70B1 could be targeted to the PM via interaction with PA in a growing pollen tube, since its localization largely overlaps with the PA maximum, although direct binding has not been demonstrated so far (Sekereš *et al.*, 2017). In general, PM targeting of Arabidopsis EXO70B1

could be driven by various protein interactors such as RIN4 (Sabol *et al.*, 2017) and RIC7 in stomatal guard cells (Hong *et al.*, 2016). Direct experiments and data from protein–protein interaction databases implicate that different EXO70 isoforms interact with different NO_3-induced (NOI)-domain containing proteins to a varying degree (Afzal *et al.*, 2013; Sabol *et al.*, 2017)—certainly an important issue for future studies.

Arabidopsis EXOB2: specialized for defence

EXO70B2 is the closest paralogue of EXO70B1 in Arabidopsis; on the other hand, the EXO70B1/EXO70B2 pair has the lowest sequence similarity of Arabidopsis EXO70 isoform sister pairs and, for instance, EXO70B1 is less related to EXO70B2 than to the tobacco NtEXO70B1 orthologue (Sekereš *et al.*, 2017). Divergence of EXO70B1 and EXO70B2 may be an evolutionary novelty of the Brassicaceae family, possibly not relevant for other angiosperm groups (for a detailed phylogenetic analysis, see Cvrčková *et al.*, 2012; Sekereš *et al.*, 2017). EXO70B2 mRNA expression is induced by various pathogens and elicitors (Pečenková *et al.*, 2011). The *exo70B2* mutant plants are more susceptible to infection by *P. syringae* (Pečenková *et al.*, 2011; Stegmann *et al.*, 2012) and the oomycete *Hyaloperenospora arabidopsidis* (Stegmann *et al.*, 2012) than WT plants. The mutants also exhibit deviations in defensive papilla formation upon infection by the fungus *B. graminis* (Pečenková *et al.*, 2011). Unlike WT plants, the *exo70B2* mutants do not up-regulate expression of several defence markers after PAMP (pathogen-associated molecular pattern) treatment, do not build up protection against *Pseudomonas* infection upon flagellin (flg22) pre-treatment, and inhibition of their primary root growth by flg22 is less pronounced than in WT plants (Stegmann *et al.*, 2012).

EXO70B2 is capable of homodimerization and heterodimerization with another pathogen-related isoform, EXO70H1 (Pečenková *et al.*, 2011). In addition, the EXO70B2 role in plant defence may be related to its transient association with SNARE proteins, mainly SNAP33 and SYP121 (Pečenková *et al.*, 2011; Zhao *et al.*, 2015; J. Ortmannová *et al.*, unublished data). Molecular determinants of EXO70B2 recruitment to the membrane are unclear, but, unlike EXO70B1, EXO70B2 is not translocated to the PM when co-expressed with RIN4 in *N. benthamiana* leaves. It weakly interacts, however, with RIN4-like protein NOI6; EXO70B2 might also be recruited to the PM by one or more of the many other NOI-domain-containing proteins (Afzal *et al.*, 2013; Sabol *et al.*, 2017). EXO70B2 does not seem to participate in ABA-induced stomatal closure, but it is implicated in the mannitol-induced stomatal closure (Seo *et al.*, 2016).

To conclude, unlike EXO70A, involved in housekeeping exocytosis, clade B EXO70 isoforms are involved in autophagic trafficking of mostly defence-related cargos through the prevacuolar compartment and MVBs to the vacuole but also to the extracellular space (cell wall and apoplast). Current evidence indicates that the EXO70B-assisted trafficking pathway may bypass the Golgi apparatus. For apoplast delivery, EXO70Bs might require a PM-associated recruitment protein. The function of EXO70Bs also varies depending on the cell type (e.g. stomata), age of the plant, and also strongly on environmental conditions.

EXO70C—a non-canonical EXO70 protein moderating growth rate in tip-growing cells

Arabidopsis EXO70C1 and EXO70C2 are specifically transcribed in root hair trichoblasts and pollen at a very high level, exceeding the transcript levels of core exocyst subunits (Synek *et al.*, 2017). At the protein level, C subfamily EXO70s are the most abundant EXO70 isoforms in both Arabidopsis and tobacco pollen (Grobei *et al.*, 2009; Sekereš *et al.*, 2017), suggesting a possible specific role in tip growth. Surprisingly, unlike EXO70A isoforms or core exocyst subunits, EXO70C proteins do not localize to the PM and seem to be purely cytoplasmic in Arabidopsis root hairs and Arabidopsis and tobacco pollen tubes, even when overexpressed (Sekereš *et al.*, 2017; Synek *et al.*, 2017). However, the effects of their overexpression in tobacco pollen tube indicate misregulated growing tip polarity (Sekereš *et al.*, 2017), and both *exo70C1* (Li *et al.*, 2010) and *exo70C2* (Synek *et al.*, 2017) mutants display a partial male transmission defect.

Mutant *exo70C2* pollen tubes growing in the style or *in vitro* are shorter than WT pollen tubes. Surprisingly, this is not due to a slower growth rate or loss of pollen tube polarity. On the contrary, mutant pollen tubes can elongate up to twice as fast as WT tubes, but cannot sustain such a rapid growth, which often results in bursting of their fast growing tips, evident as local release of cytoplasmic content. Burst pollen tubes cease to grow, regenerate, and often start a new period of fast growth and burst again. This stop and go mode of growth in cycles results in overall shorter pollen tube length compared with WT pollen tubes. This phenomenon of tip bursting, probably resulting from overstretching and weakening of the cell wall at the apex due to disrupted balance between the rate of delivery of cell wall biogenesis components and an excessive speed of elongation, suggests that the C clade of the EXO70.2 subfamily is a negative regulator or moderator of secretion (Synek *et al.*, 2017).

EXO70D, EXO70E, and EXO70F (and FX in grasses)

These three clades of the EXO70.2 subfamily are so far poorly characterized, with published data only for EXO70E. However, transcriptome data suggest a cell type-specific engagement in the endodermis or stomata for EXO70D (Winter *et al.*, 2007; Hruz *et al.*, 2008).

Arabidopsis EXO70E2 localizes to cytoplasmic punctae when overexpressed in cell culture, and this localization is unaffected by inhibitors commonly used to dissect plant cell membrane trafficking. The structures resemble inclusion bodies but turned out to be double-membrane compartments reminiscent of autophagosomes that can fuse with the PM, releasing a large exosome to the apoplast (Wang *et al.*, 2010). These EXO70E2-containing particles sequester exocyst subunits and other proteins upon overexpression in Arabidopsis cell culture (Wang *et al.*, 2010; Ding *et al.*, 2014) and do not co-localize with known membrane compartment markers

including the autophagy marker Atg8e under normal conditions (Wang *et al.*, 2010). However, upon autophagy induction, the EXO70E2-containing structures co-localize with Atg8e and Atg8f and move with them into the vacuolar lumen (Lin *et al.*, 2015).

The closest tobacco homologue of Arabidopsis EXO70E2, NtEXO70E2, is not naturally expressed in tobacco pollen; however, when ectopically expressed, yellow fluorescent protein (YFP):NtEXO70E2 in pollen tubes localizes to mobile puncta with negligible cytoplasmic signal, even at a low level of expression (Sekereš *et al.*, 2017). Strangely, Arabidopsis EXO70E2 induces the above-described double-membrane compartments even when expressed in mammalian cells—an extremely heterologous system for the plant-specific protein (Ding *et al.*, 2014). It is thus evident that the EXO70E2 protein either hijacks the autophagy machinery in various species, or directly strongly deforms membranes in a manner analogous to the action of BAR domains, as proposed for mammalian EXO70 (Zhao *et al.*, 2013), or forms aggregates that are very potent autophagy cargo in both animal and plant cells, thus resulting in autophagy induction. It is currently difficult to figure out the biological function of EXO70E2, because most subcellular localization data are based on 35S promoter-driven overexpression in Arabidopsis or in cell cultures. Unless the protein is studied in its native environment under a physiological level of expression, overexpression artefacts are difficult to avoid and interpretation of the results is problematic. EXO70E2 could play a role in a specific subtype of autophagic processes connected to an unconventional secretory pathway involving exosome production, especially in the root cap (Lin *et al.*, 2015; P. Sabol *et al.*, unpublished observations).

Using strong expression of eight different Arabidopsis EXO70 isoforms in protoplasts under the 35S promoter, Wang *et al.* (2010) found that three of them (EXO70A1, EXO70B1, and EXO70E2) form punctate autophagosome-like double-membrane structures and co-localize in these structures. However focusing in detail on EXO70E2, they observed that these structures are not targeted to the vacuole upon starvation conditions, but rather are secreted to the apoplast (Wang *et al.*, 2010). Based on these observations, the authors proposed the existence of a new plant-specific endomembrane exocyst-positive compartment in plants—EXPO—involved in unconventional secretion (Wang *et al.*, 2010; Ding and Wang, 2017). We have shown, however, that the EXO70B1 paralogue is involved in autophagy, and EXPO-like structures are also formed when the EXO84b exocyst subunit is expressed under the 35S promoter, while expression controlled by the native promoter does not lead to formation of such structures (supplementary fig. 5 of Kulich *et al.*, 2013). In Arabidopsis *exo70b1* mutants, more exosomal structures possibly related to autophagosomes (similar to proposed EXPOs but also to paramural bodies) are secreted to the apoplast (supplementary fig. 3 of Kulich *et al.*, 2013). As indicated above, currently only the EXO70E2 isoform is considered to be localized in some cells (especially in the root cap) to EXPO-like structures; new observations also indicate vacuolar re-targeting of these structures upon autophagy induction (Lin *et al.*, 2015). As autophagosomes are known to be able to fuse with the PM and participate in the unconventional protein secretion, we prefer to interpret the EXO70E2 compartment as also related to the so-called secretory autophagy pathway (for a review, see, for example, Ponpuak *et al.*, 2015).

Unfortunately, no mutant-based functional studies of Arabidopsis EXO70E2 or its closest homologue EXO70E1 have been reported so far, and the latter remains entirely uncharacterized. The closest homologue of Arabidopsis EXO70E1, NtEXO70E1b, is expressed in tobacco pollen and localizes to the inverted cone of secretory and recycling vesicles at the tip of growing tobacco pollen tubes, although the functional significance of this subcellular localization is unclear (Sekereš *et al.*, 2017). A very interesting new protein involved in the effective defence against herbivorous planthoppers BPH6 was uncovered recently in rice—it functions by stimulation of exocytosis via interaction with the exocyst mediated by direct binding with EXO7OE1 (Guo *et al.*, 2018).

Also the EXO70F clade is still awaiting characterization in Arabidopsis. While in the dicots this clade underwent only moderate diversification, in the grasses its FX subclade underwent a massive evolutionary expansion, suggesting a possible role in defence (Cvrčková *et al.*, 2012). Consistent with this hypothesis, silencing of one of the barley F subfamily EXO70s increased susceptibility towards grass powdery mildew (Ostertag *et al.*, 2013), rice OsEXO70-F2 and OsEXO70-F3 form complexes with the avirulence factor AVR-Pii, and OsEXO70-F3 contributes to *Pii*-mediated resistance against incompatible *Magnaporthe oryzae* strains expressing *AVR-Pii* (Fujisaki *et al.*, 2015).

EXO70H

While encoded by only a few paralogues in monocot genomes, EXO70H is the most diversified clade in dicots. The H clade EXO70 paralogues display a striking example of independent EXO70 duplications specific for many angiosperm taxa (Cvrčková *et al.*, 2012). It is also noteworthy that the rate of substitutions detected between EXO70 genes from tobacco (*Nicotiana tabacum*) and its parental species (*N. sylvestris* and *N. tomentosiformis*) was very low for the EXO70A clade but highest among all clades for EXO70H (Sekereš *et al.*, 2017). The EXO70H clade thus seems to be subject to rapid evolution in dicots compared with other EXO70 clades. Also, non-orthologous EXO70H isoforms are expressed in Arabidopsis and tobacco pollen (Sekereš *et al.*, 2017; Synek *et al.*, 2017), further pointing to the rapid evolution of this clade. Eight EXO70H isoforms are found in the Arabidopsis genome; thus, it is the most numerous clade of EXO70s in Arabidopsis. Nonetheless, very limited information is available regarding the biological functions of EXO70H isoforms, with only a few of them characterized at least basically.

The functionally best described member of the H clade is Arabidopsis EXO70H4. It is one of the most up-regulated genes in developing trichomes (Jakoby *et al.*, 2008), where it regulates polarized callose-rich cell wall deposition during secondary thickening, including a noteworthy structure on the stalk above the trichome base denominated as the Ortmannian ring (Kulich *et al.*, 2015). This SCW ring-like build-up is

enriched mainly in callose but also in other cell wall components, and probably forms a physical barrier separating the plant body from the trichome SCW. EXO70H4 localizes to sites of prospective cell wall deposition in trichomes together with other exocyst subunits and recruits callose synthases to these sites, namely GLUCAN SYNTHASE LIKE (GSL) 5, also known as POWDERY MILDEW RESISTANT 4 (PMR4), and GSL10 (Kulich *et al.*, 2018). The EXO70H4-dependent callose deposition is also a pre-requisite for silica deposition in the cell wall. Importantly, this function of EXO70H4 in trichomes seems to be highly specific and cannot be replaced by any other Arabidopsis EXO70H isoforms, including closely related EXO70H3. While limited to trichomes under normal conditions, EXO70H4 expression is induced in pavement epidermal cells upon flg22 or chitin treatments, suggesting a role in callose deposition also during reaction to pathogen attack (Kulich *et al.*, 2018). EXO70H4 expression is negatively regulated by methyl jasmonates (Hruz *et al.*, 2008), conceivably linking EXO70H4 with herbivore resistance. On the other hand, positive regulation by UV-B light through the CONSTITUTIVE PHOTOMORPHOGENETIC 1 (COP1) E3 ubiquitin ligase pathway was reported (Oravecz *et al.*, 2006) and EXO70H4-dependent UV light stimulation of Arabidopsis trichome SCW thickening was observed (Kulich *et al.*, 2015). Recently we described very specific PM lipid domains in mature Arabidopsis trichomes separated by the callose Ortmannian ring. The upper PA- and phosphatidylserine-rich domain above the ring binds the EXO70H4 isoform preferentially, while the basal domain enriched in PIP_2 binds preferentially EXO70A1 (Kubátová *et al.*, 2019). This observation supports the hypothesis that some EXO70 isoforms in the same cell might target the exocyst (or exocyst subcomplexes) to specific cortical PM domains (Žárský *et al.*, 2009). In the same report, capturing of EXO70H4-positive membranes within the trichome secondary cell wall was uncovered using electron microscopy (Kubátová *et al.*, 2019).

Based on both experimental and bioinformatic data, a hypothesis on miRNA interference with EXO70 mRNAs was proposed for the EXO70H clade (Kulich *et al.*, 2018). An interesting question of stoichiometry arises from transcriptomic and proteomic data (Jakoby *et al.*, 2008; for pollen summarized in Synek *et al.*, 2017), where other exocyst subunits are not as abundant as EXO70H4 itself. In yeast and mammals, each exocyst subunit seems to be present in 1:1 stoichiometry already at the transcript level, but this is not always the case in plants. It was demonstrated that EXO70H4 is trapped within the SCW so that it does not recycle, in contrast to other exocyst subunits (Kubátová *et al.*, 2019)—this may well explain non-stoichiometry of EXO70H4 in trichomes (Kulich *et al.,* 2015, 2018). The *Cucumis sativus* EXO70H4 isoform was also found to be highly up-regulated during development of its multicellular fruit trichomes (Chen *et al.*, 2014). This suggests a conserved role for EXO70H4 across a variety of eudicot clades and between multicellular and unicellular trichomes (Kulich *et al.*, 2015).

A role in defence against pathogens has also been described for the EXO70H1 paralogue, which is expressed in response to treatment with the elf18 peptide. LOF mutation in the EXO70H1 locus results in enhanced susceptibility towards *P. syringae*. However, the detailed mechanism of EXO70H1 action in defence is unknown. Surprisingly, Arabidopsis EXO70H1 localizes to the nucleus when expressed in *N. benthamiana* epidermis (Pečenková *et al.*, 2011). Also tobacco NtEXO70H1/2 and NtEXO70H5-8b localize to the nucleus in growing pollen tubes (Sekereš *et al.*, 2017). The high ratio of nuclear to cytoplasmic localization of several tobacco EXO70H isoforms is consistent with their possible function within the nucleus. This is further supported by richness of nuclear proteins within the putative Arabidopsis EXO70H1 interactome (Žárský *et al.*, 2013). EXO70H1pro::GUS (β-glucuronidase) and EXO70H2pro::GUS were found to be expressed specifically in the elongation and root hair formation root region (Li *et al.*, 2010). The paralogue EXO70H2 has been followed in the context of iron transport and homeostasis regulation where it was identified as a potential downstream regulatory target of the histone acetyltransferase GENERAL CONTROL NON-REPRESSED PROTEIN 5 (GCN5; Xing *et al.*, 2015).

In *Medicago truncatula*, an EXO70H clade member (Medtr4g062330) is induced upon *Rhizobium* infection, co-localizes to the infection thread tip with vapyin (VPN) and its interactor, the E3 ligase LIN, and is required, together with these two proteins, for normal infection thread development (Liu *et al.*, 2019). For unclear reasons, Liu *et al.* consider Medtr4g062330 an EXO70H4 orthologue, although a previous phylogenetic analysis locates this protein clearly inside a clade that contains Arabidopsis EXO70H5, H6, H7, and H8, but not EXO70H4 (Zhang *et al.*, 2015).

The EXO70.3 subfamily

The ancestral EXO70.3 subfamily comprises two clades, EXO70G and EXO70I, with clade I apparently lost in the Brassicaceae including Arabidopsis (Eliáš *et al.*, 2003; Cvrčková *et al.*, 2012). However, the reliability of resolution between the G and I clades varies somewhat depending on the methods of phylogenetic analysis used, becoming less distinct with inclusion of divergent sequences that necessitate exclusion of unreliably aligned sequence portions from the analysis (e.g. Cvrčková *et al.*, 2012). A phylogenetic analysis focusing exclusively on angiosperm EXO70.3 subfamily members that can be reliably aligned along their whole length clearly confirms the existence of these two clades, as well as the presence of an EXO70I clade member in grapevine, a basal rosid (Fig. 2).

In our previously published analysis of EXO70 evolution, based on the final published *Selaginella* genome assembly, we concluded that lycopods possibly lost the EXO70.3 subfamily (Cvrčková *et al.*, 2012). However, in an earlier study, including data from a pre-release of the *Selaginella* genome, we identified a gene, SmEXO70.3, which clearly clusters within the EXO70.3 subfamily (Synek *et al.*, 2006). This gene is, however, located on a genomic fragment that has been excluded from the final genome release and its sequence has never been deposited in GenBank [it remains, however, available in the supplementary data of our report (Synek *et al.*, 2006)]. After critical re-evaluation of related *Selaginella* sequence data, we

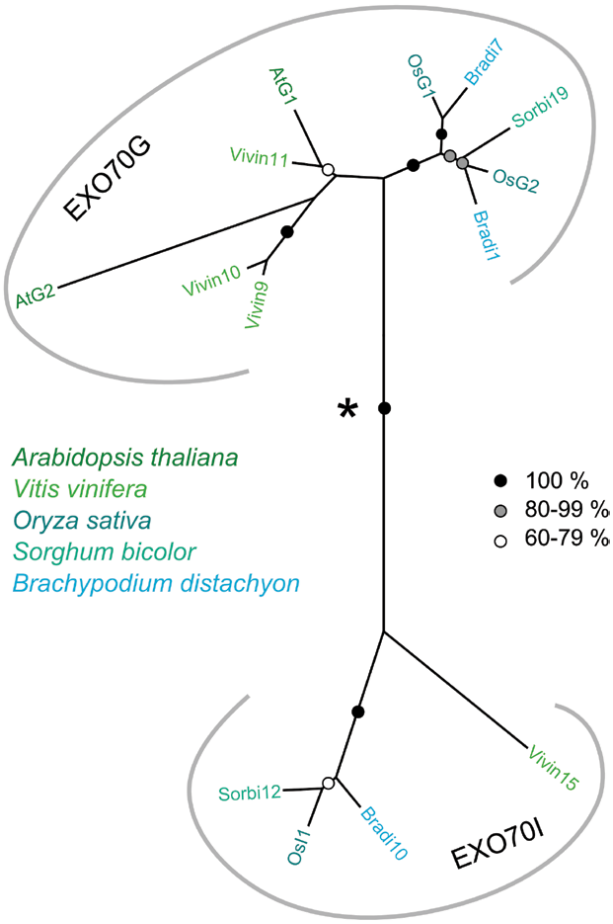

Fig. 2. Relationships between clades within the angiosperm EXO70.3 subfamily. The maximum likelihood phylogenetic tree was constructed using the method and data described previously (Cvrčková *et al.*, 2012). One incomplete *Sorghum bicolor* sequence has been omitted to preserve alignment length. The asterisk denotes the presumed position of the root as inferred from a preliminary tree including also *A. thaliana* EXO70A1 (not shown). For terminology, see legend to Fig. 1. Bootstrap support is indicated by symbols (branches without a symbol had bootstrap support between 50% and 60%).

go back to our original conclusion (also indicated in Rawat *et al.*, 2017), that also lycopods, including *Selaginella*, harbour all three land plant EXO70 subfamilies (see Fig. 1).

Members of the Arabidopsis EXO70G clade are awaiting functional characterization. The sole published report focusing on functional characterization of a member of this particular clade describes the mutant phenotype and protein localization of EXO70.3d in the moss *Physcomitrella patens*. The *exo70.3d* LOF mutant shows pleiotropic developmental deviations in protonemata, gametophores, sexual organs, and sporophytes. It is obvious that while the gene is not essential for cell survival, its function is important for multicellular development and possibly for communication between cells, as the egg cell in archegonia is initiated but not differentiated properly, and the mutant is thus unable to form the sporophyte (Rawat *et al.*, 2017).

Only a few functional studies exist for members of the EXO70I clade, which is absent in Arabidopsis. Expression of *M. truncatula* EXO70I is induced by arbuscular mycorrhizal symbiosis; in *exo70i* mutant plants, the branching of developing arbuscules is aberrant and incorporation of membrane cargo into the peri-arbuscular membrane is impaired. EXO70I:YFP specifically accumulates near the hyphal tips of developing arbuscules. The scaffold protein VPN co-localizes with *M. truncatula* EXO70I and specifically interacts with this isoform, but not with EXO70A1 or EXO70B2, and is likely to act in EXO70I recruitment to its target membrane domain (Zhang *et al.*, 2015).

EXO70I-mediated trafficking to the developing peri-arbuscular membrane is likely to involve the whole EXO70I-containing exocyst complex, because the core exocyst subunit EXO84b also localizes to sites of symbiotic fungal penetration in *Medicago* and *Daucus carota*. Unlike mature arbuscules, the developing arbuscules recruit green fluorescent protein (GFP):EXO84b to tips and branches in carrot (Genre *et al.*, 2012). Although the GFP:EXO70I was also reported to accumulate near tips of the infection threads during rhizobial nodulation of *Medicago* cells (Gavrin *et al.*, 2017), mutation in *Medicago* EXO70I does not affect symbiotic interactions with nodule bacteria (Zhang *et al.*, 2015).

Non-canonical EXO70 domain-containing proteins

A legume-specific group of EXO70 domain-containing proteins was discovered in soybean. Their EXO70 domain is close to EXO70B but the 12 proteins form a distinct phylogenetic subgroup, and were named the EXO70J subfamily. Many of them contain a transmembrane domain homologous to one from a WRKY-related protein. The transmembrane domain-containing GmEXO70J1, 6, 7, 10, and 12 localize to the Golgi apparatus when expressed in *N. benthamiana*, unlike GmEXO70J3, which does not contain the transmembrane domain. While their cellular function is unknown, EXO70J subfamily members were hypothesized to participate in Golgi apparatus restructuralization and fragmentation (Chi *et al.*, 2015). This would be in agreement with the capability of the animal EXO70 to directly deform the PM (Zhao *et al.*, 2013). Expression of EXO70J paralogues increases in leaves during senescence (Chi *et al.*, 2015), but they are also expressed in many other tissues (Wang *et al.*, 2016). Viral-induced silencing of either transmembrane domain GmEXO70J7 or soluble GmEXO70J8 leads to premature leaf senescence. Furthermore, amiRNA silencing of GmEXO70J7 or (also transmembrane) GmEXO70J9 leads to a reduced number of nodules (Wang *et al.*, 2016). Strangely, expression of GmEXO70J7 and GmEXO70J9 decreases upon soybean inoculation with *Rhizobium* (Wang *et al.*, 2016). While hypotheses about the physiological role of J subfamily EXO70s include nitrogen transport, senescence regulation, nutrient elongation, and cell elongation (Chi *et al.*, 2015; Wang *et al.*, 2016), conclusive functional studies still remain to be done.

An EXO70-like domain is also present, together with NB and LRR domains, in a large protein, RGA2a, encoded by the *Sr33* locus that confers resistance of *Aegilops tauschii* to *Puccinia graminis* (Periyannan *et al.*, 2013); a homologue was also reported from *Triticum urartu* (Ling *et al.*, 2013). While there is genetic evidence that these proteins have a defence-related role, mechanistic data are still lacking.

Regulation of the cellular EXO70 repertoire by targeted degradation

Bioinformatic analyses uncovered an over-representation of Atg8-interacting motifs (AIMs) in exocyst subunits, including many EXO70 isoforms (Tzfadfia and Galili, 2013; Cvrčková and Žárský, 2013). Therefore, distinct EXO70 isoforms could be involved in autophagy and autophagy-derived unconventional trafficking pathways that bypass the Golgi apparatus, as shown for EXO70B1 (Kulich *et al.*, 2013). Alternatively, EXO70 isoforms could act as adaptors targeting their specific protein interactors for selective autophagy. Such specific targeting for degradation has been recently demonstrated in the case of the brassinosteroid pathway regulator BES1 (BRASSINOSTEROID INSENSITIVE 1-EMS SUPRESSOR 1), whose degradation is mediated by the DSK2 (DOMINANT SUPRESSOR OF KAR 2) adaptor, which directly interacts with ATG8e via the AIMs (Nolan *et al.*, 2017). The AIMs of EXO70 proteins might also directly target EXO70 isoforms for degradation, as recently suggested for Arabidopsis EXO70B2. Besides induction of its proteasomal degradation, flg22 treatment also induces EXO70B2 relocalization to the microsomal fraction, co-localization with autophagosomes dependent on the C-terminal AIMs, and subsequent vacuolar degradation (Teh *et al.*, 2019). This is in agreement with the hypothesis that EXO70 isoforms within the exocyst complex may be replaced according to the needs of cell differentiation or by biotic or abiotic stimuli-induced expression of required isoforms and regulated proteolysis of those not required under the particular circumstances (Žárský *et al.*, 2013). The degradation of EXO70B2 is regulated by its direct interactors, the plant U-box-type ubiquitin ligase 22 and 23 (PUB22 and PUB23; Stegmann *et al.*, 2012). PUB22 is itself subject to proteasomal degradation but it is stabilized by flg22 treatment; thus flg22 increases ubiquitin ligase activity of PUB22, resulting in a negative feedback loop that clears EXO70B2 once it is no longer needed (Stegmann *et al.*, 2012).

Other polyubiquitin ligases, PUB18 and its related isoform PUB19, induce proteolytic degradation of EXO70B1 in an ABA-regulated manner, controlling EXO70B1 function in ABA-induced stomatal closure. Like PUB22, PUB18 is itself targeted to degradation due to self-ubiquitination, resulting thus in a tight regulatory feedback loop between a stress signalling mediator, EXO70, and a specific E3 ubiquitin ligase. Interestingly, the specificity of EXO70B1–PUB18 and EXO70B2–PUB22 interactions depends on the U-box N-terminal (UND) domain of PUB18. Upon swapping of the domain to PUB22, the specificity of interaction with the EXO70 isoforms is reversed (Seo *et al.*, 2016).

Since the division of labour between EXO70B1 and EXO70B2 is probably specific to Brassicaceae and thus relatively recent, specific 'wiring' of the machinery regulating EXO70 degradation can evolve rapidly and might be taxon specific. Indeed, while the E3 ubiquitin ligase ARMADILLO REPEAT CONTAINING 1 (ARC1) directly binds and primes EXO70A1 for degradation in Brassica (Samuel *et al.*, 2009; Liu *et al.*, 2016), Arabidopsis ARC1 is a non-functional pseudogene (Kitashiba *et al.*, 2011). Thus, EXO70A1 is subject to different regulatory mechanisms even in closely related genera. This indicates that specific degradation of EXO70 isoforms is a well-regulated process possibly allowing exchange of EXO70 isoforms associated with the core exocyst subunits, facilitating formation of alternative exocyst complexes in plants (Žárský *et al.*, 2013; Pečenková *et al.*, 2017).

Conclusions

Over the last 10 years, new insights into the plant exocyst function in general, and that of EXO70 subunits in particular, indicate the necessity to revise our original model based on the assumption of exocysts being exclusively involved in exocytosis and membrane recycling (Žárský *et al.*, 2009). It turned out that the most evolutionarily dynamic EXO70 subfamily, EXO70.2, often participates in non-canonical (i.e. non-simple exocytosis) functions. EXO70B clade members are involved in autophagy (Kulich *et al.*, 2013), while EXO70Cs even perform a moderating function limiting the speed of cell expansion in tip-growing cell types (Synek *et al.*, 2017).

Ten years ago we hypothesized that specialized EXO70s may be responsible for delivering cargos to specific cortical domains of the cell, thus generating compositional and structural diversity of the plasmalemma, cell wall, and the apoplast (Žárský *et al.*, 2009). However, it is nowadays clear that delivery (including, importantly, that of CesA complexes) to a variety of cortical domains can be mediated by exocyst complexes containing the same basal major exocytotic EXO70A subunit, representing the only clade of the EXO70.1 subfamily with specificity determined by cell type-specific protein and lipid interactors (Oda *et al.*, 2015; Kalmbach *et al.*, 2017; Vukašinović *et al.*, 2017).

The examples of EXO70H4, but also the EXO70B isoforms, representatives of the class EXO70.2, indicate that these EXO70 paralogues might be important for secondary wall modifications (callose and silica deposition in the case of EXO70H4, and local modifications of the cell wall during biotic interactions in the case of EXO70B2), and possibly also for specific cases of autophagy, as observed for EXO70B1-dependent anthocyanin import to the vacuole. Over-representation of AIMs in class EXO70.2 EXO70 subunits (Cvrčková and Žárský, 2013), in some cases supported by experimental data, suggests a specific mechanism of down-regulation by autophagy for some of these paralogues (and possbly also their interactors).

The EXO70.3 subfamily remains mostly uncharacterized. Its EXO70I clade paralogues seem to be important for symbiotic interactions (consistent with this clade being absent in Brassicaceae including Arabidopsis). However, the phenotype

of a LOF mutant in the moss *P. patens* EXO70.3 representative indicates the importance of this subfamily for development of a multicellular body.

Since different EXO70 paralogues compete for the same exocyst core subunits, we proposed a hypothesis about the contribution of the exocyst complex to the coordination of the endomembrane dynamics (Žárský *et al.*, 2013; Pečenková *et al.*, 2017). Most of the experimental work on plant exocysts still needs to be done, and we can expect that such an endeavour will be an interesting journey.

Acknowledgements

We thank current and past members of our team, especially Ivan Kulich, Martin Potocký, Peter Sabol, and Jitka Ortmannová, for contributing ideas as well as unpublished observations. This work was supported by the Czech Science Foundation (CSF/GACR) projects 18-18290J, 18-12579S, and 19-02242J; and by the Ministry of Education, Youth and Sports of CR project European Regional Development Fund-Project 'Centre for Experimental Plant Biology': no. CZ.02.1.01/0.0/0.0/16_019/0000738.

References

Afzal AJ, Kim JH, Mackey D. 2013. The role of NOI-domain containing proteins in plant immune signaling. BMC Genomics **14**, 327.

Bodemann BO, Orvedahl A, Cheng T, *et al.* 2011. RalB and the exocyst mediate the cellular starvation response by direct activation of autophagosome assembly. Cell **144**, 253–267.

Chen C, Liu M, Jiang L, Liu X, Zhao J, Yan S, Yang S, Ren H, Liu R, Zhang X. 2014. Transcriptome profiling reveals roles of meristem regulators and polarity genes during fruit trichome development in cucumber (*Cucumis sativus* L.). Journal of Experimental Botany **65**, 4943–4958.

Chi Y, Yang Y, Li G, Wang F, Fan B, Chen Z. 2015. Identification and characterization of a novel group of legume-specific, Golgi apparatus-localized WRKY and Exo70 proteins from soybean. Journal of Experimental Botany **66**, 3055–3070.

Cole RA, McInally SA, Fowler JE. 2014. Developmentally distinct activities of the exocyst enable rapid cell elongation and determine meristem size during primary root growth in Arabidopsis. BMC Plant Biology **14**, 386.

Conze LL, Berlin S, Le Bail A, Kost B. 2017. Transcriptome profiling of tobacco (*Nicotiana tabacum*) pollen and pollen tubes. BMC Genomics **18**, 581.

Cvrčková F, Grunt M, Bezvoda R, Hála M, Kulich I, Rawat A, Žárský V. 2012. Evolution of the land plant exocyst complexes. Frontiers in Plant Science **3**, 159.

Cvrčková F, Žárský V. 2013. Old AIMs of the exocyst: evidence for an ancestral association of exocyst subunits with autophagy-associated Atg8 proteins. Plant Signaling & Behavior **8**, e27099.

Dellago H, Löscher M, Ajuh P, *et al.* 2011. Exo70, a subunit of the exocyst complex, interacts with SNEV(hPrp19/hPso4) and is involved in pre-mRNA splicing. The Biochemical Journal **438**, 81–91.

Ding Y, Wang J. 2017. Analysis of exocyst-positive organelle (EXPO)-mediated unconventional protein secretion (UPS) in plant cells. Methods in Molecular Biology **1662**, 231–241.

Ding Y, Wang J, Chun Lai JH, *et al.* 2014. Exo70E2 is essential for exocyst subunit recruitment and EXPO formation in both plants and animals. Molecular Biology of the Cell **25**, 412–426.

Drdová E, Klejchová M, Janko K, Hála M, Soukupová H, Cvrčková F, Žárský V. 2019. Developmental plasticity of Arabidopsis hypocotyl is dependent on exocyst complex function. Journal of Experimental Botany **70**, 1255–1265.

Drdová EJ, Synek L, Pečenková T, Hála M, Kulich I, Fowler JE, Murphy AS, Žárský V. 2013. The exocyst complex contributes to PIN auxin efflux carrier recycling and polar auxin transport in Arabidopsis. The Plant Journal **73**, 709–719.

Eliáš M, Drdová E, Ziak D, Bavlnka B, Hála M, Cvrčková F, Soukupová H, Žárský V. 2003. The exocyst complex in plants. Cell Biology International **27**, 199–201.

Fendrych M, Synek L, Pečenková T, Drdová EJ, Sekereš J, de Rycke R, Nowack MK, Žárský V. 2013. Visualization of the exocyst complex dynamics at the plasma membrane of *Arabidopsis thaliana*. Molecular Biology of the Cell **24**, 510–520.

Fendrych M, Synek L, Pečenková T, *et al.* 2010. The Arabidopsis exocyst complex is involved in cytokinesis and cell plate maturation. The Plant Cell **22**, 3053–3065.

Fujisaki K, Abe Y, Ito A, *et al.* 2015. Rice Exo70 interacts with a fungal effector, AVR-Pii, and is required for AVR-Pii-triggered immunity. The Plant Journal **83**, 875–887.

Gavrin A, Kulikova O, Bisseling T, Fedorova EE. 2017. Interface symbiotic membrane formation in root nodules of *Medicago truncatula*: the role of synaptotagmins MtSyt1, MtSyt2 and MtSyt3. Frontiers in Plant Science **8**, 201.

Genre A, Ivanov S, Fendrych M, Faccio A, Žárský V, Bisseling T, Bonfante P. 2012. Multiple exocytotic markers accumulate at the sites of perifungal membrane biogenesis in arbuscular mycorrhizas. Plant & Cell Physiology **53**, 244–255.

Grobei MA, Qeli E, Brunner E, Rehrauer H, Zhang R, Roschitzki B, Basler K, Ahrens CH, Grossniklaus U. 2009. Deterministic protein inference for shotgun proteomics data provides new insights into Arabidopsis pollen development and function. Genome Research **19**, 1786–1800.

Guo J, Xu C, Wu D, *et al.* 2018. Bph6 encodes an exocyst-localized protein and confers broad resistance to planthoppers in rice. Nature Genetics **50**, 297–306.

Hála M, Cole R, Synek L, *et al.* 2008. An exocyst complex functions in plant cell growth in Arabidopsis and tobacco. The Plant Cell **20**, 1330–1345.

He B, Xi F, Zhang X, Zhang J, Guo W. 2007. Exo70 interacts with phospholipids and mediates the targeting of the exocyst to the plasma membrane. The EMBO Journal **26**, 4053–4065.

Heider MR, Munson M. 2012. Exorcising the exocyst complex. Traffic **13**, 898–907.

Hong D, Jeon BW, Kim SY, Hwang JU, Lee Y. 2016. The ROP2–RIC7 pathway negatively regulates light-induced stomatal opening by inhibiting exocyst subunit Exo70B1 in Arabidopsis. New Phytologist **209**, 624–635.

Hruz T, Laule O, Szabo G, Wessendorp F, Bleuler S, Oertle L, Widmayer P, Gruissem W, Zimmermann P. 2008. Genevestigator v3: a reference expression database for the meta-analysis of transcriptomes. Advances in Bioinformatics **2008**, 420747.

Jakoby MJ, Falkenhan D, Mader MT, Brininstool G, Wischnitzki E, Platz N, Hudson A, Hülskamp M, Larkin J, Schnittger A. 2008. Transcriptional profiling of mature Arabidopsis trichomes reveals that NOECK encodes the MIXTA-like transcriptional regulator MYB106. Plant Physiology **148**, 1583–1602.

Kalmbach L, Hématy K, De Bellis D, Barberon M, Fujita S, Ursache R, Daraspe J, Geldner N. 2017. Transient cell-specific EXO70A1 activity in the CASP domain and Casparian strip localization. Nature Plants **3**, 17058.

Kitashiba H, Liu P, Nishio T, Nasrallah JB, Nasrallah ME. 2011. Functional test of Brassica self-incompatibility modifiers in *Arabidopsis thaliana*. Proceedings of the National Academy of Sciences, USA **108**, 18173–18178.

Koumandou VL, Dacks JB, Coulson RM, Field MC. 2007. Control systems for membrane fusion in the ancestral eukaryote; evolution of tethering complexes and SM proteins. BMC Evolutionary Biology **7**, 29.

Kubátová Z, Pejchar P, Potocký M, Sekereš J, Žárský V, Kulich I. 2019. Arabidopsis trichome contains two plasma membrane domains with different lipid compositions which attract distinct EXO70 subunits. International Journal of Molecular Sciences **20**, 3803.

Kulich I, Cole R, Drdová E, Cvrčková F, Soukup A, Fowler J, Žárský V. 2010. Arabidopsis exocyst subunits SEC8 and EXO70A1 and exocyst interactor ROH1 are involved in the localized deposition of seed coat pectin. New Phytologist **188**, 615–625.

Kulich I, Pečenková T, Sekereš J, Smetana O, Fendrych M, Foissner I, Höftberger M, Žárský V. 2013. Arabidopsis exocyst subcomplex

containing subunit EXO70B1 is involved in autophagy-related transport to the vacuole. Traffic **14**, 1155–1165.

Kulich I, Vojtíková Z, Glanc M, Ortmannová J, Rasmann S, Žárský V. 2015. Cell wall maturation of Arabidopsis trichomes is dependent on exocyst subunit EXO70H4 and involves callose deposition. Plant Physiology **168**, 120–131.

Kulich I, Vojtíková Z, Sabol P, Ortmannová J, Neděla V, Tihlaříková E, Žárský V. 2018. Exocyst subunit EXO70H4 has a specific role in callose synthase secretion and silica accumulation. Plant Physiology **176**, 2040–2051.

Kulich I, Žárský V. 2014. Autophagy-related direct membrane import from ER/cytoplasm into the vacuole or apoplast: a hidden gateway also for secondary metabolites and phytohormones? International Journal of Molecular Sciences **15**, 7462–7474.

Li S, Chen M, Yu D, Ren S, Sun S, Liu L, Ketelaar T, Emons AM, Liu CM. 2013. EXO70A1-mediated vesicle trafficking is critical for tracheary element development in Arabidopsis. The Plant Cell **25**, 1774–1786.

Li S, van Os GM, Ren S, Yu D, Ketelaar T, Emons AM, Liu CM. 2010. Expression and functional analyses of EXO70 genes in Arabidopsis implicate their roles in regulating cell type-specific exocytosis. Plant Physiology **154**, 1819–1830.

Lin Y, Ding Y, Wang J, *et al.* 2015. Exocyst-positive organelles and autophagosomes are distinct organelles in plants. Plant Physiology **169**, 1917–1932.

Ling HQ, Zhao S, Liu D, *et al.* 2013. Draft genome of the wheat A-genome progenitor *Triticum urartu*. Nature **496**, 87–90.

Liu CW, Breakspear A, Stacey N, *et al.* 2019. A protein complex required for polar growth of rhizobial infection threads. Nature Communications **10**, 2848.

Liu J, Zhang H, Lian X, Converse R, Zhu L. 2016. Identification of interacting motifs between armadillo repeat containing 1 (ARC1) and exocyst 70 A1 (Exo70A1) proteins in *Brassica oleracea*. The Protein Journal **35**, 34–43.

Liu J, Zhao Y, Sun Y, He B, Yang C, Svitkina T, Goldman YE, Guo W. 2012. Exo70 stimulates the Arp2/3 complex for lamellipodia formation and directional cell migration. Current Biology **22**, 1510–1515.

Liu J, Zuo X, Yue P, Guo W. 2007. Phosphatidylinositol 4,5-bisphosphate mediates the targeting of the exocyst to the plasma membrane for exocytosis in mammalian cells. Molecular Biology of the Cell **18**, 4483–4492.

Liu N, Hake K, Wang W, Zhao T, Romeis T, Tang D. 2017. CALCIUM-DEPENDENT PROTEIN KINASE5 associates with the truncated NLR protein TIR-NBS2 to contribute to exo70B1-mediated immunity. The Plant Cell **29**, 746–759.

Loraine AE, McCormick S, Estrada A, Patel K, Qin P. 2013. RNA-seq of Arabidopsis pollen uncovers novel transcription and alternative splicing. Plant Physiology **162**, 1092–1109.

Lu H, Liu J, Liu S, Zeng J, Ding D, Carstens RP, Cong Y, Xu X, Guo W. 2013. Exo70 isoform switching upon epithelial–mesenchymal transition mediates cancer cell invasion. Developmental Cell **27**, 560–573.

Martin-Urdiroz M, Deeks MJ, Horton CG, Dawe HR, Jourdain I. 2016. The exocyst complex in health and disease. Frontiers in Cell and Developmental Biology **4**, 24.

Morgera F, Sallah MR, Dubuke ML, Gandhi P, Brewer DN, Carr CM, Munson M. 2012. Regulation of exocytosis by the exocyst subunit Sec6 and the SM protein Sec1. Molecular Biology of the Cell **23**, 337–346.

Munson M, Novick P. 2006. The exocyst defrocked, a framework of rods revealed. Nature Structural & Molecular Biology **13**, 577–581.

Nolan TM, Brennan B, Yang M, Chen J, Zhang M, Li Z, Wang X, Bassham DC, Walley J, Yin Y. 2017. Selective autophagy of BES1 mediated by DSK2 balances plant growth and survival. Developmental Cell **41**, 33–46.

Novick PJ. 2014. A Rab effector called the Exocyst and related vesicle tether complexes. In: Wittinghofer A, ed. Ras superfamily small G proteins: biology and mechanisms 2. Cham: Springer, 67–79.

Oda Y, Iida Y, Nagashima Y, Sugiyama Y, Fukuda H. 2015. Novel coiled-coil proteins regulate exocyst association with cortical microtubules in xylem cells via the conserved oligomeric golgi-complex 2 protein. Plant & Cell Physiology **56**, 277–286.

Ogura T, Goeschl C, Filiault D, Mirea M, Slovak R, Wolhrab B, Satbhai SB, Busch W. 2019. Root system depth in arabidopsis is shaped by EXOCYST70A3 via the dynamic modulation of auxin transport. Cell **178**, 400–412.e16.

Oravecz A, Baumann A, Máté Z, Brzezinska A, Molinier J, Oakeley EJ, Adám E, Schäfer E, Nagy F, Ulm R. 2006. CONSTITUTIVELY PHOTOMORPHOGENIC1 is required for the UV-B response in Arabidopsis. The Plant Cell **18**, 1975–1990.

Ostertag M, Stammler J, Douchkov D, Eichmann R, Hückelhoven R. 2013. The conserved oligomeric Golgi complex is involved in penetration resistance of barley to the barley powdery mildew fungus. Molecular Plant Pathology **14**, 230–240.

Pečenková T, Hála M, Kulich I, Kocourková D, Drdová E, Fendrych M, Toupalová H, Žárský V. 2011. The role for the exocyst complex subunits Exo70B2 and Exo70H1 in the plant–pathogen interaction. Journal of Experimental Botany **62**, 2107–2116.

Pečenková T, Janda M, Ortmannová J, Hajná V, Stehlíková Z, Žárský V. 2017. Early Arabidopsis root hair growth stimulation by pathogenic strains of *Pseudomonas syringae*. Annals of Botany **120**, 437–446.

Pečenková T, Sabol P, Kulich I, Ortmannová J, Žárský V. 2016. Constitutive negative regulation of R proteins in Arabidopsis also via autophagy related pathway? Frontiers in Plant Science **7**, 260.

Periyannan S, Moore J, Ayliffe M, *et al.* 2013. The gene Sr33, an ortholog of barley Mla genes, encodes resistance to wheat stem rust race Ug99. Science **341**, 786–788.

Pommereit D, Wouters FS. 2007. An NGF-induced Exo70–TC10 complex locally antagonises Cdc42-mediated activation of N-WASP to modulate neurite outgrowth. Journal of Cell Science **120**, 2694–2705.

Ponpuak M, Mandell MA, Kimura T, Chauhan S, Cleyrat C, Deretic V. 2015. Secretory autophagy. Current Opinion in Cell Biology **35**, 106–116.

Rauch L, Hennings K, Aepfelbacher M. 2014. A role for exocyst in maturation and bactericidal function of staphylococci-containing endothelial cell phagosomes. Traffic **15**, 1083–1098.

Rawat A, Brejšková L, Hála M, Cvrčková F, Žárský V. 2017. The *Physcomitrella patens* exocyst subunit EXO70.3d has distinct roles in growth and development, and is essential for completion of the moss life cycle. New Phytologist **216**, 438–454.

Robinson NG, Guo L, Imai J, Toh-E A, Matsui Y, Tamanoi F. 1999. Rho3 of *Saccharomyces cerevisiae*, which regulates the actin cytoskeleton and exocytosis, is a GTPase which interacts with Myo2 and Exo70. Molecular and Cellular Biology **19**, 3580–3587.

Rybak K, Steiner A, Synek L, *et al.* 2014. Plant cytokinesis is orchestrated by the sequential action of the TRAPPII and exocyst tethering complexes. Developmental Cell **29**, 607–620.

Sabol P, Kulich I, Žárský V. 2017. RIN4 recruits the exocyst subunit EXO70B1 to the plasma membrane. Journal of Experimental Botany **68**, 3253–3265.

Safavian D, Zayed Y, Indriolo E, Chapman L, Ahmed A, Goring DR. 2015. RNA silencing of exocyst genes in the stigma impairs the acceptance of compatible pollen in Arabidopsis. Plant Physiology **169**, 2526–2538.

Samuel MA, Chong YT, Haasen KE, Aldea-Brydges MG, Stone SL, Goring DR. 2009. Cellular pathways regulating responses to compatible and self-incompatible pollen in Brassica and Arabidopsis stigmas intersect at Exo70A1, a putative component of the exocyst complex. The Plant Cell **21**, 2655–2671.

Sekereš J, Pejchar P, Šantrůček J, Vukašinović N, Žárský V, Potocký M. 2017. Analysis of exocyst subunit EXO70 family reveals distinct membrane polar domains in tobacco pollen tubes. Plant Physiology **173**, 1659–1675.

Seo DH, Ahn MY, Park KY, Kim EY, Kim WT. 2016. The N-terminal UND motif of the Arabidopsis U-Box E3 ligase PUB18 is critical for the negative regulation of ABA-mediated stomatal movement and determines its ubiquitination specificity for exocyst subunit Exo70B1. The Plant Cell **28**, 2952–2973.

Sivaram MV, Saporita JA, Furgason ML, Boettcher AJ, Munson M. 2005. Dimerization of the exocyst protein Sec6p and its interaction with the t-SNARE Sec9p. Biochemistry **44**, 6302–6311.

Stegmann M, Anderson RG, Ichimura K, Pečenková T, Reuter P, Žárský V, McDowell JM, Shirasu K, Trujillo M. 2012. The ubiquitin ligase PUB22 targets a subunit of the exocyst complex required for PAMP-triggered responses in Arabidopsis. The Plant Cell **24**, 4703–4716.

Stegmann M, Anderson RG, Westphal L, Rosahl S, McDowell JM, Trujillo M. 2013. The exocyst subunit Exo70B1 is involved in the immune response of *Arabidopsis thaliana* to different pathogens and cell death. Plant Signaling & Behavior **8**, e27421.

Synek L, Schlager N, Eliáš M, Quentin M, Hauser MT, Žárský V. 2006. AtEXO70A1, a member of a family of putative exocyst subunits specifically expanded in land plants, is important for polar growth and plant development. The Plant Journal **48**, 54–72.

Synek L, Vukašinović N, Kulich I, Hála M, Aldorfová K, Fendrych M, Žárský V. 2017. EXO70C2 is a key regulatory factor for optimal tip growth of pollen. Plant Physiology **174**, 223–240.

Tan X, Feng Y, Liu Y, Bao Y. 2016. Mutations in exocyst complex subunit SEC6 gene impaired polar auxin transport and PIN protein recycling in Arabidopsis primary root. Plant Science **250**, 97–104.

Teh OK, Lee CW, Ditengou FA, *et al*. 2019. Phosphorylation of the exocyst subunit Exo70B2 contributes to the regulation of its function. bioRxiv 266171. [Preprint].

TerBush DR, Maurice T, Roth D, Novick P. 1996. The exocyst is a multiprotein complex required for exocytosis in *Saccharomyces cerevisiae*. The EMBO Journal **15**, 6483–6494.

Tu B, Hu L, Chen W, *et al.* 2015. Disruption of OsEXO70A1 causes irregular vascular bundles and perturbs mineral nutrient assimilation in rice. Scientific Reports **5**, 18609.

Tzfadia O, Galili G. 2013. The Arabidopsis exocyst subcomplex subunits involved in a golgi-independent transport into the vacuole possess consensus autophagy-associated atg8 interacting motifs. Plant Signaling & Behavior **8**, 26732.

Vaškovičová K, Žárský V, Rösel D, Nikolič M, Buccione R, Cvrčková F, Brábek J. 2013. Invasive cells in animals and plants: searching for LECA machineries in later eukaryotic life. Biology Direct **8**, 8.

Vukašinović N, Oda Y, Pejchar P, Synek L, Pečenková T, Rawat A, Sekereš J, Potocký M, Žárský V. 2017. Microtubule-dependent targeting of the exocyst complex is necessary for xylem development in Arabidopsis. New Phytologist **213**, 1052–1067.

Vukašinović N, Žárský V. 2016. Tethering complexes in the Arabidopsis endomembrane system. Frontiers in Cell and Developmental Biology **4**, 46.

Wang J, Ding Y, Wang J, Hillmer S, Miao Y, Lo SW, Wang X, Robinson DG, Jiang L. 2010. EXPO, an exocyst-positive organelle distinct from multivesicular endosomes and autophagosomes, mediates cytosol to cell wall exocytosis in Arabidopsis and tobacco cells. The Plant Cell **22**, 4009–4030.

Wang Z, Li P, Yang Y, Chi Y, Fan B, Chen Z. 2016. Expression and functional analysis of a novel group of legume-specific WRKY and Exo70 protein variants from soybean. Scientific Reports **6**, 32090.

Wen TJ, Hochholdinger F, Sauer M, Bruce W, Schnable PS. 2005. The roothairless1 gene of maize encodes a homolog of sec3, which is involved in polar exocytosis. Plant Physiology **138**, 1637–1643.

Winter D, Vinegar B, Nahal H, Ammar R, Wilson GV, Provart NJ. 2007. An 'Electronic Fluorescent Pictograph' browser for exploring and analyzing large-scale biological data sets. PLoS One **2**, e718.

Wu B, Guo W. 2015. The exocyst at a glance. Journal of Cell Science **128**, 2957–2964.

Wu J, Tan X, Wu C, Cao K, Li Y, Bao Y. 2013. Regulation of cytokinesis by exocyst subunit SEC6 and KEULE in *Arabidopsis thaliana*. Molecular Plant **6**, 1863–1876.

Xing J, Wang T, Liu Z, *et al.* 2015. GENERAL CONTROL NONREPRESSED PROTEIN5-mediated histone acetylation of FERRIC REDUCTASE DEFECTIVE3 contributes to iron homeostasis in Arabidopsis. Plant Physiology **168**, 1309–1320.

Yoshimoto K, Jikumaru Y, Kamiya Y, Kusano M, Consonni C, Panstruga R, Ohsumi Y, Shirasu K. 2009. Autophagy negatively regulates cell death by controlling NPR1-dependent salicylic acid signaling during senescence and the innate immune response in Arabidopsis. The Plant Cell **21**, 2914–2927.

Yue P, Zhang Y, Mei K, Wang S, Lesigang J, Zhu Y, Dong G, Guo W. 2017. Sec3 promotes the initial binary t-SNARE complex assembly and membrane fusion. Nature Communications **8**, 14236.

Žárský V, Cvrčková F, Potocký M, Hála M. 2009. Exocytosis and cell polarity in plants—exocyst and recycling domains. New Phytologist **183**, 255–272.

Žárský V, Kulich I, Fendrych M, Pečenková T. 2013. Exocyst complexes multiple functions in plant cells secretory pathways. Current Opinion in Plant Biology **16**, 726–733.

Zhang C, Brown MQ, van de Ven W, *et al*. 2016. Endosidin2 targets conserved exocyst complex subunit EXO70 to inhibit exocytosis. Proceedings of the National Academy of Sciences, USA **113**, E41–E50.

Zhang X, Pumplin N, Ivanov S, Harrison MJ. 2015. EXO70I is required for development of a sub-domain of the periarbuscular membrane during arbuscular mycorrhizal symbiosis. Current Biology **25**, 2189–2195.

Zhao J, Zhang X, Wan W, Zhang H, Liu J, Li M, Wang H, Xiao J, Wang X. 2018. Identification and characterization of the EXO70 gene family in polyploid wheat and related species. International Journal of Molecular Sciences **20**, 60.

Zhao T, Rui L, Li J, Nishimura MT, Vogel JP, Liu N, Liu S, Zhao Y, Dangl JL, Tang D. 2015. A truncated NLR protein, TIR-NBS2, is required for activated defense responses in the exo70B1 mutant. PLoS Genetics **11**, e1004945.

Zhao Y, Liu J, Yang C, *et al.* 2013. Exo70 generates membrane curvature for morphogenesis and cell migration. Developmental Cell **26**, 266–278.

9 Literature cited

A

Abou-Saleh, R.H., Hernandez-Gomez, M.C., Amsbury, S., Paniagua, C., Bourdon, M., Miyashima, S., et al. (2018) *Interactions between callose and cellulose revealed through the analysis of biopolymer mixtures*. *Nat. Commun.*, **9**, 4538.

Ager, F. (2003) *Nuclear micro-probe analysis of Arabidopsis thaliana leaves*. *Nuclear Instruments and Methods in Physics Research Section B: Beam Interactions with Materials and Atoms*, **210**, 401–406.

Ager, F.J., Ynsa, M.D., Domínguez-Solís, J.R., Gotor, C., Respaldiza, M.A., and Romero, L.C. (2002) *Cadmium localization and quantification in the plant Arabidopsis thaliana using micro-PIXE*. *Nuclear Instruments and Methods in Physics Research Section B: Beam Interactions with Materials and Atoms*, **189**, 494–498.

Alassimone, J., Naseer, S., and Geldner, N. (2010) *A developmental framework for endodermal differentiation and polarity*. *Proc. Natl. Acad. Sci. U. S. A.*, **107**, 5214–5219.

Antonescu, C.N., Danuser, G., and Schmid, S.L. (2010) *Phosphatidic acid plays a regulatory role in clathrin-mediated endocytosis*. *Mol. Biol. Cell*, **21**, 2944–2952.

B

Bannister, J.V. and Hill, H.A.O. (1980) *Chemical and Biochemical Aspects of Superoxide and Superoxide Dismutase*. North Holland.

Barratt, D.H.P., Kölling, K., Graf, A., Pike, M., Calder, G., Findlay, K., et al. (2011) *Callose synthase GSL7 is necessary for normal phloem transport and inflorescence growth in Arabidopsis*. *Plant Physiol.*, **155**, 328–341.

Bashline, L., Li, S., and Gu, Y. (2014) *The trafficking of the cellulose synthase complex in higher plants*. *Ann. Bot.*, **114**, 1059–1067.

Baskin, T.I. (2001) *On the alignment of cellulose microfibrils by cortical microtubules: a review and a model*. *Protoplasma*, **215**, 150–171.

Böhlenius, H., Mørch, S.M., Godfrey, D., Nielsen, M.E., and Thordal-Christensen, H. (2010) *The multivesicular body-localized GTPase ARFA1b/1c is important for callose deposition and ROR2 syntaxin-dependent preinvasive basal defense in barley*. *Plant Cell*, **22**, 3831–3844.

Bouché, N., Fait, A., Bouchez, D., Møller, S.G., and Fromm, H. (2003) *Mitochondrial succinic-semialdehyde dehydrogenase of the gamma-aminobutyrate shunt is required to restrict levels of reactive oxygen intermediates in plants*. *Proc. Natl. Acad. Sci. U. S. A.*, **100**, 6843–6848.

Bove, J., Vaillancourt, B., Kroeger, J., Hepler, P.K., Wiseman, P.W., and Geitmann, A. (2008) *Magnitude and Direction of Vesicle Dynamics in Growing Pollen Tubes Using Spatiotemporal Image Correlation Spectroscopy and Fluorescence Recovery after Photobleaching*. *Plant Physiology*, **147**, 1646–1658.

Bringmann, M., Li, E., Sampathkumar, A., Kocabek, T., Hauser, M.-T., and Persson, S. (2012) *POM-POM2/cellulose synthase interacting1 is essential for the functional association of cellulose synthase and microtubules in Arabidopsis*. *Plant Cell*, **24**, 163–177.

Brininstool, G., Kasili, R., Simmons, L.A., Kirik, V., Hülskamp, M., and Larkin, J.C. (2008) *Constitutive Expressor Of Pathogenesis-related Genes5 affects cell wall biogenesis and trichome development*. *BMC Plant Biol.*, **8**, 58.

Brownfield, L., Doblin, M., Fincher, G.B., and Bacic, A. (2009) *Biochemical and Molecular Properties of Biosynthetic Enzymes for (1,3)-β-Glucans in Embryophytes, Chlorophytes and Rhodophytes*. In: *Chemistry, Biochemistry, and Biology of 1-3 Beta Glucans and Related Polysaccharides* , pp. 283–326.

Brugiére, T. and Exley, C. (2017) *Callose-associated silica deposition in Arabidopsis*. *J. Trace Elem. Med. Biol.*, **39**, 86–90.

Bucher, G.L., Tarina, C., Heinlein, M., Di Serio, F., Meins, F., and Iglesias, V.A. (2001) *Local expression of enzymatically active class I β-1, 3-glucanase enhances symptoms of TMV infection in tobacco*. *Plant J.*, **28**, 361–369.

Burk, D.H. and Ye, Z.-H. (2002) *Alteration of oriented deposition of cellulose microfibrils by mutation of a katanin-like microtubule-severing protein*. *Plant Cell*, **14**, 2145–2160.

C

Cai, G., Faleri, C., Del Casino, C., Emons, A.M.C., and Cresti, M. (2011) *Distribution of callose synthase, cellulose synthase, and sucrose synthase in tobacco pollen tube is controlled in dissimilar ways by actin filaments and microtubules*. *Plant Physiol.*, **155**, 1169–1190.

Černý, M., Habánová, H., Berka, M., Luklová, M., and Brzobohatý, B. (2018) *Hydrogen Peroxide: Its Role in Plant Biology and Crosstalk with Signalling Networks*. *Int. J. Mol. Sci.*, **19**.

Chapple, C.C., Vogt, T., Ellis, B.E., and Somerville, C.R. (1992) *An Arabidopsis mutant defective in the general phenylpropanoid pathway*. *Plant Cell*, **4**, 1413–1424.

Chen, C., Liu, M., Jiang, L., Liu, X., Zhao, J., Yan, S., et al. (2014) *Transcriptome profiling reveals roles of meristem regulators and polarity genes during fruit trichome development in cucumber (Cucumis sativus L.)*. *J. Exp. Bot.*, **65**, 4943–4958.

Chen, X.-Y., Liu, L., Lee, E., Han, X., Rim, Y., Chu, H., et al. (2009) *The Arabidopsis callose synthase gene GSL8 is required for cytokinesis and cell patterning*. *Plant Physiol.*, **150**, 105–113.

Chiba, Y., Mitani, N., Yamaji, N., and Ma, J.F. (2009) *HvLsi1 is a silicon influx transporter in barley*. *Plant J.*, **57**, 810–818.

Choi, Y.E., Harada, E., Wada, M., Tsuboi, H., Morita, Y., Kusano, T., and Sano, H. (2001) *Detoxification of cadmium in tobacco plants: formation and active excretion of crystals containing cadmium and calcium through trichomes*. *Planta*, **213**, 45–50.

Cole, R.A. and Fowler, J.E. (2006) *Polarized growth: maintaining focus on the tip*. *Curr. Opin. Plant Biol.*, **9**, 579–588.

Connick, V.J. (2011) *The Impact of Silicon Fertilisation on the Chemical Ecology of the Grapevine, Vitis Vinifera; Constitutive and Induced Chemical Defenses Against Arthropod Pests and Their Natural Enemies*.

Cosgrove, D.J. and Jarvis, M.C. (2012) *Comparative structure and biomechanics of plant primary and secondary cell walls*. *Frontiers in Plant Science*, **3**.

Coskun, D., Deshmukh, R., Sonah, H., Menzies, J.G., Reynolds, O., Ma, J.F., et al. (2019) *The controversies of silicon's role in plant biology*. *New Phytol.*, **221**, 67–85.

Crowell, E.F., Bischoff, V., Desprez, T., Rolland, A., Stierhof, Y.-D., Schumacher, K., et al. (2009) *Pausing of Golgi bodies on microtubules regulates secretion of cellulose synthase complexes in Arabidopsis*. *Plant Cell*, **21**, 1141–1154.

Cui, W. and Lee, J.-Y. (2016) *Arabidopsis callose synthases CalS1/8 regulate plasmodesmal permeability during stress*. *Nat Plants*, **2**, 16034.

Currie, H.A. and Perry, C.C. (2007) *Silica in plants: biological, biochemical and chemical studies*. *Ann. Bot.*, **100**, 1383–1389.

Cvrčková, F., Grunt, M., Bezvoda, R., Hála, M., Kulich, I., Rawat, A., and Zárský, V. (2012) *Evolution of the land plant exocyst complexes*. *Front. Plant Sci.*, **3**, 159.

D

Dai, X., Wang, G., Yang, D.S., Tang, Y., Broun, P., Marks, M.D., et al. (2010) *TrichOME: a comparative omics database for plant trichomes*. *Plant Physiol.*, **152**, 44–54.

Dar, M.I., Khan, F.A., Rehman, F., Masoodi, A., Ansari, A.A., Varshney, D., et al. (2015) *Roles of Brassicaceae in Phytoremediation of Metals and Metalloids*. *Phytoremediation*, 201–215.

Das, K. and Roychoudhury, A. (2014) *Reactive oxygen species (ROS) and response of antioxidants as ROS-scavengers during environmental stress in plants*. *Frontiers in Environmental Science*, **2**.

Daudi, A. and O'Brien, J. (2012) *Detection of Hydrogen Peroxide by DAB Staining in Arabidopsis Leaves*. *BIO-PROTOCOL*, **2**.

Derksen, J., Rutten, T., Lichtscheidl, I.K., de Win, A.H.N., Pierson, E.S., and Rongen, G. (1995) *Quantitative analysis of the distribution of organelles in tobacco pollen tubes: implications for exocytosis and endocytosis*. *Protoplasma*, **188**, 267–276.

Deshmukh, R.K., Vivancos, J., Guérin, V., Sonah, H., Labbé, C., Belzile, F., and Bélanger, R.R. (2013) *Identification and functional characterization of silicon transporters in soybean using comparative genomics of major intrinsic proteins in Arabidopsis and rice*. *Plant Mol. Biol.*, **83**, 303–315.

Domínguez-Solís, J.R., López-Martín, M.C., Ager, F.J., Ynsa, M.D., Romero, L.C., and Gotor, C. (2004) *Increased cysteine availability is essential for cadmium tolerance and accumulation in Arabidopsis thaliana*. *Plant Biotechnol. J.*, **2**, 469–476.

Dong, X., Hong, Z., Chatterjee, J., Kim, S., and Verma, D.P.S. (2008) *Expression of callose synthase genes and its connection with Npr1 signaling pathway during pathogen infection*. *Planta*, **229**, 87–98.

Dong, X., Hong, Z., Sivaramakrishnan, M., Mahfouz, M., and Verma, D.P.S. (2005) *Callose synthase (CalS5) is required for exine formation during microgametogenesis and for pollen viability in Arabidopsis*. *Plant J.*, **42**, 315–328.

Dörmann, P., Kim, H., Ott, T., Schulze-Lefert, P., Trujillo, M., Wewer, V., and Hückelhoven, R. (2014) *Cell-autonomous defense, re-organization and trafficking of membranes in plant-microbe interactions*. *New Phytol.*, **204**, 815–822.

Drakakaki, G., van de Ven, W., Pan, S., Miao, Y., Wang, J., Keinath, N.F., et al. (2012) *Isolation and proteomic analysis of the SYP61 compartment reveal its role in exocytic trafficking in Arabidopsis*. *Cell Res.*, **22**, 413–424.

E

Eggert, D., Naumann, M., Reimer, R., and Voigt, C.A. (2014) *Nanoscale glucan polymer network causes pathogen resistance*. *Sci. Rep.*, **4**, 4159.

Elias, M., Drdova, E., Ziak, D., Bavlnka, B., Hala, M., Cvrckova, F., et al. (2003) *The exocyst complex in plants*. *Cell Biol. Int.*, **27**, 199–201.

Ellinger, D., Glöckner, A., Koch, J., Naumann, M., Stürtz, V., Schütt, K., et al. (2014) *Interaction of the Arabidopsis GTPase RabA4c with its effector PMR4 results in complete penetration resistance to powdery mildew*. *Plant Cell*, **26**, 3185–3200.

Ellinger, D., Naumann, M., Falter, C., Zwikowics, C., Jamrow, T., Manisseri, C., et al. (2013) *Elevated early callose deposition results in complete penetration resistance to powdery mildew in Arabidopsis*. *Plant Physiol.*, **161**, 1433–1444.

Ellinger, D. and Voigt, C.A. (2014) *Callose biosynthesis in Arabidopsis with a focus on pathogen response: what we have learned within the last decade*. *Ann. Bot.*, **114**, 1349–1358.

Enns, L.C., Kanaoka, M.M., Torii, K.U., Comai, L., Okada, K., and Cleland, R.E. (2005) *Two callose synthases, GSL1 and GSL5, play an essential and redundant role in plant and pollen development and in fertility*. *Plant Mol. Biol.*, **58**, 333–349.

Epstein, E. (2001) *Chapter 1 Silicon in plants: Facts vs. concepts*. In: *Studies in Plant Science* , pp. 1–15.

Epstein, E. (2009) *Silicon: its manifold roles in plants*. *Ann. Appl. Biol.*, **155**, 155–160.

Epstein, E. (1994) *The anomaly of silicon in plant biology*. *Proc. Natl. Acad. Sci. U. S. A.*, **91**, 11–17.

Esch, J.J., Chen, M., Sanders, M., Hillestad, M., Ndkium, S., Idelkope, B., et al. (2003) *A contradictory GLABRA3 allele helps define gene interactions controlling trichome development in Arabidopsis*. *Development*, **130**, 5885–5894.

Evert, R.F. and Derr, W.F. (1964) *Callose Substance in Sieve Elements*. *Am. J. Bot.*, **51**, 552.

Exley, C. and Guerriero, G. (2019) *A reappraisal of biological silicification in plants? New Phytol.*, **223**, 511–513.

F

Fang, J.-Y. and Ma, X.-L. (2006) *In vitro simulation studies of silica deposition induced by lignin from rice*. *J. Zhejiang Univ. Sci. B*, **7**, 267–271.

Fauteux, F., Chain, F., Belzile, F., Menzies, J.G., and Bélanger, R.R. (2006) *The protective role of silicon in the Arabidopsis-powdery mildew pathosystem*. *Proc. Natl. Acad. Sci. U. S. A.*, **103**, 17554–17559.

Frerigmann, H., Böttcher, C., Baatout, D., and Gigolashvili, T. (2012) *Glucosinolates are produced in trichomes of Arabidopsis thaliana*. *Front. Plant Sci.*, **3**, 242.

Fry, S.C., Nesselrode, B.H.W.A., Miller, J.G., and Mewburn, B.R. (2008) *Mixed-linkage (1-->3,1-->4)-beta-D-glucan is a major hemicellulose of Equisetum (horsetail) cell walls*. *New Phytol.*, **179**, 104–115.

Fujita, S., De Bellis, D., Edel, K.H., Köster, P., Andersen, T.G., Schmid-Siegert, E., et al. (2020) *SCHENGEN receptor module drives localized ROS production and lignification in plant roots*. *EMBO J.*, **39**, e103894.

Fukuda, N., Hokura, A., Kitajima, N., Terada, Y., Saito, H., Abe, T., and Nakai, I. (2008) *Micro X-ray fluorescence imaging and micro X-ray absorption spectroscopy of cadmium hyper-accumulating plant, Arabidopsis halleri ssp. gemmifera, using high-energy synchrotron radiation*. *Journal of Analytical Atomic Spectrometry*, **23**, 1068.

G

García-Hernández, M., Murphy, A., and Taiz, L. (1998) *Metallothioneins 1 and 2 have distinct but overlapping expression patterns in Arabidopsis*. *Plant Physiol.*, **118**, 387–397.

Ghanmi, D., McNally, D.J., Benhamou, N., Menzies, J.G., and Bélanger, R.R. (2004) *Powdery mildew of Arabidopsis thaliana: a pathosystem for exploring the role of silicon in plant–microbe interactions*. *Physiological and Molecular Plant Pathology*, **64**, 189–199.

Gierlinger, N., Sapei, L., and Paris, O. (2008) *Insights into the chemical composition of Equisetum hyemale by high resolution Raman imaging*. *Planta*, **227**, 969–980.

Goto, M., Ehara, H., Karita, S., Takabe, K., Ogawa, N., Yamada, Y., et al. (2003) *Protective effect of silicon on phenolic biosynthesis and ultraviolet spectral stress in rice crop*. *Plant Science*, **164**, 349–356.

Grégoire, C., Rémus-Borel, W., Vivancos, J., Labbé, C., Belzile, F., and Bélanger, R.R. (2012) *Discovery of a multigene family of aquaporin silicon transporters in the primitive plant Equisetum arvense*. *Plant J.*, **72**, 320–330.

Gross, G.G. (1977) *Cell wall-bound malate dehydrogenase from horseradish*. *Phytochemistry*, **16**, 319–321.

Guerriero, G., Hausman, J.-F., and Legay, S. (2016) *Silicon and the Plant Extracellular Matrix*. *Front. Plant Sci.*, **7**, 463.

Gu, H.-H., Qiu, H., Tian, T., Zhan, S.-S., Deng, T.-H.-B., Chaney, R.L., et al. (2011) *Mitigation effects of silicon rich amendments on heavy metal accumulation in rice (Oryza sativa L.) planted on multi-metal contaminated acidic soil*. *Chemosphere*, **83**, 1234–1240.

Guo, W., Grant, A., and Novick, P. (1999) *Exo84p is an exocyst protein essential for secretion*. *J. Biol. Chem.*, **274**, 23558–23564.

Guseman, J.M., Lee, J.S., Bogenschutz, N.L., Peterson, K.M., Virata, R.E., Xie, B., et al. (2010) *Dysregulation of cell-to-cell connectivity and stomatal patterning by loss-of-function mutation in Arabidopsis chorus (glucan synthase-like 8)*. *Development*, **137**, 1731–1741.

Gutierrez-Alcala, G., Gotor, C., Meyer, A.J., Fricker, M., Vega, J.M., and Romero, L.C. (2000) *Glutathione biosynthesis in Arabidopsis trichome cells*. *Proc. Natl. Acad. Sci. U. S. A.*, **97**, 11108–11113.

Gutierrez, R., Lindeboom, J.J., Paredez, A.R., Emons, A.M.C., and Ehrhardt, D.W. (2009) *Arabidopsis cortical microtubules position cellulose synthase delivery to the plasma membrane and interact with cellulose synthase trafficking compartments*. *Nat. Cell Biol.*, **11**, 797–806.

Gu, Y., Kaplinsky, N., Bringmann, M., Cobb, A., Carroll, A., Sampathkumar, A., et al. (2010) *Identification of a cellulose synthase-associated protein required for cellulose biosynthesis*. *Proc. Natl. Acad. Sci. U. S. A.*, **107**, 12866–12871.

H

Handley, R., Ekbom, B., and Agren, J. (2005) *Variation in trichome density and resistance against a specialist insect herbivore in natural populations of Arabidopsis thaliana*. *Ecological Entomology*, **30**, 284–292.

He, B. and Guo, W. (2009) *The exocyst complex in polarized exocytosis*. *Current Opinion in Cell Biology*, **21**, 537–542.

He, B., Xi, F., Zhang, X., Zhang, J., and Guo, W. (2007) *Exo70 interacts with phospholipids and mediates the targeting of the exocyst to the plasma membrane*. *EMBO J.*, **26**, 4053–4065.

He, C., Wang, L., Liu, J., Liu, X., Li, X., Ma, J., et al. (2013) *Evidence for "silicon" within the cell walls of suspension-cultured rice cells*. *New Phytol.*, **200**, 700–709.

He, J.Y., Ren, Y.F., Zhu, C., and Jiang, D. (2013) *Change of Photosynthetic Gas Exchange and Chlorophyll Fluorescence of Cd-Sensitive Mutant Rice in Response to Cd Stress*. *Advanced Materials Research*, **807-809**, 336–341.

Heilmann, M. and Heilmann, I. (2015) *Plant phosphoinositides-complex networks controlling growth and adaptation*. *Biochim. Biophys. Acta*, **1851**, 759–769.

Henzler, T. and Steudle, E. (2000) *Transport and metabolic degradation of hydrogen peroxide in Chara corallina: model calculations and measurements with the pressure probe suggest transport of H(2)O(2) across water channels*. *J. Exp. Bot.*, **51**, 2053–2066.

Hirschi, K.D., Korenkov, V.D., Wilganowski, N.L., and Wagner, G.J. (2000) *Expression of arabidopsis CAX2 in tobacco. Altered metal accumulation and increased manganese tolerance*. *Plant Physiol.*, **124**, 125–133.

Hokura, A., Onuma, R., Kitajima, N., Terada, Y., Saito, H., Abe, T., et al. (2006) *2-D X-ray Fluorescence Imaging of Cadmium Hyperaccumulating Plants by Using High-energy Synchrotron Radiation X-ray Microbeam*. *Chemistry Letters*, **35**, 1246–1247.

Hong, Z., Delauney, A.J., and Verma, D.P. (2001) *A cell plate-specific callose synthase and its interaction with phragmoplastin*. *Plant Cell*, **13**, 755–768.

Hong, Z., Zhang, Z., Olson, J.M., and Verma, D.P. (2001) *A novel UDP-glucose transferase is part of the callose synthase complex and interacts with phragmoplastin at the forming cell plate*. *Plant Cell*, **13**, 769–779.

Hruz, T., Laule, O., Szabo, G., Wessendorp, F., Bleuler, S., Oertle, L., et al. (2008) *Genevestigator v3: a reference expression database for the meta-analysis of transcriptomes*. *Adv. Bioinformatics*, **2008**, 420747.

Huang, L., Chen, X.-Y., Rim, Y., Han, X., Cho, W.K., Kim, S.-W., and Kim, J.-Y. (2009) *Arabidopsis glucan synthase-like 10 functions in male gametogenesis*. *J. Plant Physiol.*, **166**, 344–352.

Hülskamp, M. (2004) *Plant trichomes: a model for cell differentiation*. *Nature Reviews Molecular Cell Biology*, **5**, 471–480.

Hülskamp, M., Miséra, S., and Jürgens, G. (1994) *Genetic dissection of trichome cell development in Arabidopsis*. *Cell*, **76**, 555–566.

I

Iglesias, V.A. and Meins, F. (2000) *Movement of plant viruses is delayed in a beta-1,3-glucanase-deficient mutant showing a reduced plasmodesmatal size exclusion limit and enhanced callose deposition*. *Plant J.*, **21**, 157–166.

Inanaga, S., Okasaka, A., and Tanaka, S. (1995) *Does silicon exist in association with organic compounds in rice plant? Soil Sci. Plant Nutr.*, **41**, 111–117.

Isaure, M.-P., Fayard, B., Sarret, G., Pairis, S., and Bourguignon, J. (2006) *Localization and chemical forms of cadmium in plant samples by combining analytical electron microscopy and X-ray spectromicroscopy. Spectrochimica Acta Part B: Atomic Spectroscopy*, **61**, 1242–1252.

Isaure, M.-P., Huguet, S., Meyer, C.-L., Castillo-Michel, H., Testemale, D., Vantelon, D., et al. (2015) *Evidence of various mechanisms of Cd sequestration in the hyperaccumulator Arabidopsis halleri, the non-accumulator Arabidopsis lyrata, and their progenies by combined synchrotron-based techniques*. *J. Exp. Bot.*, **66**, 3201–3214.

Iwasaki, K. and Matsumura, A. (1999) *Effect of silicon on alleviation of manganese toxicity in pumpkin (Cucurbita moschata Duch cv. Shintosa). Soil Sci. Plant Nutr.*, **45**, 909–920.

J

Jacobs, A.K., Lipka, V., Burton, R.A., Panstruga, R., Strizhov, N., Schulze-Lefert, P., and Fincher, G.B. (2003) *An Arabidopsis Callose Synthase, GSL5, Is Required for Wound and Papillary Callose Formation*. *Plant Cell*, **15**, 2503–2513.

Jakoby, M.J., Falkenhan, D., Mader, M.T., Brininstool, G., Wischnitzki, E., Platz, N., et al. (2008) *Transcriptional profiling of mature Arabidopsis trichomes reveals that NOECK encodes the MIXTA-like transcriptional regulator MYB106*. *Plant Physiol.*, **148**, 1583–1602.

James, D.G. (2003) *Field evaluation of herbivore-induced plant volatiles as attractants for beneficial insects: methyl salicylate and the green lacewing, Chrysopa nigricornis*. *J. Chem. Ecol.*, **29**, 1601–1609.

Jovanović, S.V., Kukavica, B., Vidović, M., Morina, F., and Menckhoff, L. (2018) *Class III Peroxidases: Functions, Localization and Redox Regulation of Isoenzymes*. *Antioxidants and Antioxidant Enzymes in Higher Plants*, 269–300.

K

Kalmbach, L., Hématy, K., De Bellis, D., Barberon, M., Fujita, S., Ursache, R., et al. (2017) *Transient cell-specific EXO70A1 activity in the CASP domain and Casparian strip localization*. *Nat Plants*, **3**, 17058.

Kaufman, P.B., Dayanandan, P., Takeoka, Y., Bigelow, W.C., Jones, J.D., and Iler, R. (1981) *Silica in Shoots of Higher Plants*. In: *Silicon and Siliceous Structures in Biological Systems* , pp. 409–449.

Kauss, H. (1985) *Callose biosynthesis as a Ca2+-regulated process and possible relations to the induction of other metabolic changes*. *J. Cell Sci. Suppl.*, **2**, 89–103.

Kauss, H., Waldmann, T., and Quader, H. (1990) *Ca2 as a Signal in the Induction of Callose Synthesis*. *Signal Perception and Transduction in Higher Plants*, 117–131.

Kerr, E.M. and Fry, S.C. (2004) *Extracellular cross-linking of xylan and xyloglucan in maize cell-suspension cultures: the role of oxidative phenolic coupling*. *Planta*, **219**, 73–83.

Kido, N., Yokoyama, R., Yamamoto, T., Furukawa, J., Iwai, H., Satoh, S., and Nishitani, K. (2015) *The matrix polysaccharide (1;3,1;4)-β-D-glucan is involved in silicon-dependent strengthening of rice cell wall*. *Plant Cell Physiol.*, **56**, 268–276.

Kim, M.J., Ciani, S., and Schachtman, D.P. (2010) *A peroxidase contributes to ROS production during Arabidopsis root response to potassium deficiency*. *Mol. Plant*, **3**, 420–427.

Kjellbom, P., Snogerup, L., Stöhr, C., Reuzeau, C., McCabe, P.F., and Pennell, R.I. (1997) *Oxidative cross-linking of plasma membrane arabinogalactan proteins*. *Plant J.*, **12**, 1189–1196.

Kleine-Vehn, J., Wabnik, K., Martinière, A., Łangowski, Ł., Willig, K., Naramoto, S., et al. (2011) *Recycling, clustering, and endocytosis jointly maintain PIN auxin carrier polarity at the plasma membrane. Mol. Syst. Biol.*, **7**, 540.

Klinger, C.M., Klute, M.J., and Dacks, J.B. (2013) *Comparative genomic analysis of multi-subunit tethering complexes demonstrates an ancient pan-eukaryotic complement and sculpting in Apicomplexa*. *PLoS One*, **8**, e76278.

Kooijman, E.E., Chupin, V., Fuller, N.L., Kozlov, M.M., de Kruijff, B., Burger, K.N.J., and Rand, P.R. (2005) *Spontaneous curvature of phosphatidic acid and lysophosphatidic acid*. *Biochemistry*, **44**, 2097–2102.

Koumandou, V.L., Dacks, J.B., Coulson, R.M.R., and Field, M.C. (2007) *Control systems for membrane fusion in the ancestral eukaryote; evolution of tethering complexes and SM proteins*. *BMC Evol. Biol.*, **7**, 29.

Kubátová, Z., Pejchar, P., Potocký, M., Sekereš, J., Žárský, V., and Kulich, I. (2019) *Trichome Contains Two Plasma Membrane Domains with Different Lipid Compositions Which Attract Distinct EXO70 Subunits*. *Int. J. Mol. Sci.*, **20**.

Kulich, I., Cole, R., Drdová, E., Cvrcková, F., Soukup, A., Fowler, J., and Zárský, V. (2010) *Arabidopsis exocyst subunits SEC8 and EXO70A1 and exocyst interactor ROH1 are involved in the localized deposition of seed coat pectin*. *New Phytol.*, **188**, 615–625.

Kulich, I., Pečenková, T., Sekereš, J., Smetana, O., Fendrych, M., Foissner, I., et al. (2013) *Arabidopsis exocyst subcomplex containing subunit EXO70B1 is involved in autophagy-related transport to the vacuole*. *Traffic*, **14**, 1155–1165.

Kulich, I., Vojtíková, Z., Glanc, M., Ortmannová, J., Rasmann, S., and Žárský, V. (2015) *Cell wall maturation of Arabidopsis trichomes is dependent on exocyst subunit EXO70H4 and involves callose deposition*. *Plant Physiol.*, **168**, 120–131.

Kulich, I., Vojtíková, Z., Sabol, P., Ortmannová, J., Neděla, V., Tihlaříková, E., and Žárský, V. (2018) *Exocyst Subunit EXO70H4 Has a Specific Role in Callose Synthase Secretion and Silica Accumulation*. *Plant Physiol.*, **176**, 2040–2051.

Küpper, H., Lombi, E., Zhao, F.J., and McGrath, S.P. (2000) *Cellular compartmentation of cadmium and zinc in relation to other elements in the hyperaccumulator Arabidopsis halleri*. *Planta*, **212**, 75–84.

L

Langowski, L., Růzicka, K., Naramoto, S., Kleine-Vehn, J., and Friml, J. (2010) *Trafficking to the outer polar domain defines the root-soil interface*. *Curr. Biol.*, **20**, 904–908.

Łangowski, Ł., Wabnik, K., Li, H., Vanneste, S., Naramoto, S., Tanaka, H., and Friml, J. (2016) *Cellular mechanisms for cargo delivery and polarity maintenance at different polar domains in plant cells*. *Cell Discov*, **2**, 16018.

Law, C. and Exley, C. (2011) *New insight into silica deposition in horsetail (Equisetum arvense)*. *BMC Plant Biol.*, **11**, 112.

Leroux, O., Leroux, F., Mastroberti, A.A., Santos-Silva, F., Van Loo, D., Bagniewska-Zadworna, A., et al. (2013) *Heterogeneity of silica and glycan-epitope distribution in epidermal idioblast cell walls in Adiantum raddianum laminae*. *Planta*, **237**, 1453–1464.

Leshem, Y., Melamed-Book, N., Cagnac, O., Ronen, G., Nishri, Y., Solomon, M., et al. (2006) *Suppression of Arabidopsis vesicle-SNARE expression inhibited fusion of H2O2-containing vesicles with tonoplast and increased salt tolerance*. *Proc. Natl. Acad. Sci. U. S. A.*, **103**, 18008–18013.

Levy, A., Erlanger, M., Rosenthal, M., and Epel, B.L. (2007) *A plasmodesmata-associated beta-1,3-glucanase in Arabidopsis*. *Plant J.*, **49**, 669–682.

Li, E., Bhargava, A., Qiang, W., Friedmann, M.C., Forneris, N., Savidge, R.A., et al. (2012) *The Class II KNOX gene KNAT7 negatively regulates secondary wall formation in Arabidopsis and is functionally conserved in Populus*. *New Phytologist*, **194**, 102–115.

Li, S., Chen, M., Yu, D., Ren, S., Sun, S., Liu, L., et al. (2013) *EXO70A1-mediated vesicle trafficking is critical for tracheary element development in Arabidopsis*. *Plant Cell*, **25**, 1774–1786.

Li, Z., Fernie, A.R., and Persson, S. (2016) *Transition of primary to secondary cell wall synthesis*. *Science Bulletin*, **61**, 838–846.

Lin, C.-Y., Trinh, N.N., Fu, S.-F., Hsiung, Y.-C., Chia, L.-C., Lin, C.-W., and Huang, H.-J. (2013) *Comparison of early transcriptome responses to copper and cadmium in rice roots*. *Plant Mol. Biol.*, **81**, 507–522.

Liu, H., Zhou, L.H., Jiao, J., Liu, S., Zhang, Z., Lu, T.J., and Xu, F. (2016) *Gradient Mechanical Properties Facilitate Arabidopsis Trichome as Mechanosensor. ACS Appl. Mater. Interfaces*, **8**, 9755–9761.

Liu, J., Zuo, X., Yue, P., and Guo, W. (2007) *Phosphatidylinositol 4,5-bisphosphate mediates the targeting of the exocyst to the plasma membrane for exocytosis in mammalian cells*. *Mol. Biol. Cell*, **18**, 4483–4492.

Liu, S., Jiao, J., Lu, T.J., Xu, F., Pickard, B.G., and Genin, G.M. (2017) *Arabidopsis Leaf Trichomes as Acoustic Antennae*. *Biophys. J.*, **113**, 2068–2076.

Liu, Y., Su, Y., and Wang, X. (2013) *Phosphatidic acid-mediated signaling*. *Adv. Exp. Med. Biol.*, **991**, 159–176.

Livingston, S.J., Quilichini, T.D., Booth, J.K., Wong, D.C.J., Rensing, K.H., Laflamme-Yonkman, J., et al. (2019) *Cannabis glandular trichomes alter morphology and metabolite content during flower maturation*. *Plant J.*

Luyckx, M., Hausman, J.-F., Lutts, S., and Guerriero, G. (2017) *Silicon and Plants: Current Knowledge and Technological Perspectives*. *Front. Plant Sci.*, **8**, 411.

M

Madson, M., Dunand, C., Li, X., Verma, R., Vanzin, G.F., Caplan, J., et al. (2003) *The MUR3 Gene of Arabidopsis Encodes a Xyloglucan Galactosyltransferase That Is Evolutionarily Related to Animal Exostosins*. *The Plant Cell*, **15**, 1662–1670.

Ma, J., Cai, H., He, C., Zhang, W., and Wang, L. (2015) *A hemicellulose-bound form of silicon inhibits cadmium ion uptake in rice (Oryza sativa) cells*. *New Phytologist*, **206**, 1063–1074.

Ma, J.F., Mitani, N., Nagao, S., Konishi, S., Tamai, K., Iwashita, T., and Yano, M. (2004) *Characterization of the silicon uptake system and molecular mapping of the silicon transporter gene in rice*. *Plant Physiol.*, **136**, 3284–3289.

Ma, J.F. and Yamaji, N. (2006) *Silicon uptake and accumulation in higher plants*. *Trends Plant Sci.*, **11**, 392–397.

Ma, J.F., Yamaji, N., Mitani, N., Tamai, K., Konishi, S., Fujiwara, T., et al. (2007) *An efflux transporter of silicon in rice*. *Nature*, **448**, 209–212.

Marks, M.D., Wenger, J.P., Gilding, E., Jilk, R., and Dixon, R.A. (2009) *Transcriptome analysis of Arabidopsis wild-type and gl3-sst sim trichomes identifies four additional genes required for trichome development*. *Mol. Plant*, **2**, 803–822.

Martinez, C., Montillet, J.L., Bresson, E., Agnel, J.P., Dai, G.H., Daniel, J.F., et al. (1998) *Apoplastic Peroxidase Generates Superoxide Anions in Cells of Cotton Cotyledons Undergoing the Hypersensitive Reaction toXanthomonas campestrispv. malvacearumRace 18*. *Molecular Plant-Microbe Interactions*, **11**, 1038–1047.

Martiniere, A., Lavagi, I., Nageswaran, G., Rolfe, D.J., Maneta-Peyret, L., -T. Luu, D., et al. (2012) *Cell wall constrains lateral diffusion of plant plasma-membrane proteins*. *Proceedings of the National Academy of Sciences*, **109**, 12805–12810.

Martin, T.F.J. (2015) *PI(4,5)P2-binding effector proteins for vesicle exocytosis*. *Biochimica et Biophysica Acta (BBA) - Molecular and Cell Biology of Lipids*, **1851**, 785–793.

Martin-Urdiroz, M., Deeks, M.J., Horton, C.G., Dawe, H.R., and Jourdain, I. (2016) *The Exocyst Complex in Health and Disease*. *Front Cell Dev Biol*, **4**, 24.

McCormick, S. (1993) *Male Gametophyte Development*. *Plant Cell*, **5**, 1265.

Mhamdi, A. and Van Breusegem, F. (2018) *Reactive oxygen species in plant development*. *Development*, **145**.

Mitani, N., Ma, J.F., and Iwashita, T. (2005) *Identification of the silicon form in xylem sap of rice (Oryza sativa L.)*. *Plant Cell Physiol.*, **46**, 279–283.

Mitani, N., Yamaji, N., Ago, Y., Iwasaki, K., and Ma, J.F. (2011) *Isolation and functional characterization of an influx silicon transporter in two pumpkin cultivars contrasting in silicon accumulation*. *Plant J.*, **66**, 231–240.

Mitani, N., Yamaji, N., and Ma, J.F. (2009) *Identification of maize silicon influx transporters*. *Plant Cell Physiol.*, **50**, 5–12.

Mittler, R., Vanderauwera, S., Suzuki, N., Miller, G., Tognetti, V.B., Vandepoele, K., et al. (2011) *ROS signaling: the new wave? Trends Plant Sci.*, **16**, 300–309.

Mohnen, D. (2008) *Pectin structure and biosynthesis*. *Curr. Opin. Plant Biol.*, **11**, 266–277.

Montpetit, J., Vivancos, J., Mitani-Ueno, N., Yamaji, N., Rémus-Borel, W., Belzile, F., et al. (2012) *Cloning, functional characterization and heterologous expression of TaLsi1, a wheat silicon transporter gene*. *Plant Mol. Biol.*, **79**, 35–46.

Moravcevic, K., Oxley, C.L., and Lemmon, M.A. (2012) *Conditional peripheral membrane proteins: facing up to limited specificity*. *Structure*, **20**, 15–27.

Moscatelli, A., Ciampolini, F., Rodighiero, S., Onelli, E., Cresti, M., Santo, N., and Idilli, A. (2007) *Distinct endocytic pathways identified in tobacco pollen tubes using charged nanogold*. *J. Cell Sci.*, **120**, 3804–3819.

Murphy, A. and Taiz, L. (1995) *Comparison of metallothionein gene expression and nonprotein thiols in ten Arabidopsis ecotypes. Correlation with copper tolerance*. *Plant Physiol.*, **109**, 945–954.

N

Nedukha, O.M. (2015) *Callose: Localization, functions, and synthesis in plant cells*. *Cytology and Genetics*, **49**, 49–57.

Newman, R.H., Hill, S.J., and Harris, P.J. (2013) *Wide-angle x-ray scattering and solid-state nuclear magnetic resonance data combined to test models for cellulose microfibrils in mung bean cell walls*. *Plant Physiol.*, **163**, 1558–1567.

Nielsen, M.E., Feechan, A., Böhlenius, H., Ueda, T., and Thordal-Christensen, H. (2012) *Arabidopsis ARF-GTP exchange factor, GNOM, mediates transport required for innate immunity and focal accumulation of syntaxin PEN1*. *Proc. Natl. Acad. Sci. U. S. A.*, **109**, 11443–11448.

Nishimura, M.T., Stein, M., Hou, B.-H., Vogel, J.P., Edwards, H., and Somerville, S.C. (2003) *Loss of a callose synthase results in salicylic acid-dependent disease resistance*. *Science*, **301**, 969–972.

Noctor, G., Reichheld, J.-P., and Foyer, C.H. (2018) *ROS-related redox regulation and signaling in plants*. *Semin. Cell Dev. Biol.*, **80**, 3–12.

O

Oblessuc, P.R., Matiolli, C.C., and Melotto, M. (2020) *Novel molecular components involved in callose-mediated Arabidopsis defense against Salmonella enterica and Escherichia coli O157:H7*. *BMC Plant Biol.*, **20**, 16.

Oda, Y. and Fukuda, H. (2012) *Secondary cell wall patterning during xylem differentiation*. *Curr. Opin. Plant Biol.*, **15**, 38–44.

Oda, Y. and Fukuda, H. (2013) *The dynamic interplay of plasma membrane domains and cortical microtubules in secondary cell wall patterning*. *Front. Plant Sci.*, **4**.

Oda, Y., Iida, Y., Nagashima, Y., Sugiyama, Y., and Fukuda, H. (2015) *Novel coiled-coil proteins regulate exocyst association with cortical microtubules in xylem cells via the conserved oligomeric golgi-complex 2 protein*. *Plant Cell Physiol.*, **56**, 277–286.

Oda, Y., Mimura, T., and Hasezawa, S. (2005) *Regulation of secondary cell wall development by cortical microtubules during tracheary element differentiation in Arabidopsis cell suspensions*. *Plant Physiol.*, **137**, 1027–1036.

Oravecz, A., Baumann, A., Máté, Z., Brzezinska, A., Molinier, J., Oakeley, E.J., et al. (2006) *CONSTITUTIVELY PHOTOMORPHOGENIC1 is required for the UV-B response in Arabidopsis*. *Plant Cell*, **18**, 1975–1990.

P

Paradez, A., Wright, A., and Ehrhardt, D.W. (2006) *Microtubule cortical array organization and plant cell morphogenesis*. *Curr. Opin. Plant Biol.*, **9**, 571–578.

Parra-Vega, V., Corral-Martínez, P., Rivas-Sendra, A., and Seguí-Simarro, J.M. (2015) *Induction of Embryogenesis in Brassica Napus Microspores Produces a Callosic Subintinal Layer and Abnormal Cell Walls with Altered Levels of Callose and Cellulose*. *Front. Plant Sci.*, **6**, 1018.

Pleskot, R., Cwiklik, L., Jungwirth, P., Žárský, V., and Potocký, M. (2015) *Membrane targeting of the yeast exocyst complex*. *Biochim. Biophys. Acta*, **1848**, 1481–1489.

Potikha, T. and Delmer, D.P. (1995) *A mutant of Arabidopsis thaliana displaying altered patterns of cellulose deposition*. *The Plant Journal*, **7**, 453–460.

Potocký, M., Pleskot, R., Pejchar, P., Vitale, N., Kost, B., and Zárský, V. (2014) *Live-cell imaging of phosphatidic acid dynamics in pollen tubes visualized by Spo20p-derived biosensor*. *New Phytol.*, **203**, 483–494.

Q

Qadota, H., Python, C.P., Inoue, S.B., Arisawa, M., Anraku, Y., Zheng, Y., et al. (1996) *Identification of yeast Rho1p GTPase as a regulatory subunit of 1,3-beta-glucan synthase*. *Science*, **272**, 279–281.

R

Reynolds, O.L., Padula, M.P., Zeng, R., and Gurr, G.M. (2016) *Silicon: Potential to Promote Direct and Indirect Effects on Plant Defense Against Arthropod Pests in Agriculture*. *Front. Plant Sci.*, **7**, 744.

Richmond, T.A. and Somerville, C.R. (2001) *Integrative approaches to determining Csl function*. In: *Plant Cell Walls* , pp. 131–143.

Rodrigues Oblessuc, P., Vaz Bisneta, M., and Melotto, M. (2019) *Common and unique Arabidopsis proteins involved in stomatal susceptibility to Salmonella enterica and Pseudomonas syringae*. *FEMS Microbiol. Lett.*

Roosens, N.H.C.J., Willems, G., and Saumitou-Laprade, P. (2008) *Using Arabidopsis to explore zinc tolerance and hyperaccumulation*. *Trends Plant Sci.*, **13**, 208–215.

Roppolo, D., De Rybel, B., Dénervaud Tendon, V., Pfister, A., Alassimone, J., Vermeer, J.E.M., et al. (2011) *A novel protein family mediates Casparian strip formation in the endodermis*. *Nature*, **473**, 380–383.

Ruegger, M. and Chapple, C. (2001) *Mutations that reduce sinapoylmalate accumulation in Arabidopsis thaliana define loci with diverse roles in phenylpropanoid metabolism*. *Genetics*, **159**, 1741–1749.

S

Sabol, P., Kulich, I., and Žárský, V. (2017) *RIN4 recruits the exocyst subunit EXO70B1 to the plasma membrane*. *J. Exp. Bot.*, **68**, 3253–3265.

Sagi, M. and Fluhr, R. (2001) *Superoxide production by plant homologues of the gp91(phox) NADPH oxidase. Modulation of activity by calcium and by tobacco mosaic virus infection*. *Plant Physiol.*, **126**, 1281–1290.

Salt, D.E., Prince, R.C., Pickering, I.J., and Raskin, I. (1995) *Mechanisms of Cadmium Mobility and Accumulation in Indian Mustard*. *Plant Physiology*, **109**, 1427–1433.

Samuels, A.L. (1995) *Cytokinesis in tobacco BY-2 and root tip cells: a new model of cell plate formation in higher plants*. *J. Cell Biol.*, **130**, 1345–1357.

Sandell, E.B. (1945) *Colorimetric Determination of Traces of Metals*. *Soil Science*, **59**, 481.

Sanderfoot, A.A., Assaad, F.F., and Raikhel, N.V. (2000) *The Arabidopsis Genome. An Abundance of Soluble N-Ethylmaleimide-Sensitive Factor Adaptor Protein Receptors*. *Plant Physiology*, **124**, 1558–1569.

Sangster, A.G., Hodson, M.J., and Tubb, H.J. (2001) *Chapter 5 Silicon deposition in higher plants*. *Silicon in Agriculture*, 85–113.

Sarret, G., Saumitou-Laprade, P., Bert, V., Proux, O., Hazemann, J.-L., Traverse, A., et al. (2002) *Forms of zinc accumulated in the hyperaccumulator Arabidopsis halleri*. *Plant Physiol.*, **130**, 1815–1826.

Sarret, G., Willems, G., Isaure, M.-P., Marcus, M.A., Fakra, S.C., Frérot, H., et al. (2009) *Zinc distribution and speciation in Arabidopsis halleri x Arabidopsis lyrata progenies presenting various zinc accumulation capacities*. *New Phytol.*, **184**, 581–595.

Scheller, H.V. and Ulvskov, P. (2010) *Hemicelluloses*. *Annu. Rev. Plant Biol.*, **61**, 263–289.

Schuetz, M., Benske, A., Smith, R.A., Watanabe, Y., Tobimatsu, Y., Ralph, J., et al. (2014) *Laccases direct lignification in the discrete secondary cell wall domains of protoxylem*. *Plant Physiol.*, **166**, 798–807.

Sekereš, J., Pejchar, P., Šantrůček, J., Vukašinović, N., Žárský, V., and Potocký, M. (2017) *Analysis of Exocyst Subunit EXO70 Family Reveals Distinct Membrane Polar Domains in Tobacco Pollen Tubes*. *Plant Physiol.*, **173**, 1659–1675.

Sekereš, J., Pleskot, R., Pejchar, P., Žárský, V., and Potocký, M. (2015) *The song of lipids and proteins: dynamic lipid-protein interfaces in the regulation of plant cell polarity at different scales*. *J. Exp. Bot.*, **66**, 1587–1598.

Seregin, I.V. and Ivanov, V.B. (1997) *Histochemical investigation of cadmium and lead distribution in plants*. *Russ. J. Plant Physiol.*, **44**, 791–796.

Sharma, P., Jha, A.B., Dubey, R.S., and Pessarakli, M. (2012) *Reactive Oxygen Species, Oxidative Damage, and Antioxidative Defense Mechanism in Plants under Stressful Conditions*. *Journal of Botany*, **2012**, 1–26.

Shen, X., Zhou, Y., Duan, L., Li, Z., Eneji, A.E., and Li, J. (2010) *Silicon effects on photosynthesis and antioxidant parameters of soybean seedlings under drought and ultraviolet-B radiation*. *J. Plant Physiol.*, **167**, 1248–1252.

Shikanai, Y., Yoshida, R., Hirano, T., Enomoto, Y., Li, B., Asada, M., et al. (2020) *Callose synthesis suppresses cell death induced by low-calcium conditions in leaves*. *Plant Physiol.*

Shi, X., Sun, X., Zhang, Z., Feng, D., Zhang, Q., Han, L., et al. (2015) *GLUCAN SYNTHASE-LIKE 5 (GSL5) plays an essential role in male fertility by regulating callose metabolism during microsporogenesis in rice*. *Plant Cell Physiol.*, **56**, 497–509.

Shi, Y., Wang, Y., Flowers, T.J., and Gong, H. (2013) *Silicon decreases chloride transport in rice (Oryza sativa L.) in saline conditions*. *J. Plant Physiol.*, **170**, 847–853.

Sinlapadech, T., Stout, J., Ruegger, M.O., Deak, M., and Chapple, C. (2007) *The hyper-fluorescent trichome phenotype of the brt1 mutant of Arabidopsis is the result of a defect in a sinapic acid: UDPG glucosyltransferase. Plant J.*, **49**, 655–668.

Sjolund, R.D. (1997) *The Phloem Sieve Element: A River Runs through It. Plant Cell*, **9**, 1137–1146.

Somerville, C. (2004) *Toward a Systems Approach to Understanding Plant Cell Walls. Science*, **306**, 2206–2211.

Stone, B.A. and Clarke, A.E. (1992) *Chemistry and biology of 1,3-β-Glucans*. Intl Specialized Book Service Inc.

Suo, B., Seifert, S., and Kirik, V. (2013) *Arabidopsis GLASSY HAIR genes promote trichome papillae development. J. Exp. Bot.*, **64**, 4981–4991.

Synek, L., Schlager, N., Eliás, M., Quentin, M., Hauser, M.-T., and Zárský, V. (2006) *AtEXO70A1, a member of a family of putative exocyst subunits specifically expanded in land plants, is important for polar growth and plant development. Plant J.*, **48**, 54–72.

Szymanski, D.B., Lloyd, A.M., and Marks, M.D. (2000) *Progress in the molecular genetic analysis of trichome initiation and morphogenesis in Arabidopsis. Trends Plant Sci.*, **5**, 214–219.

T

Tamai, K. and Ma, J.F. (2003) *Characterization of silicon uptake by rice roots. New Phytol.*, **158**, 431–436.

Taylor, N.G. (2000) *Multiple Cellulose Synthase Catalytic Subunits Are Required for Cellulose Synthesis in Arabidopsis. THE PLANT CELL ONLINE*, **12**, 2529–2540.

TerBush, D.R., Maurice, T., Roth, D., and Novick, P. (1996) *The Exocyst is a multiprotein complex required for exocytosis in Saccharomyces cerevisiae. EMBO J.*, **15**, 6483–6494.

Tewari, R.K., Kumar, P., and Sharma, P.N. (2006) *Antioxidant responses to enhanced generation of superoxide anion radical and hydrogen peroxide in the copper-stressed mulberry plants. Planta*, **223**, 1145–1153.

Thiele, K., Wanner, G., Kindzierski, V., Jürgens, G., Mayer, U., Pachl, F., and Assaad, F.F. (2009) *The timely deposition of callose is essential for cytokinesis in Arabidopsis. Plant J.*, **58**, 13–26.

Tissier, A. (2012) *Glandular trichomes: what comes after expressed sequence tags? Plant J.*, **70**, 51–68.

Töller, A., Brownfield, L., Neu, C., Twell, D., and Schulze-Lefert, P. (2008) *Dual function of Arabidopsis glucan synthase-like genes GSL8 and GSL10 in male gametophyte development and plant growth. Plant J.*, **54**, 911–923.

Trinh, N.-N., Huang, T.-L., Chi, W.-C., Fu, S.-F., Chen, C.-C., and Huang, H.-J. (2014) *Chromium stress response effect on signal transduction and expression of signaling genes in rice. Physiol. Plant.*, **150**, 205–224.

V

Vanzin, G.F., Madson, M., Carpita, N.C., Raikhel, N.V., Keegstra, K., and -D. Reiter, W. (2002) *The mur2 mutant of Arabidopsis thaliana lacks fucosylated xyloglucan because of a lesion in fucosyltransferase AtFUT1. Proceedings of the National Academy of Sciences*, **99**, 3340–3345.

Vatén, A., Dettmer, J., Wu, S., Stierhof, Y.-D., Miyashima, S., Yadav, S.R., et al. (2011) *Callose biosynthesis regulates symplastic trafficking during root development. Dev. Cell*, **21**, 1144–1155.

Verma, D.P. and Hong, Z. (2001) *Plant callose synthase complexes. Plant Mol. Biol.*, **47**, 693–701.

Verma, D.P.S. (2001) *CYTOKINESIS AND BUILDING OF THE CELL PLATE IN PLANTS. Annu. Rev. Plant Physiol. Plant Mol. Biol.*, **52**, 751–784.

Vivancos, J., Labbé, C., Menzies, J.G., and Bélanger, R.R. (2015) *Silicon-mediated resistance of Arabidopsis against powdery mildew involves mechanisms other than the salicylic acid (SA)-dependent defence pathway. Molecular Plant Pathology*, **16**, 572–582.

Vogel, J. and Somerville, S. (2000) *Isolation and characterization of powdery mildew-resistant Arabidopsis mutants. Proc. Natl. Acad. Sci. U. S. A.*, **97**, 1897–1902.

Voigt, C.A. (2014) *Callose-mediated resistance to pathogenic intruders in plant defense-related papillae. Frontiers in Plant Science*, **5**.

Voigt, C.A. (2016) *Cellulose/callose glucan networks: the key to powdery mildew resistance in plants? New Phytologist*, **212**, 303–305.

Vukašinović, N., Oda, Y., Pejchar, P., Synek, L., Pečenková, T., Rawat, A., et al. (2017) *Microtubule-dependent targeting of the exocyst complex is necessary for xylem development in Arabidopsis. New Phytol.*, **213**, 1052–1067.

Vukašinović, N. and Žárský, V. (2016) *Tethering Complexes in the Arabidopsis Endomembrane System. Front Cell Dev Biol*, **4**, 46.

W

Wang, H.-S., Yu, C., Fan, P.-P., Bao, B.-F., Li, T., and Zhu, Z.-J. (2014) *Identification of Two Cucumber Putative Silicon Transporter Genes in Cucumis sativus. J. Plant Growth Regul.*, **34**, 332–338.

Wang, Z., Li, X., Wang, X., Liu, N., Xu, B., Peng, Q., et al. (2019) *Arabidopsis Endoplasmic Reticulum-Localized UBAC2 Proteins Interact with PAMP-INDUCED COILED-COIL to Regulate Pathogen-Induced Callose Deposition and Plant Immunity. Plant Cell*, **31**, 153–171.

Watteau, F. and Villemin, G. (2001) *Ultrastructural study of the biogeochemical cycle of silicon in the soil and litter of a temperate forest. Eur. J. Soil Sci.*, **52**, 385–396.

Wawrzynska, A., Rodibaugh, N.L., and Innes, R.W. (2010) *Synergistic activation of defense responses in Arabidopsis by simultaneous loss of the GSL5 callose synthase and the EDR1 protein kinase. Mol. Plant. Microbe. Interact.*, **23**, 578–584.

Werker, E. (2000) *Trichome diversity and development*. *Advances in Botanical Research*, 1–35.

Wrzaczek, M., Brosché, M., and Kangasjärvi, J. (2013) *ROS signaling loops — production, perception, regulation*. *Current Opinion in Plant Biology*, **16**, 575–582.

X

Xie, B., Wang, X., and Hong, Z. (2010) *Precocious pollen germination in Arabidopsis plants with altered callose deposition during microsporogenesis*. *Planta*, **231**, 809–823.

Xie, B., Wang, X., Zhu, M., Zhang, Z., and Hong, Z. (2010) *CalS7 encodes a callose synthase responsible for callose deposition in the phloem*. *Plant J.*, **65**, 1–14.

Y

Yamaji, N., Chiba, Y., Mitani-Ueno, N., and Feng Ma, J. (2012) *Functional characterization of a silicon transporter gene implicated in silicon distribution in barley*. *Plant Physiol.*, **160**, 1491–1497.

Yamaji, N., Mitatni, N., and Ma, J.F. (2008) *A transporter regulating silicon distribution in rice shoots*. *Plant Cell*, **20**, 1381–1389.

Yan, A., Pan, J., An, L., Gan, Y., and Feng, H. (2012) *The responses of trichome mutants to enhanced ultraviolet-B radiation in Arabidopsis thaliana*. *J. Photochem. Photobiol. B*, **113**, 29–35.

Yeo, A.R., Flowers, S.A., Rao, G., Welfare, K., Senanayake, N., and Flowers, T.J. (1999) *Silicon reduces sodium uptake in rice (Oryza sativa L.) in saline conditions and this is accounted for by a reduction in the transpirational bypass flow*. *Plant, Cell & Environment*, **22**, 559–565.

Z

Zarra, I., Sánchez, M., Queijeiro, E., Peña, M.J., and Revilla, G. (1999) *The cell wall stiffening mechanism in Pinus pinaster Aiton: regulation by apoplastic levels of ascorbate and hydrogen peroxide*. *Journal of the Science of Food and Agriculture*, **79**, 416–420.

Zárský, V., Cvrcková, F., Potocký, M., and Hála, M. (2009) *Exocytosis and cell polarity in plants - exocyst and recycling domains*. *New Phytol.*, **183**, 255–272.

Zárský, V. and Potocký, M. (2010) *Recycling domains in plant cell morphogenesis: small GTPase effectors, plasma membrane signalling and the exocyst*. *Biochem. Soc. Trans.*, **38**, 723–728.

Žárský, V., Sekereš, J., Kubátová, Z., Pečenková, T., and Cvrčková, F. (2019) *Three subfamilies of exocyst EXO70 family subunits in land plants: early divergence and ongoing functional specialization*. *J. Exp. Bot.*

Zhang, X., Pumplin, N., Ivanov, S., and Harrison, M.J. (2015) *EXO70I Is Required for Development of a Sub-domain of the Periarbuscular Membrane during Arbuscular Mycorrhizal Symbiosis*. *Curr. Biol.*, **25**, 2189–2195.

Zhang, Y., Liu, C.-M., Emons, A.-M.C., and Ketelaar, T. (2010) *The plant exocyst*. *J. Integr. Plant Biol.*, **52**, 138–146.

Zhao, F.J., Lombi, E., Breedon, T., and S., P.M. (2000) *Zinc hyperaccumulation and cellular distribution in Arabidopsis halleri*. *Plant, Cell & Environment*, **23**, 507–514.

Zhong, R., Burk, D.H., Morrison, W.H., 3rd, and Ye, Z.-H. (2002) *A kinesin-like protein is essential for oriented deposition of cellulose microfibrils and cell wall strength*. *Plant Cell*, **14**, 3101–3117.

Zhong, R., Lee, C., and Ye, Z.-H. (2010) *Evolutionary conservation of the transcriptional network regulating secondary cell wall biosynthesis*. *Trends Plant Sci.*, **15**, 625–632.

Zhong, R. and Ye, Z.-H. (2009) *Secondary Cell Walls*. *Encyclopedia of Life Sciences*.

Zhong, R. and Ye, Z.-H. (2015) *Secondary cell walls: biosynthesis, patterned deposition and transcriptional regulation*. *Plant Cell Physiol.*, **56**, 195–214.

Zhong, R. and Ye, Z.-H. (2014) *Transcriptional Regulation of Biosynthesis of Cell Wall Components during Xylem Differentiation*. *Plant Cell Wall Patterning and Cell Shape*, 351–377.

Zhou, L.H., Liu, S.B., Wang, P.F., Lu, T.J., Xu, F., Genin, G.M., and Pickard, B.G. (2017) *The Arabidopsis trichome is an active mechanosensory switch*. *Plant Cell Environ.*, **40**, 611–621.

Zhu, X., Li, S., Pan, S., Xin, X., and Gu, Y. (2018) *CSI1, PATROL1, and exocyst complex cooperate in delivery of cellulose synthase complexes to the plasma membrane*. *Proc. Natl. Acad. Sci. U. S. A.*, **115**, E3578–E3587.

Zhu, Y. and Gong, H. (2014) *Beneficial effects of silicon on salt and drought tolerance in plants*. *Agronomy for Sustainable Development*, **34**, 455–472.